PLASMA ASSISTED DEPOSITION USING AN UNBALANCED MAGNETRON

by

HUSSEIN ABIDJWAD JA'FER

A doctoral thesis submitted in partial fulfilment of the requirements for the award of Doctor of Philosophy of the Loughborough University of Technology.

March 1993

Supervisor: Prof. R.P. Howson B.Sc. Ph.D.

Department of Physics

DEDICATION: To

My parents, brothers and sisters

My wife (Bushrah) and my children: Alaa, Wiam, Ali and Haythem

With my thanks for their patience and belief.

ABSTRACT

It is well known that ion bombardment of growing films can strongly influence their microstructure and consequently their physical properties. The available technology for ion assisted deposition, particularly where separate sources are used for the deposition flux and the ion flux, is difficult to implement in many production situations. The planar magnetron provides a controllable ion flux while retaining the many other desirable features of simplicity, high deposition rate, geometric versatility and tolerance of reactive gases. This assists in the implementation of ion beam assisted deposition in both research and production.

The unbalanced magnetron is a new type of planar deposition source that gives the normal deposition behaviour of a planar magnetron plus a beam of ions whose intensity at the substrate can be varied independently of the deposition flux by changing the magnetic field configuration. It is shown by using the unbalanced magnetron the reactivity of the plasma and the deposited film properties can be improved. For a high floating potential and ion bombardment of the deposited film, the partial pressure of oxygen required is considerably lower. The use of the unbalanced magnetron for reactively sputtered titanium nitride and titanium oxide on glass substrates at room temperature result in an improvement in the deposited film optical and electrical properties.

The type and degree of film modification due to the ion bombardment of the growing films depend on the kinetic energy of incident ions and the ratio of the fluxes of bombarding ions and condensing atoms. In addition, bombardment of the substrate surface before coating begins results in a variety of induced surface modifications that are generally beneficial to film adhesion. The design and construction of an unbalanced magnetron providing a high current density with high floating potential are described here.

It has been observed that the high energy reflected neutral species at magnetron voltages around 500 V may cause a radiation type damage, which in turn influences the microstructure and morphology and, hence, the film properties and film stresses. The design of a low voltage magnetron operating at voltages between 50-500 volts is described here. This design was shown to give TiN films of improved quality.

By modifying the filament position in conjunction with the magnetic field, a plasma source based on the unbalanced magnetron has been achieved. Using this, a plasma beam assisted magnetron system for low voltage sputtering of sensitive material was demonstrated.

ACKNOWLEDGEMENTS

I would like to express my gratitude to my supervisor Professor R. P. Howson for his supervision and discussion throughout this project. My great thanks also go to my director of research Professor K. R. A. Ziebeck for his continuous support and personal efforts in different matters and difficulties which I and my family have experienced. I would like also to thank Dr A. G. Spencer and Dr G. W. Hall for their assistance and scientific discussion and Mr E. M. Stenlake for his technical assistance and useful discussion. My thanks also to all technical staff in the work shop for their help and to Mr J. Bates from metallurgical department who did the SEM investigation of some of the samples.

I would like also to thank Dr. H. Barankova and Dr. S. Kadlec from Institute of Physics, Prague, for their scientific discussion and collaboration during their visit.

Again I would like deeply to thank Dr. A. G. Spencer and Dr. G. W. Hall for their kindness and offers of assistance throughout all my difficulties and for their help in reading my thesis.

My thanks also go to the members of the physics department for their friendship and hospitality.

I would like very much to thank all my friends who have shown a remarkable character of unity and love. Finally my thanks go to the Ministry of Higher Education and Scientific Research of the Republic of Iraq for giving me the opportunity to continue my postgraduate studies.

List of Contents

Chapter-1

Introduction 1

1.1 References 8

Chapter-2

Theory and back ground 12

2.1 Glow discharge initiation 12

2.2 Plasma discharge 15

2.2.1 Plasma measurement 15

2.2.2 Debye length 17

2.2.3 Ion Current 19

2.2.4 Floating potential 20

2.2.5 Magnetic effect 22

2.3 Sputtering phenomena 23

2.4 The magnetron 26

2.4.1 Target sputtering 29

2.4.2 The unbalanced magnetron 33

2.4.2.1 Magnetron plasma confinement 35

2.4.2.2 I-V plasma characteristics and electron temperature 37

2.4.2.3 Film modification by ion bombardment 39

2.5 Reactive sputter deposition 42

2.5.1 Controlling the process by monitoring system 45

2.6 References 47

Chapter-3

Measurement techniques for thin films 53

3.1 Talystep system 53

3.2 The ellipsometer 53

3.3 The spectrophotometer 54

3.4 The film resistivity 55

3.5 References 57

Chapter-4

Vacuum considerations 58

4.1 The effects on magnetron potential 58

4.2 Plasma parameters 60

4.3 Impurity and film properties 61

4.4 References 65

Chapter-5

Substrate effects from an unbalanced magnetron 66

5.1 Unbalanced magnetron design and I-V characteristics 66

5.1.1 I-V magnetron characteristics 67

5.2 Magnetron efficiency 69

5.3 Ion current and floating potential 70

5.4 Heat load measurements 71

5.5 Plasma radial distribution 73

5.6 Auxiliary magnet effects 74

5.6.1 Controlling the unbalanced magnetron performance 75

5.7 Applications 76

5.7.1 Titanium oxide 76

5.7.2 Titanium nitride 77

5.7.2.1 The load-lock system 77

5.7.2.2 The getter box system 80

5.7.3 Indium-tin oxide 82

5.8 References 85

Chapter-6

Comparison between an arc evaporation and the unbalanced magnetron 89

6.1 Arc evaporation source 90

6.2 Plasma properties 91

6.3 The reactive process 92

6.3.1 Gas flow control 92

6.3.2 Film products 92

6.4 Other remarks 94

6.5 References 95

Chapter-7

High ion current performance from an unbalanced magnetron (UM) 96

7.1 Magnetron design 98

7.1.1 I-V magnetron characteristics of the new UM 99

7.2 Substrate effects from UM 99

7.2.1 Floating potential and ion current measurements 99

7.2.2 Floating potential and ion current distribution with beam axis 102

7.2.3 Auxiliary magnet effects 102

7.3 Plasma activation 103

7.4 Applications 103

7.4.1 PECVD 103

7.4.1.1 Diamond-like carbon deposition 104

7.4.1.2 Silicon oxide 106

7.4.1.3 Titanium oxide 107

7.4.2 Polymer and positive photoresist etching 109

7.4.2.1 Plasma parameter effects 110

7.4.2.2 Selective surfaces 111

7.5 References 113

Chapter-8

Low voltage magnetron 117

8.1 Hollow cathode enhanced magnetron process 118

8.2 Thin film stresses 119

8.3 Thermionic electron assisted magnetron process 122

8.4 Low voltage magnetron design and optimisation 123
8.4.1 Filament position effects 124
8.4.2 I-V magnetron characteristics 124
8.4.3 Low working gas pressure 125
8.5 Plasma properties 126
8.6 Sputtering rate of low voltage magnetron 126
8.7 Applications 127
8.7.1 Low voltage reactive sputtering of TiN 127
8.7.2 Getter box system 129
8.8 References 131
Chapter-9
Plasma source based an unbalanced magnetron 133
9.1 Hall effect ion source 133
9.1.1 Operation 133
9.2 Plasma-source based on the unbalanced magnetron 135
9.2.1 Design and optimisation 135
9.2.2 The source performance 138
9.2.3 Axis and radial beam profile 139
9.2.4 Argon and oxygen pressure effects 140
9.2.5 Auxiliary magnet effects 141
9.3 Applications 142
9.3.1 Metal low voltage sputtering 142
9.3.1.1 Copper plate sputtering 142
9.3.1.2 Copper target based an unbalanced magnetron sputtering 144
9.3.2 Low voltage ITO sputtering 145
9.4 References 148
Chapter-10
Conclusions 149

CHAPTER-1

INTRODUCTION

The rapid growth in sputtering since the early 1960's has been due to the use of the technique for the fabrication of thin films and to the increasing use of films in modern technology. This is a rebirth of the sputtering technology, which developed in the half century following the discovery of the sputtering phenomenon by Grove (Refs. 1,2). During that period, the technique was widely used for the preparation of metallic films, which were generally employed as reflectors (Ref. 3). When improvements in vacuum technology made possible the routine attainment of pressures in the 10^{-4} Torr range, evaporation displaced sputtering for this application. A cursory examination of the literature shows that films containing almost every element in the periodic table have been prepared, many of them by the radio frequency (RF) sputtering technique first described by Anderson et al as recently as 1962 (Refs. 3,5). Essentially all the reported film deposition work has been carried out in a glow discharge environment, maintained by the application of either direct current DC or RF (13.56 MHz) power in various configurations.

There has been a large number of review articles devoted to various aspects of sputtering. A brief history of the development of sputtering can be found in a review article by Wehner and Anderson (Ref. 6) and by Bishop (Ref. 2). For detailed information on sputtering theory and basic understanding, the reader is referred to References 6-9. Sputtering apparatuses can assume an almost unlimited variety of configurations, depending on the application. The simplest is the planar diode (Refs. 6,10,11) which consists of two planar electrodes, typically 10 to 30 cm in diameter, which are placed facing one another at a spacing of 5 to 10 cm. One electrode contains the target. The substrates are placed on the other one. Planar diodes have played a major role in the

development of sputtering technology in the 1960's and 1970's. The substrates in a planar diode are in contact with the plasma. This makes it relatively easy to execute the processes of substrate sputter cleaning and bias sputtering. However, the heating associated with plasma and electron bombardment prevents the use of planar diodes for coating thermally sensitive substrates. In diode sputtering, electrons emitted from the cathode by ion bombardment are accelerated to near the full applied potential in the cathode dark space, and enter the negative glow as so-called primary electrons, where they collide with gas atoms and produce the ions required to sustain the discharge. At low pressures, ions are produced far from the cathode where their chances of being lost to the walls are great. Therefore, ionization efficiencies are low, and self-sustained discharges can not be maintained in planar diodes at pressures below about 10 mTorr (Refs. 12,13). At high pressures, the sputtered atom transport is reduced by collisional scattering (Ref. 10). In order for a glow to operate at lower pressure or in the same pressure but with an intense plasma, then, it is necessary to provide some source of electrons other than those emitted through secondary emission of ions.

Therefore, thermionically sputtered glow has been used (Refs. 14,15), so called Triode sputtering. In a Triode source, a heated filament is added to a diode source to provide electrons to sustain the glow discharge, independent of the target. In this manner, ionization efficiency is increased, and thus the discharge is able to operate at lower pressures (0.5 to 1 mTorr) and lower target voltage (Ref. 16). As a result, higher deposition rates can be achieved with triodes than with planar diodes. The main disadvantage of the Triode source is the system complexity, especially the shortened lifetime of the filament.

If, instead of increasing the number of electrons emitted at the cathode, the efficiency of the available electrons is increased, it will be possible to sputter at lower pressure, or, if

the pressure is not reduced, to obtain grater current for a given applied voltage. In this case the magnetic field is used to enhance the glow discharge via the electrons, the influence on the much heavier ions being negligible. The addition of a static magnetic field to the plasma, perpendicular to the plane of the electrodes, causes the electrons to move in a spiral path, effectively increasing the path length of the electron many times. The result is that collisions are now more likely, and the net density of ions and electrons in the plasma increases.

In 1858 Gassiot first passed a comment that placing a magnet close to the plasma caused some distortion of it (Ref. 17). If the magnetic field is oriented parallel to the cathode surface, the electric field ExB effects will be observed. This was the first thought about magnetron sources, when the magnetic fields are used in concert with cathode surface to form electron trap, which are so configured that the ExB electron-drift currents can close on themselves (Ref. 18). This method led to an almost unlimited variety of magnetron configurations. The first operation in the magnetron mode for sputtering appears to have been achieved by Penning and Moubis using configurations of cylindrical-post magnetron (Ref. 19) and cylindrical-hollow magnetron (Ref. 20). These two shapes of cylindrical magnetron are described in Reference 18. The most active development of cylindrical magnetron technology has occurred over the period 1969 to 1980 by Thornton (Refs. 18,21). Thornton gives not only the basic understanding of the magnetron characteristics (Refs. 22,23) but also the related effects in the deposited film by this technique compared with others (Refs. 24-26).

An alternative to the cylindrical magnetron is the conical geometry, often known generally as a "S-gun". In this case, the cathode has the form of an open, high-angle cone. the magnetic field lines from either a large, single permanent magnet or an electromagnet located behind the cathode, traverse the cathode surface almost parallel to it. The ExB

drift path is circular, and inclined at an angle parallel to the cathode surface. The sputter Gun and S-Gun were invented by Clark (Ref. 27). For more details the reader is directed to References 16 and 28.

The geometry of the ExB drift current is unimportant and hence dozens of geometric permutations have been invented using the same basic effect. An alternative to the S-Gun are the planar magnetrons. The magnets in this design are arranged so that there is at least one region in front of the cathode surface where the locus of magnetic field lines parallel to the cathode surface is a closed path (Ref. 29). One of the first descriptions of a planar magnetron device may have been that of Kesaev and Pashkova (Ref. 30) who used the magnetic field to constrain the motion of the cathode spot in a mercury arc lamp. The two well known shapes of the planar magnetron are the circular (Ref. 31) and the rectangular planar magnetron (Ref. 32). These are described in Reference 29. Generally, the electron confinement in a magnetron tunnel significantly increases the efficiency and as a result, a magnetron can operate at low pressure (1-3 mTorr) and low voltage (300-500 V). The current density at the cathode of a magnetron is a maximum where the magnetic field lines are tangential to the surface of the cathode (Ref. 33). Therefore, the erosion of the target is nonuniform.

The dc magnetron discharge is characterised by a superlinear dependence of the current on the cathode voltage. This behaviour is understood in terms of gas heating and rarefaction resulting from collisions with sputtered atoms (Refs. 34,35). An investigation with particular reference to magnetron characteristics has recently been made by Rossnagel et al (Refs. 36-40). The magnetic field does not directly affect the ion motion, however, because of electrostatic attraction the ions move with the electrons, keeping the plasma neutral. In a conventional magnetron, most of the discharge is confined close to the cathode surface, and therefore bombardment of the growing film by electrons and

ions in minimised.

It is well known that ion bombardment of growing films can strongly influence their microstructure and consequently, their physical properties (Refs. 39-41). The available technology for ion assisted deposition (Refs. 42-44) particularly where separate sources are used for the deposition flux and the ion flux, is difficult to implement in many production situations. There is an ability to provide a controllable ion flux from a planar magnetron while retaining the many other desirable features of , simplicity, high deposition rate, geometric versatility and tolerance of reactive gases. This assists in the implementation of ion beam assisted deposition in both research and production.

As early as 1986 (Refs. 45-47), Window and Savvides developed a new type of planar deposition source, which gives the normal deposition behaviour of a planar magnetron, plus a beam of ions whose intensity at the substrate can be varied independently of the deposition flux by changing the magnetic field configuration. This is called an "Unbalanced" magnetron. It was anticipated that enhanced bombardment would lead to improved film properties and film densification at low deposition temperatures. Recent work by Howson et al (Refs. 48-52), Musil et al (Refs. 53-56) and others (Refs. 57,58) has indeed shown that the unbalanced magnetrons can be used to stimulate increased ion densities in the region surrounding the substrate. The design of unbalanced magnetrons can take a variety of geometries depending on the ion flux density that is required and the uniformity of the beam at the substrate. This can be seen in the review by W. Munz (Ref. 61).

The coating sources and systems described in references 45 to 60 are mostly laboratorial and single magnetron systems. One of the first industrial systems was described by Teer (Refs. 62,63). This technology considered in multi-cathode system. A greatly extended

and more flexible design is current under development at Hauzer Techno Coating Europe B.V. (Ref. 61). Recently Rohde et al (Refs. 64-66) have developed a so called dual-cathode system. In this design face to face unbalanced magnetron was used. Generally, multi-magnetron systems are capable of coating pieces as large as 15 cm in diameter and approximately 40 cm in length, or a number of smaller parts.

The improvement of optical and electrical properties of deposited films is seen readily using the unbalanced magnetron (Refs. 52,54,59,60), and efficient uses in industrial products and hard coatings of TiN and TiC (Refs. 60,66,67). With high ion current performance and floating potential from an unbalanced magnetron, polymer etching and diamond-like carbon deposition was achieved (Ref. 51). The unbalanced magnetron offers the possibility of creating plasma conditions similar to those which are normally attainable only in typical "ion plating" processes. This makes it possible introduce the uncontested advantages of cathode sputtering, namely its exact controllability and its ability to deposit alloys without problems into hard material coating. This promising coating instrument should also be made accessible to other fields of application, in particular wherever dense ceramic coatings, i.e. high-melting materials, are to be deposited onto heat-sensitive substrates. Examples are oxide coatings used to coat architectural glass or in the modern packaging industry, currently deposited primarily using the balanced magnetron.

It has recently been demonstrated that the injection of electrons into the race track of a magnetron independently of these supplied by the sputtering process at the cathode, can result in a much lower operating potential for the magnetron and allows it to operate at lower pressure (Refs. 68,69). It seems that this is a very important development, in that it reduces the energy with which high energy neutrals will bombard the growing film (causing radiation-type damage) and will allow for more efficient operation of the

magnetron. Accordingly we have created an unbalanced magnetron (Ref. 70) which can operate at very low voltages and pressures, and have evaluated its use in reactive sputtering.

In the work reported by ULvac group (Ref. 71), significant improvements in the properties of indium-tin oxide films could be obtained if oxide targets were sputtered at low voltages. TiN coating onto glass substrates at room temperature using a low voltage unbalanced magnetron also show significant results where the film resistivity drops by half (Ref. 72). The use of thermionic electrons injected from a high temperature filament not only reduces the magnetron potential but also enhances the unbalanced magnetron performance (ion current and floating potential). These advantages have been taken into account and with small adjustment of the filament position followed by a series of investigations, a plasma source providing high current, low voltage ions was achieved (Ref. 73). The use of this source for low voltage sputtering is also investigated. Directing this source to either a biased plate target or other unbalanced magnetron, low voltage sputtering of highly sensitive material can be achieved. ITO film deposition by using this technique is still on going.

1.1 References

1- W. R. Grove, Phil. Trans. Roy. Soc., 142 (1852) 142.

2- C. A. Bishop, " The deposition of coating onto polymer substrates by planar magnetron sputtering", Ph.D thesis, LUT, 1986.

3- W. D. Westwood, "Progress in surface science", V. 17, P. 71, Pergamon press, 1978.

4- G. S. Anderson, W. N. Mayer and G. K. Wehner, J. Appl. Phys., 10 (1962) 2991.

5- G. K. Wehner and G. S. Anderson, " Handbook of thin film technology", (eds., L. I. Maissel and R. Glang), Mcgraw-Hill, New York, 1970.

6- L. I. Maissel and R. Glang, " Handbook of thin film technology", Mcgraw-Hill book company, 1970.

7- B. Behrisch, "Sputtering by particle bombardment", Topics Appl. Phys., 47, Spriger verlag, New york, 1981.

8- B. Chapman. "Glow discharge processes", a Wiley-Interscience publication, New York, 1980.

9- P. C. Zalm, "Hanbook of ion beam processing technology", (eds., J. J. Cuomo and S. M. Rossnagel), Noyes publication, New Jersey, 1989.

10- R. F. Bunshah, "Deposition technologies for film and coatings", Noyes publication, 1982.

11- R. V. Stuart, "Vacuum technology, thin films, and sputtering", academic press, 1983.

12- E. Kay, Tech. Met. Res., 1, part 3 (1968) 1269.

13- J. L. Vossen and W. Kern, " Thin film processes 1", Academic press, New York, 1978.

14- E. C. Muly and A. J. Aronson, J. Vac. Sci. Technol., 6 (1969) 128.

15- T. C. Tinsone and J. B. Bindell, J. Vac. Sci. Technol., 11 (1974) 519.

16- J. L. Vossen and W. Kern, " Thin film processes 2", Academic press, New York, 1991.

17- J. P. Gassiot, Phil. Trans. Roy. Soc. London, 148 (1858) 1

Proc. Roy. Soc., 9 (1858) 146.

18- J. A. Thornton, J. Vac. Sci. Technol., 15 (1978) 171.

19- F. M. Penning and J. H. A. Moubis, Proc., K. Ned. Akad. Wet., 43 (1940) 41.

20- F. M. Penning, Physica (Utrecht), 3 (1936) 873.

21- J. A. Thornton and A. S. Penfold,"Thin film processes", (eds., J. L. Vossen and W. Kern), Academic press, New York, 1978.

22- J. A. Thornton, Thin Solid Films, 80 (1981) 80.

23- J. A. Thornton, Thin Solid Films, 54 (1978) 23.

24- J. A. Thornton and W. W. Anderson, J. Vac. Sci. Technol., 18 (1981) 199.

25- J. A. Thornton and D. W. Hoffman, J. Vac. Sci. Technol., 18 (1981) 203.

26- J. A. Thornton and D. W. Hoffman, J. Vac. Sci. Technol., A 3, (1985) 576.

27- P. J. Clarke, U. S. Patent, 3, 616 (1971) 450.

28- D. B. Fraser, "Thin film processes", (eds., J. L. Vossen and W. Kern), Academic press, 1978.

29- R. K. Waits, "Thin film processes", (eds., J. L. Vossen and W. Kern), Academic press, 1978.

30- I. G. Kesaev and V. V. Pashkova, Sov. Phys. Tech. Phys., 4 (1959) 254.

31- S. Schiller, U. Heisig and K. Goedicke, "Thin Solid Films", 40 (1977) 327.

32- T. V. Vorous, Solid State Technology, 19 (12), (1976) 62.

33- A. E. Wendt, M. A. Lieberman and H. Meuth, J. Vac. Sci. Technol., A 6, 3 (1988) 1827.

34- S. M. Rossnagel, J. Vac. Sci. Technol., A 6, (1988) 19.

35- S. M. Rossnagel, J. Vac. Sci. Technol., A 6, (1988) 1821.

36- S. M. Rossnagel and H. R. Kaufman, J. Vac. Sci. Technol., A 4 (1986) 1822.

37- S. M. Rossnagel and H. R. Kaufman, J. Vac. Sci. Technol., A 5 (1987) 2276.

38- S. M. Rossnagel and H. R. Kaufman, J. Vac. Sci. Technol., A 5 (1987) 88.

39- S. M. Rossnagel, J. Vac. Sci. Technol., A 7 (1989) 1025.

40- S. M. Rossnagel and J. J. Cuomo, Vacuum, 38 (1988) 73.

41- O. Auciello and R. Kelly, "Ion modification of surfaces", Elsevier, Amsterdam, 1984.

42- H. R. Kaufman, J. J. Cuomo and J. M. E. Harper, J. Vac. Sci. Technol., 21, (1982) 725.

43- J. E. Sundgren and H. T. G. Hentzell, J. Vac. Sci. Technol., A 4 (1986) 2259.

44- Y. H. Kim, Y. S. Chaug, N. J. Chou and J. Kim, J. Vac. Sci. Technol., A 5 (1987) 2690.

45- B. Window and N . Savvides, J. Vac. Sci. Technol., A 4 (2), (1986) 196.

46- B. Window and N. Savvides, J. Vac. Sci. Technol., a 4 (3), (1986) 453.

47- N. Savvides and B. Window, J. Vac. Sci. Technol., A 4 (3), (1986) 857.

48- A. G. Spencer, K. Oka and R. P. Howson, Vacuum, 38 (1988) 8.

49- R. P. Howson, A. G. Spencer, K. Oka, and R. W. Lewin, J. Vac. Sci. Technol., A 7 (3), (1989) 1230.

50- R. P. Howson, H. A. Ja'fer, A. G. Spencer, Thin Solid Films, 193/194 (1990) 127.

51- H. A. Ja'fer, R. P. Howson, A. G. Spencer and M. Stenlake, IPAT, Brussele, 1991.

52- R. P. Howson, H. A. Ja'fer, J. Vac. Sci. Technol.,A, Vol . 10 (1992) 1784-1790.

53- J. Musil and S. Kadlec, Vacuum, 40 (1990) 435.

54- S. Kadlec, J. Musil, W. D. Munz, G. Hakanson and J. E. Sundgren, Surf. Coat. Technol., 39 (1989) 487.

55- S. Kadlec, J. Musil, V. Valvoda, W. D. Munz, H. Petersein and J. Schroeder, Vacuum, 41 (1990) 2233.

56- S. Kadlec, J. Musil and W. D. Munz, J. Vac. Sci. Technol., A 8 (3), (1990) 1318.

57- N. Savvides and B. Window, J. Vac. Sci. Technol., A 4 (3), (1986) 504.

58- B. Window and G. L. Harding, J. Vac. Sci. Technol., A 8 (3), (1990) 1277.

59- K. Oka, R. P. Howson, R. W. Lewin and A. G. Spencer, Proc. Soc. Photo-Opto. Instrum. Eng., 1019 (1988) 40.

60- J. Musil, S. Kadlec, J. Vyskocil and V. Poulek, Surf. Coat. Tech., 39/40 (1989) 301.

61- W. D. Munz, Surf. Coat. Tech., 48 (1991) 81.

62- D. G. Teer, Surf. Coat. Tech., 35 (1988) 901.

63- D. G. Teer, Surf. Coat. Tech., 39/40 (1989) 565.

64- S. L. Rohde, W. Sproul, J. R. Rohde, J. Vac. Sci. Technol., A 9 (3), (1991) 1178.

65- S. L. Rohde, I. Petrov, W. D. Sproul, S. A. Barnett and M. E. Graham, Thin Solid Films, 193/194 (1990) 117.

66- S. L. Rohde, L. Hultman, M. S. Wong and W. D. Sproul, Surf. Coat. Tech., 50 (1992) 255.

67- D.G. Teer, IPAT, BrusselS, 1991.

68- J. J. Cuomo and S. M. Rossnagel, J. Vac. Sci. Technol., A 4, (1986) 393.

69- B. K. Steenbeck, E. Steinbeiss, G. Schmidt and G. Bruchlos, Vacuum, 42 (1991) 39.

70- R. P. Howson, H. A. Ja'fer, to be published in Vacuum, 1993.

71- S. Ishibashi, Y. Higuchi, N. Nakamura, Y. Ota and K. Nakamura, Proc. 1st. Int'l Sympo. on ISSP, Tokyo, 1991.

72- R. A. Swady, H. A. Ja'fer and R. P. Howson, to be published in Vacuum, 1993.

73- H. A. Ja'fer and R. P. Howson, to be published in Vacuum, 1993.

CHAPTER-2

THEORY AND BACKGROUND

2.1 Glow Discharge Initiation

The most widely used method in laboratory and in technology for obtaining a plasma is the electrical gas discharge. In nature an example of this phenomenon is seen in lightning, in technology, typical examples are electric spark, electric arcs, sputter sources for thin film deposition and etching, and other gas discharge devices. Ionization in a discharge depends on the production of an electron avalanche. This process is of the same type as a chain reaction in chemistry or multiplication of microbes in an epidemic. This process can be clearly explained by considering an evacuated glass tube with two internal metal plates separated by a distance d Fig. 1 (Ref. 1) and biased by an external dc power supply. If a low pressure inert gas is introduced into the chamber, a charged particle (electron) may be liberated near the negatively biased electrode (the cathode). The cause of this electron could be the passage of a cosmic ray through the apparatus, the decay of a radionuclide in the metal, photo-electron field emission by the sun or by the fluorescent lights, field emission from the metal plate, or a host of other processes (Ref. 1). Because of the applied electric field, the electron will start to accelerate toward the anode.

Gas pressure and the applied electric field are related parameters, and together produce an electron avalanche. If the gas pressure is low enough, an electron will not suffer any collisions as it proceeds to the anode where it will be collected. Hence, there will be no free charge left in the apparatus. If the pressure is high enough, however, the electron will collide with neutral atoms along its path. When the applied electric field is low, the electron will not gain sufficient energy to ionise the atoms. It will simply drift at a speed determined by its mobility. These can be attached to the neutral gas by electrostatic

Fig.2.1 Discharge apparatus.

Fig.2.2 Discharge generated by a D.C. power supply (Ref. 3).

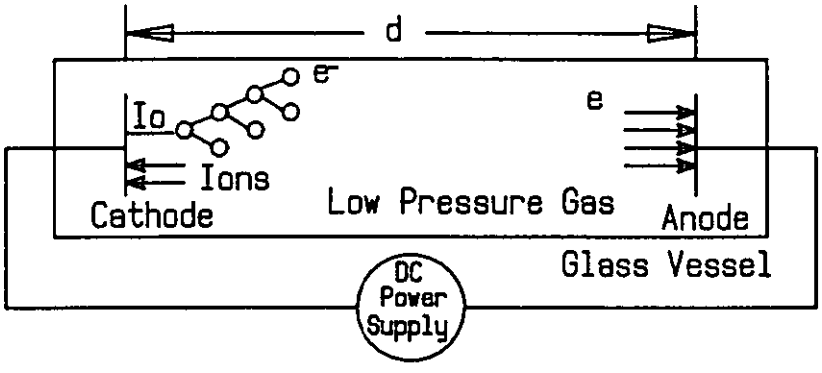

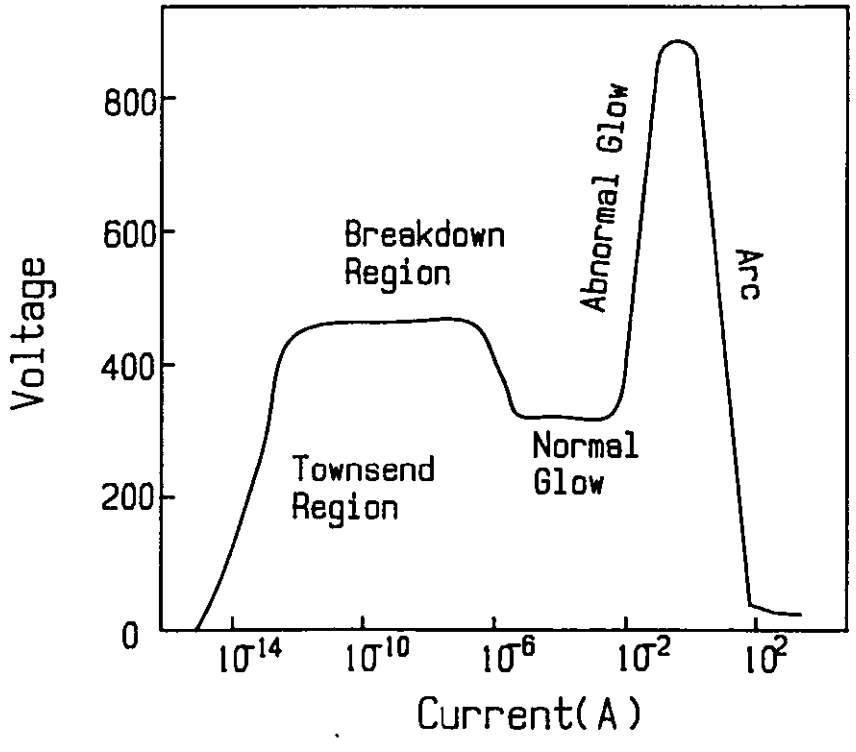

means, when the gas atom is sufficiently electronegative. These negative ion, however, have substantially smaller mobility .

It is necessary, then, that the applied electric field be large enough. Hence the energy imparted to electron in their mean free paths is sufficient to knock out at least one electron from an atom on impact. In this time, the ions will drift to the cathode and the electrons to the anode. As a result of ions impact to the cathode and the electrons to the anode the secondary electrons will be emitted. But only those released from the cathode are useful. The secondary electrons that ejected from the anode will simply return to it . The current of electrons toward the anode has been calculated by Townsend, this was of the form; (Ref. 2)

$$I = I_0 \frac{\exp(\alpha d)}{1 - \beta(\exp(\alpha d) - 1)}$$

where:

I_0= The current of electrons from the cathode due to the external source (e.g. photo-emission)

β= The ion impact secondary electron emission coefficient.

α= The first Townsend coefficient; the number of ionizations per unit distance.

From this equation two cases can be seen; i) for small value of α, β and d, the denominator is unity, so the only current that flows is that released from the cathode by the photons, but amplified slightly by small value of $\exp(\alpha d)$, ii) for moderate or large values of α, β, and d, such that the denominator equals zero or is negative, the current

grows faster than exponentially, and breakdown occurs. At the same point the equation fails, because it does not take into account the decrease of neutral atoms in the system because of ionization or the change of potential in the system, and so forth (Ref. 1). The current that flows in such an apparatus is shown versus voltage in Fig. 2. At low voltages, the current grows with the voltage until the ionization probability, related to α, approaches a value large enough to breakdown the gas. Then the Townsend region occurs, and the voltage is constant as the current rapidly rises.

When the gas is highly ionised, i.e. it is a plasma, the electric field between the two plates (electrodes) has been drastically altered. A sheath exists at the cathodes still promoting the acceleration of ions to the cathode and of secondary electrons into the plasma. The glow does not cover all the cathode. An effort to increase the voltage increases the glowing area and the current. This is termed the normal glow. Note that the voltage required to maintain the normal glow is less than that required to achieve breakdown.

Finally, when the entire cathode is covered with a glow, the I-V characteristic changes, The current does increase with the voltage (see Fig. 2), and the abnormal glow has been obtained. This type of glow discharge has been found to be the dominant discharge in diode sputtering equipment.

In the glow discharge the dominant criteria is the cathode sheath. As will be shown later this sheath has a several distinct regions. Attached to the cathode is cathode fall region. There, the ions extracted from the plasma by the cathode fall are limited in current by electrostatic repulsion because the electron density there is less than the ion density.

The law describing this was derived by Langmuir and Child (Ref. 3,4) for plane parallel geometry and is:

$$J_s\ (A/cm^2) = \frac{5.5 \times 10^{-6}\ V_s^{3/2}}{M^{1/2}\ d_s^2}$$

where:

V_S = Voltage drop in fall region in volts

d_S = Sheath thickness in cm. and

M = Atomic mass of working gas in amu

From this equation the thickness of the fall region;the so called dark space, has been estimated to be ≈ 0.5 mm for magnetron sputtering, which is less than ordinary diode sputtering.

2.2 Plasma Discharge

In principle, a plasma is an ionised gas, that is a gas in which at least a proportion of the atoms or molecules is broken down into charge carriers. Its dimension should be less than Debye length. Freely moving electrons can transport electric current ; in other words, a plasma is a conducting gas . In plasma the particles can be forced to move in regular fashion by using the magnetic field.

2.2.1 Plasma Measurements

To specify the plasma behaviour there are some important parameters like ion and electron density, ion and electron temperature and Debye length need to be known. In plasma diagnostics a reasonable method to characterise the plasma parameters can be achieved (Ref. 5).

In our investigation an electrostatic or Langmuir probe (Ref. 6) has been used. A metal probe is inserted into the plasma and the current to the probe measured as a function of

the probe potential (I-V characteristic). An important property of plasmas emerges clearly in the probe method (i.e. plasmas do not obey Ohm's law). The electron current is determined simply by the magnitude of the charge which transported by the positive potential. This current is found to approach a limiting value which is independent of potential. This current limit is called the (saturation current) and is determined by the charge which is transported by the electrons that strike the surface of the probe in their thermal motion . If the thermal speed of the electron is known the plasma density can be found from the saturation current. The thermal velocity is calculated from the electron temperature, which is found by inspecting the slope of the voltage-current characteristic.

In an unperturbed plasma (Ref. 5) elementary gas kinetic theory shows that the number of particles of a given species crossing unit area per unit time (from one side) is:

$$\Gamma = \frac{1}{4} n v$$

If the plasma were unperturbed these would be eliminated by electrons

$$I_e = \frac{1}{4} eAN_e v \qquad 2.1$$

where:

e = Charge of the electron

N_e= Electron density

v = Average velocity of the electron

A = Probe area

Electron velocity is related to the electron temperature T_e by the expression:

$$v = \left(\frac{8KT_e}{\pi M_e}\right)^{1/2} \qquad 2.2$$

where:

M_e= Electron mass

K = Boltzmann constant

The electron temperature can be determined with respect to the I-V characteristic of the probe on region in which the probe has a negative potential relative to the plasma potential(retarding region). In this region the probe repels the electrons and the surface of the probe can only be reached by these electrons in the Boltzmann distribution which have energy sufficient to over come the potential difference ($V - V_p$) where V is a probe potential and V_p is a plasma potential.

Hence,

$$I = I_\infty \exp\left(\frac{-eV}{KT_e}\right) \qquad 2.3$$

By plotting the current I as a function of the probe potential V on logarithmic scale, the slope in the retarding region this will allows us to determine the temperature T_e. By using equation 2.1 the plasma density can be estimated.

2.2.2 Debye Length

Any charge imbalance in an ionised plasma, sets up electric fields that tend to limit its extent and neutralise it Fig. 1 (Ref. 7). It has been shown (Ref. 8) that the sheath thickness is always related to a plasma parameter known as the Debye shielding distance (Debye length), which depends on the temperature and densities of the various species of charged particles present.

If the resultant potential at any radius r is V(r), the concentrations of positive ions,N_i and electrons, N_e, in this field can be predicted from the position distribution form of the

Fig.2.3 Appearance of Debye shielding distance in an ionized plasma (Ref.7).

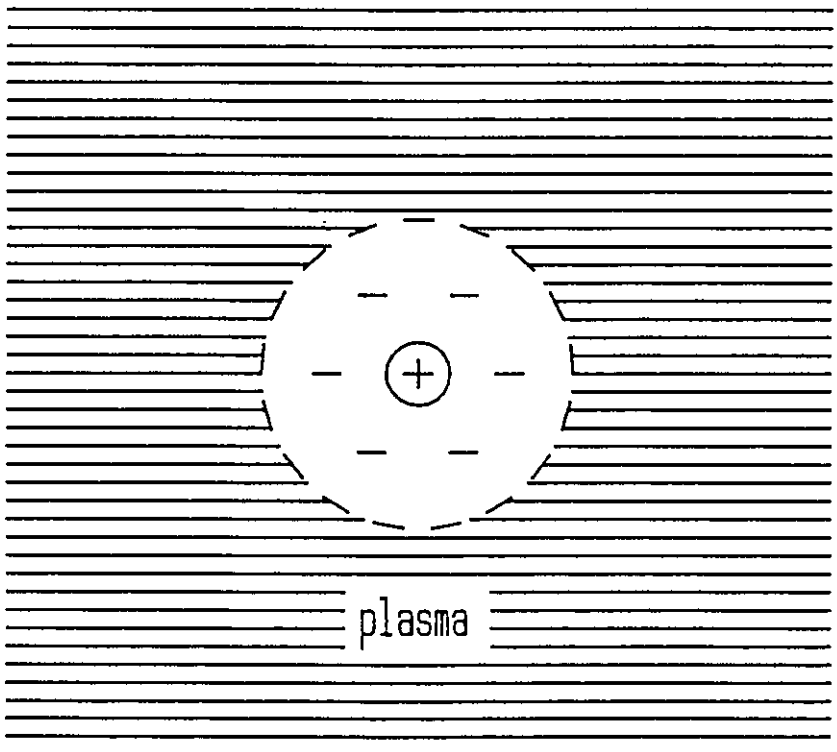

Boltzmann law.

Hence,

$$N_e = N_\infty \exp(\frac{eV}{KT}) \qquad 2.4$$

$$N_i = N_\infty \exp(\frac{-eV}{KT}) \qquad 2.5$$

N_∞ is the electron density far from the perturbing charge where the potential V is taken as zero, and T is the temperature, assumed to be the same for both. If we suppose that eV << KT nearly everywhere, from Taylor series the exp(eV/KT) can be Approximated by (1+eV/KT) and exp(-eV/KT) by (1-eV/KT).

Then we can write

$$N_e \approx N_\infty (1+\frac{eV}{KT}) \qquad 2.6$$

$$N_i \approx N_\infty (1-\frac{eV}{KT}) \qquad 2.7$$

From Poisson's equation,for spherical symmetry,

$$\frac{1}{r}(\frac{\partial^2}{\partial r^2}) = \frac{\rho}{\varepsilon_0} = \frac{e(N_i - N_e)}{\varepsilon_0} = \frac{2N_\infty e^2 V}{\varepsilon_0 KT}$$

ρ is the real charge density in the microscopic space and ε_0 is the permittivity of free space. The solution of this equation (Ref. 4) is:

$$V = -\frac{e}{4\pi\varepsilon_0 r}\exp(\frac{-r}{\lambda_D})$$

where:

$$\lambda_D = \left(\frac{2KT\varepsilon_0}{N_\infty e^2}\right)^{1/2} \qquad 2.8$$

Because the ion-electron mass ratio M_i/M_e is large, it is assumed that the positive ion concentration is unperturbed, so that the ions do not move but form a uniform background of positive charge, and only the electron varies according to Boltzmann's law in this case the factor 2 is omitted from equation 2.8, and T is always the electron temperature. The final expression to equation 2.8 is:

$$\lambda_D = \left(\frac{KT_e}{N_\infty e^2}\right)^{1/2} \qquad 2.9$$

From equation 2.8 we can say ,roughly, that the plasma screens the charge of an individual particle for distances greater than lambda. The ratio of probe dimension to Debye length is therefore very important when a probe method is to be used for plasma investigation.

2.2.3 Ion Current

The most important criterion in probe characteristic is the sheath formation around the probe, which has been demonstrated by Bohm (1949) (Refs. 4,9). The effect of this region is to increase the velocity of ions entering the probe sheath.

Fig. 4 (Ref. 10) shows the potential variation near a negative electrode. In the sheath region, it is difficult to relate the ion current density to $N_{i\infty}$ of ions in the bulk plasma, because there is a quasi-neutral presheath region where a potential drop V_p of the order of half of the electron temperature occurs, that is:

$$V(0) = \frac{1}{2}\left(\frac{KT_e}{e}\right)$$

To determine the ion presheath density can be assumed to obey a Boltzmann

Fig.2.4 The positive space charge sheath (Ref.10).

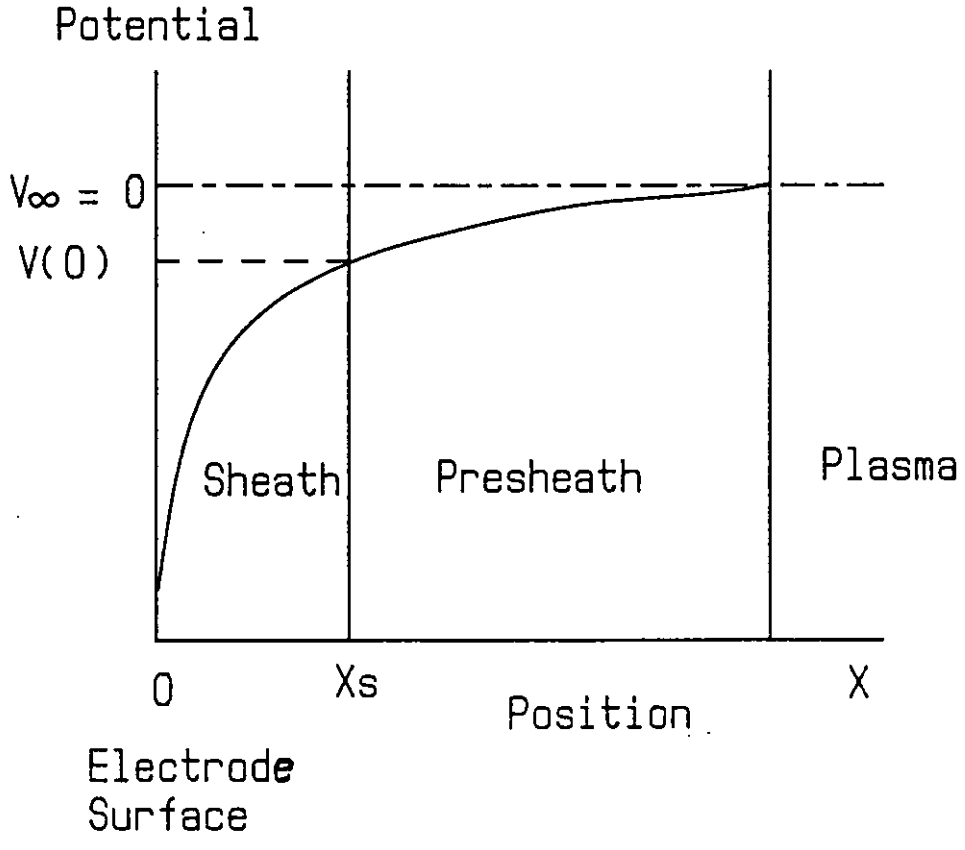

distribution. Hence,

$$N_i(0) = N_{i\infty}\exp(\frac{-e\,V_p}{KT_e})$$

Therefore

$$\frac{N_i(0)}{N_{i\infty}} = 0.6$$

The ion Speed In terms of temperature is:

$$V_i = (\frac{KT_e}{M_i})^{1/2}$$

The ion current, which flows due to the electric field is:

$$I_i(0) = eN_i(0)\,V_i\,S_s$$

where S_s is the surface area of ion sheath, for simplicity we assume that $S_s = A_s$. Where A_s Is the probe area. The ion current that flows to the probe is then:

$$I_i(0) = 0.6\,N_{i\infty}(\frac{KT_e}{M_i})^{1/2}A_s \qquad 2.10$$

2.2.4 Floating Potential

The true potential on the substrate in glow discharge sputtering has been studied extensively (Refs. 3,11-13). From I-V plasma characteristics, the floating potential can be defined as the point where the amount of electrons and ions to arrive at a probe must be the same in order to obtain the zero current of a probe. This potential usually arises because of the higher mobility of electrons as opposed to ions. So that, electrons arrive at the isolated substrate surface much faster than ions. Residual electrons which cannot recombine on the surface form a negative electric field there. This negative electric field reduces the speed of electrons. It increases until the ion and electron currents become the

same. This mechanism is called ambipolar diffusion, and the floating potential is the negative potential formed by it. As a result the sheath around the substrate (dark space) will be formed. The electrons which enter this sheath and reaching the substrate, should have an energy equal to $e(V_p-V_f)$. From Maxwell-Boltzmann distribution function

$$I_e(V_f) = I_e \exp(\frac{-eV_f}{KT_e}) \qquad 2.11$$

From Equations 2. 1 and 2.11

$$I_e(V_f) = \frac{1}{4} eN_e(\frac{8KT_e}{\pi M_e})^{1/2} A_s \exp(\frac{-eV_f}{KT_e})$$

At V_f Point,the criterion for net zero current becomes

$$I_e(V_f) = I_i(0)$$

exp

$$\frac{1}{4} eN_{e\infty}(\frac{8KT_e}{\pi M_e})^{1/2} A_s (\frac{-eV_f}{KT_e}) = 0.6\, e\, N_{i\infty}(\frac{KT_e}{M_i})^{1/2} A_s$$

$$\exp(\frac{-eV_f}{KT_e}) = 2.4\,(\frac{KT_e}{M_i})^{1/2}(\frac{\pi M_e}{8KT_e})^{1/2}$$

$$V_f = \frac{KT_e}{e} \mathrm{Ln}(\frac{M_e}{2.26M_i})^{1/2} \qquad 2.12$$

Equation 2.12 tells us that the floating potential is related to the electron temperature T_e and the masses of the electron M_e and M_i involved in the discharge .

2.2.5 Magnetic Effect

The motion of the particles in an ordinary gas is limited only by the collisions which they undergo with each other or with walls. The motion of plasma particles, however, can be constrained by a magnetic field. Plasmas can be confined in a magnetic trap. Plasma particles are constrained to circle around the lines of force of the magnetic field although they can move freely along the magnetic field. The combination of free motion along the field lines and gyration around the lines results in a helical motion. The particle motion across the magnetic field is thus greatly restricted although the motion along the field is essentially as before. therefore, the electric probe is unsuitable for absolute measurements in a magnetic field. The ratio of gyration radius (r) to the typical dimension A of the probe, plays a significant role for controlling the magnetic field effects. If $r >> A$, then, the previous treatment should apply. For probes which capture electrons this cannot be done because the electron Larmor radius is too small. The ion radius is thousands of times larger (for comparable T_e and T_i) by the factor $\sqrt{(M_e/M_i)}$ (Ref. 5). Therefore absolute measurements can be made with an electric probe in a magnetic field if the ion current is used rather than electron current,and the probe significantly negative. So that most of electrons are reflected, then the electron density will be governed as before by the thermal Boltzmann distribution.

The ions, being relatively unaffected (for $r >> A$) by the magnetic field satisfy the same equations as before. So the ion current, which depends only on Ne and ion dynamics, is just as before. The electron current will also maintain its exponential dependence on the Bohm potential V(0). So that analysis of the current slope will again provide T_e. As will be shown later, the first thing that happens to the probe characteristic when a magnetic field is present is that the electron saturation current is decreased since the electron flow is impeded. This was the evident as a reduction in the ratio of electron to ion saturation

current as the magnetic field behind the probe increases.

2.3 Sputtering Phenomena

Sputtering of target atoms from a solid surface under ion bombardment has long been studied for both the physical understanding of the collisional processes involved, and for various practical reasons as well, for example sputter surface cleaning or sputter thin film deposition in large scale technical application, or as a research tool for high resolution depth profiling SIMS (Ref. 14,15), or in plasma wall interaction problems (erosion of first wall materials and plasma contamination in fusion devices (Ref. 16)). A detailed compilation of sputtering yields of different beam and target species is given by Andersen and Bay (Ref. 17 chapter 4) and Behrisch (Ref. 18). Sigmund and Robinson (Ref. 17 chapter 2 and 3), Jackson (Ref. 19) and Harrison (Ref. 20) gives a numerous explanations and theoretical concepts in predicting the sputtering yield.

Knockon sputtering by ion bombardment has been classified to three different situations as shown in Fig 5; (A) the single knockon regime, (B) the linear cascade regime, and (C) the spike regime. In the single knockon regime, the bombarding ion transfers energy to target atoms which, possibly after having undergone a small number of further collisions, are ejected through the surface if energetic enough to overcome binding forces. The linear cascade is different from the spike regime by the spatial density of moving atoms which is small in the former and large in the latter. The closest regime to the magnetron sputtering are the linear cascade collisions (Refs. 17,21). In this region ,the processes that are possible are shown in Fig. 5B. These are :- The emission of neutral particles by knowing the target sputter yield this can be estimated. As a result of high energetic ion bombardment of the target surface, secondary electron emission will take place. These electrons are very important in the sputtering technique, which is not only sustain the discharge but control the plasma chemistry by excitation, dissociation and ionization of

Fig.2.5 Processes possible for a cathode subjected to ion bombardment.

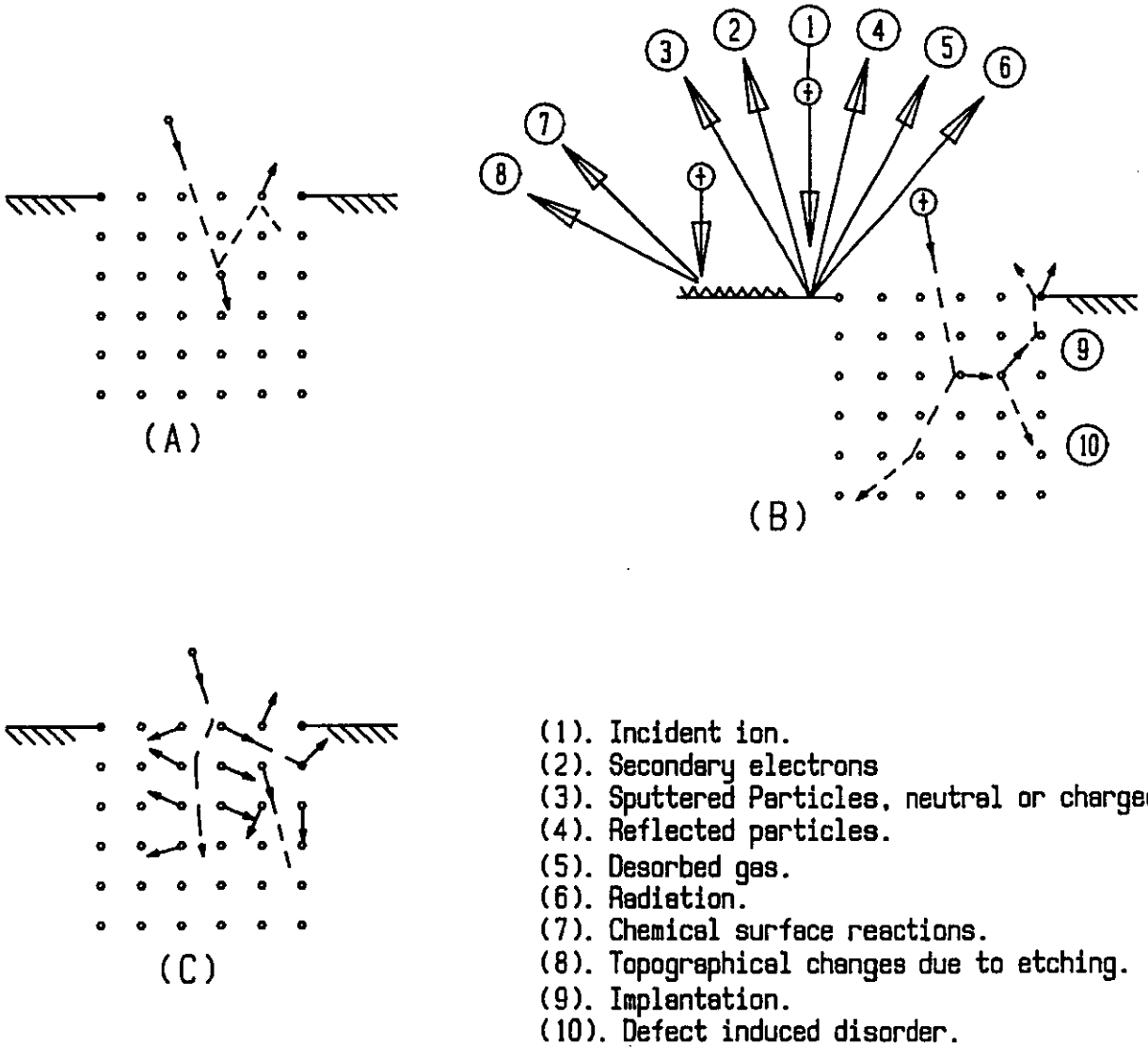

(1). Incident ion.
(2). Secondary electrons
(3). Sputtered Particles, neutral or charged.
(4). Reflected particles.
(5). Desorbed gas.
(6). Radiation.
(7). Chemical surface reactions.
(8). Topographical changes due to etching.
(9). Implantation.
(10). Defect induced disorder.

the working atmosphere (Ref. 4). Positive and negative secondary ions are created. The positive ions are a very small fraction of the sputter flux. Nevertheless, these ions can not escape through the dark space but draws back to the target surface as a consequence of the high negative target potential. In contrast to that, the negative ions will be accelerated. As will be seen in chapter 6, the ions are very important in controlling thin film properties. Unfortunately though, the fraction of these ions in sputtering equipment is not much as in arc evaporation.

The sputtering rate is measured by the sputtering yield Y, which defined as the mean number of atoms removed from the surface of a solid per incident particle. The sputtering yields depend on ion energy, mass and angle of incidence, the mass of the target atoms, the crystallinity and the crystal orientation of the target, but they are usually nearly independent of the temperature (Ref. 22). Below a threshold energy which is about 20-40 ev for normally incident ions, almost no sputtering takes place. Above this threshold the yields increase with increasing incident energy and reach the maximum in the energy region of 5-50 KeV (Ref. 10). The decrease of the sputtering yield at higher energies is related to the larger penetration of the ions into the solid and the lower energy deposition in surface layer. At the same energy, Larger mass ions usually give larger sputtering yields than lighter ions (Ref. 17,18). A theoretical basis for yield calculation was laid by P.Sigmund (Ref. 23). Subsequently, many numerical models have appeared (Ref. 24), and they are reviewed by Zalm (Ref. 25). Nevertheless the development of theory given by Sigmund resulted in anomalies.

The simple formula for low energy sputtering has been given by Steinbruchel (Ref. 26), which followed directly from Sigmund's theory. From combining results from various papers,the sputtering yield is:

$$Y = \frac{5.2}{U} \frac{Z_t}{(Z_t^{2/3} + Z_p^{2/3})^{3/4}} \left(\frac{Z_p}{Z_t + Z_p}\right)^{0.67} E^{1/2}$$

where:

E= Ion energy (keV)

U= Target binding energy (eV)

Z_t & Z_p= Atomic number of target atoms and projectile ions

M_t & M_p= Atomic masses for target material and projectile ions

In (Ref. 26) the comparison of experimental (Ref. 27) and theoretical (Ref. 28) sputtering yield for single charge of Ar atom at 600 eV for different material has been illustrated. In the following section, the sputtering yield of magnetron targets for several materials has been calculated and compared with other references. The sputtering rate for a copper target with an ion incidence angle of 40° to the target surface and between 50 to 600 eV of ion energy has been investigated in chapter 9 .

2.4 The Magnetron

The purpose of using a magnetic field in a sputtering system is to make more efficient use of the electrons, and cause them to produce more ionization. In a conventional glow discharge electrons are soon lost by recombination at the walls. Magnetic effects can be initially discussed in terms of the motion of isolated electrons (Refs. 21,29,30). A moving charge in a magnetic field is subjected to a force:

$$F = B\,q\,V$$

where:

q = The charge on the particle

V = Particle velocity

B = The applied magnetic field

The direction of the force is perpendicular to both the magnetic field and the velocity. the force will produce an acceleration that is inversely proportional to the mass of the charge (Ref. 10). This force, then will cause the particle to move in an orbital path as shown in Fig. 6 (Ref. 2). The orbit can be calculated from this equation (Refs. 3,31):

$$r = \frac{mv_{\perp}}{qB}$$

where:

$v_{\perp}$ = The velocity perpendicular to the magnetic field and

m = The mass of the particle.

The particle motion along the field is unimpeded, so that if it has a component of velocity along the field line its net motion is a spiral along the field line, as shown in Fig. 6b.

Fig.2.6 The motion of the electron in a magnetic field only; a) viewed perpendicular to the page and b) the same motion viewed from the side (Ref.2).

Fig.2.7 The motion of an electron in combined electric and magnetic fields.

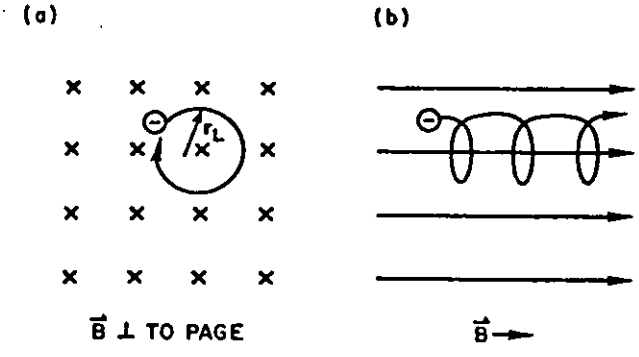

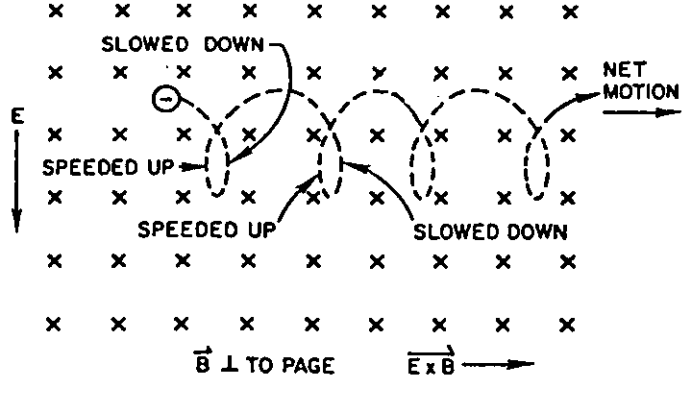

The charged particle will also undergo a drift motion across the magnetic field if an electric field E is present as shown in Fig. 7. When the electric field is applied, the electron experiences a constant force, in this case oriented towards the top of the page. This has the effect of slowing down the particle on the downward side of the orbit. Reducing the velocity is, in this case, equivalent to reducing the energy. The result is that the orbit becomes effectively smaller on the upward path of the orbit, the electron is accelerated and its effective radius increases. The result of this cyclical motion is an effective drift to the right, in the direction perpendicular to both the electric and magnetic fields. This is known as the ExB drift.

The actual path of the electron can be quite complex and has only recently been treated with monte carlo techniques (Ref. 32). For magnetron case, however, Rossnagel and Kaufman (Ref. 33) have measured the general ExB drift current. This was done by placing a small magnetic field probe on the axis of the magnetron, measuring the strength of the magnetic field induced by the circulating current, and calculating the current necessary to produce the field.

The electric field in front of the magnetron is greatly altered by the presence of the conducting plasma so that the bulk of the applied potential is dropped across a small region close to the cathode surface. This region corresponds to the cathode dark space in a glow discharge, but in a magnetron the dark space is small as shown in Fig. 8 (Ref. 34). Assuming that the magnetic field is uniform and parallel to the target surface and the E field across the dark space is normal to the target surface. Accelerating across the applied potential V the electron will gain a velocity v,

$$v = \left(\frac{2qV}{m}\right)^{0.5}$$

Fig.2.8 The approximate potential thicknesses of each region for the magnetron plasma (Ref.34).

Fig.2.9 An approximate to the electron path where B is parallel to the target (Ref. 29).

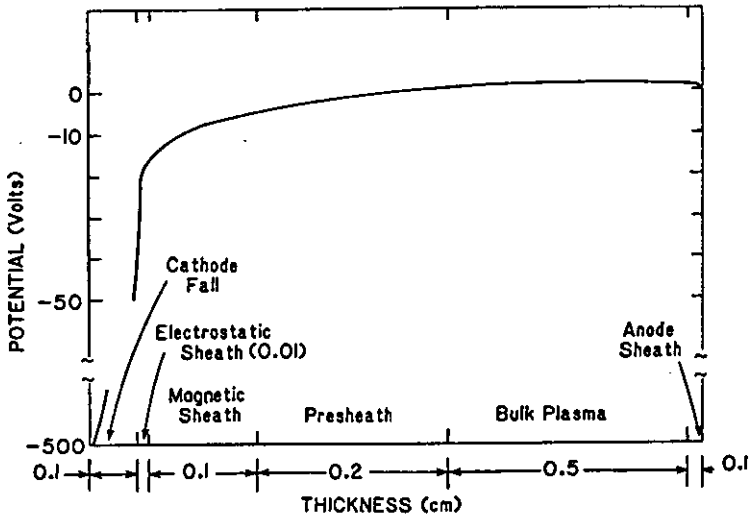

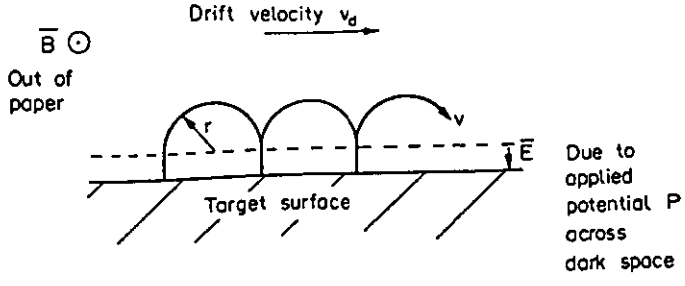

where:

q = Electron charge

m = Electron rest mass

The introduction of these electrons with the B field will produce a circular path of radius r, see Fig. 9. Using a typical magnetron operating parameter of V = 500 V and B = 500 gauss gives the electron path radius as r = 1.5 mm, i.e. larger than or comparable to the cathode dark space. So that the cathode fall region is too short to allow the drift approximation to be valid. Once in the magnetic sheath the drift approximation is valid even for these 500 eV electron. These drift velocities are about 3×10^7 cm/sec (Ref. 34) a small fraction of their total velocity (v/π) (Ref. 21). To prevent this large drift velocity removing an electron from the discharge, the drift path must form a loop. any loop will do and common shapes are circular or two parallel sides with semicircular ends, but some more tortuous paths have been used (Ref. 35).

The magnetic field is generally provided from a simple magnetic circuit behind the target and the field from this arrangement will be dome shape. Only at the centre of the target is the magnetic field parallel to the target and normal to the electron velocity. A way from the central region the field is at some angle (α) to the target (Fig. 10). As they accelerate across the dark space the electrons will therefore gain a component velocity $V_{av} = v \sin(\alpha)$ parallel to the B field. This velocity will carry the electron along the magnetic field line across the dome and down on the other side, where it may be mirrored by the converging B field. Because of the magnetic mirror effect and energy loss to the plasma (via instabilities, for example) it is highly unlikely that the hot electrons will ever again reach the cathode. However, quite a small value of alpha (about 20°) makes drift velocity v_d and V_{av} comparable and then the electron movement will not be along the drift direction but diagonally across the dome field (Refs. 36,37). Generally, these drifts take

Fig.2.10 The effect of an inclined B field on the electron motion

Fig.2.11 Motion of electron drifts in a magnetron (Ref.34).

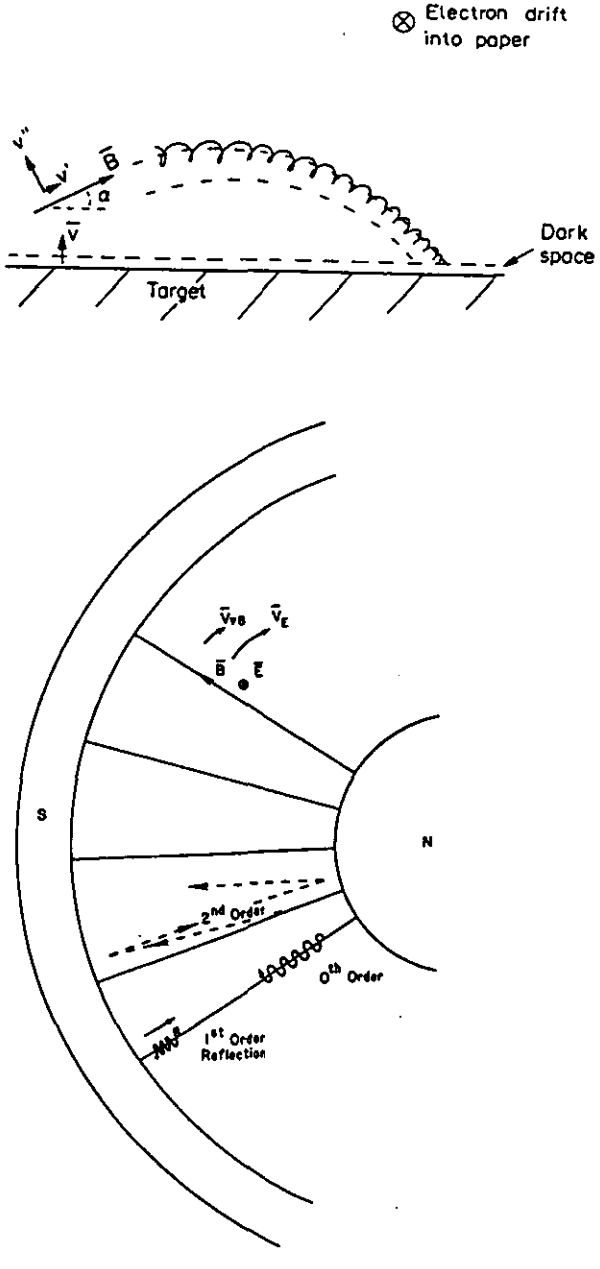

the electrons on orbits around the magnetron (Fig. 11). The net pattern of their motion is a zig-zag between the inner and outer poles. Figure 11 shows that at the zero order, only the cyclotron motion around B is included. The first order correction to the motion includes reflection as the electrons enter regions of increasing B. The second order description includes drift motion due to the crossed E and B fields and the grad B (see Ref. 34, page 198 and 255).

Electron created by ion impacts on the target where B is parallel to the target surface will have a small velocity across the dome. Electrons created at or reflected from a point on the target where the magnetic field is not parallel to it will move across the dome through the region where B is parallel to the target. So the highest electron density will be in this region. The creation rate of ions will be higher here and, if the ions do not move larger distance from their point of creation. The maximum sputtering of the target will be beneath this region.

2.4.1 Target Sputtering

To obtain the actual target sputter yield, one must know the ion flux (target current) and the target lost mass (atom flux) from the sputtering condition such as the target current and voltage, and the total operation time. The actual target sputter yield can be estimated by this equation:

$$y = 96352\frac{R}{J\,t\,W}$$

where:

R = Target lost mass (gm)

J = Target current (A)

t = Operating time (sec)

W = Target atomic weight (gm/mole)

Target lost mass (R) was measured within an error of ∓ 0.0005 g. Ion flux is estimated as a single argon atom charge (Ar^+) at normal incidence. The calculations have been done for several targets as shown in Table 1. This is compared with Ref. 38 . For comparison the interpolation of the sputter voltage need to be considered. As can be seen in this Table, the measured yield is almost 60-65% of the predicted reading. This discrepancy can be related to several reasons, (Ref. 39), such as:

1- The magnetron current is not carried across the dark space solely by ions.

2- The ion energy is less than the energy gained by the fall across the applied potential.

3- The target has some oxidation.

4- redeposition of backscattered material onto the target (present of virtual source) (Refs. 40,41).

5- There is argon included in the sputtered target.

All of these parameters are almost related to three main conditions; the target, vacuum and discharge conditions. For lower atomic weight material sputtered at high argon pressure (10 to 100 mTorr), more backscattering of material will take place. There was a considerable deposition from the backscattered material seen when targets like Al and Si were used. Such coatings are usually noted in the dead zone areas of the magnetron (outer and inner poles of the magnetron). The degree at which the back deposited material is eroded from the target surface depends greatly on the type of the deposit (metal, metal oxide, and/or metal nitride) and also on the location on the target surface onto which the backscattered material is deposited. Rizk et al (Ref. 40) and Nyaiesh (Ref. 41) assumed that the redeposit of the backscattered material is due to a presence of virtual sources located with height (h) from the magnetron. They found that the deposit diameter (formed in the dead zone area) to be dependent on the height of the virtual source, while the latter

Table 2.1 Target sputtering yields of various materials in argon compared with reference 38 (page 4-48).

Target Material	Sputtering Voltage V	Sputtering Yield	Sputtering Yield (Ref. 38)	
			200 V	600 V
Al	550	0.451	0.35	1.2
Ti	472	0.296	0.2	0.6
Pd	356	1.033	1.0	2.4
Ag	400	1.297	1.6	3.4
Pt	617	0.985	0.6	1.6
Au	520	1.574	1.1	2.8

was found to be affected by gas pressure and gas type. For height measurement this equation is used:

$$h = n\lambda\frac{\cos\alpha}{P}$$

where:

n = Number of collisions the sputtered atoms suffer with the sputtering gas (as a result they lose their initial energy and cool down to the gas temperature at the height, h).

λ = Sputtered atom mean free path (cm)

P = Discharge pressure (mTorr)

α = Angle of scattering of sputtered atoms by Ar gas atom, which is,

$$\alpha = \tan^{-1}\frac{M_s}{M_g}$$

where:

M_S and M_g = The mass of the sputtered atoms and gas atoms respectively.

The results that have been obtained from above calculation were h =5.6 and h=1.12 cm for argon pressures of 10 and 50 mTorr respectively. But the results shown in Table 1 were taken at argon pressures ranged between 2 to 3 mTorr. For such pressure the mean free path will be longer and by interpolating the above Figures, the height h in our system was equal to 18 cm. This is longer than the target-substrate distance or even longer than the chamber dimension, i.e. virtual source at 2 mTorr argon pressure is hardly likely to be effective.

Reactive metals are particular sensitive to small amounts of residual gas (e.g. water

vapour) which will decrease the measured yield substantially. This indicates that the reaction products at the target surface will have larger binding energies than the original metal and so a lower sputter yield. Therefore the arrival of a reactive gas at the target must result in a reduction of the sputter yield and this reduction will be most severe for the more reactive systems (e.g. Al+O or Ti+O).

The ion current across the dark space does not fully represent the magnetron current. Schiller et al (Ref. 39) have measured this and gave Figure of 75% ion current across the dark space. The ion current Ii can be represented as (Ref. 21):

$$I_i = \frac{I}{(1+\gamma)}$$

where:

γ= Secondary electron coefficient.

The secondary electron coefficient changes with the target surface and usually increases as an oxide or nitride forms (with a resulting change in the discharge voltage). For a metal (γ) is typically 0.1 (Ref. 10) and for an oxide or nitride it may rise to around 0.2 (Ref. 42).

In magnetron sputtering the cathode dark space is smaller than that of glow discharge and the used argon pressure is lower, this in turn, will lead to longer mean free path. Therefore, the ions at the cathode will have less charge exchange (Ref. 34) and have energies close to that gained by falling through the applied potential.

2.4.2 The Unbalanced Magnetron

The unbalanced magnetron has been used to simultaneously sputter and bombard the growing films with an ion flux up to 9 mA/cm^2 with floating potential of 20 to 30 V. In a conventional magnetron, most of the discharge is confined close to the cathode surface and, therefore, bombardment of the growing film by electrons and ions is minimised. By unbalancing the magnetic field the substrate bombardment can be significantly increased. The original work on the topic was performed at the CSIRO Institute in Sidney (Refs. 43-46). Soon after, this process was used at the University of Loughborough (Refs. 13,47,48) mainly to acheive an optical coating and the Academy of Sciences in Prague, Czechoslovakia, to deposit hard TiN coatings (Refs. 49-52). Since then several papers on this topic have appeared (Refs. 53-56). The reader is referred to a recent review by W. Munz (Ref. 57).

There are two types of unbalanced magnetron configurations [(Ref. 43). In type one, the flux from the central magnetron is larger than that of the outer magnet; in type two the central flux is less than the outer flux (see Fig. 1 chapter 5). Type one has been shown to give low ion and electron current at the substrate, low self-bias voltages (Ref. 43) and low heat load (Ref. 58). Type two magnetrons give large ion and electrons to the substrate by about 100 times larger than the case of type one. Electrons are channelled along a field line extending from the discharge region to the substrate. The ions are electrostatically dragged by the electrons and, therefore, bombard the substrate.

For creating an unbalanced magnetron an electromagnetic or permanent magnet can be used. In all cases, the unbalanced field required a stronger magnet in the outer pole than the inner pole. This can be designed in two ways:

1- Hiding the magnet behind the target and

2- Using an extra pole piece fixed in the front of the target.

The advantages and disadvantages of the both design depend on the required of ion bombardment, the impurity, and the target utilisation . Type 1 gives less unbalanced field directed to the substrate than type 2, and therefore has less plasma leakage to the substrate. In the case of using a thermal sensitive substrate (such as a polymer for example) with a type 2 magnetron the substrate can be severely damaged. This can be easily reduced or eliminated by using a water-cooled earth cap placed approximately 5 mm away from the centre pole. By connecting this cap to a variable resistance the plasma leakage to the substrate can be controlled.

The poles will be exposed to the plasma and are at the target potential, so that it may be possible to sputter from the poles and thus contaminate the depositing film. This can be reduced by using the correct shape to the pole pieces with respect to the magnet locations in the magnetron body and by the use of close earth shielding (Refs. 38,59). Sputtering can be reduced from the pole surface if the magnetic flux exiting the surface is arranged to be perpendicular to that surface. The electrons are removed as rapidly as possible from the vicinity of the poles such that the ionisation and thus the bombardment is minimised in that area. Poor design may go unnoticed if sputtering yield of the target material is much higher than that of the pole material. In this situation there can be net deposition into the pole pieces from the backscattered material. If the pole design cannot be altered or there is still an unacceptable level of contamination, a close-fitting earth shield could be added to suppress the plasma and consequent bombardment from that area. There are two important points which need to be considered for the location of an earth shield; one is the build up of coating on the shield especially for long magnetron operation time which may cause arcing or short the magnetron to the earth. Thus the shield needs to be cleaned occasionally which is not desirable manner for long-term operation. Secondly, using an earth shield close to the poles will suppress some of the plasma close to the target, thus the magnetron potential will be higher than usual. In the case of using a

Fig.2.12 Cross section of Leybold's sputtering system (Ref.61).

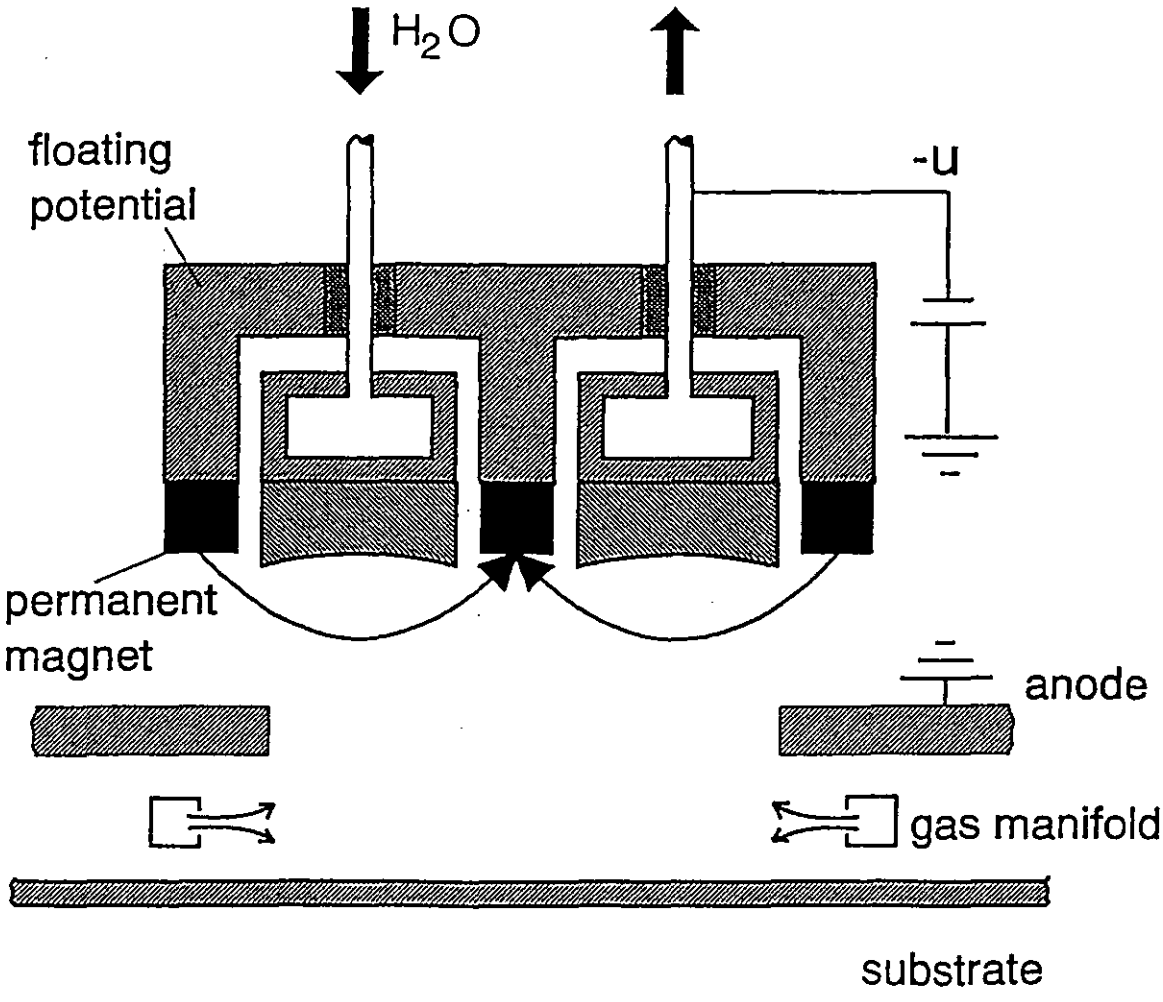

Fig.2.13 Cross section of three magnetrons with the measured magnetic field and erosion profiles.

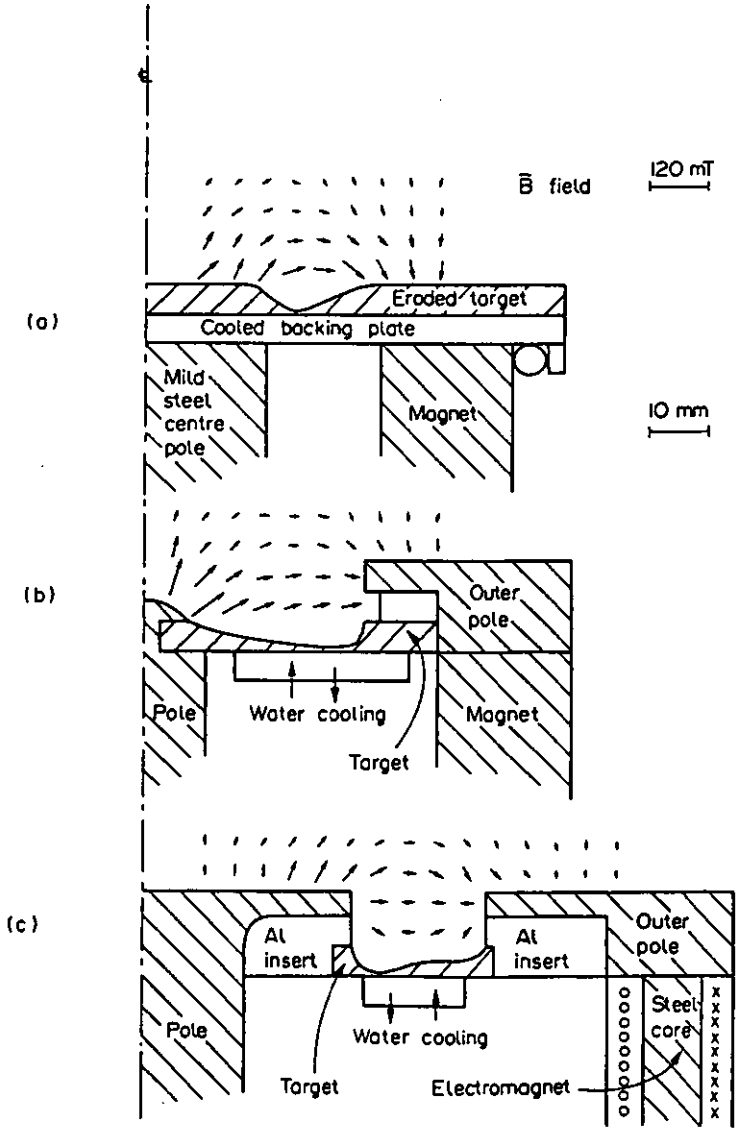

target material like Si which runs at a high voltage without fixed shield this makes the plasma hard to start up .

Recently some alternatives have been pointed out. By isolating the outer pole from the target may possibly reduce the pole sputtering (Ref. 60). In this work dip insulation was used. The insulated material is required to stand high temperatures due to the heat from the glow discharge close to the target. Again because of the high electric field drop across the insulator, the ion bombardment to it will cause an arc problem. Leybold (Ref. 61) have developed a new planar magnetron based on the patent "Interpole Target Magnetron" as shown in Fig. 12, in which the pole pieces are separated from the main target. Leybold claim this design will give a better target erosion (target utilisation), less arcing and contamination.

However, the unbalanced magnetrons of type 2 offer a good erosion profile (Fig. 13b). Allowable impurity levels vary with the application and if the highest possible purity is required, then the initial hidden pole design of Fig. 13a (type 1) is to be favoured, and target utilisation must be sacrificed unless a moving magnet or target system is used (Ref. 62).

2.4.1.1 Magnetron Plasma Confinement

Fig. 14 shows the I-V characteristic taken for the magnetron of figure 1A chapter 7. As shown in this figure, the reading has been taken in two parts, the first at the magnetron start and the second ten minutes later. Such features have been linked to plasma oscillation effects (Ref. 63). The oscillation has been measured experimentally (Ref. 63) and shown in Fig. 15. This oscillation and instability (Refs. 64,65) makes the electrons transfer across the magnetic field to the front or to the shield direction (Ref. 66).

Fig.2.14 I-V magnetron characteristic taken for hot and cold outer pole.

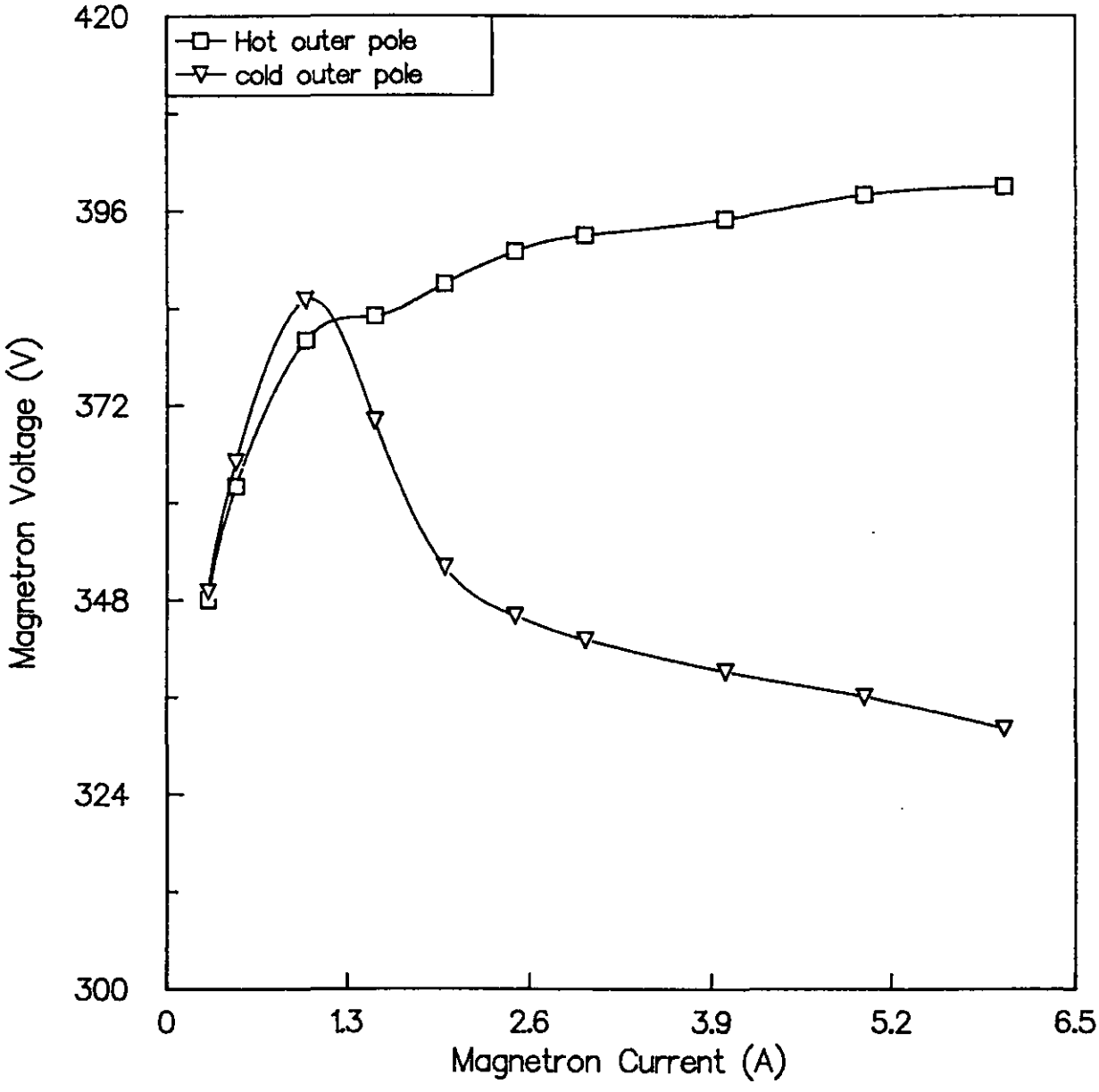

Fig.2.15 The onset of plasma oscillations in a D.C. planar magnetron (Ref.63).

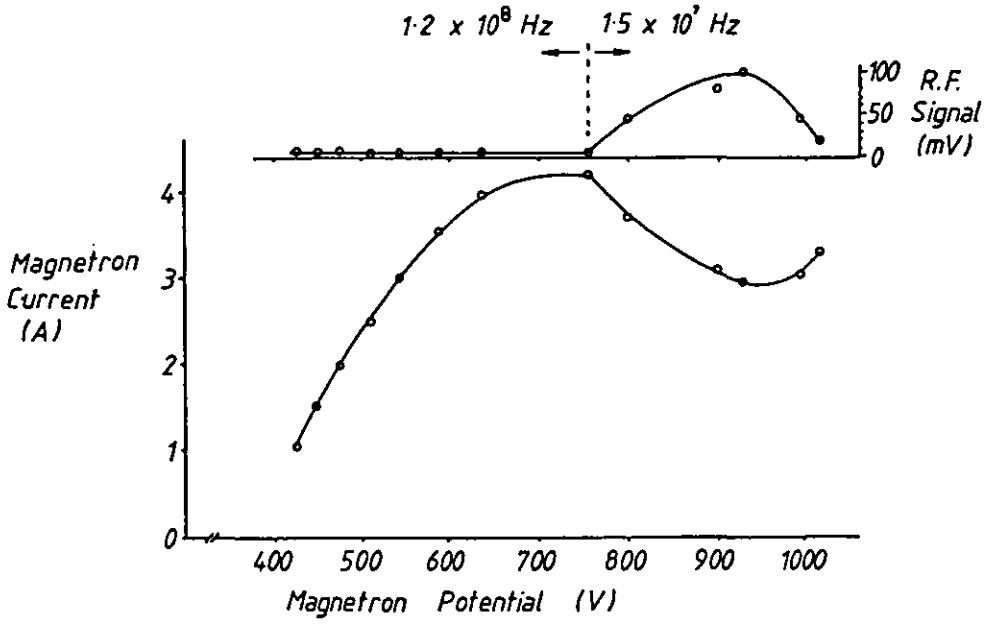

A stability criterion for oscillations has been derived for the penning discharge (Ref. 67). This is confirmed in the general case by Cap (Ref. 65). The electron cloud is stable if the plasma frequency (w_p) is less than the electron cyclotron frequency (w_{ce}). W_p can be derived from electron thermal speed (V) travel a distance of Debye length (λ_D). By inverting the time

$$W_p = \frac{V}{\lambda_D}$$

therefore,

$$W_p = \left(\frac{4 \pi n_e}{M}\right)^{1/2}$$

where:

N_e = Electron density m^{-3}

M = Electron mass (gram)

The W_{ce} can be designed from the orbit radius (Lamor radius) so

$$W_{ce} = \frac{q B}{M}$$

where B is the magnetic field strength (T). These two equations reveal that W_p is almost related to the electron density and W_{ce} is related to the magnetic strength. The observed oscillations of Fig. 15 are related to the use of thick target material which lead to lower magnetic strength. This would be expected as reducing B will reduce W_{ce}. Increasing the magnetron current will increase ne and W_p, hence the onset of oscillations as the magnetron current is increased. In the case of figure 14 an extra pole piece was fixed in front of the target (see figure 1A, chapter 7). By doing so the pole piece will extend the magnetic field from close to the target to the further in front . In the first five minutes the

pole pieces are still cool and hence the magnetic field still unaffected. In such circumstances the W_p is bigger than W_{ce} and hence oscillations will take place. Soon after the pole pieces start to warm up from the plasma and after 10 minutes they become hot and then the magnetic field set up was effected (the magnetic field at the target surface is stronger). W_{ce} is bigger than W_p and hence no oscillations takes place. To prove such features of the unusual behaviour a magnetic probe needs to be mounted inside the glow discharge so the magnetic strength can be measured. Unfortunately there was no probe which can stand high temperatures available in our laboratory. Instead, then, we have cooled the pole pieces which will keep the pole cool all the time and keep the magnetic field unaffected by the plasma heat. By doing this the I-V characteristics reveal the same reading immediately and after 10 minutes. The conclusions are consistent with the work of Figure 15. As these oscillations lead to an increase in the plasma impedance where an increasing loss of electrons leads to an increasing operation potential. So that in order to design a magnetron particular attention needs to be paid to the above because such criteria will limit the input power and reduce the magnetron efficiency.

2.4.2.2 I-V Plasma Characteristics and Electron Temperature

By using a shielded probe the characteristic of leaked plasma from unbalanced magnetron has been investigated (Ref. 13). the magnetron was operated at 500 mA, with a titanium target, 3 mTorr argon pressure and the probe 70 mm from the target surface. The typical I-V characteristic is shown in Fig. 16. When the bias is very negative over (60 V) with respect to the plasma potential, the electric field around the probe will prevent all but the highest energy electrons from reaching the probe, effectively reducing the electron current to zero. The positive ions encounter only are attracted by this electric field. The flow is termed the "ion saturation" current I_{si} and occurs when the voltage is sufficiently negative to repel nearly all the electrons in the plasma. As V is made more positive the number of

Fig.2.16 Plasma I-V characteristics of the unbalanced magnetron (magnetron current was 500 mA and 3 mTorr argon pressure).

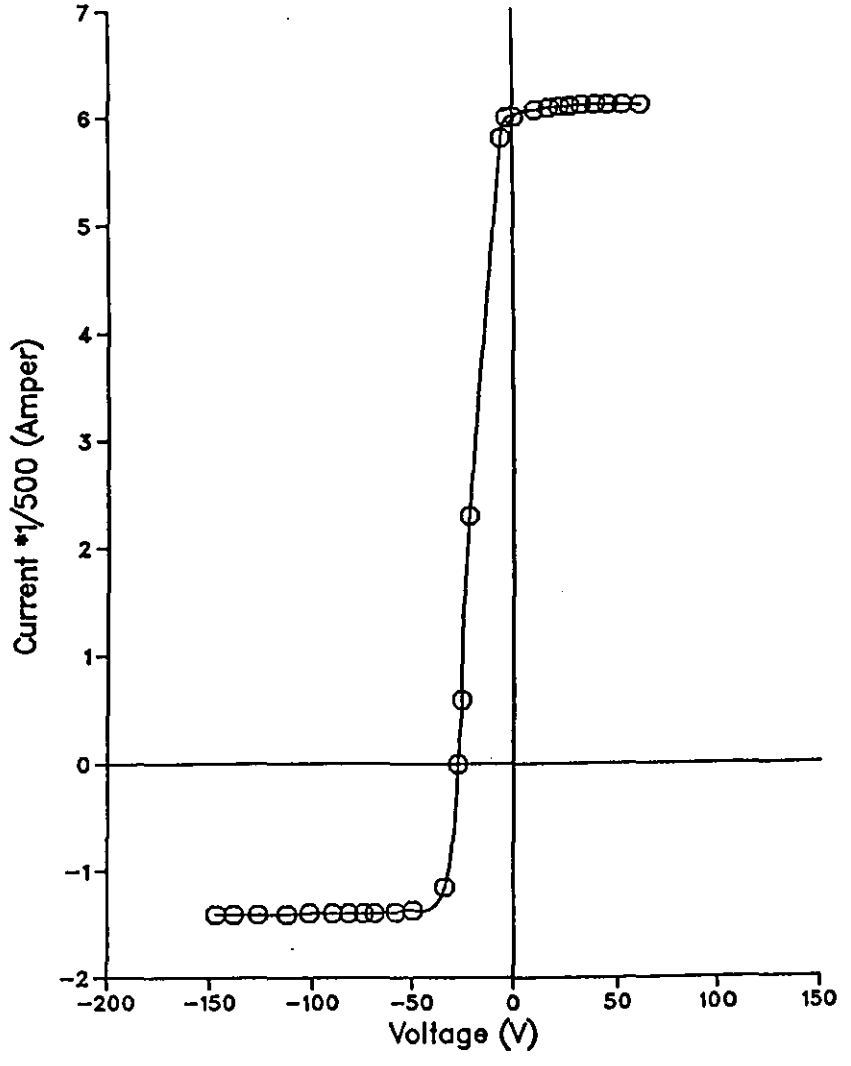

electrons which are able to overcome the repelling electric field and contribute a negative current increases exponentially. The electron current collected is equal to I_{si} at the self-bias voltage (floating Potential) V_f. V_f is less than the plasma potential V_p, because the electron thermal velocity is greater than that of the ions. Because of the greater energies of electron than ions ,the plasma potential tends to a positive potential, and is independent of discharge power. At a certain potential V_p, the flux of ions and electrons reaching the probe is totally representative of the random drift of electrons and ions, and no plasma sheath exists between the substrate probe and plasma. Voltage more positive than the plasma potential results in ions being repelled from the probe until finally an electron saturation current develops. As will be shown later the probe will be used to measure the floating potential and the saturation ion current only. These two parameters are expected to be effective in modifying thin film growth by dissipating their energy close to the substrate (Ref. 13). In the retarding region of I-V characteristic where the electrons follow Maxwelen-Boltzmann distribution, and by using equation 2.3, the electron temperature can be calculated.

Fig. 17 shows the variation of electron temperature T_e with argon pressure. because of the shorter electron mean free path at high pressure than at low argon pressure the electron temperature T_e is reduced as the argon pressure increased. From the floating potential which is illustrated on Fig. 17, and from Equation 2.12, the electron temperature can be calculated and compared with equation 2.3. Figure 18 illustrates the electron temperature as a result of magnetron current. As shown in the figure the electron temperature is nearly constant with increasing the magnetron power. This may be attributed to the energy of the secondary electrons entering the plasma being approximately constant. This is because the magnetron potential does not change

Fig.2.17 Electron temperature measured for different argon pressure (magnetron current was 500 mA).

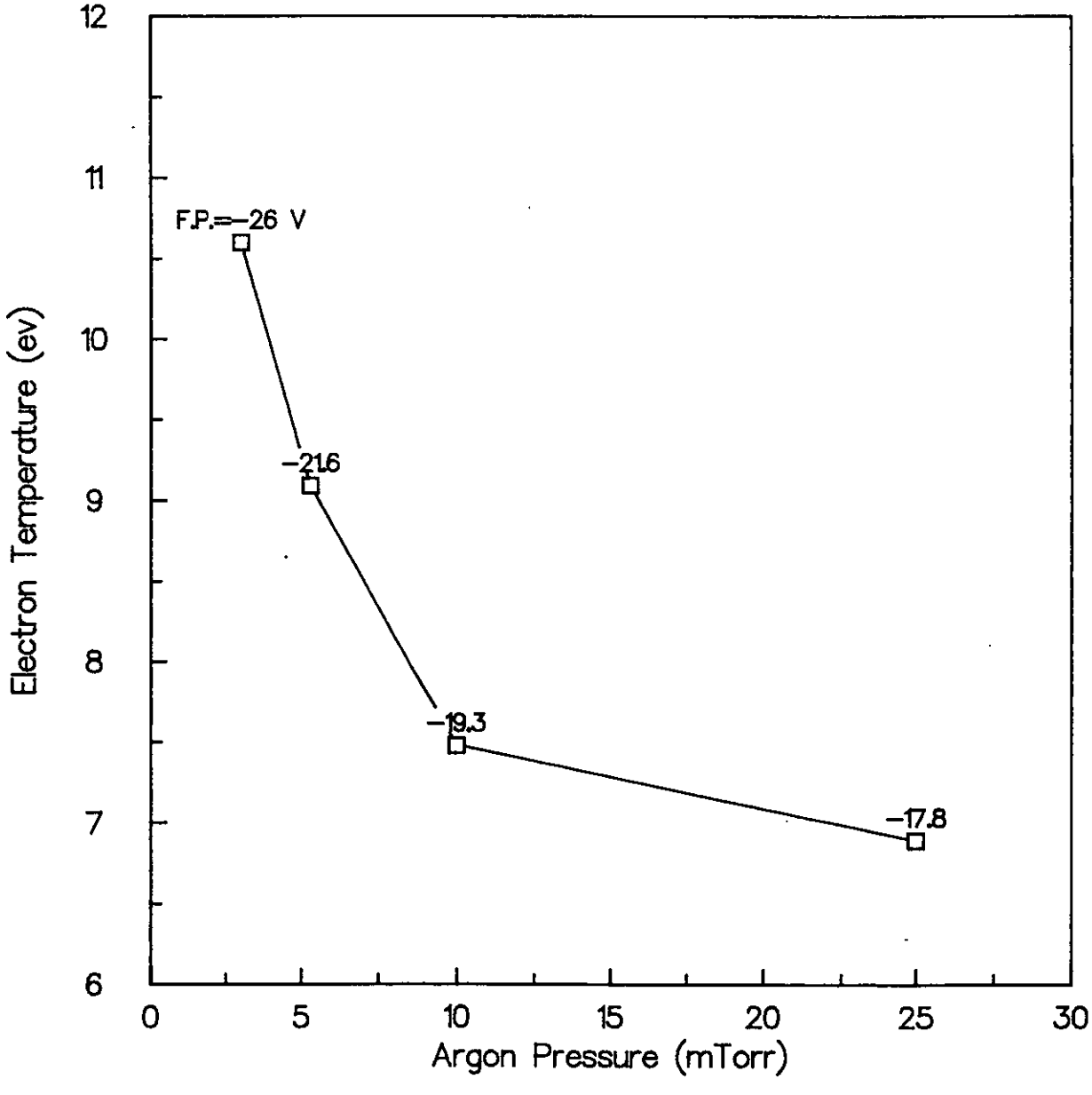

Fig.2.18 Electron temperature measured for different magnetron current (argon pressure was 3 mTorr).

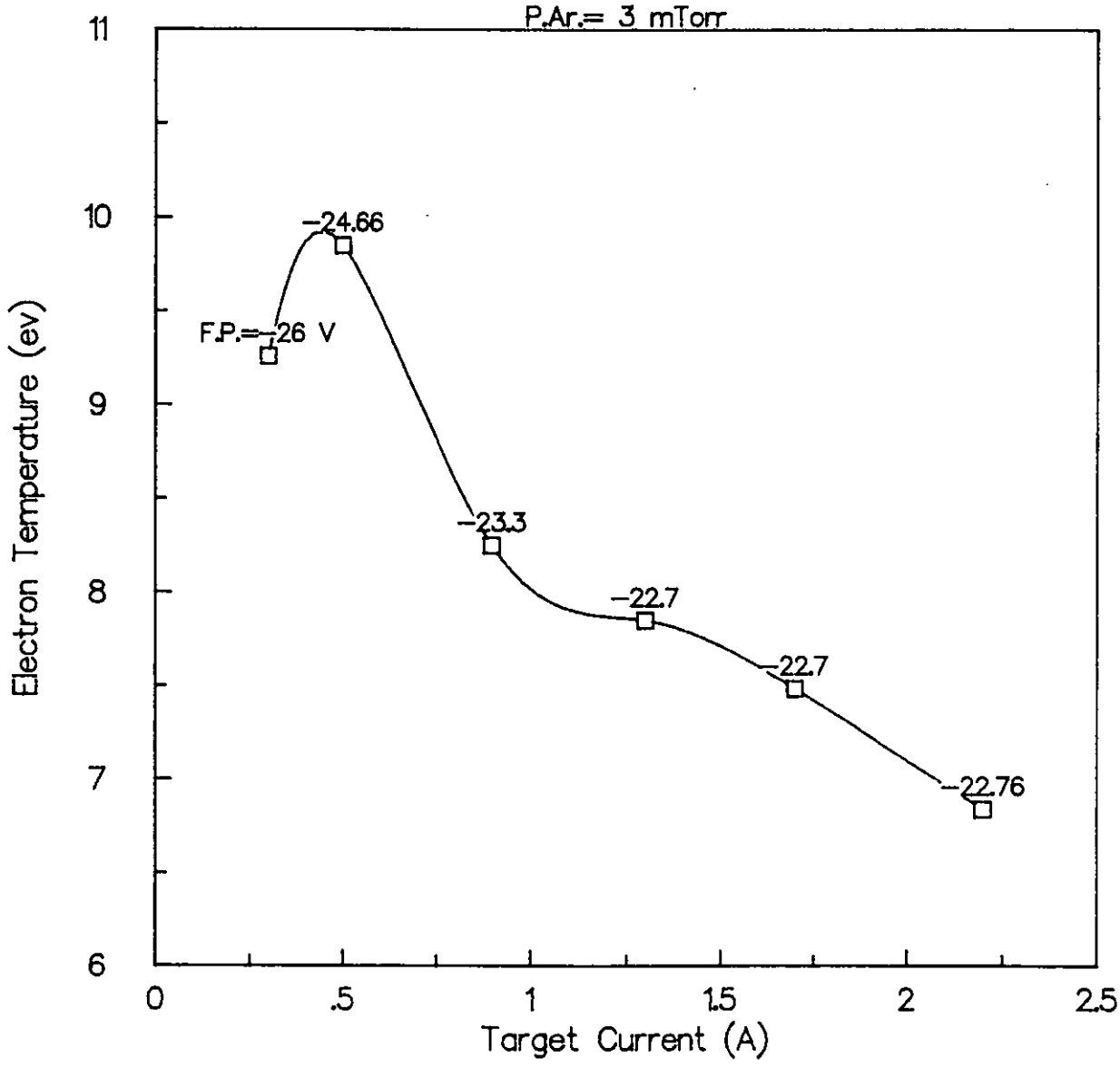

remarkably with increasing the magnetron current. The slight reduction in the electron temperature could be happened from the increase of the interaction of ions with the target sputtered atom near to the substrate surface.

2.4.2.3 Film Modification by Ion Bombardment

Ion plating according to the Bunshah definition (Ref. 68) is a generic term applied to the atomic film deposition process in which the substrate surface and/or the growing film is subjected to a flux of energetic particles sufficient to cause changes in the interfacial region or film properties compared to the non-bombardment deposition. This means that sputtering exhibits some of the essential characteristics of ion plating, eg, the ability to influence the quality of the coating by bombarding the condensate with energetic particles. Substrates exposed to a glow discharge are bombarded by energetic neutral ions and electrons. The nature and energy of the bombarding species are primarily dependent on the process parameters and geometrical location of the substrate within and/or outside the plasma zone (Refs. 69,70). Such bombardment can initiate a variety of reactions that may lead to substrate heating, substrate surface chemistry changes, re-emission or sputtering of deposited material, or gas incorporation in the growing film, as well as modification of the film morphology, crystal orientation and grain size etc. Thus, substrate bombardment can have a pronounced effect on the properties of the film. Ion bombardment during deposition often leads to film properties characteristic of depositions in the absence of ion bombardment but at significantly higher substrate temperature (Ref. 71). Fig. 19 shows Thornton's well-known diagram (Ref. 72) of the influence of temperature and pressure on the structure of the condensing film. Dense columnar coatings with a smooth surface (zone T and zone 2) are obtained only when the condensation temperature is within a certain sufficiently high range. The lower the pressure during deposition, the lower is the minimum temperature limit. Messier et al (Ref. 73) found that the minimum temperature limit for dense smooth coatings also drops

Fig.2.19 The dependence of coating structure of film on the gas pressure and substrate temperature (Ref.72).

Fig.2.20 Influence of bias voltage on the microstructure of coatings with substrate to melting point temperature (Ref.73).

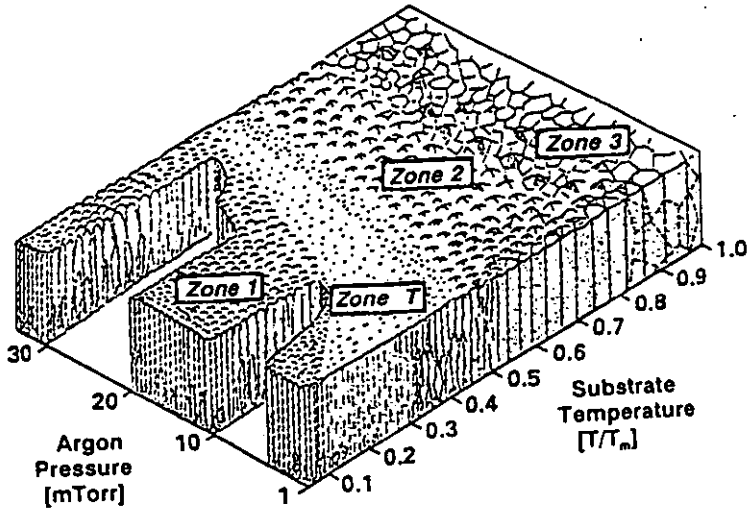

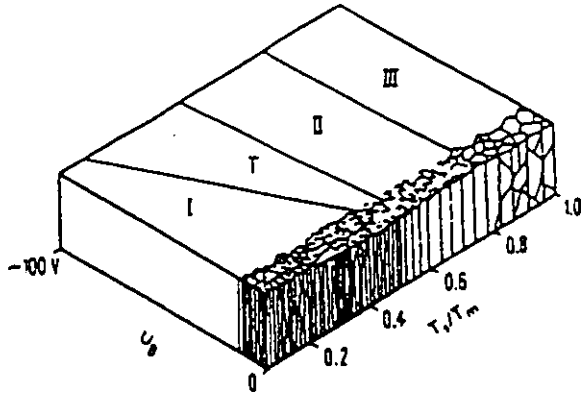

with increasing bias voltage (Fig. 20).

The effects of ion bombardment have been described by Mattox (Ref. 74) and Takagi (Ref. 75) who considered the effects produced on the surface prior to deposition, on interface formation, and during film growth. Developments in ion-assisted deposition processes have been reviewed by Matthews (Ref. 76), Bunshah (Refs. 77,78) and Thornton (Ref. 79). Ion bombardment during the deposition of Ag and Cu films has been observed to result in smaller grain sizes than those observed for evaporation (Refs. 80,81).

The beneficial of the unbalanced magnetron are seen from TEM photographs (Fig. 21) and from the film's electrical and optical properties . More experimental work is shown in chapter 5. Fig. 21 shows that the ion bombardment during the films's growth makes the film denser with a small grain size and smooth surface finish, whereas without or with less ion bombardment, the film becomes soft and a big grain size and rough surface finish. As well as the ion bombardment its energy plays a significant role by controlling the film properties . We have seen that the resistivity of TiN film is decreased from 2.25 to 1.1 Ω μm when the substrate self bias (floating potential) increases from 0 to 25 Volts.

The most significant structural effects on the film are changes in the film structure, orientation and grain size (Ref. 71). These features are directly related to the ion-to-atom arrival ratio and to the ion energies (Refs. 82-85). A model for growth modification resulting from ion bombardment was proposed by Bland et al (Ref. 86) (Fig. 22). The model assumes considerable back sputtering and scattering of back sputtered material to randomise the deposition direction and hence fill in the shadowed "valley" areas that develop in the absence of ion bombardment. Bland et al (Ref. 86) also demonstrated the

Fig.2.21 Photograph of film structure taken by TEM; a) with ion bombardment and b) without ion bombardment.

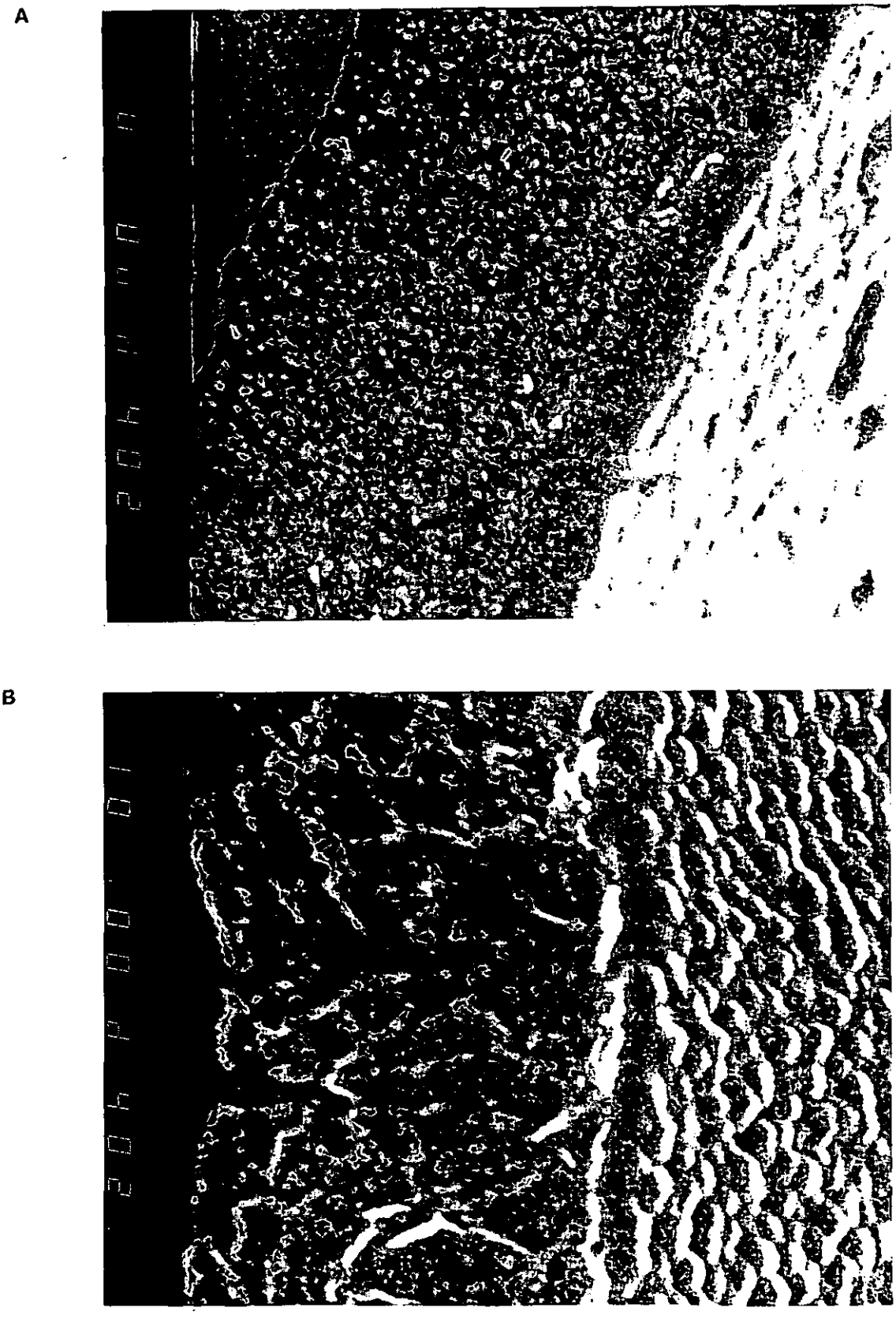

Fig.2.22 Model of growth modification by ion bombardment during deposition (Ref.86).

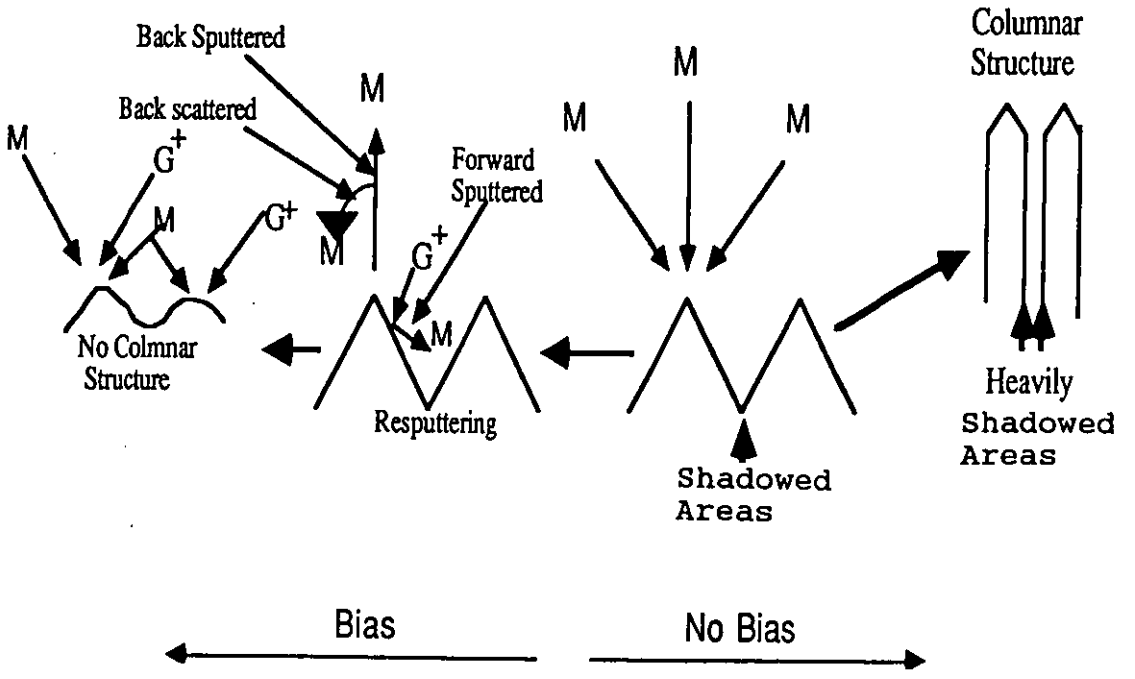

effect of ion bombardment on the density of a growing film. The density of chromium films deposited by either sputtering or electron beam evaporation was significantly enhanced in the presence of substrate bias.

Bombardment of the substrate surface before coating begins results in a variety of induced surface modifications that are generally beneficial to film adhesion (Ref. 87). Sputtering of the surface has the effect of cleaning the surface of oxides and other contaminants normally detrimental to film adhesion. Care is required in this process because it is possible for the recontamination rate to exceed the rate of contaminant removal. Bombardment during interface formation results in physical mixing between the deposition species and the substrate surface and in enhanced interdiffusion (Ref. 88). The bombarding ions tend to sputter more of the loosely bound atoms from the developing surface, with the net result that the more tightly bound atoms dominate the adhesion mechanism.

The physical properties of the film itself can be heavily modified ; stress may be increased or decreased by bombardment. In the case of the more refractory materials, ion bombardment tends to increase the film stress. Other physical properties, such as hardness and yield strength, may also be beneficially affected by bombardment. A practical benefit of these bombardment effects is the ability to deposit high quality, dense, hard film at relatively low substrate temperatures (Refs. 89,90). Stresses induced by ion bombardment or bias voltage can lead to adhesion failure (film spalling). This failure is a result of internal stresses which are classified as either intrinsic stresses caused by growth defects and structural mismatch between the film and the substrate, or thermal stresses caused by different expansion coefficients of the film and the substrate (Ref. 91). This implies that adhesion of the film is dependent on the material of the substrate.

In magnetron sputtering the coated films showed a transition from tensile to compression stress as the gas pressure was decreased (Ref. 92). That was interpreted as an increase of the energetic bombardment of the growing film. However, in magnetron sputtering the highly energetic atoms causes a film-radiation-damage which in turn influences the film properties and film stress. As will be shown in chapter 8 the use of a magnetron operated at lower voltages (Ref. 93) has shown the ability to adjust the film properties concerning the film stresses.

2.5 Reactive Sputter Deposition

Reactive sputter deposition involves the sputtering of a metal, alloy or compound in a reactive gas mixture in order to deposit a compound thin film composed of the sputtered material and the reactive species. The process of reactive sputter deposition can be very complex and involves the sputtering process, the physics of the plasma discharge, transport of sputtered and gas species, the kinetics of film growth and chemical interactions at the target and film surfaces. These all interact in some way and therefore can affect the properties of the film.

Several models were presented concerning the reaction of reactive gases with target surfaces (Refs. 94,95). The deposition of a compound with a mixture of argon and reactive gases requires a high degree of process control of the reaction inside the deposition chamber in unstable mode called transition mode. When the reactive gas is admitted to the working chamber during sputtering, the reactive gas pressure rises abruptly at specific flow rate characterised by target switching from metallic to reactive condition. When this happens the target sputtering rate drops sharply, ie, target poisoning.

The two regimes of operation, i.e. metallic cathode sputtering and compound coated

cathode sputtering, can be described by the plotting of the hysteresis effect between the flow rate, f_r of reactive species and the chamber pressure, P. (Fig. 23). A constant pressure, P_a, is maintained by the flow f_a of the non-reactive gas (Ar in this case) into the continuously pumped chamber. The deposition of the target in the Ar alone would result of the deposition of a pure metal film.

The hysteresis curve represents two stable states of a system with rapid transitions between the two states. In state A, there is negligible change in the total pressure as the reactive gas flow, f_r, is varied. In state B, the pressure rises linearly with reactive flow rate, but is lower by ΔP than the total pressure in the absence of sputtering. In state A, essentially all of the reactive gas is being incorporated in the deposited film and the atomic ratio of the reactive gas to sputtered metal in the film increases with f_r. Thus, state A can be considered as a regime in which the sputtered metal is doped with reactive gas (Metallic Mode). In state B, a constant volume of reactive gas is consumed, independent of f_r, and there is an excess of reactive gas so the formation of a stable compound is favoured (Reactive Mode).

The main cause of the transition from state A to state B and the hysteresis effect has been attributed to the formation of a compound layer on the surface of the sputtering target or cathode. The getter-pumping effect of the freshly-deposited metal films is reduced by the reduction in metal atom sputtering rate, causing the partial pressure of the reactive species (and the total pressure of the chamber) to increase. Conversion back to the metal mode (state A) occurs only when the flow of reactive gas is reduced to the point where it can no longer maintain the compound layer, which is being continuously sputtered.
A number of models describing aspects of the transition from state A to state B have been

Fig.2.23 The hysteresis curve for system pressure,p, as a function of reactive gas flow, Fr.

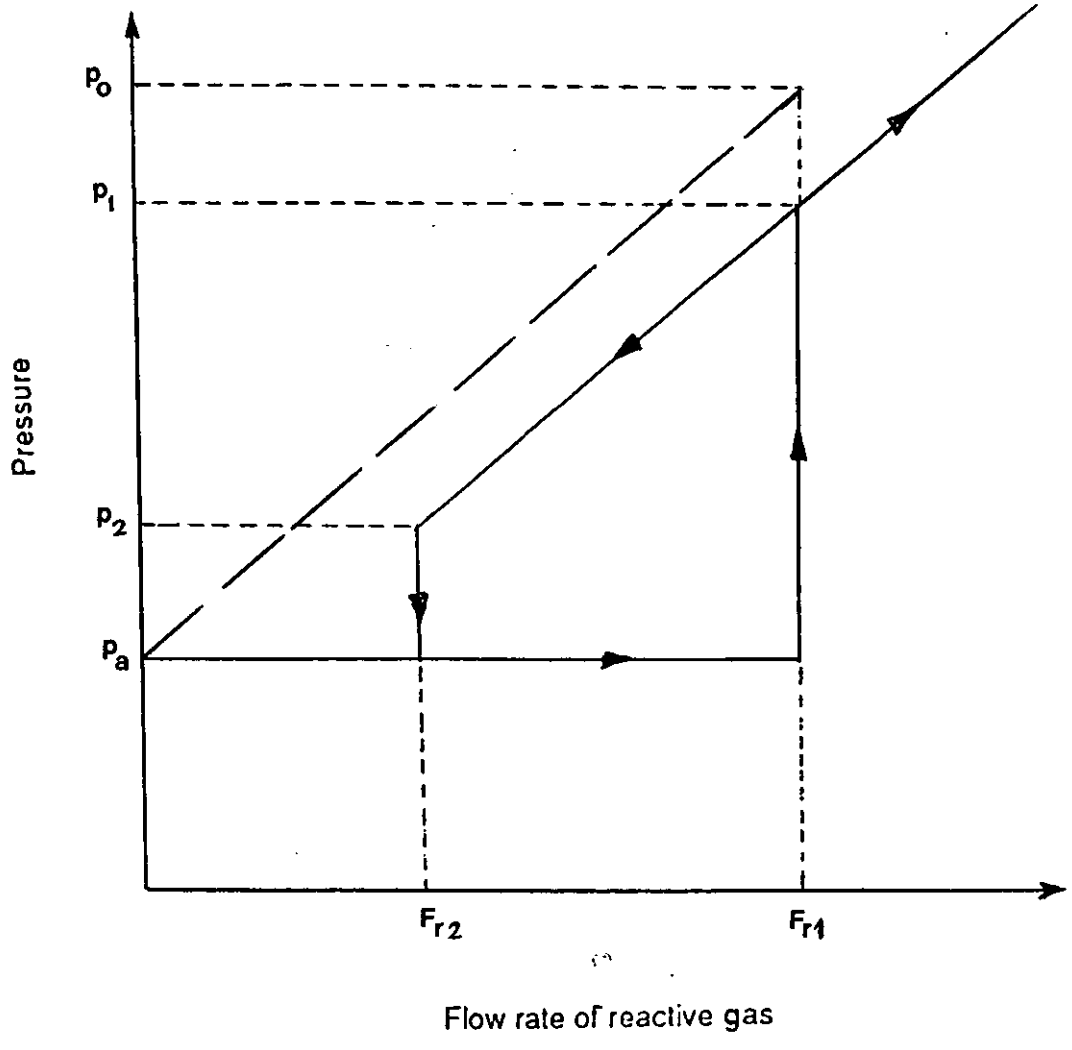

introduced (Refs. 96-101). More recent models have been developed by Larsson et al (Ref. 102) and by Berg et al (Ref. 103). These models use the consumption rate due to the gettering effect as well as exhaustion by the pump.

In most cases the sputtering yield for metal atoms from the target will decrease once a compound forms on the target surface. Some of the energy of the incident ion on the target must go to sputtering the other component of the compound. For example (Refs. 104,105) if an Al_2O_3 film is formed on the cathode surface, only 40% of atoms sputtered from the surface would be Al atoms. Thus, if the discharge power is kept constant as the transition from state A to state B occurs, the sputtering rate of Al would decrease by a minimum of 60%.

The hysteresis effect is strongly dependent on the pumping speed of the vacuum system. Okamoto and Serikawa (Ref. 106) varied the pumping speed by a factor of 20 to change the flow of Ar from 5 to 100 SCCM for the reactive sputtering of Si in Ar/N_2. They found that the hysteresis effect was dramatically reduced when the pumping speed increased until at 100 SCCM Ar flow, there was no effect. The effect of pumping speed on the shape of the pressure hysteresis curve was also explored by Kadlec et al (Ref. 107) for the reactive sputtering of TiN. Danroc et al (Ref. 108) reported the change in shape of the hysteresis curve during the reactive sputtering of TiN, as a function of both the pumping speed and the location of the N_2 inlet. The width of the hysteresis curve decreased as the Nitrogen inlet was moved closer to the pump throat.

Due to the change in the surface composition of the target in states A and B, there may often be a change in the discharge voltage and current at constant discharge power. In the case of reactively sputtered Al in Ar and O_2 mixture the voltage drops significantly, going

from state A to state B. This may be due to changes in the secondary electron coefficient of the target. The additional electrons can cause additional ionization in the plasma, resulting in a higher ion flux to the cathode, and hence a lower discharge voltage at constant power. We saw that, in the case of reactively sputtered Ti in O_2 the discharge voltages increase, rather than decrease upon transition from metallic mode to the poison target mode. This may be indicative of negative ion effects, or the less secondary electron emissions due to the type of the target metal and its compounds.

2.5.1 Controlled Process by Monitoring Systems

It is desirable to operate the target in metallic mode, but as close as possible to the critical flow for transition to rich gas mode. This usually gives an stoichiometric film structure, higher deposition rate and less trouble (for example Arcing). In reactive sputtering, the response of the magnetron in the reactive gas is not a simple linear function of the reactive gas flow for a constant power, and the conversion from metallic to rich gas mode may be rapid and difficult to control. Hence, a method of continuously adjusting the operating point to maintain constant deposition rate and film properties is necessary. This involves some means of monitoring any change in the operating point and providing a feedback control to change either the reactive gas flow or the discharge power accordingly. To monitor the operating point in such system requires a sensitive method. If the pressure increases significantly, it will be impossible to recover the operating point without essentially tracing out the hysteresis curves in Fig. 23. This is also clearly unacceptable for the deposition of homogeneous films. The parameters which change rapidly near the critical flow transition are the system pressure and the partial pressure of the reactive gas species, the discharge parameters, such as the voltage or current and the resultant film properties. An additional, observable change is the emission of light from the plasma which is indicative of both particle density as well as discharge parameters. All of these

parameters have been used as monitors (Refs. 109-119).

Optical emission from the plasma has been successfully used to drive the feedback loop in several cases (Refs. 111-113,115-118). In general, these techniques monitor either a reduction in the emission of metal species or an increase in the emission of the reactive gas species near the critical flow point. The advantage of a plasma emission monitor (PEM) is that it samples from region where the reaction is actually taking place, there is no need for differentially pumping as in the case of the residual gas analyser monitor (Refs. 109,110). This means that the response time can be much faster. The control system which was used in our Laboratory has been developed by Spencer and Howson (Ref. 115). This is shown schematically in Fig. 24. They showed that breaking the cycle which causes target poisoning by matching the admission and consumption rates to give zero surplus, can give better controlled film properties and higher deposition rates. The way the controller works is that the signal or emission intensity of the metal line is passed from the dense plasma region via an optical fibre to the optical filter which provides stable filtration of the transmitted light of the metal line concerned. This signal is transferred to the photomultiplier that is connected to the pressure controller 80-1. By adjusting the percentage of the metal line set point from the pressure controller, the piezoelectric valve will control the reactive gas consumption which will be displayed on unit 80-5 (the main gas flow displayer) and that percentage will be displayed as an output signal from the photomultiplier in terms of volts. This signal can also be transformed to a percentage of the metal line set point.

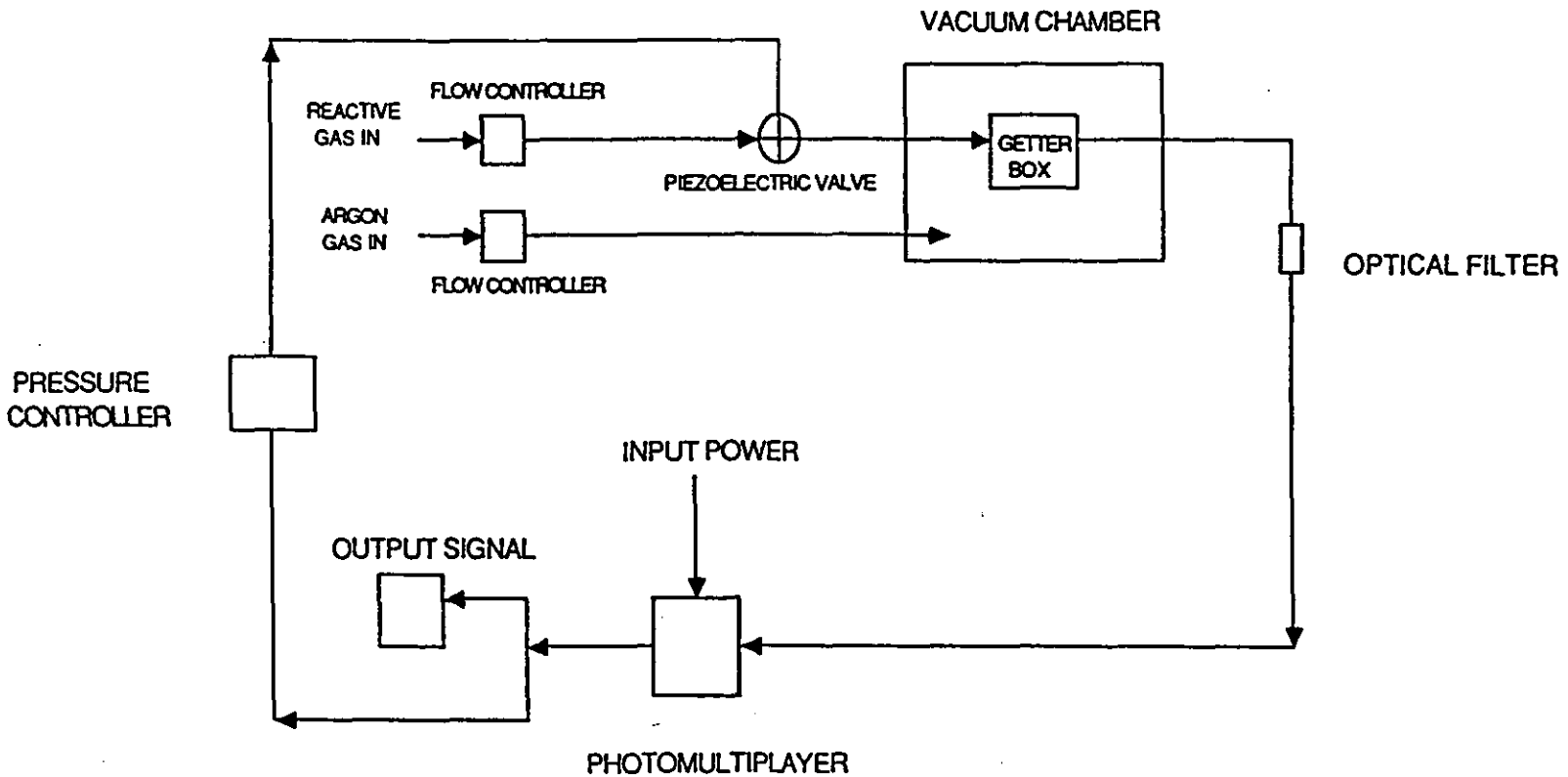

Fig 2.24 PEM system.

2.6 References

1- D. A. Frank and Kamenetskii, " Plasma the fourth state of matter", Macmillian, lleuum press, New York, (1972).

2- J. L. Vossen and W. Kern, "Thin film process II", academic press, Ney York, 1991.

3- J. L. Vossen and W. Kern,"Thin film process 1", academic press, New York, 1978.

4- F. F. Chen, "Introduction to plasma physics", Plenum press, New York, 1974.

5- I. H. Hutchinson "Principles of Plasma Diagnostics" Cambridge University Express (1990).

6- I. Langmuir and H.M.Smith, Phys. Rev., 28 (1926) 727.

7- D. Webber "Modern Physics" Penguim Books (1971).

8- J. G. Laframboise, "Theory of spherical and cylindrical langmuir probe", UTLAS report No. 100, June, 1966.

9- D.Bohm, E.H.S.Burhop, and H.S.W.Massey,in "The Characteristic of Electrical Discharges in Magnetic Field" (A.Guthric and P.K.Wakerling edts), McGraw-Hill, New York 1949.

10- B. Chapmann, "Glow discharge processes", Jhon Wiley and Sons, New York, 1980.

11- L.Holland, Thin Solid Films, 27 (1975) 63.

12- J. S. Logan, J. H. Keller, and R.G.Simmons, J. Vac. Sci. Technol., 14 (1977) 92.

13- R.P.Howson, H.A.Jafer, and A.G.Spencer, Thin Solid Films, 193/194 (1990) 127.

14- A. Benninghoven, ed. " Secondary ion mass spectrometry SIMS II-IV", springer Ser. Chem. Phys., 36, New York, 1984.

15- H. Ryssel and H. Glawisching, edts., "Ion implantation techniques", Spring-Verlang, New York, 1982.

16- D. Post and R. Behrisch, edrs, "Physics of plasma-wall interactions in controlled fusion", Plenum press, New York, 1984.

17- R. Behrisch (ed.)," Sputtering by ion bombardment I" Topics Appl. Phys. 47 (Springer-Verlag), New York, 1981.

18- R. Behrish (ed.)," Sputtering by ion bombardment II", Topics, Appl. Phys. 52, (Springer-Verlag), New York, 1983.

19- D. P. Jackson, in proc. of the symp. sputtering, ed. by Varga, Betz, and Viehbock, Inst. F. Allgem. Physik, TU Wein (1980).

20- D. E. Harrison, Radial Eff., 70 (1983).

21- A. G. Spencer, " High rate reactive magnetron sputtering", Ph. D thesis, LUT. 1988.

22- W. O. Hofer, K. Besoke and B. Stritzker, Appl. Phys., 34 (1983) 2800.

23- P. Sigmund, Phys. Rev., 184 (1969) 383 and 187 (1969) 708.

24- J. P. Biersack and W. Eckstein, Appl. Phys., A 34 (1984) 73.

25- P. C. Zalm, J. Appl. Phys., 54 (1983) 2660.

26- Ch. Steinbruchel, Appl. Phys., A 36 (1985) 37.

27- N. Laegreid and G. K. Wehner, J. Appl. Phys., 32 (1961) 365.

28- D. Rosenberg and G. K. Wehner, J. Appl. Phys., 33 (1962) 1842.

29- A. G. Spencer, C. A. Bishop, R. P. Howson, Vacuum, 37 3/4, (1987) 363.

30- L. T. Lamont, J. Vac. Sci. Technol., 14 (1977) 122.

31- H. R. Kaufman, J. Vac. Sci. Technol., B 8 (1990) 107.

32- T. J. Sheridam, M. J. Gloeckner, and J. Goree, J. Vac. Sci. Technol., A 7 (1989) 1014.

33- S. M. Rossnagel and H. R. Kaufman, J. Vac. Sci. Technol., A 5 (1987) 88.

34- D. M. Manos, "Plasma etching", Academic press, New York, 1989.

35- S. Schiller, U. Heisig, and K. Goedicke, 7th Int. Conf. on Vac. Met., Tokyo, Japan, November, 1982.

36- J. A. Thornton, J. Vac. Sci. Technol., 15 (1978) 171.

37- R. K. Waits, J. Vac. Sci. Technol., 15 (1978) 179.

38- L. I. Maissel and R. Gland, " Hanbook of thin film technology", McGraw-Hill Book, New York, 1970.

39- S. Schiller, U. Heisig, K. Geodicke, Thin Solid Films, 40 (1977) 327.

40- N. S. Rizk, A. Rizk and S. K. Habib, Vacuum, 40 (1990) 245.

41- A. R. Nyaiesh, Vacuum, 36 (1986) 307.

42- A. H. Eltoukky, B. R. Natarajan, J. E. Greene and T. L. Barr. Thin Soild Films, 69 (1980) 229.

43- B. Window and N. Savvides, J. Vac. Sci. Technol., A 4 (1986) 196.

44- B. Window and N. Savvides, J. Vac. Sci. Technol., A 4 (1986) 453.

45- N. Savvides and B. Window, J. Vac. Sci. Technol., A 4 (1986) 504.

46- B. Window and G. L.Harding, J. Vac. Sci. Technol., A 8 (1990) 1277.

47- A. G. Spencer, K. Oka, R. W. Lewin and R. P. Howson, Vacuum, 38 (1988) 857.

48- H. A. Ja'fer, R. P. Howson, E. M. Stenlake and A. G. Spencer, IPAT, May 1991, Brussels.

49- S. Kadlec, J. Musil, W-D. Munz, G. Hakansson and J-E. Sundgren, Surf. Coat. Tech., 39/40 (1989) 487.

50- S. Kadlec, J. Musil, V. Valvoda, W-D. Munz, H. Peterson and J. Schroeder, Vacuum, 41 (7-9) (1990) 2233.

51- S. Kadlec, J. Musil, W-D. Munz and V. Valvoda, Proc. 7th Int. Conf. on Ion and Plasma Assisted Technology, Edinburgh, 1989, 100.

52- S. Kadlec, J. Musil, and W-D. Munz, J. Vac. Sci. Technol., A 8 (3), (1990) 1318.

53- R. D. Arnell and R. I. Bates, vacuum, 43 (1992) 105.

54- R. D. Arnell and J. Stainsby, Proc. 11th Int. Vac. Conf. , Koln, 1989.

55- D. G. Teer, Surf. Coat. Tech., 36 (1988) 901.

56- S. L. Rohde, L. Hultman, M. S. Wong and W. D. Sproul, Surf. Coat. Technol., 50 (1992) 255.

57- W-D. Munz, Surf. Coat. Tech., 48 (1991) 81.

58- K. Oka, " Plasma activated growth of reactively sputtered optical thin films", Ph. D thesis, LUT, 1988.

59- L. Holland, British Patent 610529, accepted\18 October 1948.

60- G. Hall, personal communication, LUT, 1991.

61- S. Bei Bwenger, Proc. 1st Int'l Symp. on ISSP, 91, Tokyo, 1991.

62- K. Abe, Skobayashi, T. Kamel, T. Shimizu, and S. Aiuchi, Thin Solid Films, 96 (1982) 255.

63- A. G. Spencer, C. A. Bishop, and R. P. Howson, Vacuum, 37 3/4 (1987) 363.

64- M. F. Hoyaux, "Plasma physics and its applications, in modern physiscs", ed. D. Webber, Penguin, Harmondsworth, 1971.

65- F. F. Cap, " Handbook on plasma instabilities", academic press, New York, 1976.

66- B. B. Kadomstev, Phil. Trans. R. Soc. Lond. A 322, P. 125.

67- O. Buneman, Nature, 165 (1950) 474.

68- R. F. Bunshah, ed. " Deposition technology of films and coatings", Noyes Publishing, Park Ridge, NJ, 1982.

69- L. Holland, Surf. Sci. Tech., 11 (1980) 145.

70- L. Holland, J. Vac. Sci. Technol., 28 (1978) 437.

71- S. M. Rossnagel and J. J. Cuomo, Vacuum, 38 (2), (1988) 73.

72- J. A. Thornton, J. Vac. Sci. Technol., 11 (1974) 666.

73- R. Messier, A. P. Giri, and R. A. Roy, J. Vac. Sci. Technol., A (2), (1984) 500.

74- D. M. Mattox, in "Deposition technologies for films and coatings", R. F. Bunshah, ed., P. 244-287, Noyes Publications, Park Ridge, New Jersey, 1982.

75- T. Takagi, Thin Solid Films, 92 (1982) 1.

76- A. Matthews, J. Vac. Sci. Technol., A 3 (6), (1985) 2363.

77- R. F. Bunshah, Thin Solid Films, 107 (1983) 21.

78- R. F. Bunshah, J. Vac. Sci. Technol., A 3 (3), (1985) 553.

79- J. A. Thornton, Thin Solid Films, 107 (1983) 3.

80- F. Parmigiani, E. Kay, T. C. Huang and J. D. Swalen, Appl. Opt., 24 (1985) 3335.

81- I. C. Huang, G. Lim, F. Parmigiani and E. Kay, J. Vac. Sci. Technol., A 3 (1985) 2161.

82- Lock See Yu, J. M. E. Harper, J. J. Cuomo and D. A. Smith, J. Vac. Sci. Technol., A 4 (1986) 443.

83- P. J. Parnett and D. S. Rickerby, Thin Solid Films, 154 (1987) 403.

84- W. D. Sproul, P. J. Rudnick and M. E. Graham, Surf. Coat. Tech., 39/40 (1989) 355.

85- L. Hultmann, W-D. Munz, J. E. Sundgren, J. E. Greene, J. Musil and S. kadlec, J. Vac. Sci. Technol., A 9 (3), (1991) 434.

86- R. D. Bland, G. J. Kominiak, and D. M. Mattox, J. Vac. Sci. Technol., 11 (4) (1974) 671.

87- J. N. Avaritsiotis, R. P. Howson, M. I. Ridge, and C. A. Bishop, Trans. Ins. Met. Finish, 57 (1979) 65.

88- J. e. Greene, S. A. Barnett, J. E. Sundgren and A. Rockett, "Ion beam assisted film growth", T. Itoth, ed., Elsevier, Amesterdam, 1989, P. 104.

89- H. K. Pulker, M. Larden, R. Buhl, and E. Moll, J. Vac. Sci. Technol., A 4 (6), (1986) 2922.

90- A. J. Perry and H. K. Pulker, Thin Solid Films, 124 (1985) 323.

91- D. S. Rickerby, J. Vac. Sci. Technol., A 4 (1986) 2809.

92- J. A. Thornton and D. W. Hoffmann, J. Vac. Sci. Technol., 18 (1981) 203.

93- S. M. Rossnagel and J. J. Cuomo, Thin Solid Films, 171 (1988) 143.

94- H. F. Winters and P. Sigmund, J. Appl. Phys., 45, 11 (1974) 4760.

95- G. M. Lancaster and J. W. Rabalais, J. Phys. Chem., 83, 2 (1979) 209.

96- H. Heller, Thin Solid Films, 17 (1973) 163.

97- B. Goranchev, V. Orlinov and V. Popova, Thin Solid Films, 33 (1976) 173.

98- S. Schiller, V. Heisig, K. Steinfelder and J. Strumpfel," Proc. Int. Conf. on ion

plating and allied techniques", London, P. 211, 1984.

99- J. Affinito and R. R. Parsons, J. Vac. Sci. Technol., A 2 (1984) 1275.

100- G. Lemperiere and J. M. Poitevin, Thin Solid Films, 111 (1984) 339.

101- D. K. Hohnke, D. J. Schmatz and M. D. Hurley, Thin Solid Films, 118 (1984) 301.

102- T. Larsson, H-O. Blom, C. Nender and S. Berg, J. Vac. Sci. Technol., A 6 (1988)

103- S. Berg. H-O Blom, T. larsson and C. Nender, J. Vac. Sci. Technol., A 5 (1987) 202.

104- S. Maniv and W. D. westwood, Surf. Sci., 100 (1980) 108.

105- G. Este and W. D. Westwood, J. Vac. Sci. Technol., A 2 (1984) 1238.

106- A. Okamota and T. Serikawa, Thin Solid Films, 137 (1987) 729.

107- S. Kadlec, J. Musil and J. Vyskocil, Vacuum, 37 (1987) 729.

108- J. Danroc, A. Aubert and R. Gillet, Surf. Coat. Tech., 33 (1987) 83.

109- W. D. Sproul, Surf. Coat. Tech., 33 (1987) 73.

110- A. F. Hmiel, J. Vac. Sci. Technol., A 3 (1985) 592.

111- M. Bhushan, J. Vac. Sci. Technol., A 5 (1987) 2829.

112- S. Schiller, O. Heisig, C. Korndorfer, G. Beister, J. Reschke, K. Steinfelder and J. Strompfel, Surf. Coat. Tech., 33 (1987) 405.

113- S. Schiller, G. Beister and W. Sieber, Thin Solid Films, 111 (1984) 259.

114- S. Berg, T. Larsson, and H-O. Blom, J. Vac. Sci. Technol., A 4, 3 (1986) 594.

115- A. G. Spencer and R. P. Howson, Thin Solid Films, 186 (1990) 129.

116- R. P. Howson, A. G. Spencer, K. Oka, and R. W. Lewin, J. Vac. Sci. Technol., A 7, 3 (1989) 1230.

117- R. P. Howson, A. G. Spencer, S. A. Kazandijev and E. M. Stenlake, IPAS, 1989.

118- M. I. Ridge and R. P. Howson, Vacuum, 34 (1984) 327.

119- J. Affinito and R. R. Parsons, J. Vac. Sci. Technol., A 2 (1984) 1275.

CHAPTER-3

MEASUREMENT TECHNIQUES FOR THIN FILMS

3.1 Talystep Stylus

In stylus instruments, a diamond needle of very small dimensions (e.g. 13 μm in tip radius) is used as the arm of an electromechanical pick-up. The position of the pick-up is determined by a slider which is pressed on the area surrounding the needle to give the mean zero position. The thickness of a film is measured by traversing the stylus over the edge of the deposit, the thickness being recorded on a pen recorder as the difference in level between the film and the substrate. The substrate should generally be smooth compared with the thickness of the deposit. To ensure this, measurements are often made on a sample specimen deposited on an optically flat substrate, a portion of which is masked off. Build-up of deposit at the edge of the step is sometimes repeated. A well known instrument of this type is the Talystep, constructed by Rank Taylor-Hobson, England, and this is the one used in our Laboratory. The stylus force is adjustable from 1 to 30 mg and vertical magnification from 5000 × to 1000 000 × is possible. Although the measuring unit is mounted on an anti-vibration platform, the high sensitivity of the device demands its use on a rigid table standing on a firm floor.

3.2 The Ellipsometer

A plane-polarized light reflected from a film at non-normal incidence assumes elliptical polarisation. The ratio of minor to major axis of the reflected beam is determined by the relative phase difference Δ and azimuth Ψ(Ref. 1). The thickness and refractive index of transparent films can be determined from the values of Δ and Ψ. The apparatus used was a Gaertner L117 ellipsometer. This apparatus is shown schematically in (Fig. 1). For the results given in this work we simply determined the polariser and analyser angles (P_1,

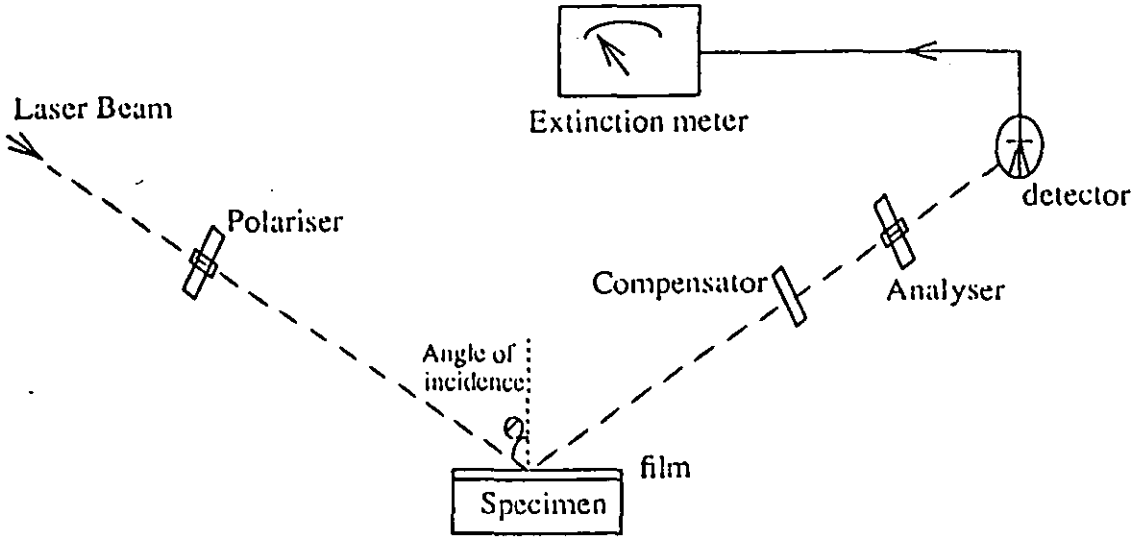

Fig. 3.1 A schematic diagram of the ellipsometer

Fig.3.2 Δ and Ψ for films of varying refractive index (n) and thickness (d) on silicon (Ref.3).

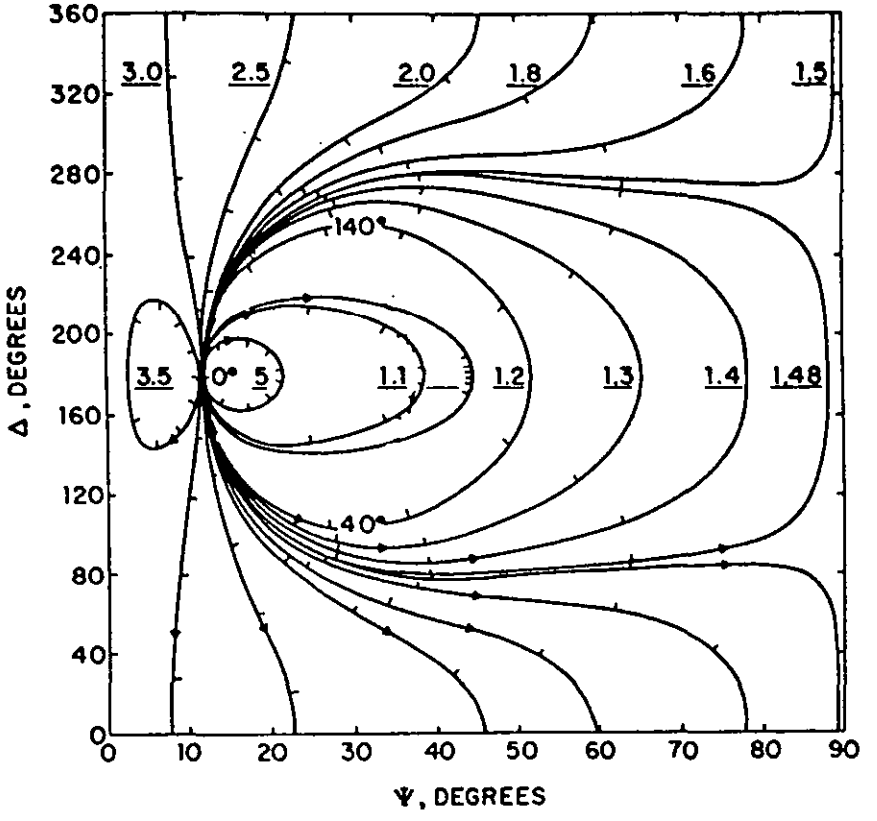

A_1 and P_2, A_2) which gave minimum detected light levels. There are 2 minima required; the first is found in the range $0 < A_1 < 90$ and $0 < P_1 < 140$ and the second is approximately at $A_2 = 180 - A_1$ and $P_2 = 90 + P_1$. Δ and Ψ are given by (Ref 2).

$$\Psi = \frac{180 - (A_2 - A_1)}{2}$$

and

$$\Delta = 360 - (P_1 + P_2)$$

The feature of this calculation is that the dependence on Δ is periodic as shown in Fig. 2 (RefS. 3 and 4), so that the solution is of the form $d = d + k \times \text{Period}$, where k is any positive integer. To obtain a unique value for d a second measurement is required and this can be obtained from stylus section 3.1 or by optical means as shown below.

3.3 The Spectrophotometer

A scanning spectrophotometer which covered the wavelength range of 170-2600 nm (model UV-VIS-NIR) was used. The explanation of this technique has been explored in references 5 and 6. This equipment was used on virtually all the coatings to provide details of the changing performance of the reflectance, transmittance and absorptance throughout the visible and near infrared spectrum to compare with changing deposition parameters.

Simplistically the optical transmittance T of a metal slab varies with thickness d as:-

$$T = T_0 \exp(-\alpha d)$$

where:

α = Absorption coefficient (Ref. 7)

$$= \frac{4 \pi k}{\lambda}$$

λ = Wave length.

k = Extinction coefficient (imaginary part of refractive index).

Assuming that d = R. t. Where R is the deposition rate and t is the deposition time , the deposition rate R can be found and hence the film thickness, d. For thicker transparent films the interference effects can also be seen. By measuring the transmittance on the spectrophotometer the interference maxima or minima occur when (Ref. 8) :

$$m.\lambda = n.d$$

where

n = The film refractive index

m = 0, 1, 2, 3, ...

In order to estimate the film thickness d from this method, several values for lambda (wave length) at maxima or minima is required. In our measurements 3 transmission peaks were enough to measure d. However, to find d from top equation m should be eliminated and the optical thickness nd can be found. From the measurement of n at 633 by the ellipsometer the film thickness can be found

3.4 The Film Resistivity

After measuring the film thickness d from the techniques mentioned above, the film resistivity (ρ) can be measured by:

$$\rho = d.R_S$$

where R_S is the film sheet resistance

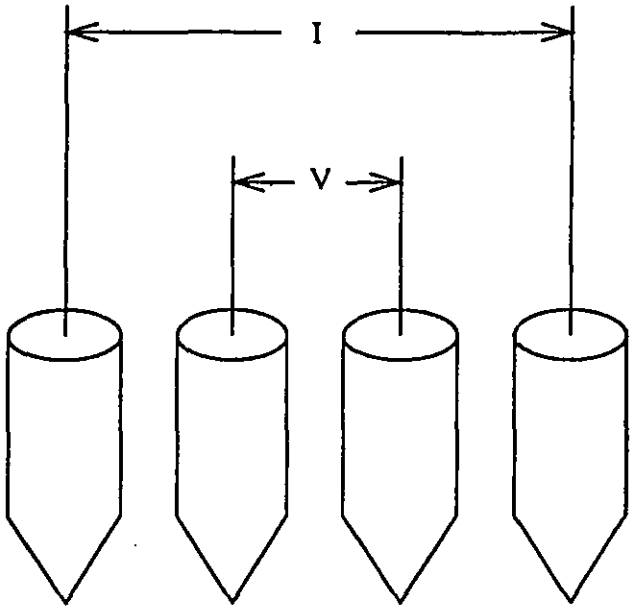

Fig. 3.3 Measurement of sheet resistance by a four probe method

By using a four point probe method (Ref. 4,9) R_S can be measured. These 4 probes are connected by springs which allow them to press against the film. The potential difference V is read between the inner probes while a known current I flows between the outer pair of probes and this allows the calculation of the surface resistance and therefore the film resistivity. Fig. 3 shows a schematic diagram for the four probe system. If the distances S between the probes are equal i.e $S_1 = S_2 = S_3 = S_4$ and S >> film thickness d, the sheet resistance can be obtained by the following equation:

$$R_S = \frac{V \pi}{I \ln 2}$$

3.5 References

1- K. L. Chopra, edt. "Thin Film Phenomena", Robert E. Publication, New York 1979.

2- Gaertner L117 Ellipsometer manual, 1977.

3- R. J. Archer, J. Opt. Soc. Am., 52 (1962) 970.

4- L. I. Maissel and R. Glang, edts."Hand Book of Thin Film Technology", McGraw-Hill Book, New York 1970.

5- R. A. Swady, "The development of vacuum technologies for the preparation of high purity thin films in simple systems", Ph. D thesis, LUT, 1992.

6- C. A. Bishop, " The deposition of coatings onto polymer substrate by planar magnetron", Ph. D thesis, LUT, 1986.

7- O. S. Heavens, "Optical properties of thin solid films", New York, 1954.

8- H. K. Pulker, "Coatings on Glass", Elsevier, New York, 1984.

9- Z. Surowiak, A. M. Margolin, I. N. Zatharchenko and S.V. Birgukov, Thin Solid Film, 176 ,(1989), 227.

CHAPTER-4

VACUUM CONSIDERATIONS

In this chapter the effect of residual gases (base pressure) on the plasma parameters, magnetron I-V characteristics and film properties and purity is investigated. In this part of investigation residual gas analysis (RGA) is used in order to study the base pressure components and then partial pressures. Coburn and Kay (Ref. 1) observed a number of ion species (H_2O^+, H_3O^+, H^+) due to the presence of residual water vapour. In the presence of a glow discharge, water molecular dissociation could happen (Ref. 2). As a result ions such as OH^-, O^+, O_2^+, O_3^+ may remain (Ref. 3). The ions present in the negative glow may reach the growing film with energies of at least a few volts (Ref. 4). In the case of the unbalanced magnetron, this energy is represented by the substrate floating potential (Ref. 5). In this investigation a batch bell-jar system is used. Its dimensions are 50 cm diameter and 60 cm height. It was pumped initially by a 1000 l/min mechanical pump and later by a diffusion pump. The RGA is connected through a tube in line with the middle of the vacuum chamber.

4.1 The Effects on Magnetron Potential

The impurities in plasma presented in UM glow discharge are found to effect the magnetron potential. In order to demonstrate this fact, magnetron potential characteristics have been studied with pumping time, with and without a nitrogen trap, with air and water vapour partial pressure as shown in Tables 1 and 2. The results were achieved with conditions of 1 A magnetron current and 2 mTorr argon pressure. The magnetron target was titanium. Table 1, column 1, shows that the magnetron voltage drops as the base pressure reduces with the pumping time. With the use of a liquid nitrogen trap (cryo-coil) (NT), the base pressure will fall about one order of magnitude for the same pumping

time. Water arrival rate at the coil is 15 L/sec/cm^2. Coil area was 500 cm^2. Considering the major condensable species as water and the sticking coefficient of 1, a pumping rate of 7500 L/sec can be achieved, which is larger than that of the diffusion pump by a factor of 100. The magnetron potential for this case is measured and shown in Table 1, column 2 to be compared with column 1. The pressure that is reached without using the NT in one hour can be reached in 20 min by using the NT. At 20 min pumping time the base pressure is reduced from 5×10^{-5} Torr to 1×10^{-5} Torr using the NT; the corresponding magnetron potential reduces from 398 V without NT to 378 with NT. Column 3 in Table 1 shows the effect of the pumping speed on the magnetron potential and the base pressure with the pumping time. In this case the diffusion pump port was reduced from 160 mm to 50 mm diameter. As shown in columns 1 and 3, the pumping speed has a significant effect on the magnetron process. At 20 min pumping time the total pressure difference between column 1 and 3 was 5×10^{-6} Torr. This small rise in the pressure, achieved by decreasing the diffusion pump port causes the magnetron potential to increase from 398 to 427 V. Also seen from column 3, in order to achieve the same base pressure of column 1, a longer pumping time is required.

To ensure that the voltage drop does not result from target sputter clean during the experiment, air and water were deliberately leaked to the vacuum chamber through a needle valve. Table 2 illustrates the magnetron potential and the total base pressure with different air and water partial pressures. Air admitted to the chamber when the base pressure was 10^{-6} Torr, water partial pressure was 4.125×10^{-8} Torr, and the magnetron voltage was 330 V. As can be seen from column 1 the magnetron voltage increases with increasing air partial pressure. If the pressure reached the same value of 20 min pumping time (3×10^{-5} Torr) the magnetron voltage reads 352 V; which is dissimilar to that at 20 min pumping time (398 V). By admitting water to the vacuum chamber the effect

Table 4-1 The effect of pumping time (base pressure) on magnetron characteristics for: 1)without nitrogen trap, 2) with nitrogen trap and 3) with lower pumping speed

	(1) without nitrogen trap		(2) with nitrogen trap		(3) with smaller diff. pump port diameter	
Pumping Time Min	Base Pressure Torr	Magnetron Voltage V	Base Pressure Torr	Magnetron Voltage V	Base Pressure Torr	Magnetron Voltage V
20	3×10^{-5}	398	1×10^{-5}	378	3.5×10^{-5}	427
40	1.8×10^{-5}	372	4×10^{-6}	354	2×10^{-5}	390
60	1×10^{-5}	360	2.8×10^{-6}	348	1.2×10^{-5}	375
90	7×10^{-6}	352	1.8×10^{-6}	342	8×10^{-6}	363
120	5×10^{-6}	346	1.6×10^{-6}	339	6×10^{-6}	358
150	4×10^{-6}	343	1.5×10^{-6}	336	4.8×10^{-6}	354
180	3.2×10^{-6}	341	1.1×10^{-6}	335	4×10^{-6}	351
240	2.7×10^{-6}	335	1×10^{-6}	334	3.4×10^{-6}	347
300	2×10^{-6}	330	1×10^{-6}	333	2.8×10^{-6}	340

Table 4-2 The effects of air and water partial pressure on magnetron characteristics.

(1) Air			(2) Water		
Air Partial pressure Torr	Base pressure Torr	Magnetron Voltage V	Water Partial Pressure Torr	Base Pressure Torr	Magnetron Voltage V
$4x10^{-9}$	$1x10^{-6}$	330	$4.12x10^{-8}$	$1x10^{-6}$	330
$7.2x10^{-8}$	$1.5x10^{-6}$	330	$1.35x10^{-7}$	$1.5x10^{-6}$	333
$1.8x10^{-7}$	$4x10^{-6}$	334	$5.25x10^{-7}$	$4x10^{-6}$	337
$1.17x10^{-6}$	$8x10^{-6}$	337	$1.17x10^{-6}$	$8x10^{-6}$	346
$1.6x10^{-6}$	$1x10^{-5}$	339	$1.6x10^{-6}$	$1x\ 10^{-5}$	353
$4.35x10^{-6}$	$3x10^{-5}$	352	$4.35x10^{-6}$	$3x10^{-5}$	394

becomes clearer as shown in Table 2 column 2. By increasing the water partial pressure to the same level of 20 min pumping time the magnetron voltage will read the same value as that measured at 3×10^{-5} Torr (see Table 1, column 1 and Table 2, column 2). The conclusion of this particular work is that the base pressure has a significant effects in magnetron potential. All the voltage measurements have been taken after 10 minutes running, because major target sputter cleaning occurs in this time. The titanium target used in this experiment was sputtered clean and was not exposed to the atmosphere for a long time. Fig. 1 shows the magnetron voltage with the running time for 1 hour and 8 hour pumping time. As can be seen from this Figure the maximum drop in magnetron voltage occurs in the first 5 minutes. This measurement has been taken for target current 1 A. Similar results were seen when 2 A target current was used.

With the use of new targets, especially for materials like aluminium or titanium, the arcing problems on the magnetron target caused by the oxide layer often happen. A target sputter clean could take a long time, depending on the surface compounds of that target and the thickness of the oxide layer. The consideration of base pressure in this case is very important. By reducing the base pressure less oxygen interaction with the target material will occur, which in turn depending on the circumstances of target surface, the sputter clean can be started immediately without any arcing. If the target surface has a greater oxide covering, reducing the base pressure will at least reduce the oxygen contamination rate, discouraging arcing on the magnetron. This will help to initiate the magnetron for sputter cleaning.

4.2 Plasma Parameters

A planar probe of 1 cm^2 area was used to measure the ion current density at a probe bias voltage of -100 V and at the floating potential of the substrate. The use of this technique showed no major effects in the plasma parameters with reducing base pressure, i.e the

Fig.4.1 Magnetron voltage variation with the running time for two pumping periods(Magnetron current was 1A).

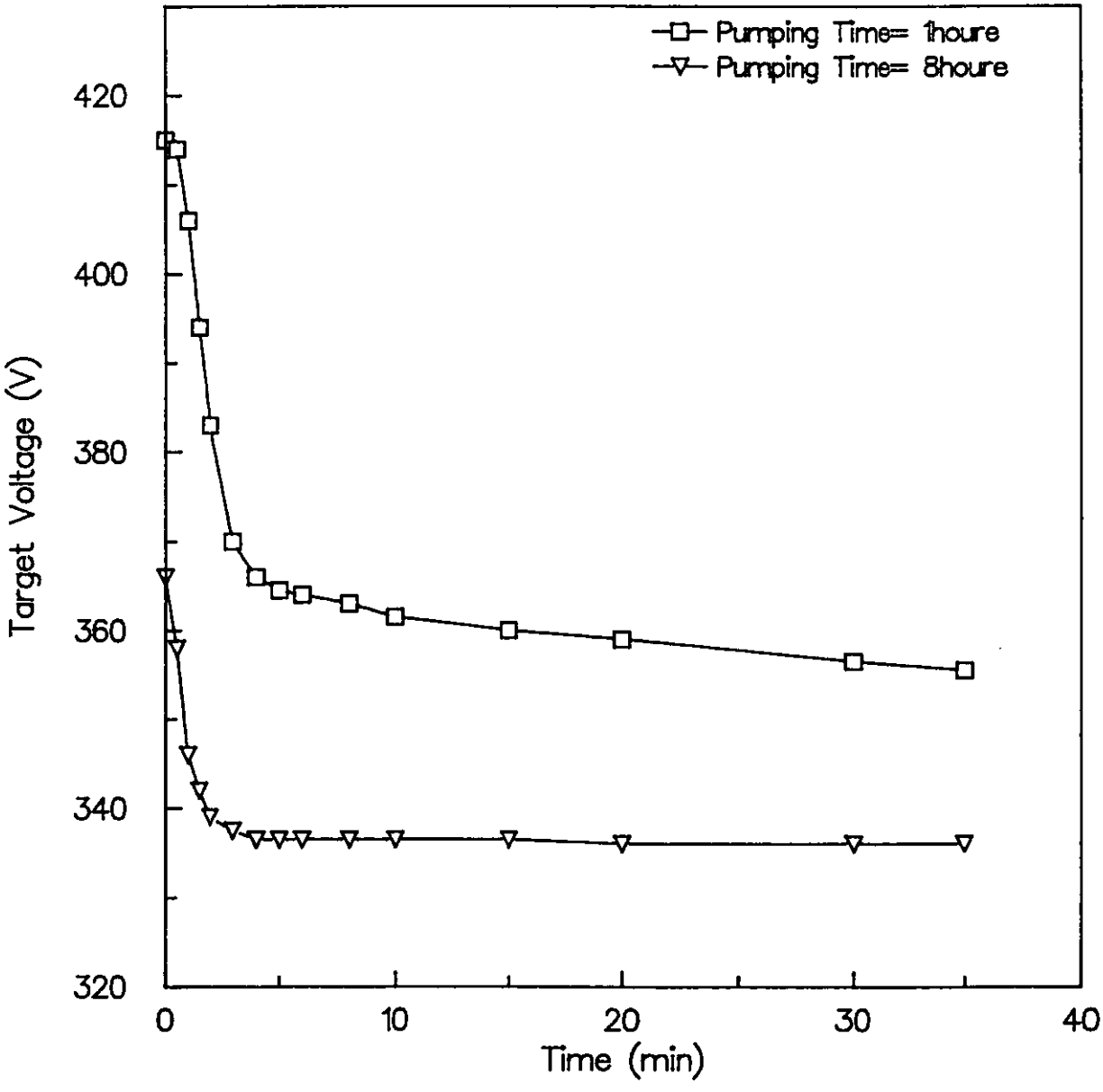

floating potential and the ion currents are almost constant with pumping time. The probe reading gives a floating potential of 35 V and ion current density of 10.2 mA/cm^2, taken for target current of 1 A and argon pressure of 2 mTorr.

In order to investigate the consequences of residual gases in the presence of the glow discharge, a special plasma diagnostic is required. The probe used in our experiment is not sufficiently sensitive to estimate the changes in the plasma parameters, especially in this range of H_2O and O_2 partial pressure. At this stage the argon ions will dominate the probe reading especially with 1 cm^2 probe area.

4.3 Impurity and Film Properties

In diode sputtering, the presence of a residual gas, such as hydrogen (Ref. 4), can produce a significant change in the sputtering rate, because of the different sputtering yields, and the changes this causes in the deposition rate. Westwood and Boynton (Ref. 6) reported that the sputtering rate increased by 20% as the hydrogen partial pressure decreased during prolonged sputtering of tantalum and platinum targets in argon. In magnetron sputtering there are no significant changes in the sputtering rate of the titanium target when reducing the base pressure.

In order to investigate the effect of residual gases on film properties, electrical sheet resistance has been measured for a set of samples. Titanium films were deposited on glass substrates with a magnetron current of 1 A and an argon pressure of 2 mTorr. Fig. 2 shows film sheet resistance as a function of the pumping time (base pressure) without using the nitrogen trap, then using the nitrogen trap, and with low pumping rate (pressure gradient effects). As can be seen from this Figure the major effect appears when the base pressure is high (at 20 min pumping time). By using the nitrogen trap the film sheet

Fig.4.2 The effects of the vacuum conditions on the Ti film properties.

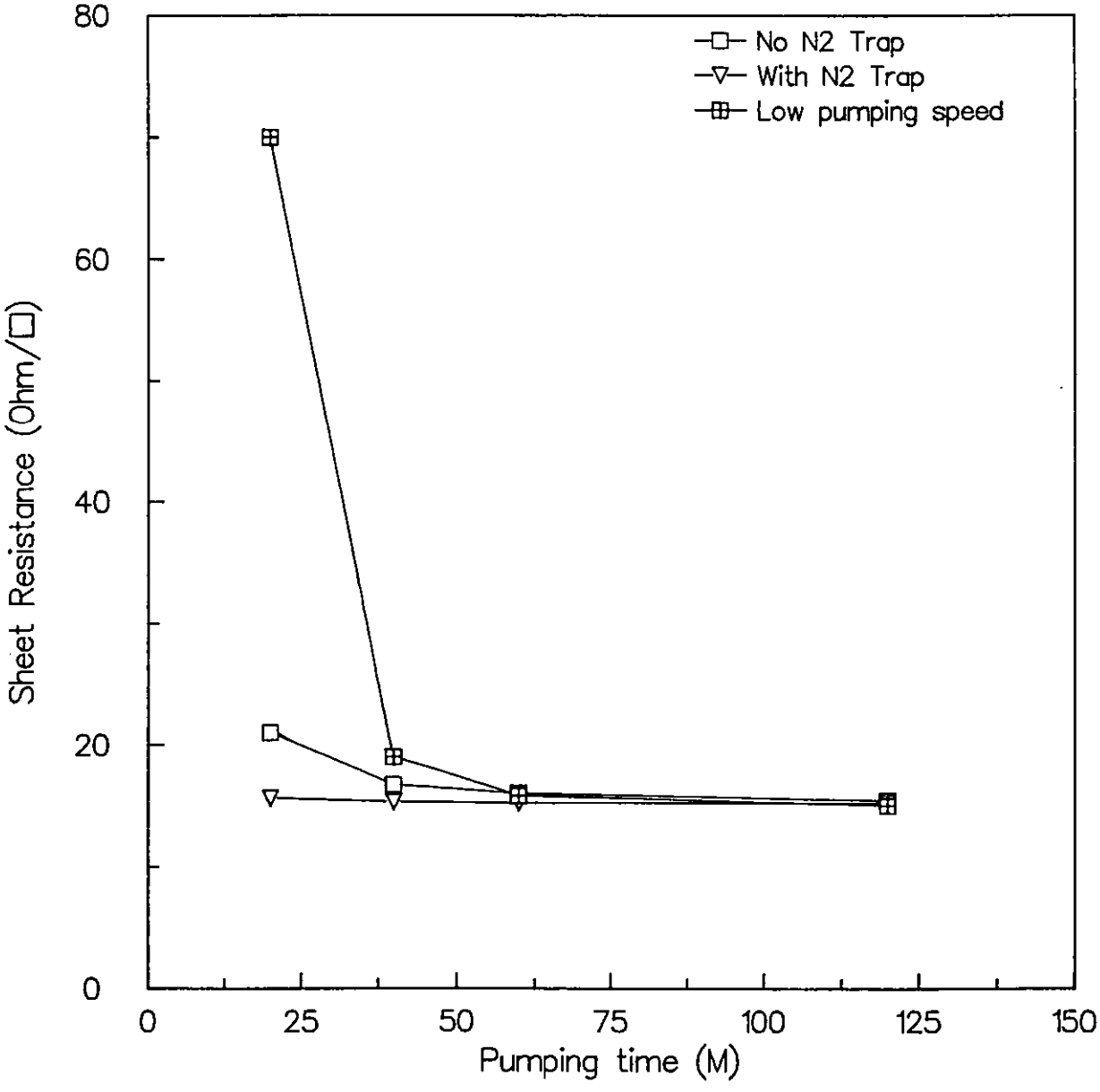

resistance is less affected, because within 20 min pumping time the NT reduces the base pressure to the same level of one hour pumping time. The advantages of using the NT is not only to save time, but during deposition much outgassing could take place, resulting from plasma/wall interaction or from other effects. So, the presence of NT will keep the pressure at the same level by condensing the water vapour that is released from the wall (water vapour is the major part of the outgassing).

The self gettering process is very useful for reducing the base pressure, especially for long process times. We have seen the chamber base pressure reduced from 3×10^{-5} to 6×10^{-7} Torr during a one hour TiN deposition .

The gettering processes can be more effective when the sputtering power is increased. Fig. 3 shows the film resistivity as a function of magnetron current. This Figure demonstrates that the resistivity reduces as the magnetron power increases and keep constant after a certain power level.

As can be seen from Fig. 2, the film purity plays a significant role in controlling the film properties. The film purity can be estimated by calculating the sputter metal to gas arrival rate ratio.

$$\text{Purity} = \frac{V_m}{V_g}$$

where:

V_m = Metal arrival rate

V_g = Incorporation gas atom arrival rate

V_m can be determined from the sputtering rate of the used target as follows:

$$V_m = \frac{R\,\rho}{M}\,Av$$

where:

ρ = Density

R = Deposition rate

M = Molecular mass in amu and

Av = Avagadro's number

V_g can be calculated from the H_2O and O_2 partial pressures. In this case the arriving gas atoms may not all be incorporated in the deposited film. Hence this number should be multiplied by the sticking coefficient of that gas. Then from the kinetic gas theory V_g will have the following formula: (Ref. 7),

$$V_g = 2\,\alpha\,P\,(2\,\pi\,m\,k\,T)^{-0.5}$$

where:

α = The sticking coefficient of the ambient gas

P = The partial pressure of the ambient gas in Pa

m = Molecular mass of gas

k = Boltzmann's constant

$= 1.38 \times 10^{-23}$ J/K

T = Absolute gas temperature in Kelvins

The O_2 sticking coefficient in many cases is found to be around 0.054 (Ref. 8); in this reference the Auger depth profile of oxygen was used to estimate the relative oxygen

Fig 4.3 The effects of magnetron current on film resistivity.

Fig.4.4 The effects of vacuum conditions on the film purity.

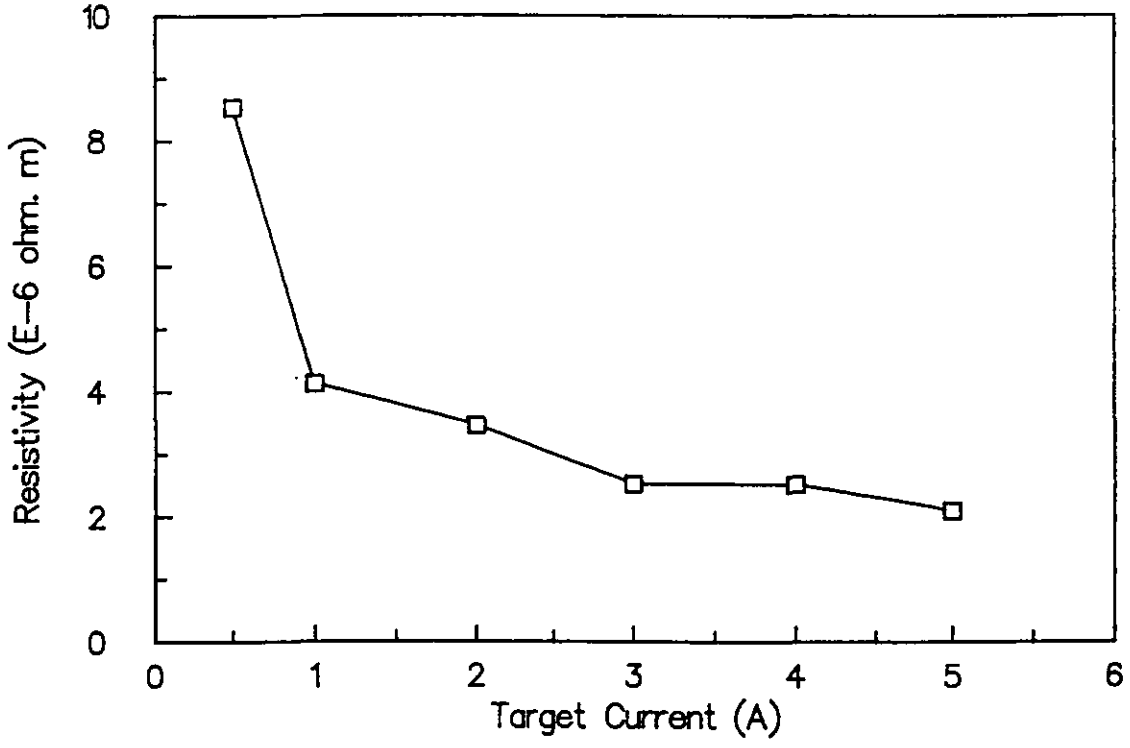

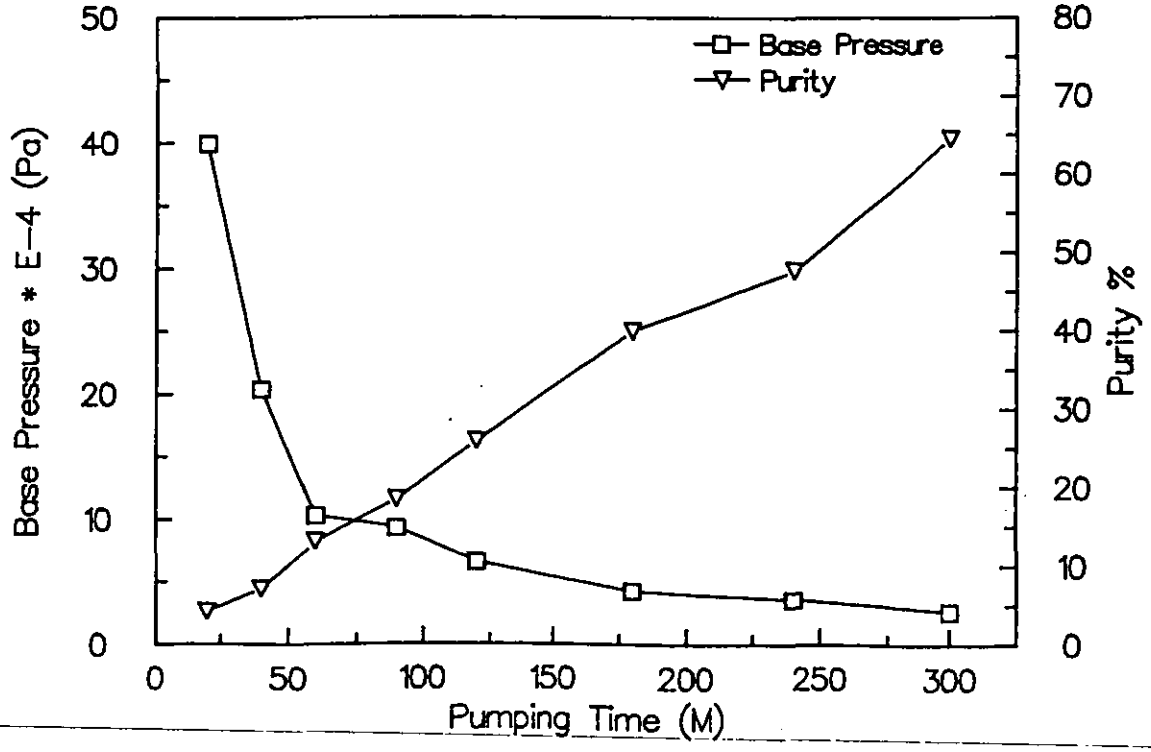

concentration on the aluminium film. By introducing some extra calculation concerning the experimental parameter they found that (α) = 0.054. For reactive In_2O_3 sputtering the oxygen utilisation is found to be around 0.05 as well (Ref. 9). However, the film purity can be simply calculated as shown in Fig. 4. This curve concerns, the data illustrated in Table 1 column 1 and the film data of Fig. 2 when no nitrogen trap is used. Since the deposition rate is constant, V_m will not change, so that, as shown in Fig. 4 the film purity will be affected only by the base pressure.

By increasing the magnetron power the deposition rate, in turn, will increase. Hence, the arrival target atoms rate in this time will be higher. If we assume the base pressure is kept constant in the case of Fig. 3, by repeating the purity calculation the expected result shows that the film purity will increase as the deposition rate or the magnetron power increases. That makes the film resistivity decreases with increasing the target current. This is almost consistence with the work done by Popov et al (Ref. 8). In their experiment they have demonstrated that O_2 concentration in a deposited aluminium film reduces with increasing magnetron power.

In another using a load-lock system, the oxygen incorporation in deposited silicon film (analysed by Auger system) is shown to be zero (Ref. 10).

Conclusions

In summary, the salient points of this chapter are that;

1- the chamber pressure has a large influence on the I-V magnetron characteristics.

2- the chamber pressure plays a significant roll in controlling the film impurity level and hence its properties.

4.4 References

1- J. W. Coburn and E. Kay, Solid State Technology, 14, 12 (1971) 49.

2- A. G. Spencer, personal communication, Physics Dept., LUT.

3- C. R. Aita, and M. E. Marhic, Vacuum, 38 (1988) 37.

4- W. D. Westwood, "progress in surface science", V. 7, P. 71, Pergamon press, UK, 1978.

5- B. Window and N. Savvides, J. Vac. Sci. Technol., A 4, (1986) 453.

6- W. D. Westwood and R. J. Boynton, J. Appl. Phys., 44 (1973) 2610.

7- L. G. Carpenter, "Vacuum technology", Adam Higler, Bristol, 1983.

8- D. N. Popov, Tz. K. Kotlarova, Tz. D. Uzunov and V. N. Gaydarova, Vacuum, 38 (1988) 1015.

9- A. G. Spencer, "High rate reactive magnetron sputtering", Physics, Dept., LUT, 1989.

10- G. W. Hall, personal communication, Physics Dept., LUT. 1992.

CHAPTER-5

SUBSTRATE EFFECTS FROM UNBALANCED MAGNETRON

Ion bombardment is not a general feature of all magnetron sources. The unbalanced magnetron has been intentionally designed to provide an ion bombardment of the growing film (Refs. 1-3). This chapter will concern the unbalanced magnetron design, performance in terms of ion and electron bombardments at the substrate and the heat load delivered to the substrate compared with that of an I-V plasma curve. The measurements concentrate on the bombarding properties of magnetrons important for thin film growth; namely the ion current on the substrate and the self-bias voltage acquired by a floating substrate. The radial distribution and pressure dependence and oxygen usage at a typical source to the substrate distance are also explained. Finally the use of this magnetron to deposit TiN and ITO are studied.

5.1 Unbalanced Magnetron Design and I-V Characteristic

The unbalanced dc magnetron of 80 mm diameter chosen for our studies is shown, with its magnetic configuration and probe circuit in Fig 1. The unbalanced magnetic field configuration is made by adding an extra fringing field to the usual magnetron trap or tunnel. The simple way to achieve the unbalanced design is to place significantly more magnet poles on the outer magnetic ring than in the centre. The motion of the secondary electrons in the unbalanced magnetron field is more complex than in the balanced situation. The electrons are trapped initially by the magnetron tunnel, and move back and forward along field lines while drifting around the track. Within the sheath, there will be the ExB drift, and out in the body of the plasma, where the electric field will be small, there will be both grad B and curvature drift components. After suffering many ionising collisions, the secondary electrons will leave the primary magnetron trap, to enter the fringing field

Fig.5.1 Lay out for the used unbalanced magnetron.

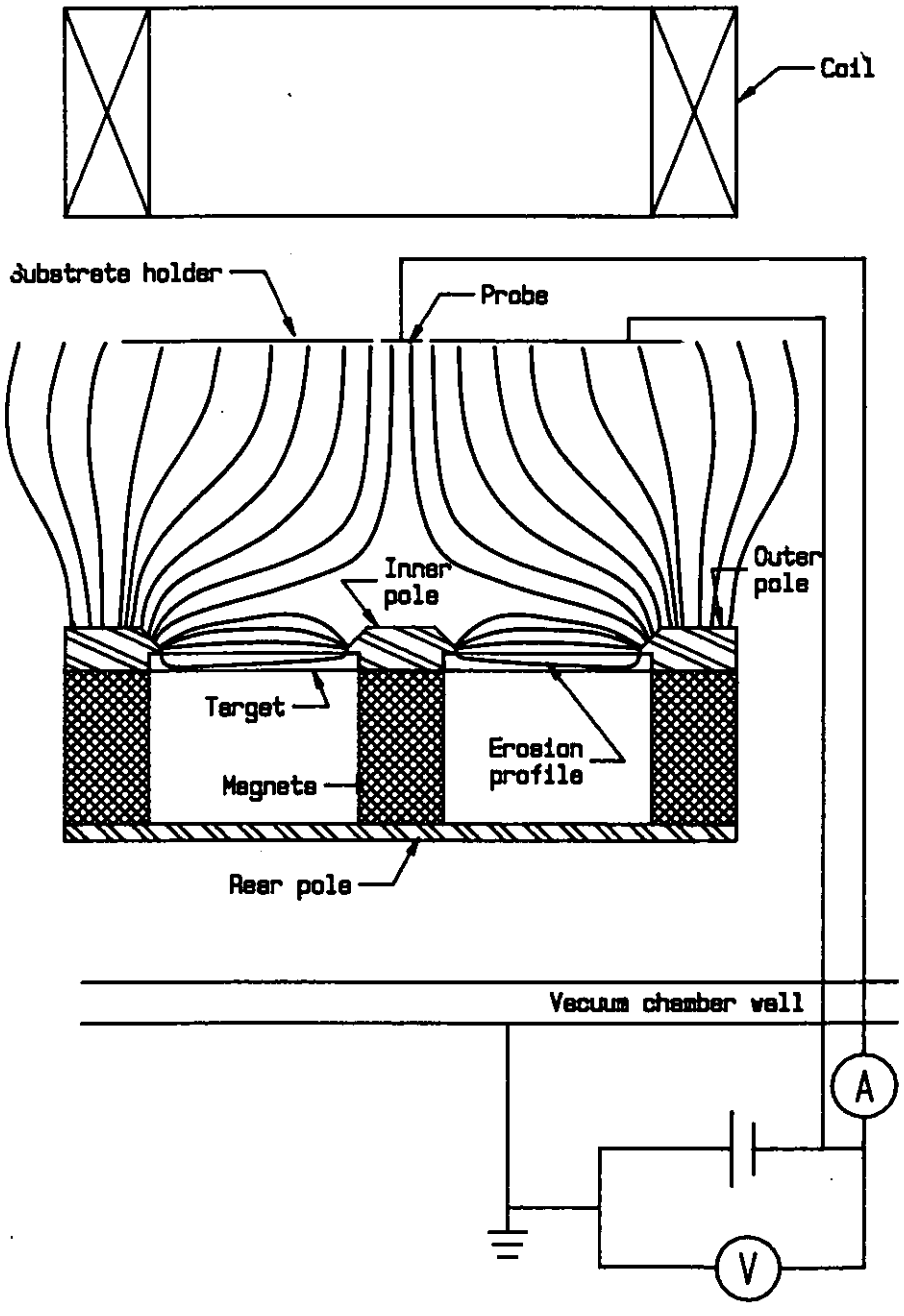

region. Although the field in this region is small, perhaps only 30-50 Gauss, the electrons have little energy, typically 50 eV, so such fields are sufficient to prevent the electrons moving across the field lines to the chamber walls or the anode. The field configuration is a magnetic bottle, with an electrostatic reflector (the cathode) at one end. To leave the trap, the electrons have to move towards the substrate.To maintain electrical neutrality in the conducting plasma, the ions move with the electrons towards the substrate.

Unbalanced magnetron can be also identified by a stream of visible plasma following the magnetic bottle shape from the target to the substrate. This enhanced emission could be of interest in optical rate control technology, as the sputtered atom flux can be more readily measured at the substrate.

5.1.1 I-V Magnetron Characteristics

By using an MDX magnetron drive, there are three options for setting the magnetron power. These are, voltage, current and power. By fixing the magnetron current constant, the voltage will be an available parameter. Hence, by controlling the magnetron at a constant pressure, the I-V characteristic for this magnetron can be determined. The relations are shown in Fig. 2. Current-voltage relationship in a magnetron has been empirically found to be (Ref. 4):

$$I = K V^n$$

where k is a constant and the exponent n is in the range of 1 to 15. The constant k and the exponent are dependent on the type of magnetron used, the cathode, and the gas species and pressure. Other effects can be seen as a result of thermalization of the sputtered atoms. In general, there is a decrease in the sputtered atom energy as a result of either

Fig.5.2 Magnetron I-V characteristic for different argon pressures.

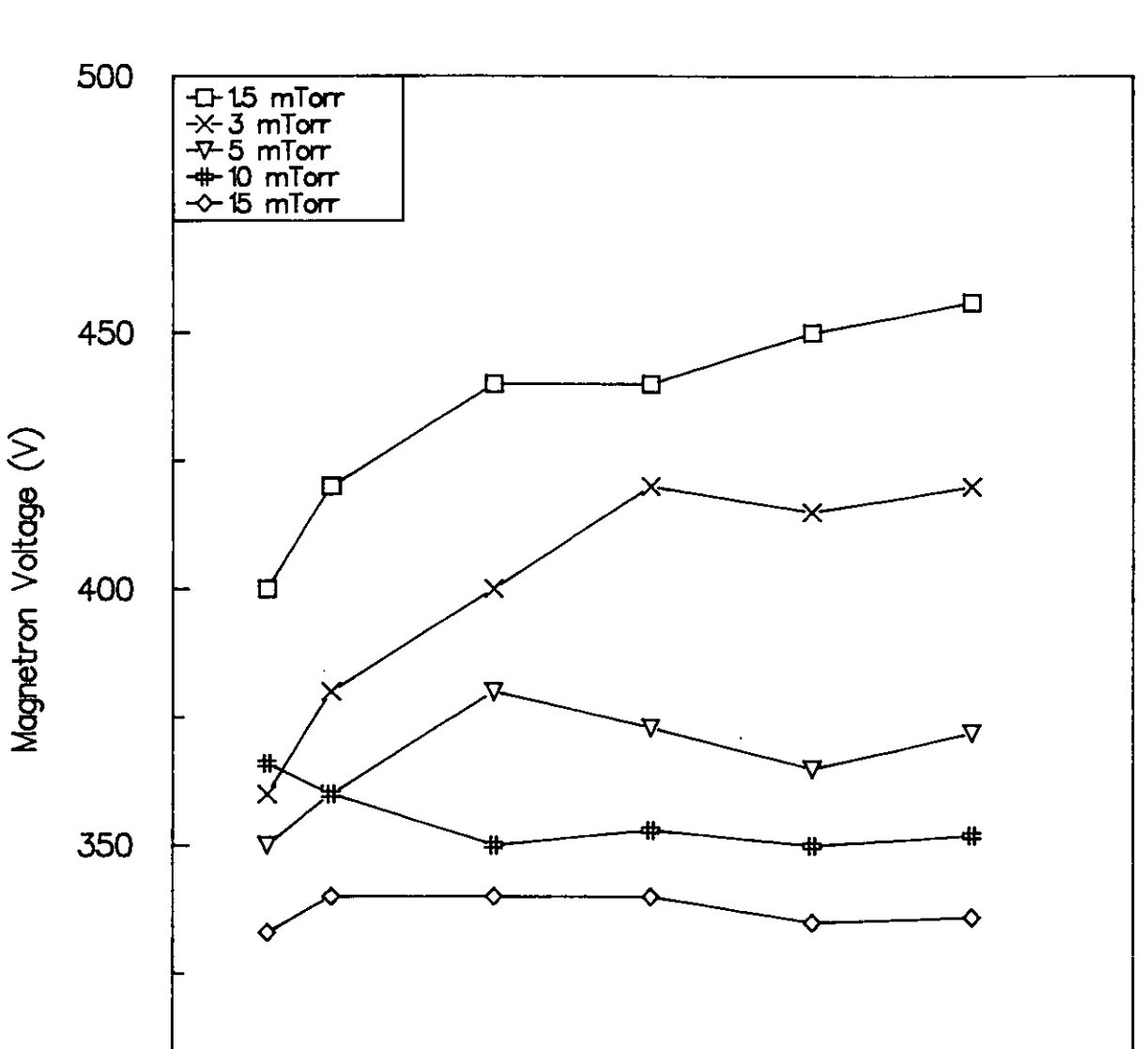

increasing pressure or cathode-to-substrate distance. During this process, however, significant amounts of thermal energy are transferred to the gas atoms, and their temperature can rise significantly (Refs. 5,6). As a result, the local density near the cathode can decrease. The effect is strongly dependent on the thermal conductivity of the gas, the sputter yield of the target, and the applied discharge power. The local reduction in gas density near the cathode has a number of significant implications for the plasma, as well as the deposition process. Ions in the plasma are created by ionization of the background gas. Reducing the local gas density by sputtered atom heating results in a more resistive plasma. This effect has shown to be dominant in setting the current-voltage relationship of the magnetron (Ref. 7).

In our experiments, the magnetron characteristics have been measured for different target materials, such as Cu, Al and Ti. The results are shown in Fig. 3. The higher the target sputter yield, the more magnetron voltage can be reached. This agrees with that determined by Rossnagel and Kaufman (Ref. 7). The magnitude of sputtered atom heating, therefore, plays the major role in determining the effective impedance of the plasma. Hence, the I-V magnetron properties can be strongly altered by changing the cathode material or the gas species. The latter has not been investigated in our experiment, we have used only argon as a working gas. In general, the I-V relation has a higher exponent n in cases where the gas rarefaction effect is weakest. This would occur for cases of low sputter yield (Ti, Al). The exponent n is smallest for cases of high sputter yield (Cu). The rarefaction of gas near the magnetron cathode has other effects. The emission of light from the plasma becomes nonlinear at high discharge currents, primarily because of the depletion of gas species (Ref. 8).

Fig.5.3 Magnetron I-V characteristics for different target materials.

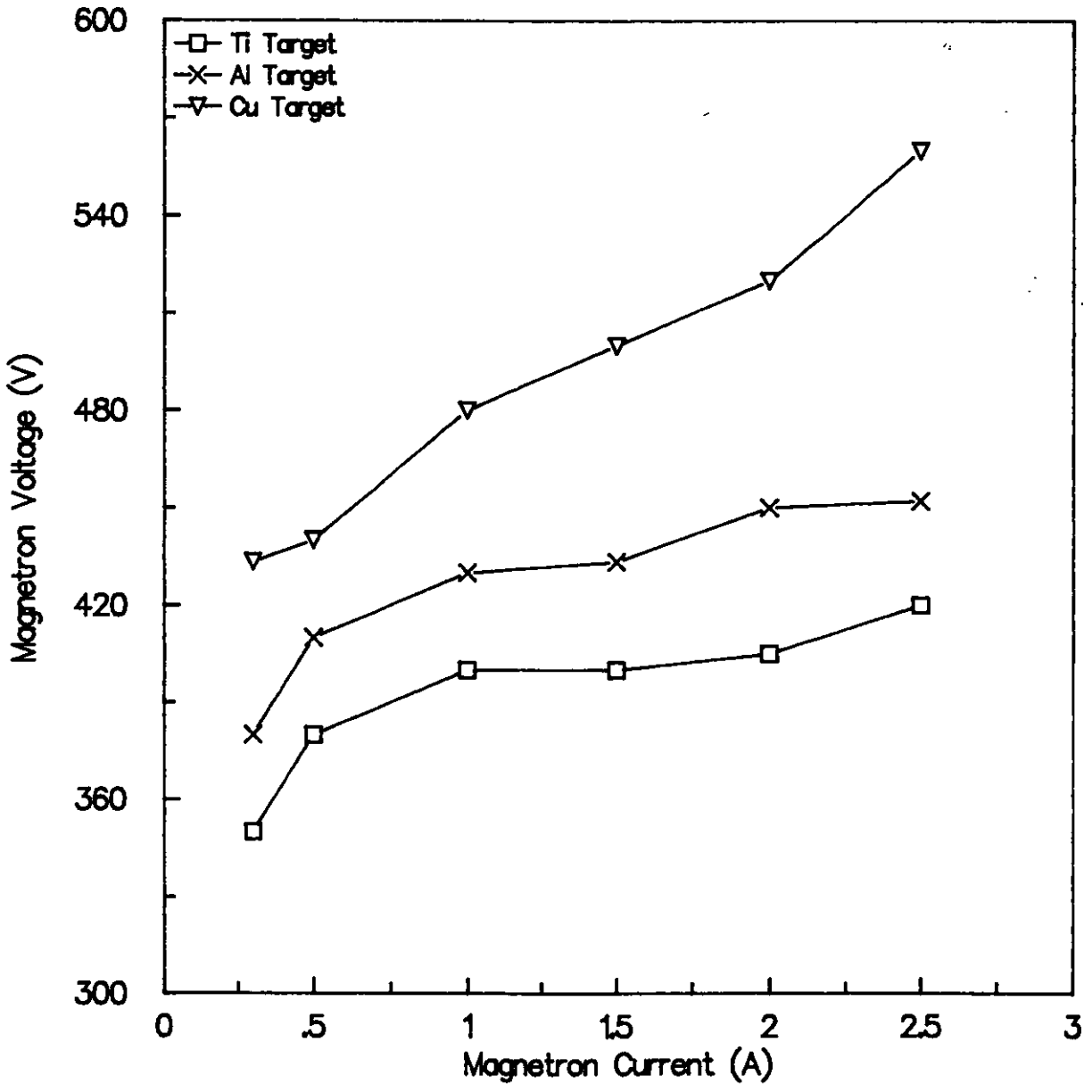

5.2 Magnetron Efficiency

Sputtering is a low temperature process. In fact, heating of the target, even if localised, can lead to evaporation of material, which is a totally different process and generally unwelcome. In order to keep the target cool, the heat generated by the discharge must be removed by water circulation. The energy dissipation of the target (Fig. 1) into the cooling water, the substrate and the plasma, was measured for a 2.2 A discharge current (Ref. 9). Platinum resistance temperature detectors were used to measure the heat losses into the cooling water; they were placed in the inlet and the outlet water pipes of the magnetron. Four-wire sensor operation was used to obtain maximum accuracy. Vacuum operation prevents any significant losses either by convection, so the energy that went into the cooling water can be calculated. The amount of heat that will be removed from the sputtered target can be calculated by the following equation:

$$Q = F\, c\, \rho\, \Delta T$$

where:

ρ = Water density

F = Water flow rate

ΔT = The increase of water temperature

c = The specific heat of water

By measuring the water flow rate and the temperature difference the removed heat can be calculated. It was equal to 82% I.V i.e.

$$Q = 0.82\ I.V$$

where:

I = Magnetron current in A

V = Magnetron voltage in V

By using glass substrates the total sputtered mass was measured; hence the total heat due

to condensation of atoms was calculated, and equalled 20% of the substrate heat. By using a movable planar probe the total energy delivered to the substrate was measured by integrating over the whole area in front of the target. The total energy that went into the substrate, including the heat of condensation, was 3% of that supplied. The rest of the energy was assumed to go into heating the plasma. The maximum power at which any magnetron can be operated depends on the efficiency of its cooling system.

5.3 Ion Current and Floating Potential

A simple planar probe of 1 cm^2 area has been used to measure substrate effects. This was used with coaxial shields at the probe edges connected to the probe potential, to reduce the edge effects (see Fig. 1). The probe was positioned on the centre-line of the target, where the dense beam of plasma is created, at a distance of 70-80 mm from its surface. Ion current density and substrate self-bias voltage have been measured for different argon pressure and for different magnetron current. These are demonstrated in Figures 4,5 and 6. Generally, the ion current increases with increasing magnetron current and with decreasing argon pressure. The floating potential increases as the argon pressure decreases, whilst almost keeping constant with the magnetron current.

The self-bias voltage is important in thin film deposition because it gives the potential reached by an insulating substrate. The growing film will then be bombarded with ions of energy equal to their charge times the voltage difference between the self-bias potential and the plasma potential, and by an equal flux of electron. From I-V plasma characteristics, the plasma potential was found to be close to ground potential. If there is no sputtered particle-gas ion collision near to the substrate surface, the floating potential will represent almost the incoming ion energy. This assumption is experimentally confirmined in the next section. From the magnetron I-V characteristics, the operating voltage for target and gas combinations is affected slightly by increasing the cathode

Fig.5.4 Argon pressure effects on the ion current density (magnetron current 500 mA).

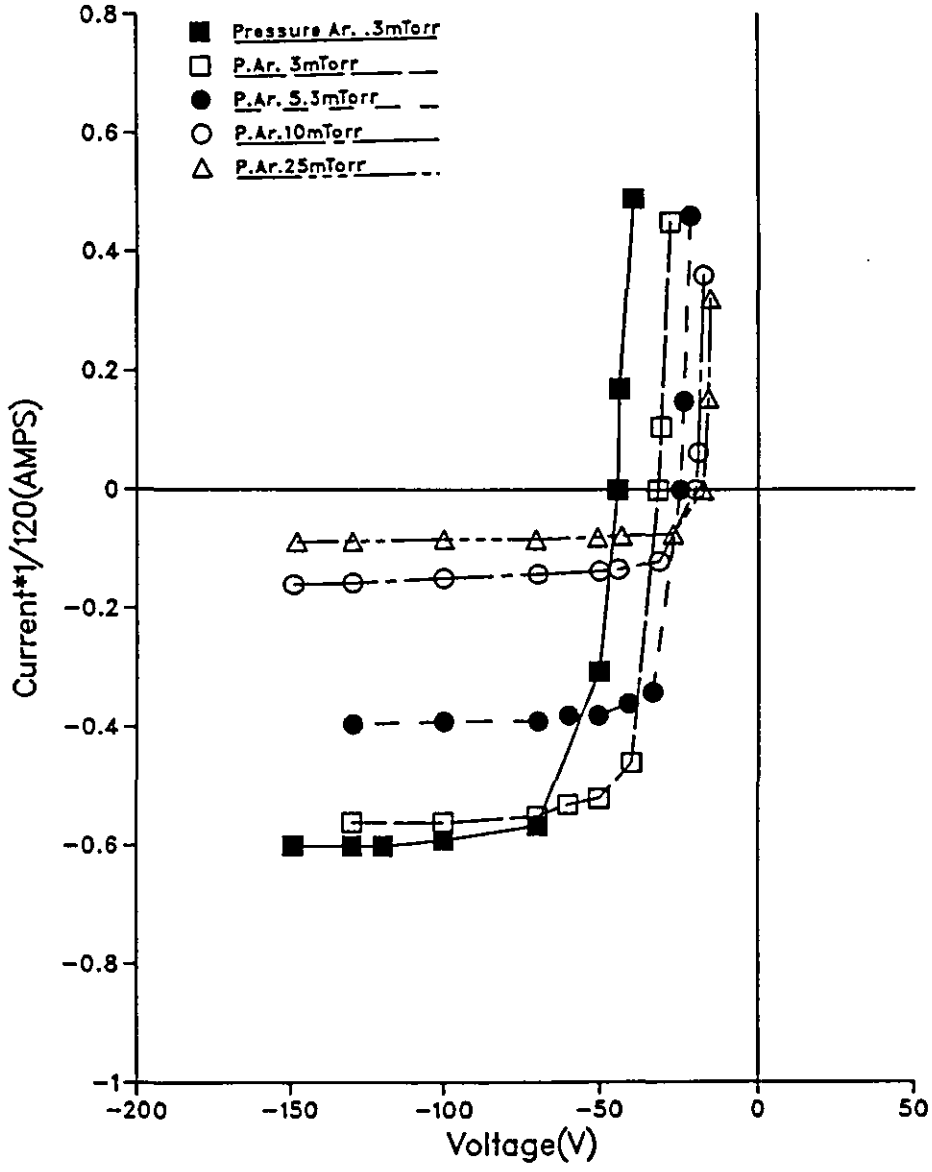

Fig.5.5 Ion current density measured with different magnetron currents and argon pressures.

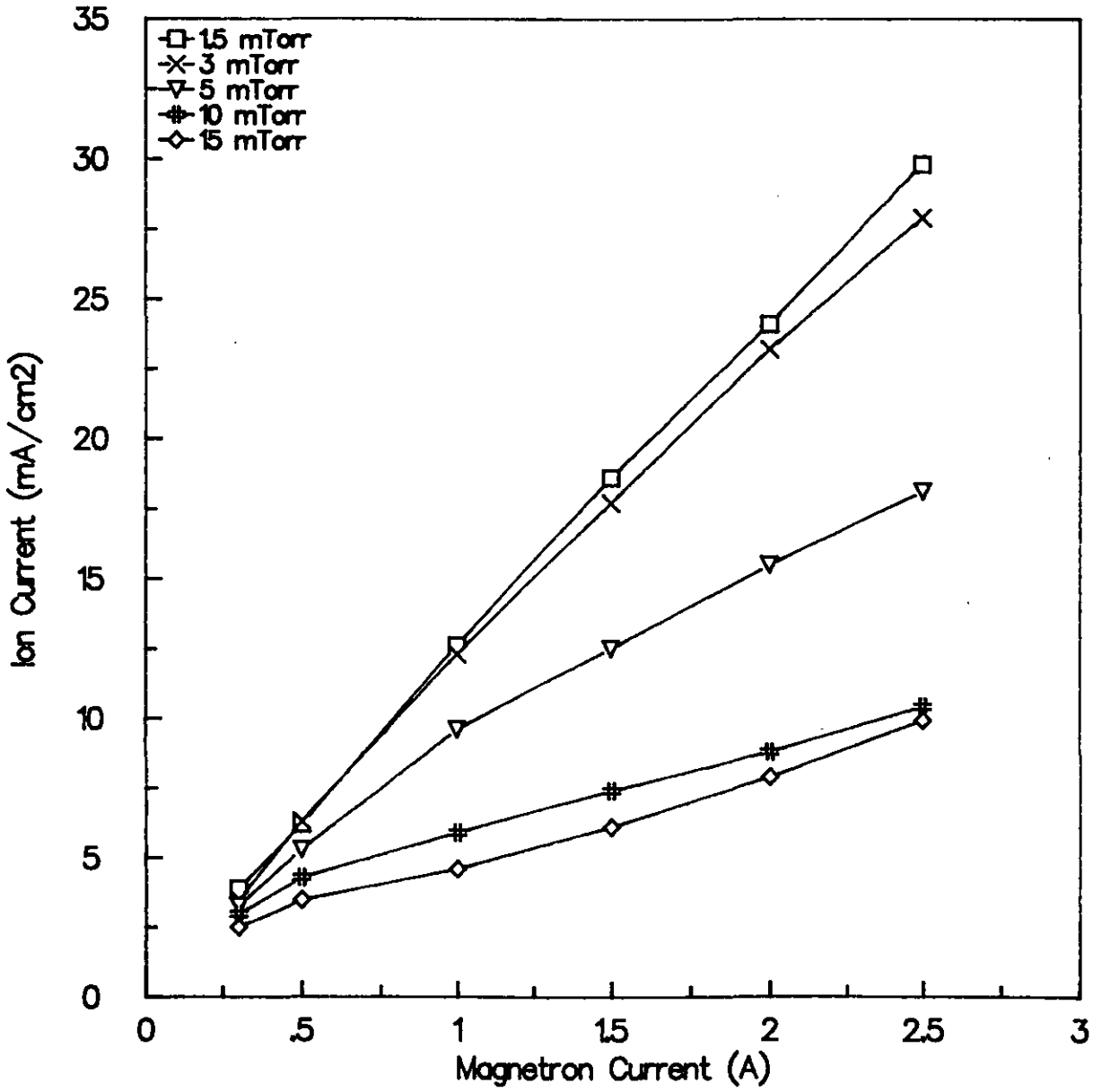

Fig.5.6 Substrate self-bias measured with different magnetron currents and argon pressures.

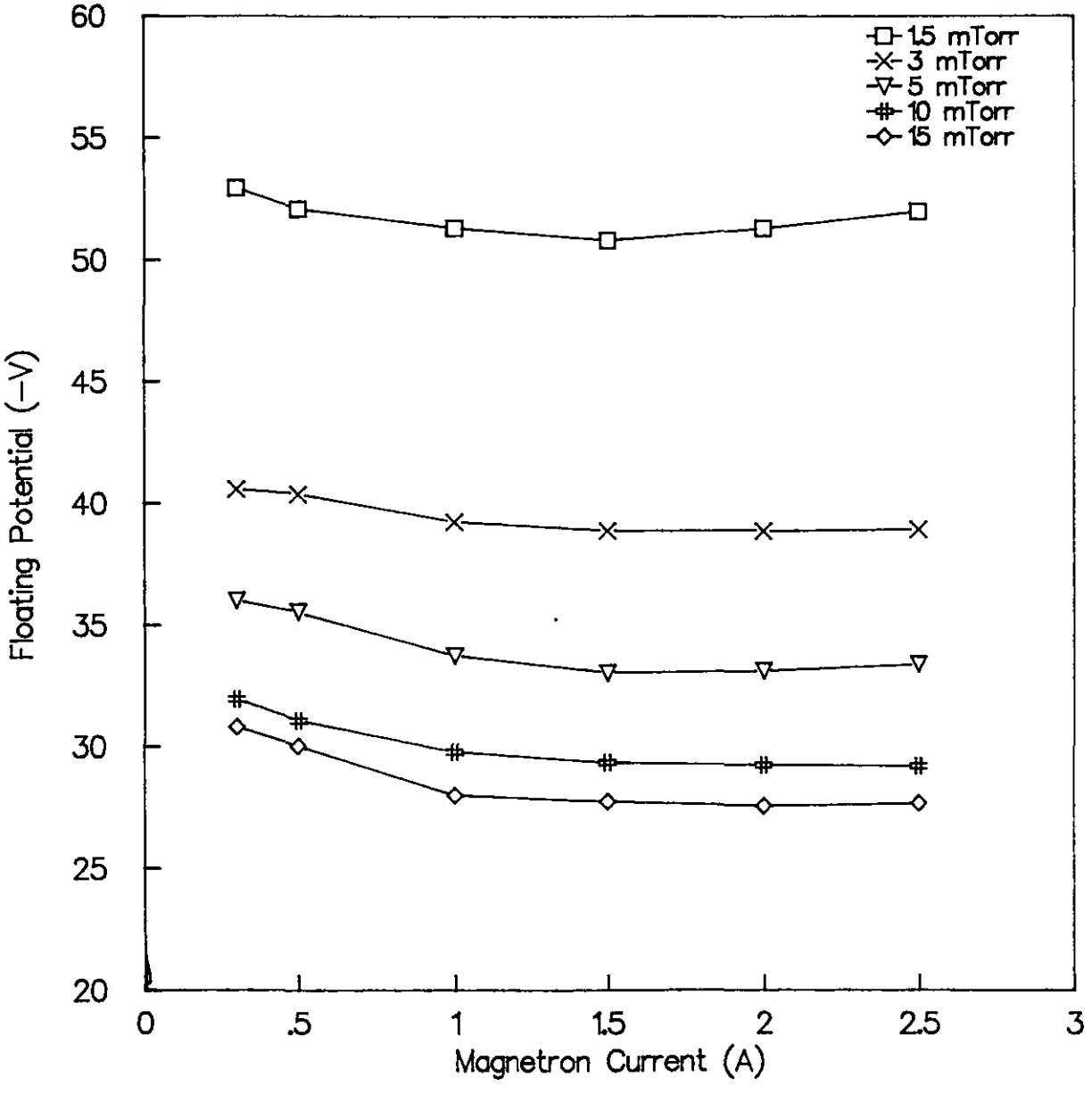

current. Thus the energy of the secondary electrons entering the plasma is approximately constant. In this case, as observed the floating potential will be fairly constant or unaffected by increasing the magnetron current. As the pressure decreases, a longer electron mean free-path will be obtained and less elastic scattering will take place. Therefore higher energy electrons will arrive at the substrate and in turn the substrate self-bias voltage will increase (Figs. 4 and 6). Ion current measurements yield different observations as the pressure decreases, the probability of ionization in the plasma decreases, as does recombination and charge exchange. The probe ion current will increase for a constant magnetron current (Figs. 4 and 5). This situation is different if thermionic cathode (hot filament) is used as will be shown in chapters 8 and 9.

5.4 Heat Load Measurement

The understanding of the various components of the cathode heat flux can also provide further understanding of the film growth environment, and for this purpose the combined heat-flux and probe current characteristics are useful (Ref. 9). For such investigations a calorimeter probe has been widely used in thin film processing (Refs. 10-12) and in many plasma reactors (Refs. 13,14). In the latter case it is used as a technique to determine the ion energy in the plasma (Ref. 15). Under steady state process conditions, energy is put into the substrate from plasma-surface interactions involving etching, deposition, recombination of radicals, electron and ion bombardment, and kinetic energy of fast neutral gas atoms.

In our experiments, the same probe described in the previous section is used. This probe was of low thermal capacity, made of stainless steel, and was used to record the initial rate of change temperature through a thermocouple welded to its back surface, from which the absorbed power density could be calculated. The power flow to the probe is approximately given by:

$$P = m\, c_p \frac{dT}{dt}$$

where:

m = The total mass

c_p = The probe specific heat capacity

By measuring the temperature history, then, P can be calculated. Fig. 7 shows the current flow to the probe as a function of negative bias, with the magnetron operating at 3 mTorr argon pressure with a target current of 500 mA. also shown is the heat loading resulting from the bombardment. The initial rate of the temperature rise was measured, rather than using the equilibrium temperature, in order to eliminate the complications of energy exchange by thermal radiation (Ref. 16). At zero net current to the probe the ion current will be approximately that which is measured at -100 V bias, and the electron current will be equal to it, so that from the current shown in Fig. 7 we have estimated the ion bombardment of the substrate, and the heat load at self-bias which was -27 V. These were 3.5 mA/cm^2 and 100 mW/cm^2 respectively. As shown in Fig. 7, the measured rate of energy dissipation in the substrate increases with increasing negative bias voltage, and this power is smaller than the calculated power from the I-V current ($I \times V$). This can be attributed to the dynamics of the sputtered particle-gas ion collision near to the substrate surface which dissipate their energy close to the substrate. It was, however, sufficiently close (75%) for the adoption of a simple model in which the majority of ions are accelerated through the floating potential to collide with the substrate, their number being indicated by the saturated ion current.

For different argon pressures, the floating potential and the heat load to the substrate have been measured, and are shown in Figs. 8 and 9 respectively. The heat load is closely related to the ion energy (floating potential). As the argon pressure decreases, the ion

Fig.5.7 Comparison of voltage multiplied by current with the measured power (target current 500mA).

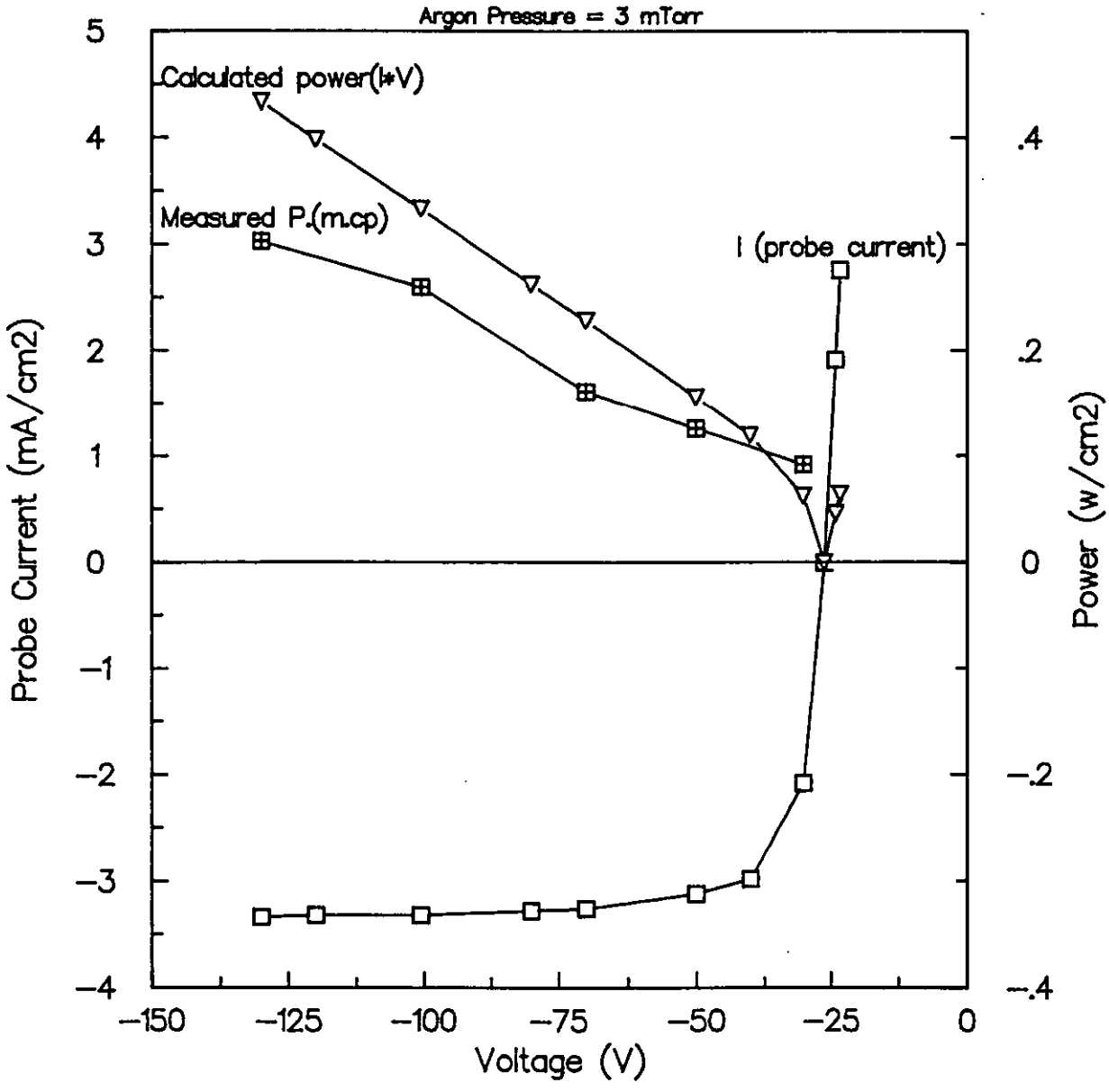

Fig.5.8 Pressure effects on the floating potential at constant target current (500 mA).

Fig.5.9 Pressure effects on the power delivered to the substrate at constant target current (500 mA).

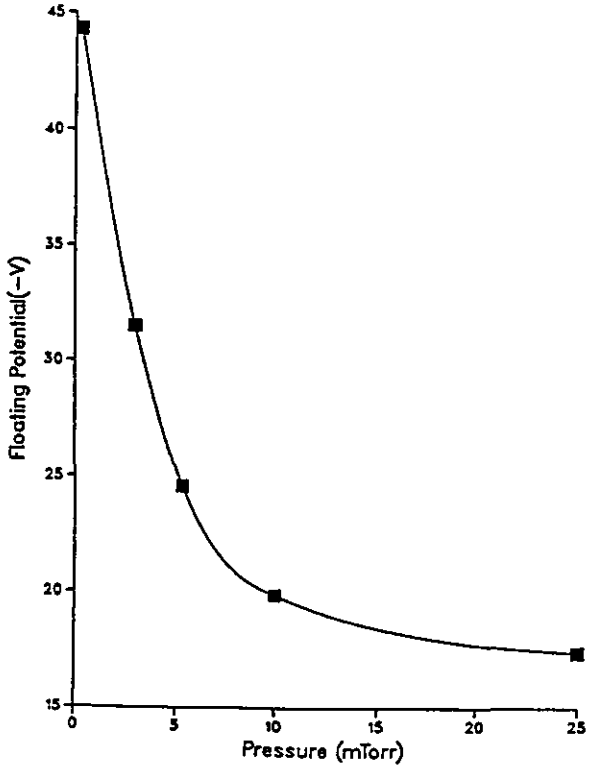

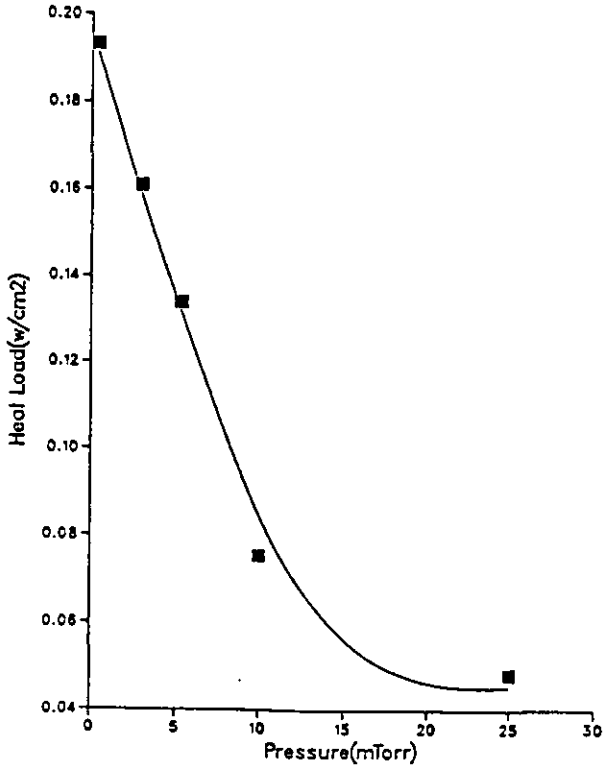

current and floating potential will increase. Consequently more heat will be delivered to the substrate. Several mean free paths are necessary to thermalize a sputtered atom. In this case, this would be about 3 mTorr in a magnetron system with a source-to-substrate distance of 70 mm. Below this pressure the radiation creates damage in the film.

When using oxygen as a reactive gas, the magnetron performance of floating potential and ion bombardment to the substrate is increased. Consequently, the heat load is seen to increase. In the presence of oxygen, electron impact dissociation accompanied by negative ion formation will take place. This and other processes lead to changes in plasma parameters observed.

5.5 Radial Distribution of Plasma and Film Deposition

The distribution of heat load and deposition rate for this magnetron was measured as a function of radial distance from the centre of the magnetron at a distance of 70 mm from the target face, as shown in Fig. 10. For this measurement it was estimated that the effective area of this unbalanced magnetron beam is approximately a 40 mm diameter circle at 70 mm distance from the target face. This gives a uniformity of ion current bombardment of $\mp$ 10%.

The beam distribution on the substrate is a major problem when using the unbalanced magnetron, especially for a stationary substrate. In the case of a moving substrate the uniformity on the coated substrate can be excellent (Refs. 17,18). For stationary substrates with circular magnetrons (Fig. 1). Many techniques can be used in order to optimise the beam uniformity in the substrate. The modification of the magnetic field by changing the outer and inner pole strength can help to give a better shape (Ref. 19). The beam distribution compensates for this deficiency by decreasing the beam performance. Other techniques can be used such as scanning the plasma beam over the substrate, or by

Fig.5.10 Heat load and deposition rate distribution with the radial distance from plasma centre beam at Argon pressure 3 mTorr and target current 500 mA.

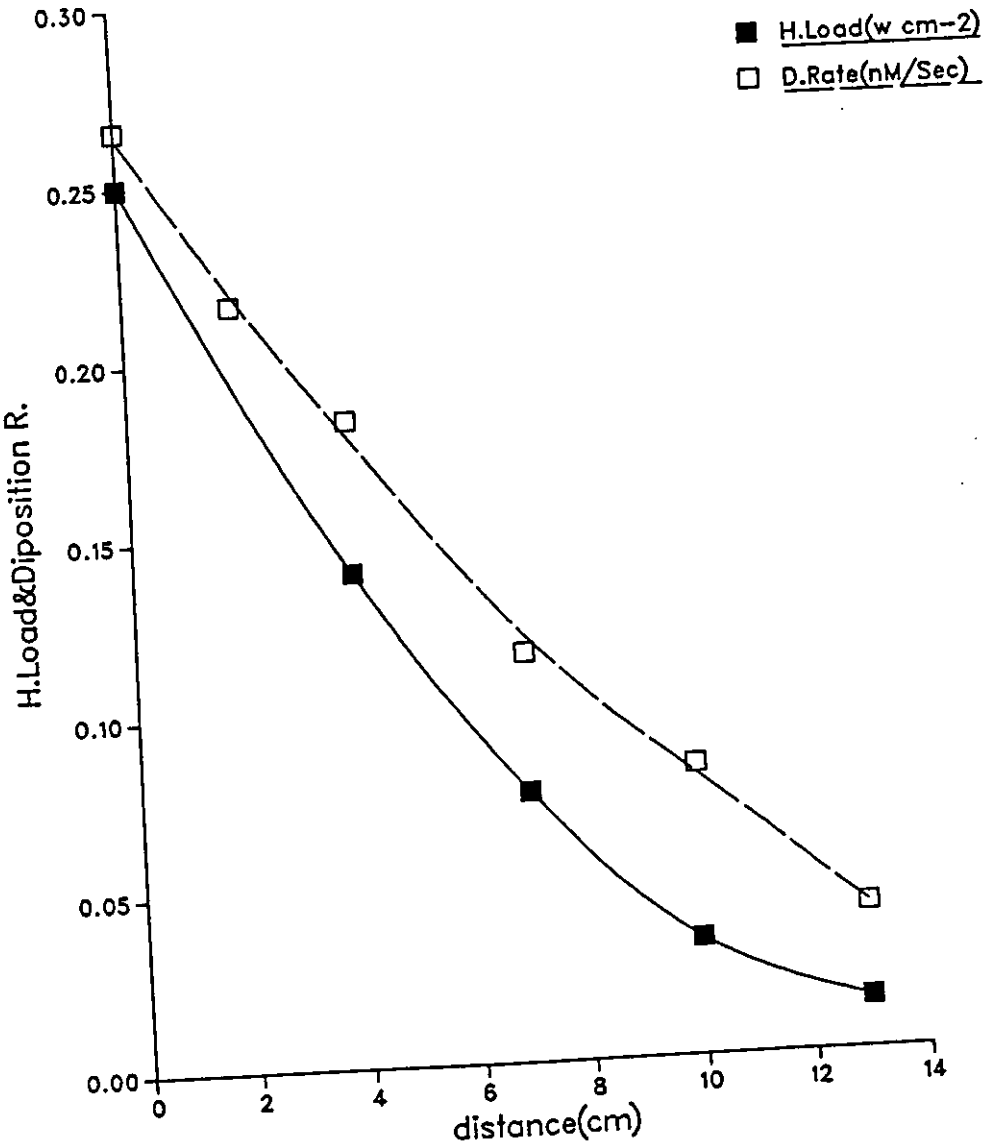

scanning the substrate around the beam. This technique, of course, will add complexityto the system.

The electron energy in such a process ranges between 2 and 30 eV; we observe that with magnets behind the substrate, the plasma can be formed to the same shape as the magnetic field configuration. Fig. 11 demonstrates this fact. By using an unbalanced magnetron facing the main one, the plasma will take the same shape of magnetic field configuration (Fig. 11).

5.6 Auxiliary Magnets Effects

To suppress the negative effects of the plasma on growing films it is necessary either to prevent energetic particles from the plasma from interaction with the film, or to completely separate the substrate from the active plasma (Ref. 20). Many investigations have been made to control the plasma parameters and film properties by using auxiliary magnets installed behind the substrate (Refs. 9,21-23). Magnetic bias has been used to increase or decrease the surface bombardment during film deposition. In our work an electromagnetic coil has been used to study the influence of the magnetic bias on the plasma extending from the magnetron (see Fig. 1). The coil has been constructed using No 24 SWG of 1 mm diameter with more than one thousand turns around a copper tube and with an outer diameter of the same size as the magnetron. The desired magnetic field strength can be achieved easily by adjusting the coil current, and either opposing or aiding magnetic field attained by reversing the polarity of the dc power supply. All the measurements have been taken as a function of the coil current. The field strength in gauss is reached by multiplying the current by a factor of 208. Normally, the magnetic strength at the probe with no current across the coil was about 40 gauss. The probe and the coil were installed at distances of 70 mm and 90 mm from the target face respectively.

Fig.5.11 A photograph shows the plasma shape for face to face magnetrons

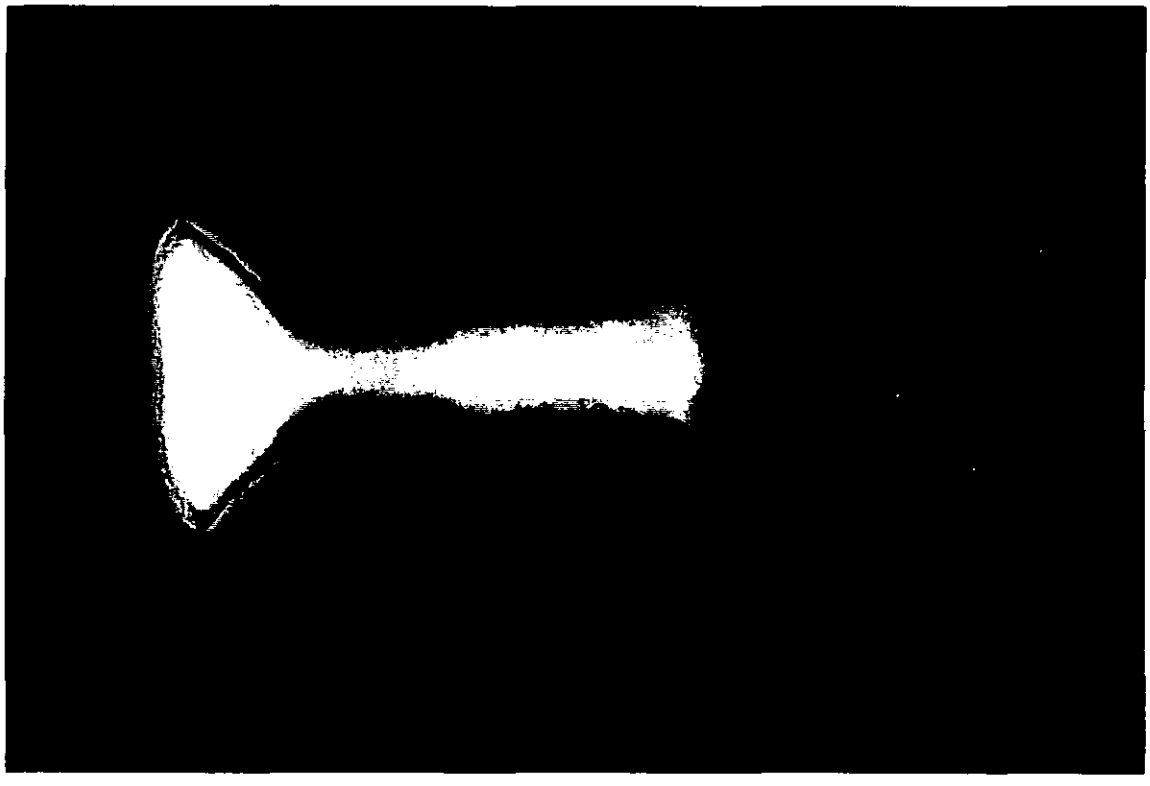

Fig.5.12 A schematic diagram of the effects of a magnetic field generator being placed behind the substrate (ref. 22).

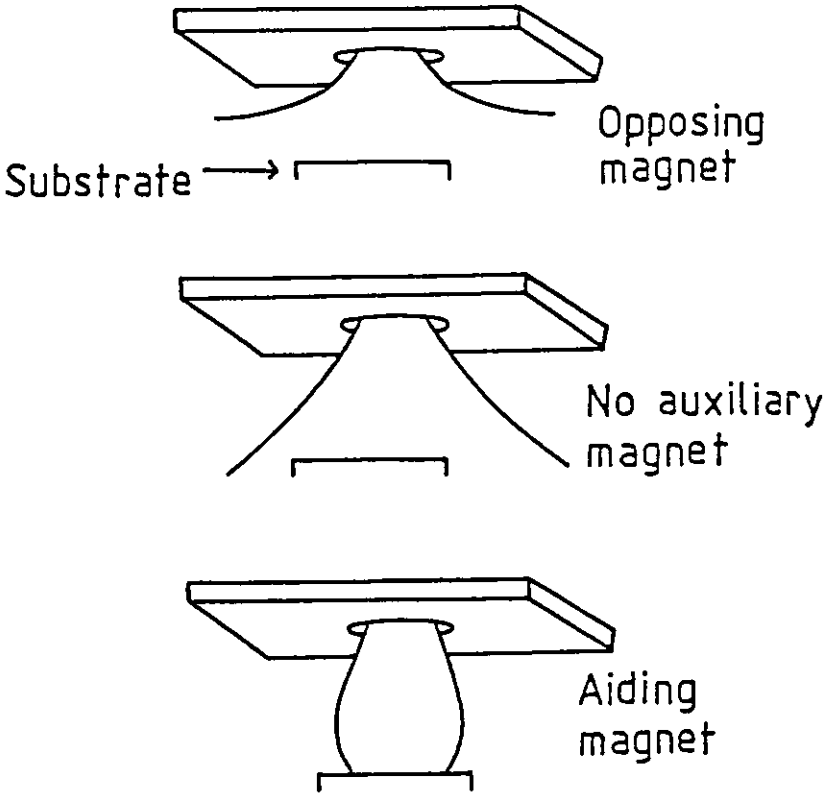

Fig.5.13 A photograph show the plasma shape for a) opposing magnet, b) no magnet and c) with aiding magnet.

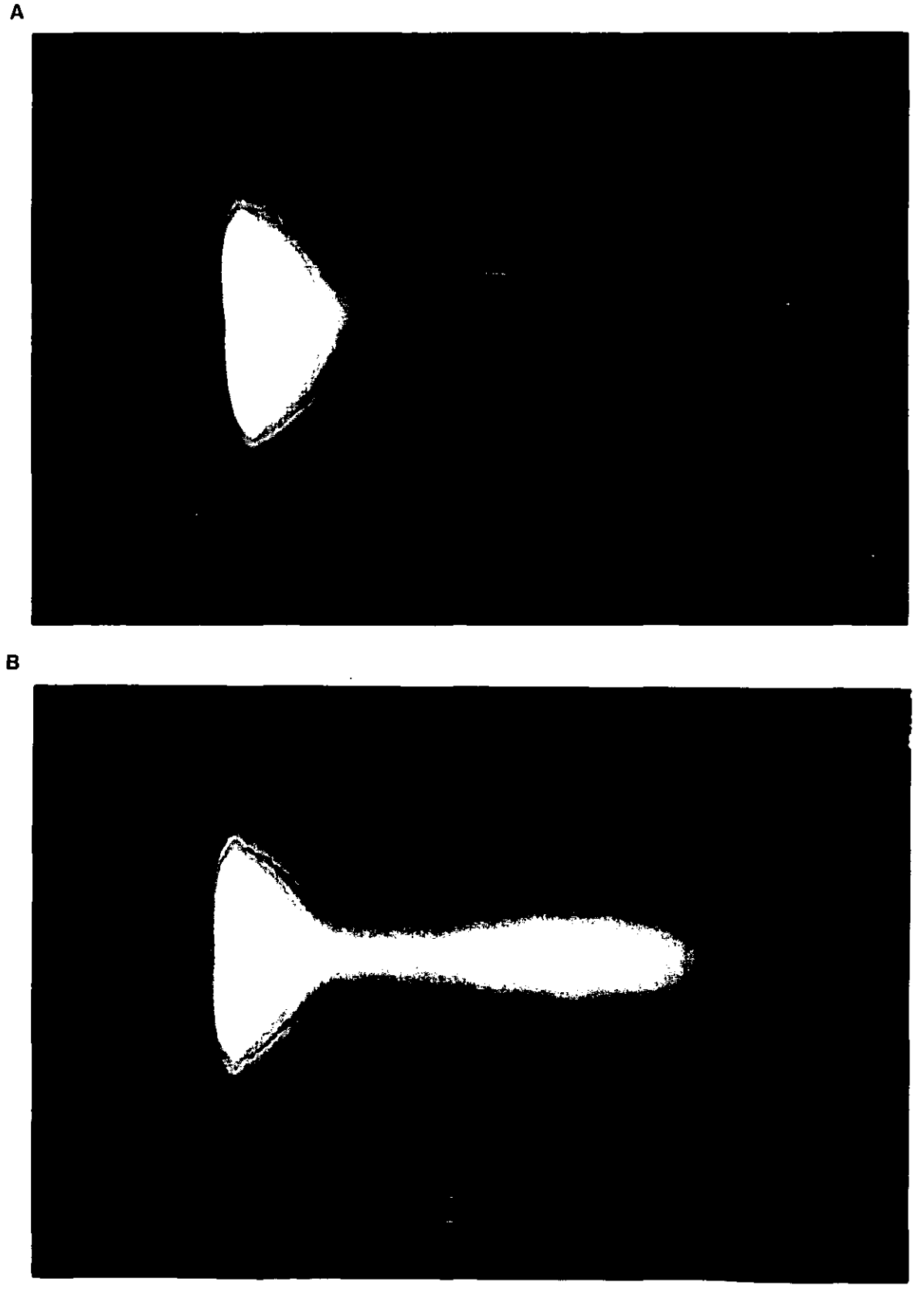

C

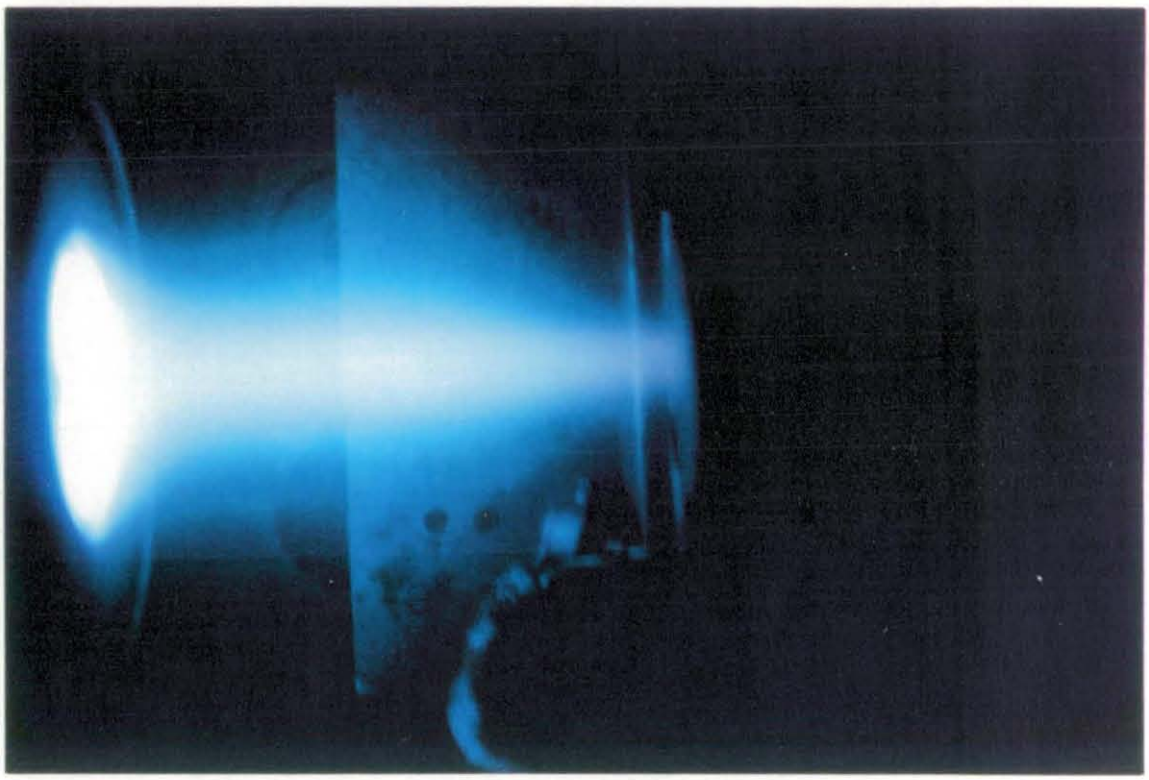

When using an unbalanced magnetron the plasma-substrate interaction is the dominant mechanism increasing substrate temperature. Our calculations show that only 3% of input power reaches the substrate, compared with d.c. diode sputtering where 40% of the input power was expended at the anode and the remainder at the cathode (Ref. 16). The substrate temperatures in this case ultimately depend upon the secondary electron emission from the cathode. However, the case of diode sputtering is rather different from magnetron sputtering because of the magnetic field used. To vary such effects as required, D. B. Fraser et al (Ref. 22) studied the influence of the auxiliary magnet on the glow extending from beneath a sputter gun into the chamber. A cylindrical magnet placed beneath the substrate, whose axis coincided with that of the sputter gun was used in tests to create an aiding or opposing field. When an magnet opposing the magnetron was used, the plasma was dispersed. With an aiding auxiliary magnet, the plasma became confined, resembling a column (Fig. 12).

In our case an electromagnet coil was used. Using this method, the unbalanced magnetron performance at the substrate can be easily controlled. Fig 13 shows photographs taken of the plasma for the three cases illustrated in Fig. 12.

5.6.1 Controlling the Unbalanced Magnetron Performance

With reference to the photographs of Fig. 12, the substrate heat load, floating potential and ion current have been measured. The magnetron was operated in the standard conditions of 500 mA current at 3 mTorr of argon pressure with different target materials. The results are illustrated in Figs. 14,15 and 16. Figures 14 and 15 show the floating potential and ion current for the case of the auxiliary magnet (coil) in aiding mode, where the magnetron outer pole and the coil have different polarity. It can clearly be seen that such a device can increase both the intensity of the ion bombardment and the energy of ions. This bombardment will depend on the type of material being sputtered, which in

Fig.5.14 The effects of the additional magnetic field and the type of the material being sputtered on the ion current density at the substrate.

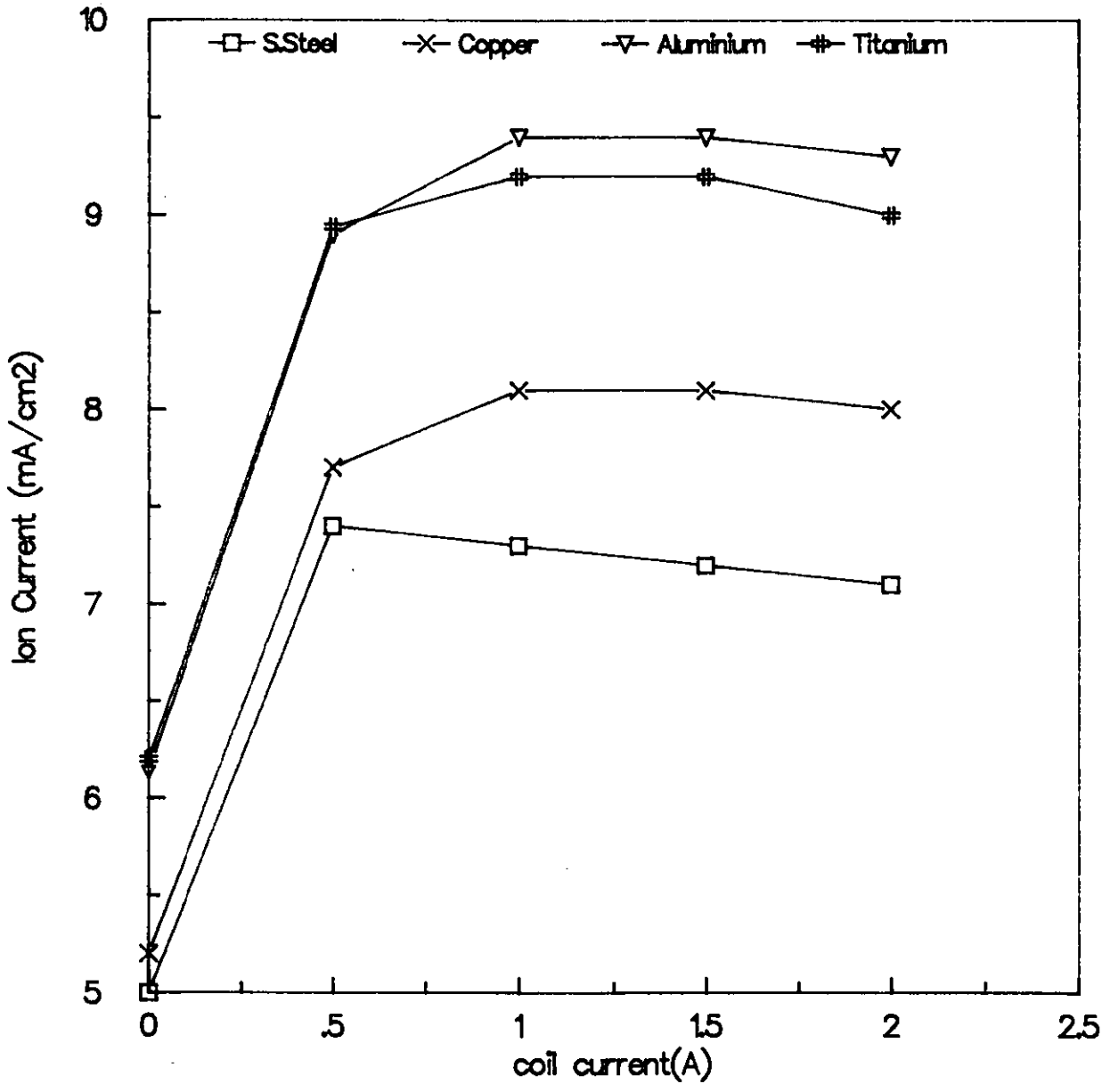

Fig.5.15 The effects of the additional magnetic field and the type of the material being sputtered on the floating potential of the substrate.

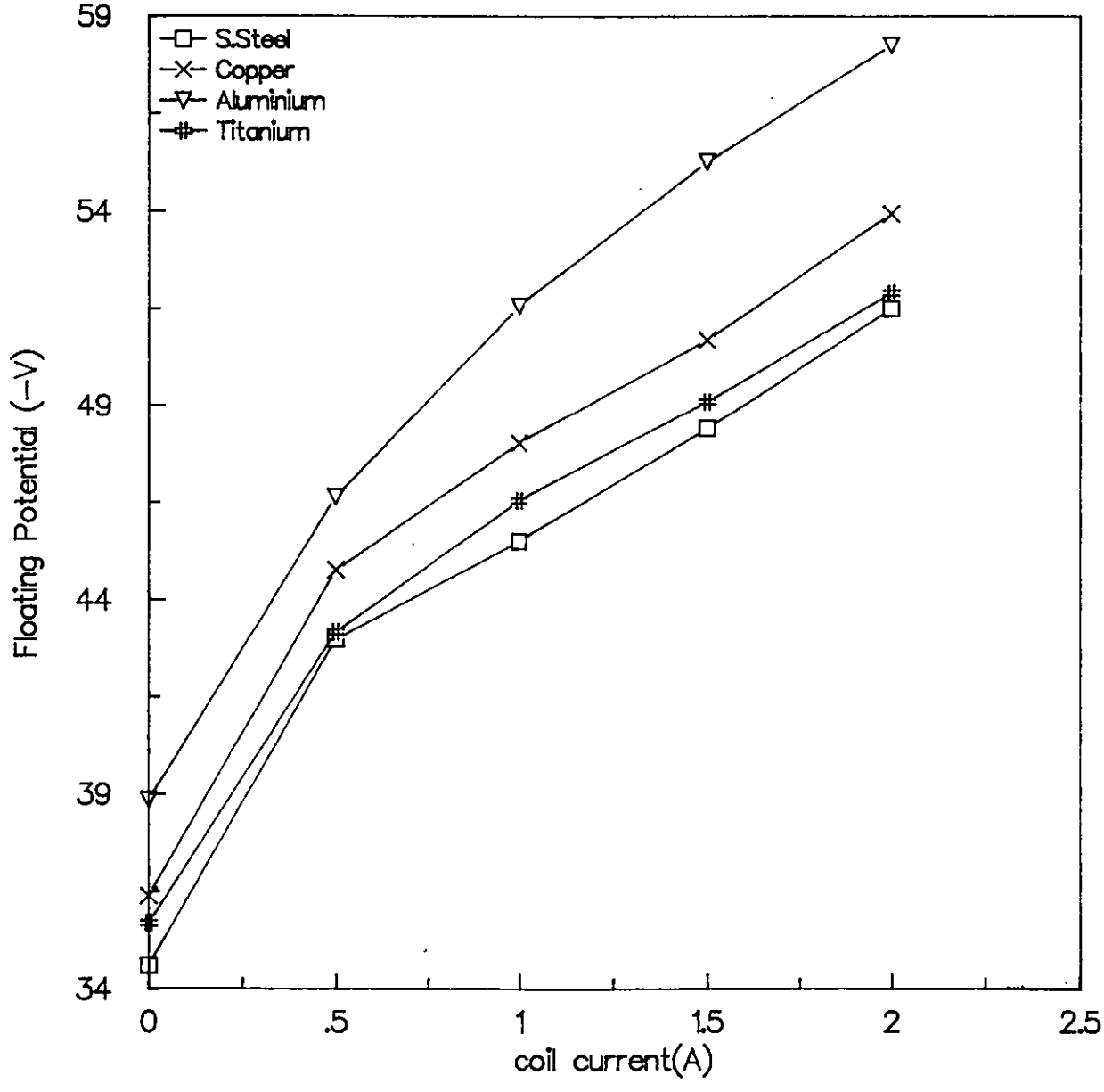

Fig.5.16 The effects of the opposing magnet on the delivered heat load and the substrate self-bias.

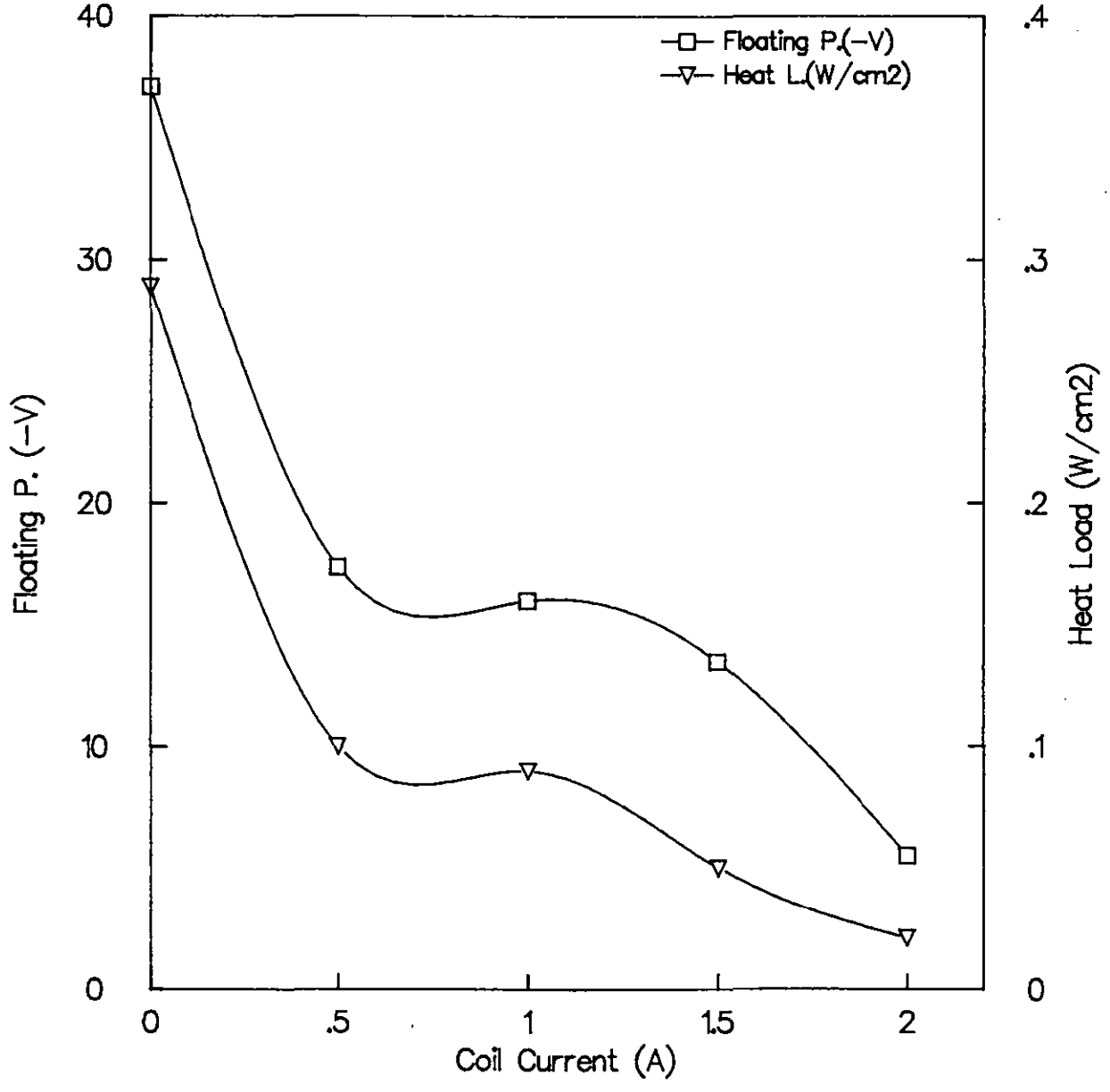

turn affects the operating potential of the magnetron. Fig. 16 shows the floating potential and the heat load for the titanium target as a function of coil current, when using the auxiliary magnet in opposing mode. With the use of a coil in opposing mode, the plasma can be moved backward or forward only by increasing or decreasing the coil current. Hence, this method allows us to control the substrate plasma environment and consequently modify optical and electrical film properties.

5.7 Applications

5.7.1 Titanium Oxide (TiO_2)

In the last decade the deposition of compound films by means of high rate reactive d.c sputtering of metal targets in an argon-reactive gas mixture has been widely investigated (for TiO_2 see Ref. 24). Howson et al have investigated the properties of TiO_2 by reactive ion plating (Ref. 25), followed by reactive magnetron sputtering (Refs. 26,27). The result of reactive magnetron processes are shown in Fig. 17. This Figure shows an optical properties of TiO_2; the refractive index at 633 nm for the different floating potentials. This result has been achieved under controlled conditions of PEM with 0.3 mTorr oxygen partial pressure, using the electromagnetron system. PEM is used in order to provide a high deposition rate of the component and better quality film by controlling the reactive gas partial pressure within the transition region. Thus, PEM is used to suppress the resulting hysteresis where the target uncontrollably switches between metal and reactive modes.

In our investigations a rectangular magnetron has been used. Single layer of TiO_2 films were made using this system in an atmosphere of Ar-O_2 mixture. In order to maintain the process in the transition region, the oxygen partial pressure was controlled by a closed

Fig.5.17 The refractive index at 633nm for different floating potential (Ref. 27).

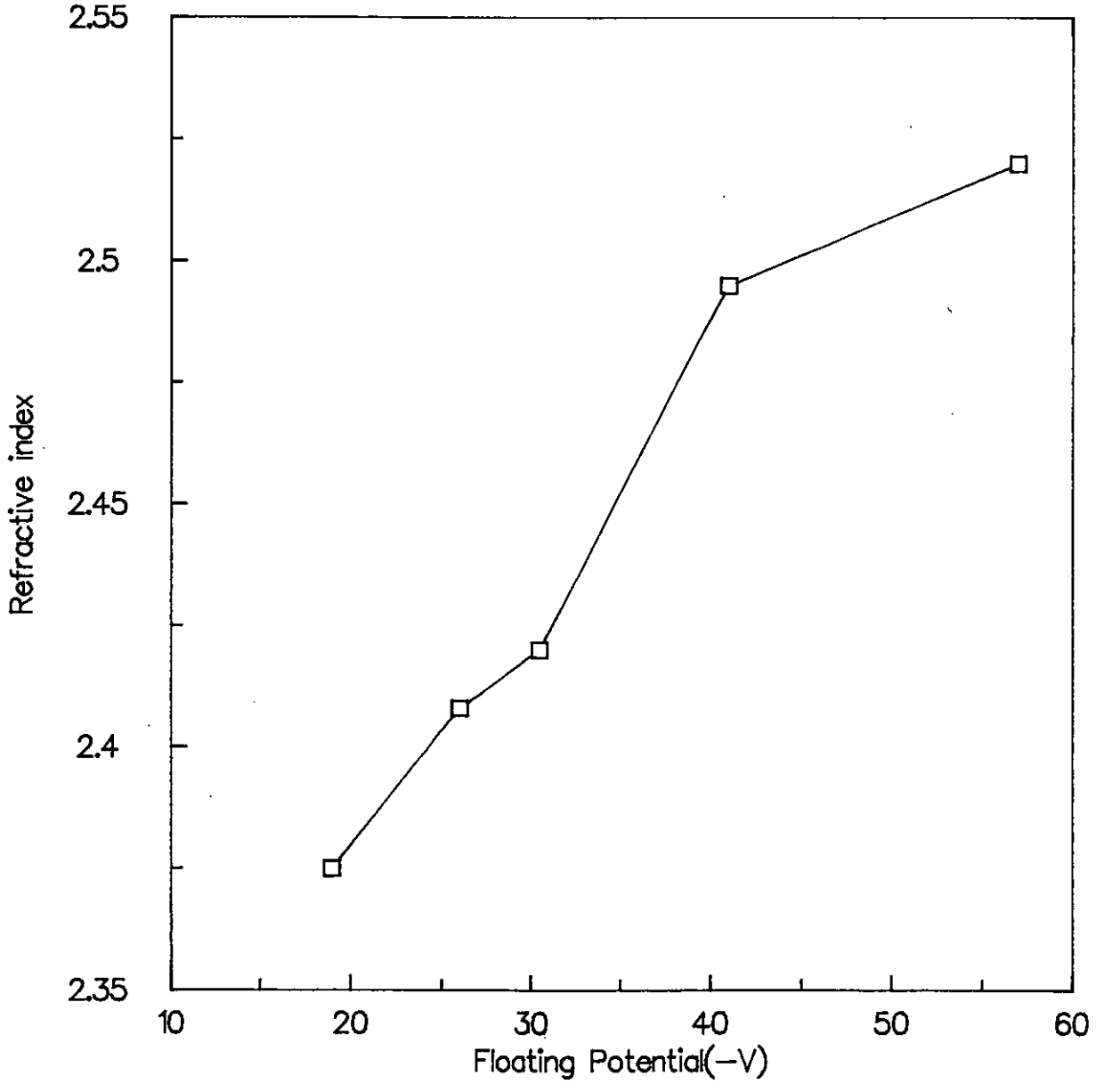

feedback loop controller. The pressure signal was used as the input signal. This experiment utilised the load-lock, which provided a rapid turnaround of samples without disturbing the discharge or pumping the vacuum system out each deposition time. The chamber used was $0.65 \times 0.45 \times 0.6$ m^3 , pumped through a 150 mm diameter orifice. The chamber was initially pumped by a rotary pump and later by a diffusion pump, giving an ultimate chamber pressure of less than 10^{-6} Torr.

By changing the magnetron from balanced to unbalanced mode the refractive index of TiO_2 increased from 2.41 to 2.54, measured at 633 nm. Magnetron power was 1 KW, argon pressure was 3 mTorr and oxygen partial pressure was 0.35 mTorr. The improvement in film refractive index and the film appearance is due to the ion bombardment of the growing film caused by increasing the activation energy and the adatom mobility at the substrate.

5.7.2 Titanium Nitride (TiN)

5.7.2.1 The Load Lock System

TiN coatings are extensively used in industry because of their wear and corrosion resistance, as well as their golden colour. such coatings have been made by sputtering (Refs. 28-32), ion plating (Ref. 33), activated reactive evaporation (Ref. 34), chemical vapour deposition (Ref. 35), plasma enhanced chemical vapour deposition (Ref. 36) and arc evaporation (Ref. 37). These coatings are used as decorative and protective agents for watch bezels, watch straps (Ref. 38), pen barrels, decorative trim, and jewellry. They are used as diffusion barrier layers for electronic applications (Ref. 39) and are further used in wear/corrosion applications such as tool bit coatings (Ref. 40).

The electrical properties of TiN characterised by high conductivity attracted large scale investigation for its application in IC technology (Refs. 31,41,42). Recently the optical

properties of TiN have been widely investigated in order to investigate the possibility of using it as a heat mirror. The inclusion of TiN with other materials and multilayers as a heat reflecting surface in a solar control system or low-emmisivity energy conservation system necessitate very well controlled films with characterised stoichiometry that could compete with noble metals (Refs. 43,44).

TiN films were produced onto glass substrate using the UM and the load-lock system, where an air to air mechanism is implemented. The differentially pumped load lock is evacuated to approximately 1 mTorr before the gate valve is opened, to allow access to the deposition chamber. Following the opening of the valve, the loading arm is pushed forward, so that the substrate locates 70 mm along the normal from the magnetron target. After deposition is completed the substrate can be removed from the chamber, the gate valve closed and the load lock vented whilst still maintaining the full base pressure of the deposition chamber.

In order to control the nitrogen partial pressure, the pressure signal was used as an input signal to an electronic system. The investigation has been made with different magnetron power, argon pressure and exposure time. It is well known that the electrical resistivity of thin films is very sensitive to composition, vacancies, grain size, porosity and film stress. We thus use four-probe measurements of resistivity to assess film quality. The ensuing results are shown in Figs. 18,19 and 20. Fig. 18 displays the effect of magnetron power on the film properties. The film resistivity decreases with increasing magnetron power. That may be attributed to less contamination with increasing power. A. Mumtaz and W. Class specified TiN colour by Auger analysis and found that the brightest film had the lowest oxygen content incorporation (Ref. 45). The use of PEM with an air to air system gives results showing that the O_2 content in the plasma reduces as the power increases.

Fig.5.18 The effects of the magnetron power in the film resistivity, deposition rate and nitrogen consumption.

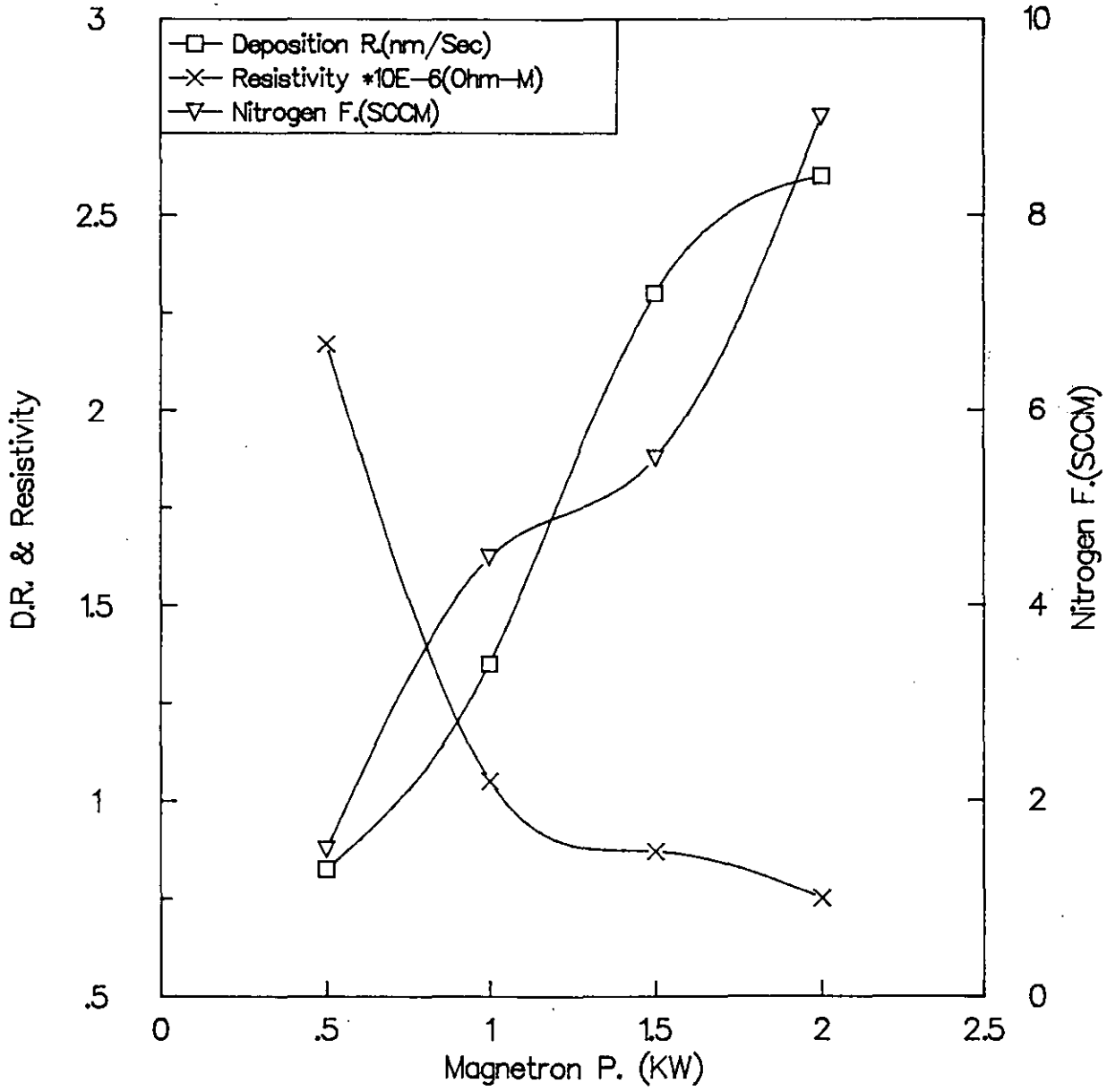

Fig. 19 shows film resistivity with argon pressure. The film resistivity increases as the pressure increases. The film appearance deteriorates as the pressure increases. Deposition under such conditions showed characteristic porous, fibrous, columnar growth (Ref. 46) and the film has large voids. By decreasing the working gas pressure, longer mean free path and higher energies will be achieved and less gas atom capture in the film will occur. Fig. 20 shows the film resistivity with exposure time. If the film thickness increases its electrical properties will improve. This happened for the case of TiN and may be attributed to an increase in the concentration of carriers. No specific investigation has carried out for this case.

TiN films obtained using the ion plating process possess a colour that is greener than the standard yellow gold. In contrast, sputtered films are slightly brown in appearance giving more redness in the film (this is seen for films produced with 1 KW, containing no stress). This has been attributed to columnar microstructure and to the slightly over nitrided films typically obtained from sputtering (Ref. 47). Films produced with high power and low pressure tend to be yellow/gold in appearance, but not as deep as the colour of films produced by an arc evaporation source. The colour of the nitrides and their metallic lustre is due to electron transitions in the energy band. It is these electrons which, on relaxation, emit the yellow light and their number is a measure of brightness (Ref. 45). Savvides and Window (Ref. 3) showed that TiN properties are improved by heating the substrate up to 500 centigrade with bias voltage around 50 V. Film stress was found to increase with increasing ion energy (bias voltage). They demonstrated that films deposited at temperature around 300 C° were observed to spall either during deposition or soon after removal from the vacuum. Our TiN films deposited on room temperature glass substrates had distinctive stress which we have not quantified. As soon as removal of the sample from the chamber is complete, the film resistivity is measured. This allowed production of thin films upto around 100 nm thick because as the thickness increases the

Fig.5.19 The effects of argon pressure in film resistivity.

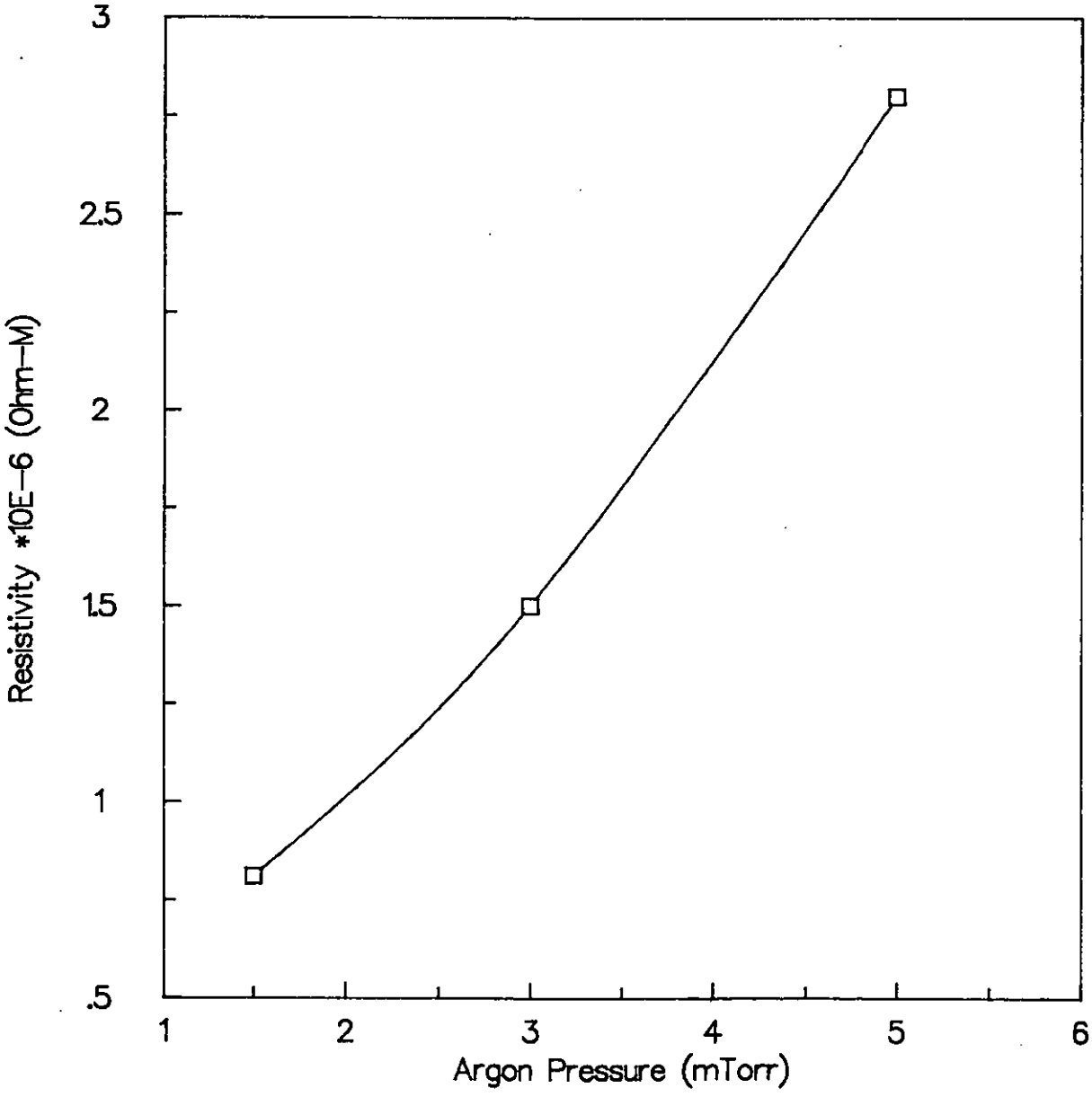

Fig.5.20 Variation in resistivity with increased exposure time.

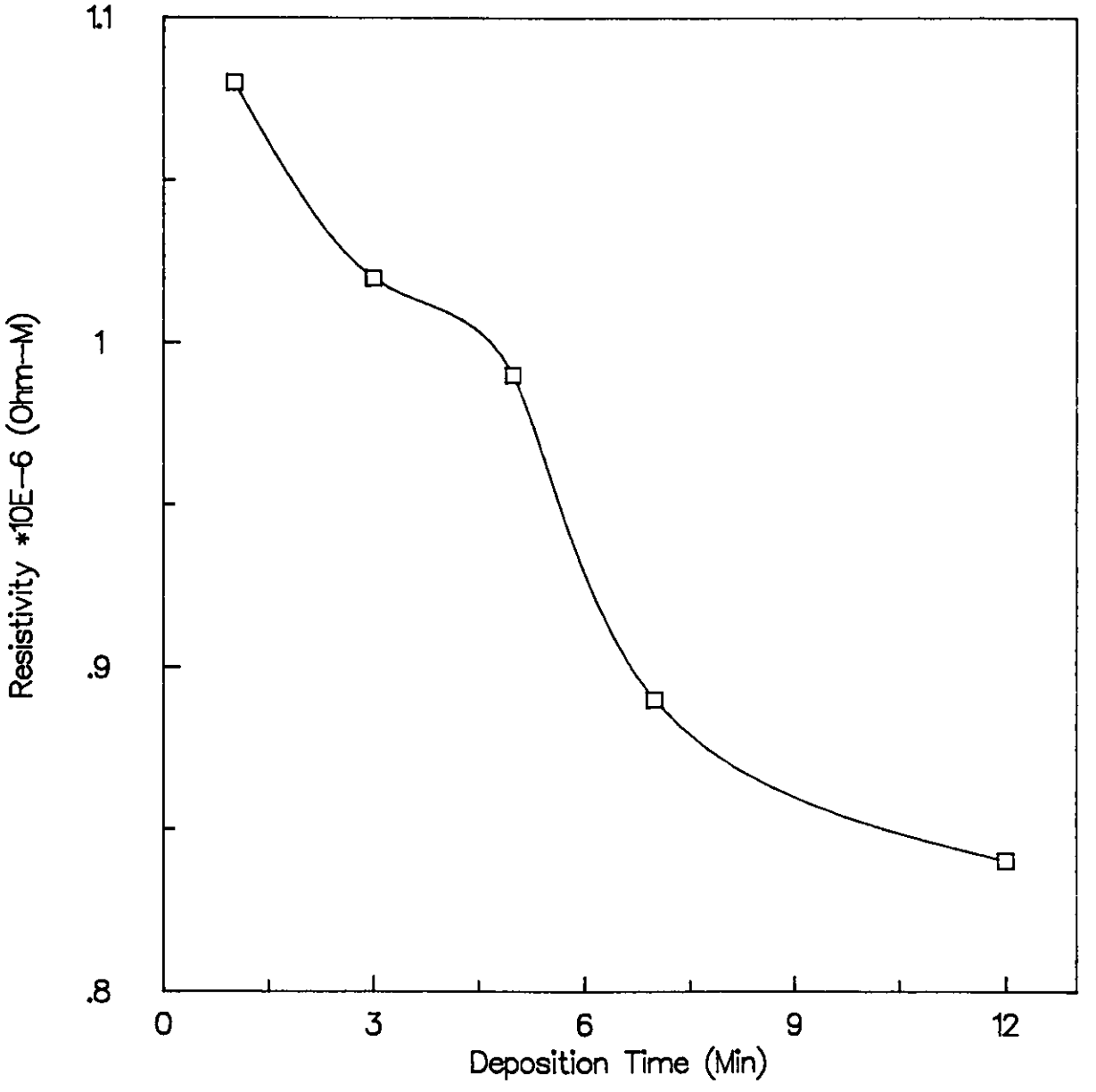

high stress results in complete adhesion failure. To achieve stabilised and good properties of TiN film, heating the substrate during deposition is required.

5.7.2.2 Getter Box System

A getter box system has been set up in our laboratory. The results obtained above have been compared with this getter box system which has been investigated with R. A. Swady (Ref. 44). The system used here has a two stage rotary pump and roots blower with a polycold meissner trap to remove water vapour. The vacuum pressure can be obtained after pumping out the system for 10 minutes is 3×10^{-5} Torr. A closed getter box within this system was designed to allow the sputtering process to take place in a confined place. This getter box is described in detail by R. P. Howson et al (Ref. 48). The argon gas is leaked from outside the getter box through a small conductance, while the reactive gas (nitrogen) flows through manifold placed between the magnetron and the substrate. The box had a sliding lid to allow sputter cleaning on a sacrificed surface. This lid can be moved to bring the substrate to the deposition zone without opening it. For controlling the reactive gas flow PEM was used (Ref. 49). The emission of titanium line is used as a feed back signal rather than the pressure signal.

The advantages of using the getter box is seen from the Al film reflection. Al optical performance is improved when a getter box was used (Ref. 48). This system is used for high rate reactive sputtering of TiO_2/TiN/TiO_2 solar control films as well (Ref. 43,44). Reactive deposition of TiN using the getter box system has also been done for both balanced and unbalanced magnetron (Refs. 44,50-52). A balanced rectangular magnetron of dimensions 250 mm × 100 mm × 3 mm was used as a titanium sputtering source. A glass substrate was used, and the target-substrate distance was 75 mm. To produce a TiN film an argon-nitrogen gas mixture was used. In this experiment the argon pressure was

Fig.5.21 Nitrogen consumption versus Ti line set point for two magnetron currents.

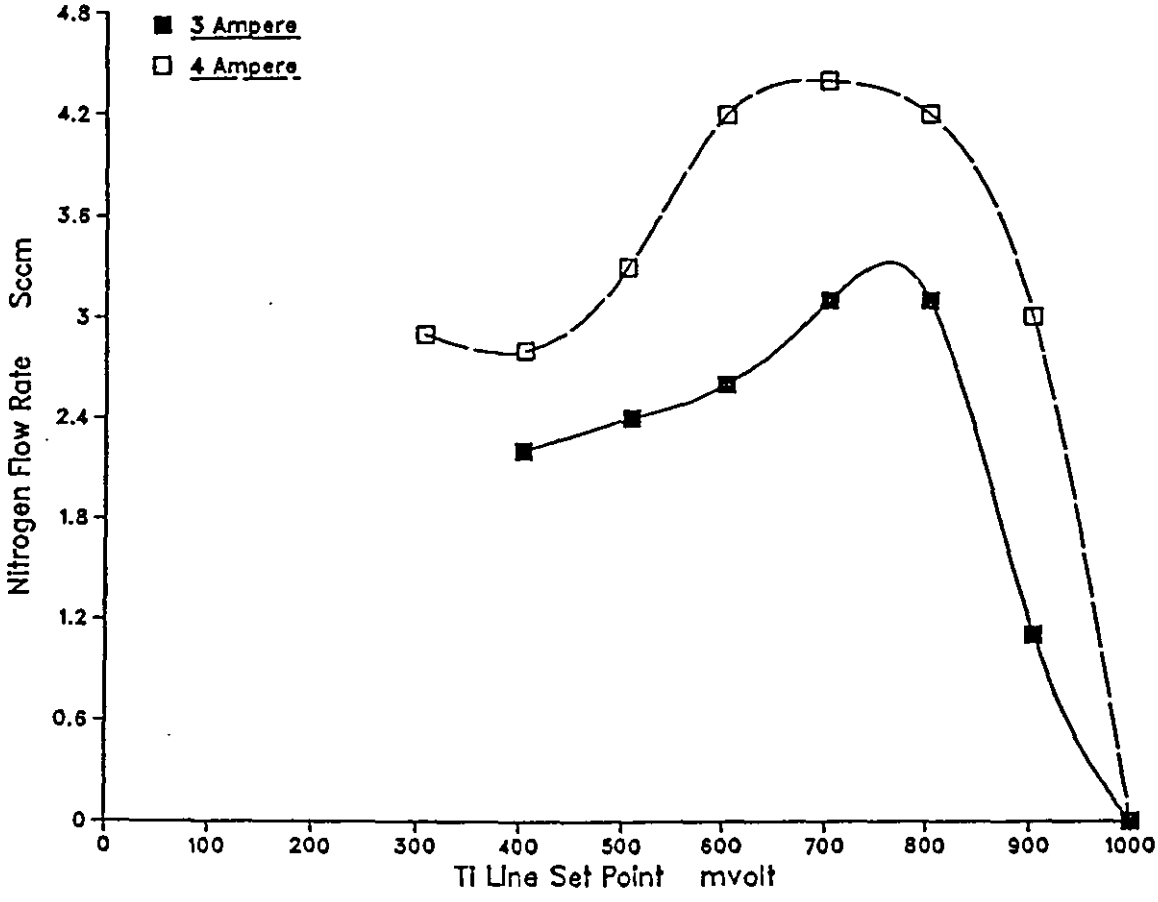

Fig 5.22 Effects of variation in nitrogen flow on film resistivity.

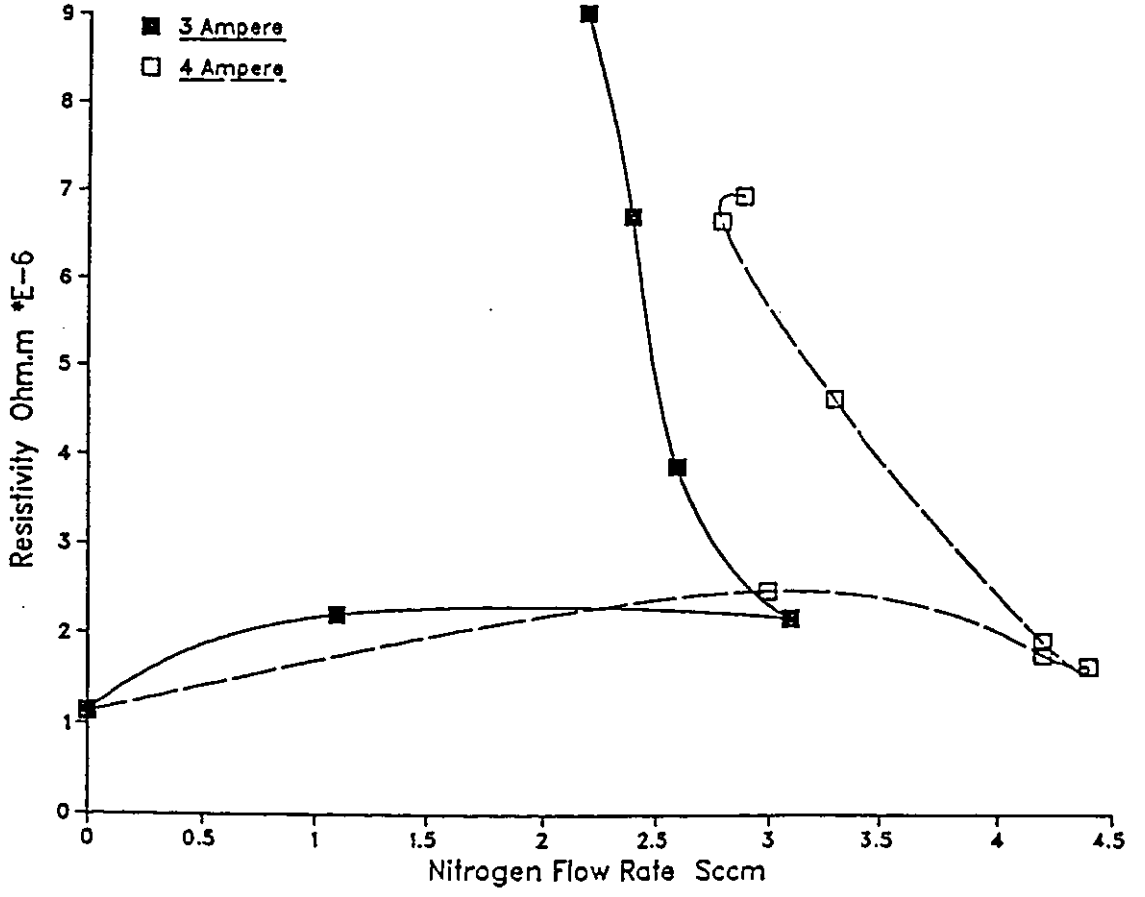

fixed to 5 mTorr. Fig. 21 shows the relationship between nitrogen flow rate and Ti line set point at wave length of 451 nm with magnetron current 3 and 4 Amperes. Fig. 22 shows the films' resistivities as a function of N_2 flow rate. As can be seen from Fig. 21, the N_2 flow rate increases with increasing Ti line set point until the maximum flow is reached; this region represents the formation of optimum TiN films, electrically and optically (Fig. 22). If the Ti line increases further the flow drops rapidly, revealing a high incorporation of titanium to the full percentage, which indicates that pure titanium has been deposited (at zero nitrogen flow). One interesting observation that can be made from these results is that the formation of optimum TiN occurs when the consumption of nitrogen gas within the system is a maximum. This fact can not be seen when manual or pressure signal control is used as in the previous section. By using the pressure signal rather than PEM, N_2 flow represents continuous increase with increasing pressure signal (input signal). Due to using a small volume (getter box) within the vacuum chamber the admitted nitrogen is assumed to be consumed totally by the film. This does in fact occur, because throughout all the process steps the total chamber pressure was constant. For the case of using the load-lock system when a large volume is used, the increase in the N_2 partial pressure with increasing the flow rate indicates an excess amount that has to be pumped by the system.

As can also be seen from Figs. 21 and 22a higher N_2 consumption is needed, with larger currents due to the higher sputtering rate which in turn requires a higher flow in the reactive process to form a compound of TiN. Fig. 23 shows the specification of TiN colours with Ti line set point at magnetron current 4 A. As shown at flow rates of 4.2 and 4.4 sccm a gold colour is formed. The use of ion bombardment, arising from the use of an unbalanced magnetron, was demonstrated to give films of improved properties. The

Fig.5.23 Specification of colours with Ti line set point for opaque TiN films at magnetron current 4 A.

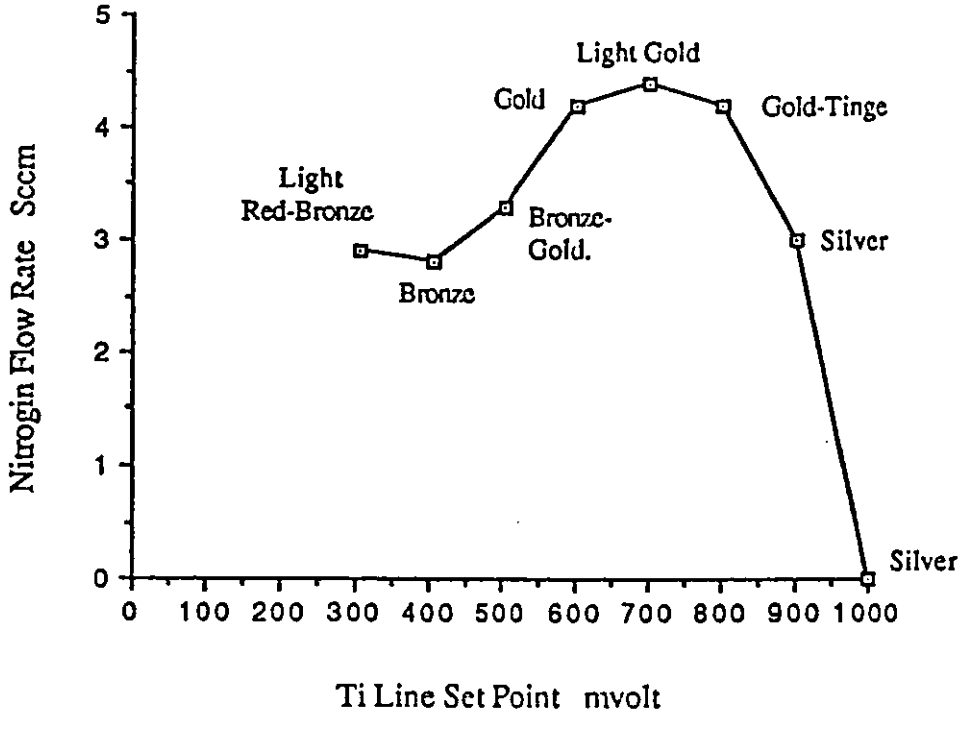

Fig.5.24 The behaviour of TiN resistivity with the nitrogen flow by using PEM and getter box system.

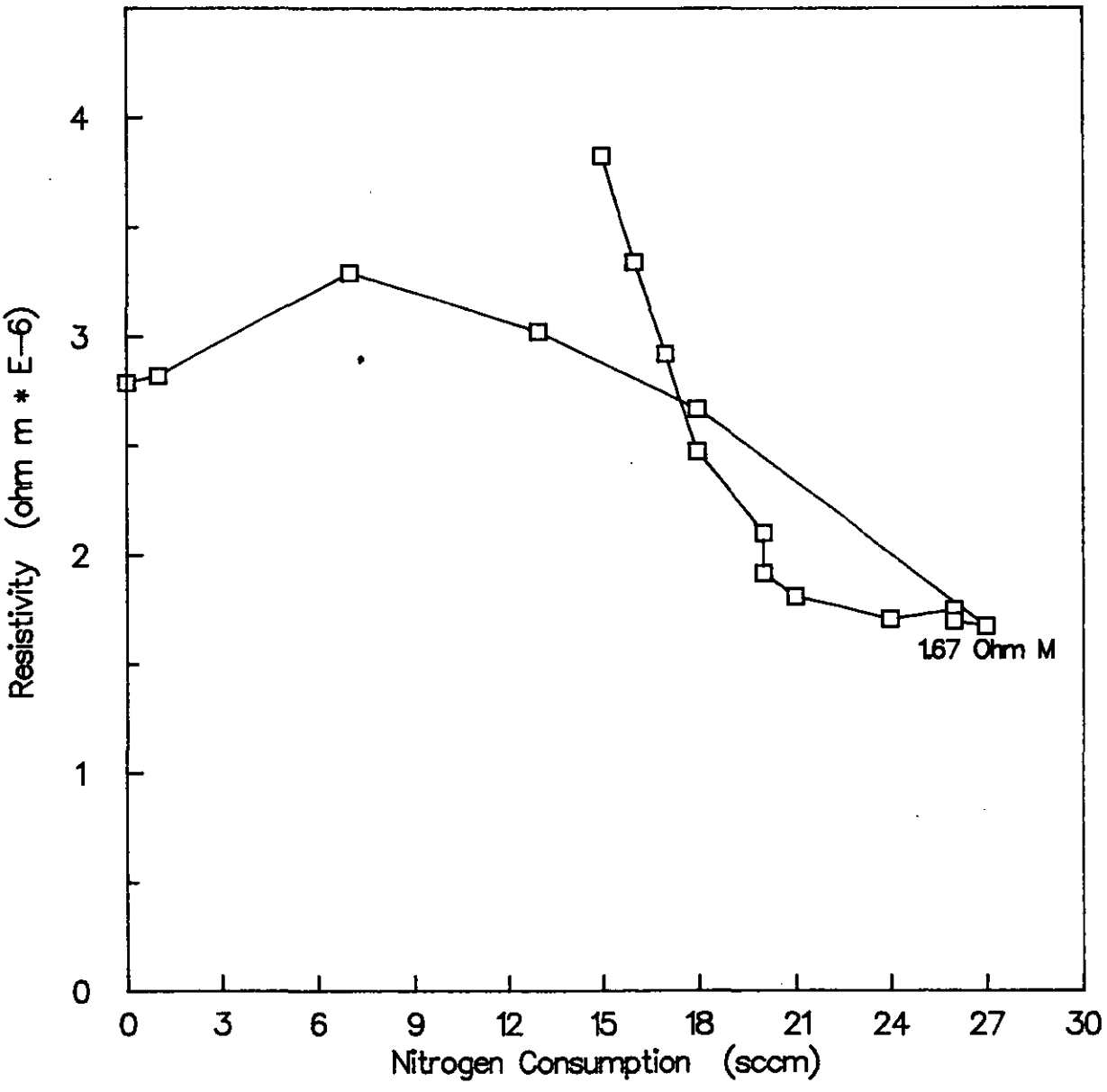

influence of the ion bombardment is to give films of lower ultimate electrical resistivity, lower than that of titanium metal. The partial pressure of nitrogen at which this is obtained is taken as that which gives stoichiometric TiN. The decrease in the resistivity obtained with ion bombardment is attributed to the increased density, which can be seen in cross section by SEM. The ensuing results are shown in Fig. 24. The results achieved using the getter box system and an unbalanced magnetron are summarised in two points:

1- electrical resistivity as low as 1.7 Ω μm

2- refractive index as low as 1.4

The load lock system with the unbalanced magnetron gave these results:

1- Minimum electrical resistivity as low as 0.8 Ω μm

2- Refractive index as low as 1.16

5.7.3 Indium-Tin Oxide (ITO)

Transparent conductive films have been used widely as window electrodes of solar cells, infrared reflective films or to prevent moisture condensation on window glasses. In recent years, thin and light weight display devices such as liquid crystal displays (LCD), electroluminescent displays (ELD) and electrochromic displays (ECD) are replacing traditional CRTs. These flat panel displays often use ITO films as the display electrode. ITO films are prepared by various methods including chemical vapour deposition (CVD), evaporation (Ref. 53), activated reactive evaporation (ARE) (Ref. 54), rf sputtering (Ref. 55), rf magnetron sputtering (Ref. 56) and dc magnetron sputtering (Refs. 52,57). The latter is widely used for making ITO film for LCDS (Ref. 58) because this method is superior in its controllability, and the films obtained show good uniformity thickness over a wide area on large size substrates.

In our laboratory within the last few years a series of investigations in depositing In_2O_3 ,

Fig.5.25 Variation in oxygen flow rate in ITO sheet resistance and magnetron potential.

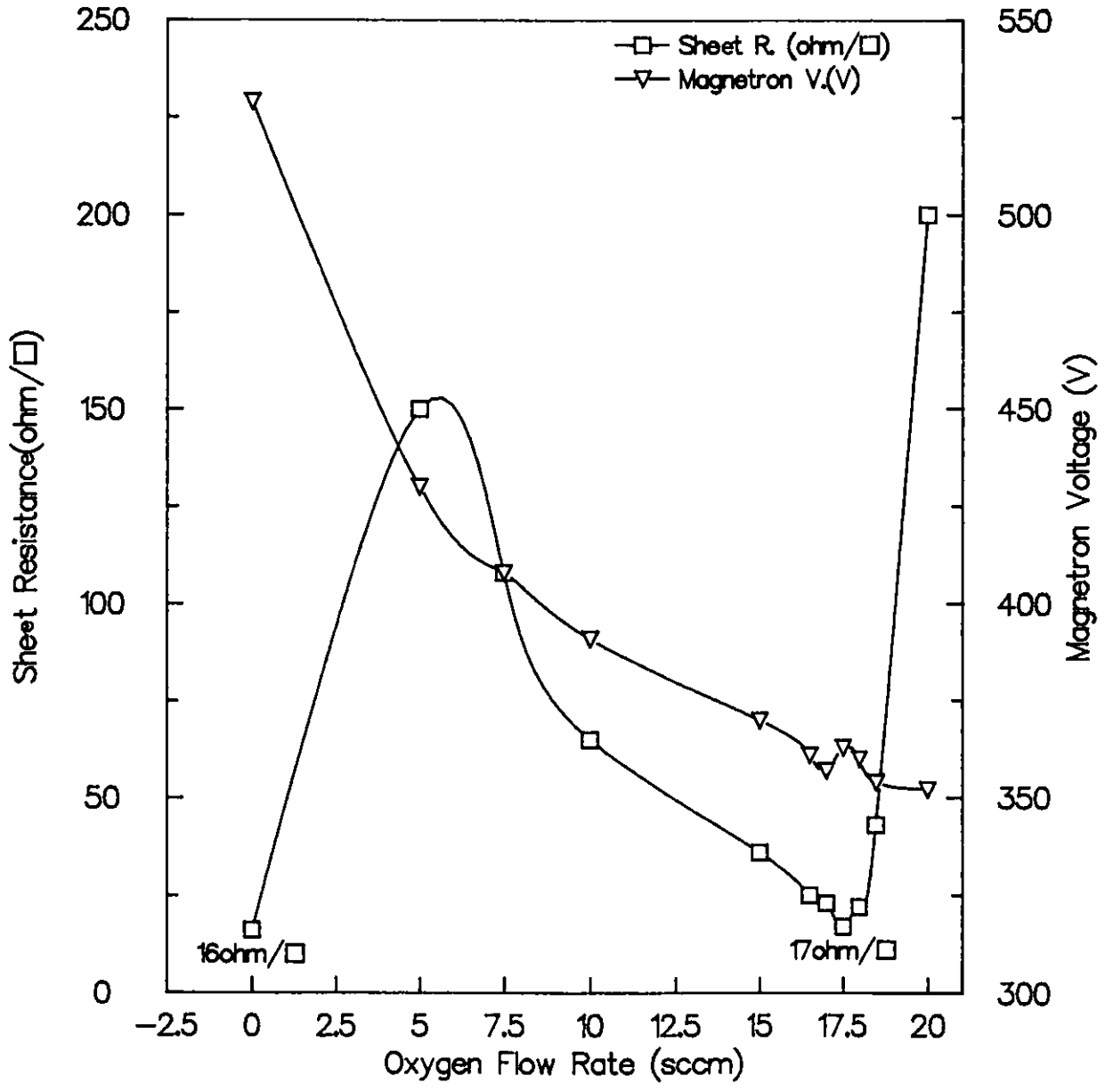

ITO and ZnO:In onto glass or flexible roll coating polymer substrate have been made (Refs. 59-62). The use of unbalanced magnetron to produce ITO on glass substrate has been investigated. This particular investigations have been made to be compared with ITO prepared at low magnetron voltages (see chapters 8 and 9). In this experiment, again the load-lock system is used. Oxygen flow rate was controlled with a piezovalve through a pressure feed back signal in order to maintain the stability in the stoichiometric region, where the conducting transmitting oxide film is formed. Using conditions of 0.5 KW magnetron power, 3 mTorr argon pressure and chamber base pressure of 3×10^{-5} Torr , a set of samples with different oxygen partial pressure was made. Fig. 25 shows the film sheet resistance and the magnetron potential for different oxygen flow rates. If the film thickness was known the film resistivity can be measured, but is found to take the same behaviour of the sheet resistance. The O_2 partial pressure is seen to increase approximately with increasing the oxygen flow rate. At the stoichiometric point a film resistivity of $4.4 \mp 0.4 \times 10^{-4}$ Ω cm and refractive index of 2 ∓ 0.2 was determined.

By using an extra magnet fastened behind the substrate, the unbalanced magnetron performance at the substrate can be increased. By doing so, the properties of ITO deposited films show no improvement. The interesting factor that is seen from this part of experiment is that the oxygen consumption reduces for higher energy and more intense ion bombardment. This is shown in Fig. 26. This happens due to the higher reactivity at the substrate when more plasma is leaked towards it. It was concluded that the surface bombardment increased the sticking coefficient or alternately, re-sputtering occurred. The deposition rate remained approximately the same for both cases.

RF biases to the substrate had not given any improvement in film electrical properties (Ref. 63). By heating the substrate during deposition and reducing the sputtering

Fig.5.26 ITO resistivity versus oxygen partial pressure for two different floating potential.

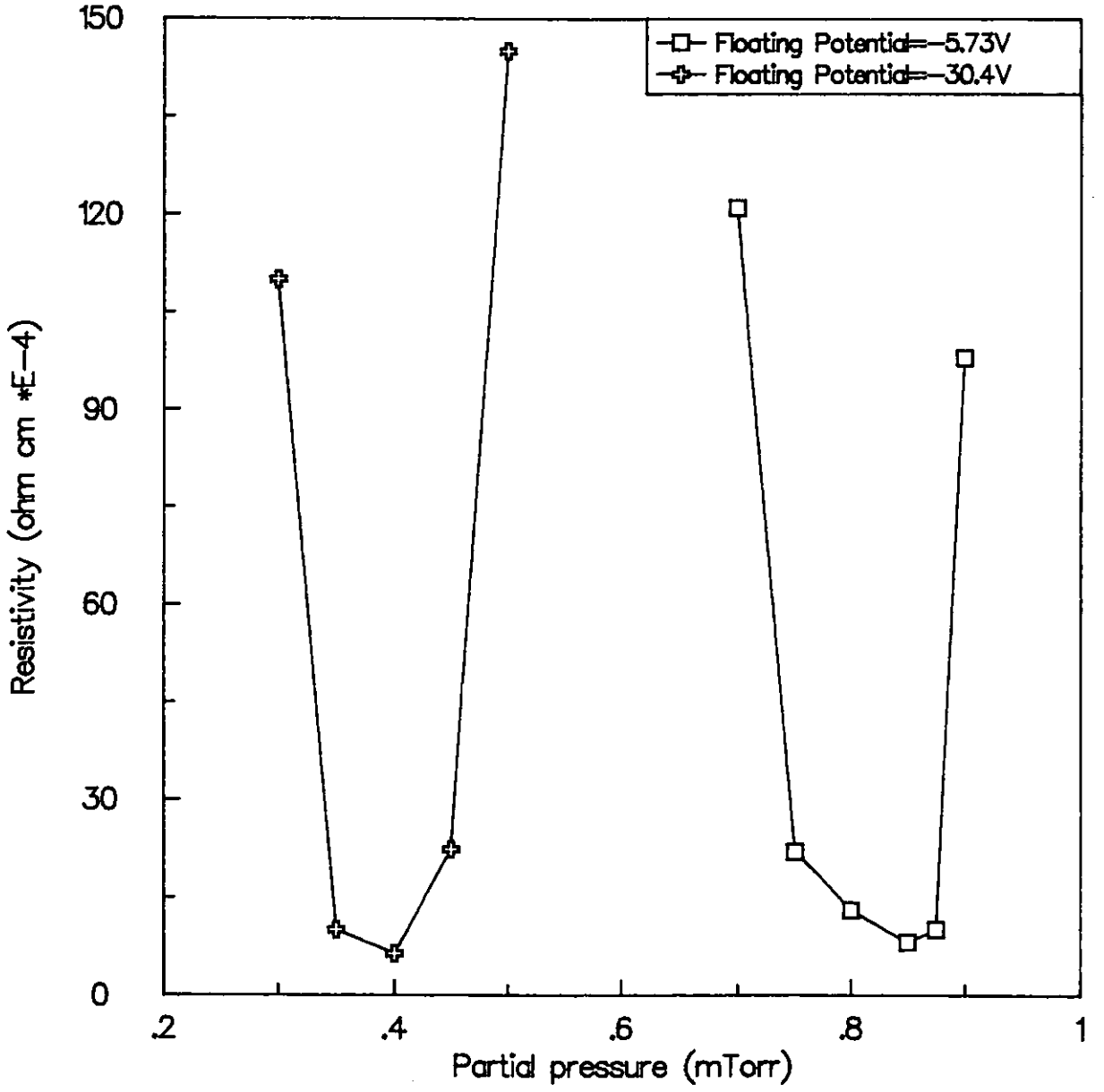

Fig.5.27 Oxygen consumption calculated by subtracting the flow without the process from the flow to the pumps and process.

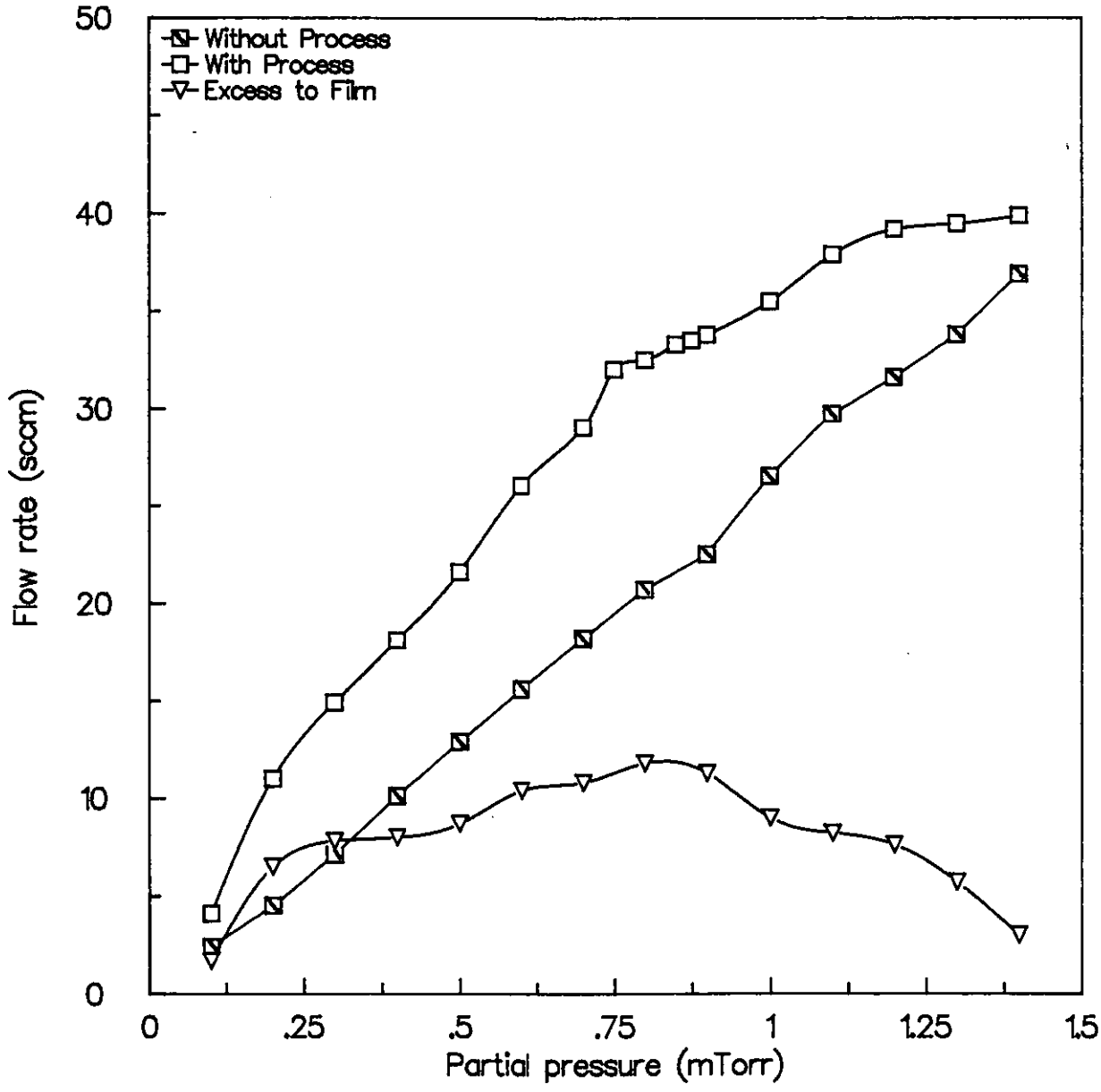

potential the resistivity has been reduced to 1×10^{-4} Ω cm (Ref. 64). However ITO deposition contaminated by iron from the magnetron outer pole reduces the film resistivity from 4×10^{-4} Ω cm to 2.5×10^{-4} Ω cm with little absorption in the blue region (Ref. 65).

By using the In line set point as an input signal to control the oxygen flow rate the same result was achieved. However, the excess O_2 flow to the ITO film was quantified by subtracting the O_2 flow rate to the pumps alone from the flow rate to the pumps and process. This is shown in Fig. 27. Here, the O_2 flow rate usually takes a maximum at or near the optimum film composition. This agrees with the results obtained by using PEM in a closed volume (getter box) as demonstrated in section 4.7.2.2. This is attributed to all the reactive gas flow going into the deposited film when the getter box is used.

Conclusions

In summary, the plasma produced by the unbalanced magnetron and its effects on the substrate in terms of ion bombardment has been investigated here.

The use of the unbalanced magnetron in the deposition of TiN result in improved optical and electrical properties.

The use of the unbalanced magnetron in TiO2 deposition leads to an increase in its refractive index to 2.54.

It has been shown that the unbalanced magnetron does yield an increase in the reactivity at the substrate which decreases considerably the oxygen partial pressure required.

5.8 References

1- B. Window and N. Savvides, J. Vac. Sci. Technol., A 4 (1986) 196.

2- B. Window and N. Savvides, J. Vac. Sci. Technol., A 4 (1986) 453.

3- N. Savvides and B. Window, J. Vac. Sci. Technol., A 4 (1986) 504.

4- J. A. Thornton and A. S. Penfold, in "Thin film processes", (J. Vossen and W. Kern, eds.), Academic press, New York, 1978.

5- D. W. Hoffman, J. Vac. Sci. Technol., A 3 (1985) 561.

6- S. M. Rossnagel, J. Vac. Sci. Technol., A 6 (1988) 19.

7- S. M. Rossnagel and H. R. Kaufman, J. Vac. Sci. Technol., 46 (1988) 223.

8- S. M. Rossnagel and K. L. Saenger, J. Vac. Sci. Technol, A 7 (1989) 968.

9- R. P. Howson, H. A. Ja'fer, and A. G. Spencer, Thin Solid Films, 193/194 (1990) 127.

10- W. Class and R. Hieronymi, Solid State Technology, 55 (1982)

11- S. A. Shivashankar and B. Robinson, J. Vac. Sci. technol., A 4 (1986) 1826.

12- R. Hieronymi, B. Sirouich and W. Class, Thin Solid Films, 96 (1982) 241.

13- R. Budny and D. Manos, J. Nucl. Mat., 121 (1984) 41.

14- P. C. Stangeby, G. M. McCracken and J. E. Vince, J. Nucl. Mat., 111/112 (1982) 81.

15- D. M. Manos and D. L. Flamm, eds., " Plasma etching", Academic press, (1989).

16- D. J. ball, J. Appl. Phys., 43 (1972) 3047.

17- D. G. Teer, Surf. Coat. Tech., 36 (1988) 901.

18- S. L. Rohde, L. Hultman, M. S Wong, and W. D. Sproul, Surf. Coat. Tech., 50 (1992) 255.

19- B. Window and C. L. Harding, J. Vac. Sci. Technol., A 8 (1990) 1277.

20- L. Bardos, Vacuum, 38 (1988) 637.

21- K. Oka, "Plasma activated growth of reactively sputtered optical films", Ph. D thesis, LUT, 1988.

22- D. B. Fraser and H. D. Cook, J. Vac. Sci. Technol., 14 (1977) 147.

23- K. Onnadiela, G. Suran, J. Sztern, Thin Solid Films, 151 (1987) 397.

24- S. Schiller, G. Beister and W. Sieber, presented at Int. Conf. Met. Conf., San Diego, Calif., April, 1983.

25- R. P. Howson, K. Suzuki, C. A. Bishop, M. I. Ridge, Vacuum, 34 (1984) 291.

26- K. Oka, R. P. Howson, R. W. lewin, A. G. spencer, presented at SPIE, Hamburg, 1988.

27- R. P. Howson. A. G. Spencer, k. Oka and R. W. Lewin, J. Vac. Sci. Technol., A 7 (1989) 1230.

28- S. Schiller, G. Beister, J. Reschke and G. Hoetzsch, J. Vac. Sci. Technol., A 5 (4), (1987) 2180.

29- J. Danvoc, A. Aubert, and R. Gillet, Surf. Coat. Tech., 33 (1987) 83.

30- J. Musil and S. Kadlec, Vacuum, 40 (1990) 435.

31- M. Wittmer, Appl. Phys. Lett., 37 (1980) 540.

32- J. Danvoc, A. Aubert, and R. Gillet, Surf. Coat. Tech., 33 (1987) 83.

33- A. J. Perry, J. Vac. Sci. Technol., A 4 (6), (1986) 2670.

34- H. Banasiak and B. Wendler, 5Th Int. Conf. on IPAT, Germany, 13 may 1985.

35- S. R. Kurtz and R. G. Gordon, Thin Solid Films, 140 (2), (1986) 277.

36- N. J. Ianno, A. V. Ahmed, and D. E. Englebert, J. Electrochemi. Soc., 136 (1), (1989) 276.

37- C. Bergman, paper presented at the 15th Int. Conf. on Metallurgical Coatings, San Diego, CA, USA, 11 April, 1988.

38- R. Buhi, H. K. Pulker, and E. Moll, Thin Solid Films, 80 (1981) 265.

39- W. J. Gaciean, P. R. Fournier, and G. K. Harb, Thin Solid Films, 60 (1979) 237.

40- B. Navinsek, A. Zabker, and J. Stefan, Vacuum, 36 (1-3), (1979) 341.

41- M. Wittmer, J. Vac. Sci. Technol., A 3 (4), (1985) 1797.

42- R. C. Ellwanger and J. M. Towner, Thin Solid Films, 161 (1988) 284.

43- A. G. Spencer, M. Georgson, C. A. Bishop, E. Stenberg, Solar Energy Materials, 18 (1988) 87.

44- R. A. Swady, "The development of vauuum technologies for the preparation of high-purity thin films in simple systems", Ph. D. Thesis, Loughborough University, 1992.

45- A. Mumtaz and W. H. Class, J. Vac. Sci. Technol., 20 (1982) 345.

46- J. A. Thornton, J. Vac. Sci. Technol., 11 (1974) 66.

47- H. Randhawa, paper presented at the 15th Int. Conf. on Mettalurgical Coatings, San Diego, CA, USA, Aprill, 11-15, 1988.

48- R. P. Howson, A. G. Spencer, S. Kazandjiev, and M. E. stenlake, 7th Int. Conf. on IPAT, Edinborough, 1989.

49- A. G. Spencer and R. P. Howson, Thin Solid Films, 186 (1990) 129.

50- R. A. Swady and R. P. Howson, 8th Int. Conf. on IPAT, Brussle, May, 1991.

51- R. P. Howson, H. A. Ja'fer, G. W. Hall, R. A. Swady, A. G. Spencer, H. Barankova, and S. Kadlec, Proc. 1st Int'l Sympo. on ISSP, Tokyo, 1991.

52- R. P. Howson, H. A. Ja'fer, J. Vac. Sci. Technol., A, Vol. 10, (1992) 1784-1790.

53- I. Hamberg and C. G. Granquist, J. Appl. Phys., 60 (1986) 11.

54- P. Nath, R. F. Bunshah, S. M. Basol, and O. M. Staffsud, Thin Solid Films, 72 (1980) 463.

55- J. C. C. Fan, F. J. Bachner, and G. H. Foley, Appl. Phys. Lett., 31 (1977) 31.

56- S. Ray, R. Banerjee, N. Basu, A. K. Batabyal, and A. K. Barua, J. Appl. Phys., 54 (1983) 3497.

57- R. P. Howson, H. Barankova and A. G. Spencer, Thin Solid Films, 196 (1991) 315.

58- H. Kitahara, T. Uchida, M. Atsumi, Y. Kaida and K. Ichikawa, Proc. 1st. Int'l Sympo. on ISSP, Tokyo, 1991.

59- M. I. Ridge and R. P. Howson, Thin Solid Films, 96 (1982) 121.

60- R. Lewin, R. P. Howson, C. A. Bishop, and M. I. Ridge, Vacuum, 36 (1986) 95.

61- R. P. Howson, M. I. Ridge and K. Suzuki, Solar Energy material, 11 (1984) 223.

62- R. P. Howson, G. W. Hall, G. W. Critchlow, and D. E. Sykes, Vacuum, 43 (1992) 167.

63- R. P. Howson, J. N. Avaritsiotis, M. I. Ridge and C. A. Bishop, Appl. Phys. Letts., 35 (2), (1981) 161.

64- S. Ishibashi, Y. Higuchi, H. Nakamura, T. Komatsu, Y. Ota, and K. Nakamura, Proc. 1st. Int'l Sympo. on ISSP, Tokyo 1991.

65- G. W. Hall, personal communication, Physics Dept., LUT.

CHAPTER-6

A COMPARISON BETWEEN AN ARC EVAPORATION SOURCE AND AN UNBALANCED MAGNETRON SPUTTERING SOURCE

Physical vapour deposition such as vacuum evaporation , sputtering and ion plating is a process extensively used for depositing many different coatings onto a wide range of substrate materials. Over the last decade coating technologies based on these techniques have found widespread industrial applications. In spite of this fact, comparison of these techniques, their possibilities, advantages and limitations including the properties of the film created still remains an open physical problem and a question widely discussed by users.

Recently, literature has appeared explaining the different features between the cathodic arc evaporation systems and magnetron sputtering system. Comparison of typical parameters for these two techniques is given by J. Musil et al (Refs. 1,2). Influence of the nitrogen partial pressure on the composition and colour of TiN coatings have also been compared (Ref. 3). A comparison between the performance of an arc evaporation source with ion selection and an unbalanced magnetron sputtering source have also been done (Ref. 4).

The film thickness distribution at large target-substrate distance and the film surface morphology and structure have also been compared for a dual purpose cathodic arc/magnetron sputtering system (Ref. 5).

6.1 Arc Evaporation Source

An arc evaporation source has been built in our laboratory. The unbalanced magnetron has many of the feature of arc source. A comparison of the unbalanced magnetron performance with that of the arc source has been made. The cathodic arc deposition (CAD) method employs a vacuum arc to generate vapour emission from a target, which is the cathode in an arc discharge circuit. Material is eroded from the target in several forms, those of greatest interest being ions and microdroplets. Ions of the target material are the species of primary importance in the film deposition. ionised vapour of the target material is deposited onto the substrate.

The CAD method is characterised by the following (Ref. 6):

1- The very high percentage of the emitted vapour that is ionised 30-100%

2- The emission of ions that are multiply charged; and

3- The high kinetic energy of the emitted ions, 10-100 eV

These characteristics yield the following benefits in coating quality and process control:

1- High film adhesion and density

2- High deposition rates with good uniformity

3- High-quality, stoichiometric coatings over a wide range of processing conditions.

4- Low substrate temperatures during deposition, and

5- Retention of alloy composition from target to deposited film.

The major disadvantage of the CAD source is that in addition to the desired vapour, it produces droplets of material being evaporated, typically of the order of micrometers, which can degrade the coating quality and surface finish.

Magnetic assisted arc evaporation has been used in order to reduce droplet formation, by increasing the cathode spot velocity (Ref. 5). It is also used to bend the arc plasma

Fig.6.1 The arc evaporation apparatus.

A: Vacuum Chamber
B: Cathode
C: Power supply
D: Ignitor
E: Gas inlet
F: Vacuum pumps
G: Resistors
H: Filament
I: Anode
J: Magnet ring
K: Magnetic coil
L: Anode-filament supply

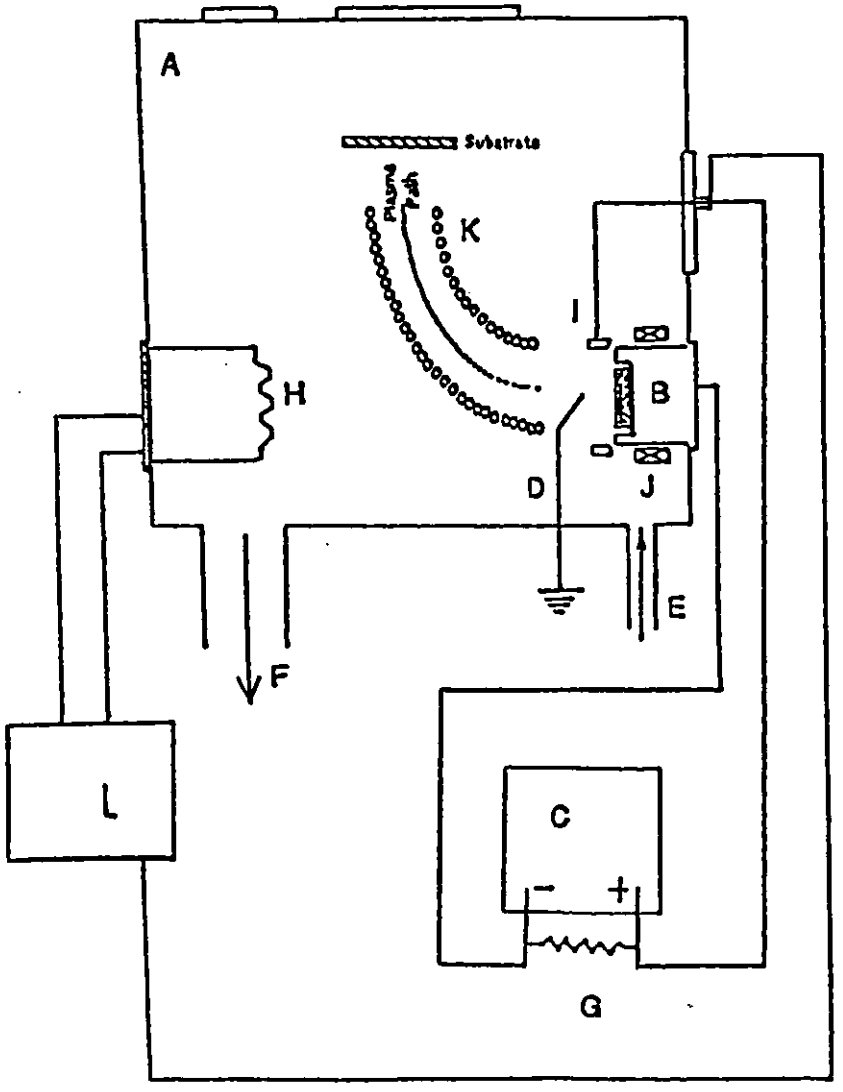

around a corner in order to filter the ions from the droplets (Ref. 7). This second technique led to a lower deposition rate and poor uniformity over a large area. Fig. 1 illustrates the CAD system used for the work presented here. An arc source was created which had magnetic stabilisation of the arc on the surface of the electrode and a solenoid to divert and direct the plasma created around the surface of the target onto the substrate and growing film surface. Less conventionally it was operated in a similar partial pressure of argon to that of the magnetron and had a hot filament and anode arrangement to create additional plasma around the target surface. This was operated at around 35 volts and a current of 3 Amps. It was hoped that such an arrangement would allow simple ignition of the arc and provide stabilisation of its operation as well as providing plasma for direction to the substrate surface (see Fig. 1). It did not provide consistent initiation of the arc and mechanical starter had to be used. The plasma beam that was directed along the axis of the solenoid, when the arc was operated at 95 Amps and 10 volts, resulted in the deposition of a thin film of the target material even though there was no direct line of sight, indicating a high proportion of ionised species in the evaporating material.

By using the technique shown in Fig. 2, the ionised sputtered material created by an unbalanced magnetron source was investigated. Bending the plasma, with an external magnetic field, to be incident on a substrate out of the direct line of sight of the target surface leads to a great reduction in the deposition rate, indicating that this plasma does not contain a large concentration of ionised sputtered material.

6.2 Plasma Properties

The same probe was used in order to investigate the plasma properties of cathodic arc system. A probe placed in the substrate position was used to give I-V characteristics and hence to give a value of the floating potential and saturated currents flowing to the film

Fig.6.2 Lay out of the unbalanced magnetron with bent plasma for metal ions investigations.

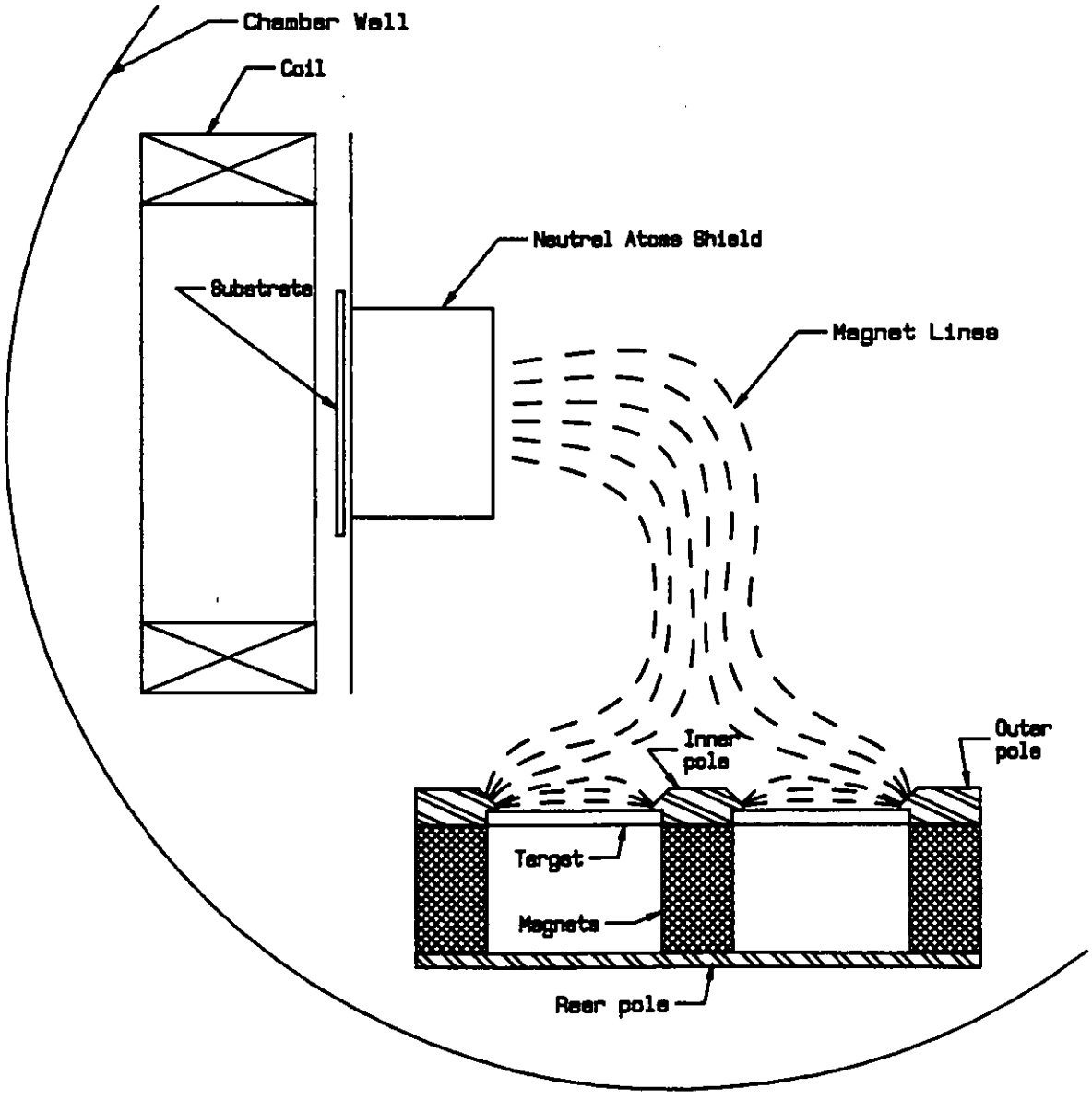

Fig.6.3 The I-V characteristics for a probe placed in the directed plasma from the arc source.

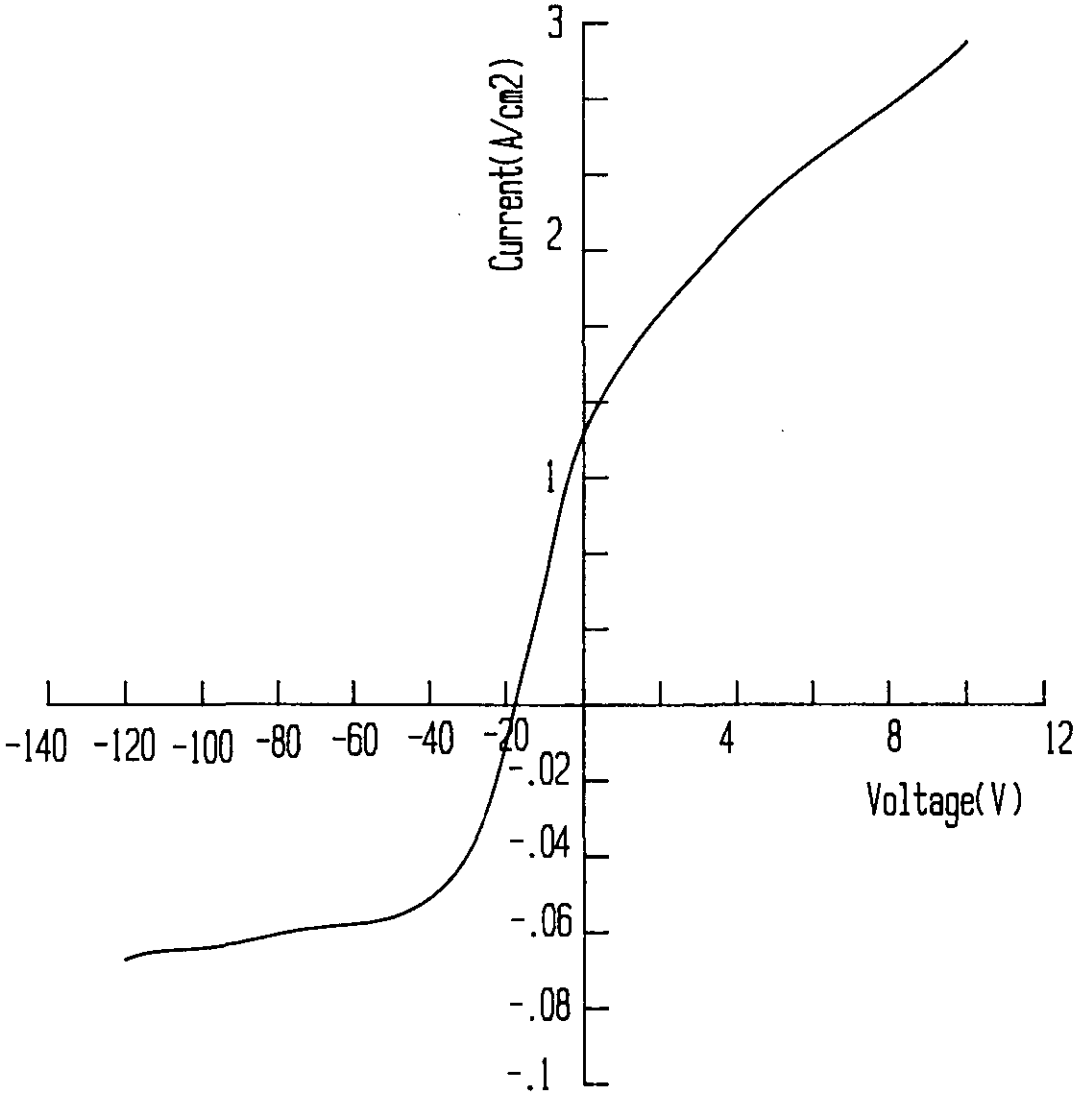

surface. These results are shown in Fig. 3. In the arc source, the floating potential has a value between 2 and 20 volts, and an ion current between 40 and 80 mA/cm^2. This did not change when the filament generated plasma was switched off and might be expected to consist almost entirely of ions of the evaporated material. The unbalanced magnetron plasma could give up to 100 mA/cm^2 ion current and floating potential up to 70 V without using oxygen or up to 100 V with oxygen (see chapters 5 and 7).

The arc evaporation process was not affected by the admission of a reactive gas and reactive processes could be undertaken with little additional problems.

6.3 Reactive Processes

6.3.1 Gas Flow Control

Commonly the admission of the reactive gas in a reactive sputtering process is done through control of the flow with a simple mechanical valve or an electronic feedback device which can indicate the magnitude of the flow. In high rate reactive sputtering with a planar magnetron conditions are often created where the process is unstable, switching between "metallic" and " oxide" sputtering modes without allowing access to the intermediate point, which is the one generally required. Control of the partial pressure of the reactive gas with rapid feedback can prevent this instability. In reactive arc evaporation (RAE), the required stoichiometry can be obtained over a wide range of reactive gas pressure.

6.3.2 Film Products

The preparation of titanium nitride by sputtering requires great care and evidently is much easier by arc evaporation. The reflectance characteristics of TiN films deposited on glass by both techniques is shown in Fig. 4. The sputtered film was prepared by a getter sputter technique using careful partial pressure control of the nitrogen added for the

Fig.6.4 The reflectance in visible region of an arc evaporated film compared to that of one reactively sputtered.

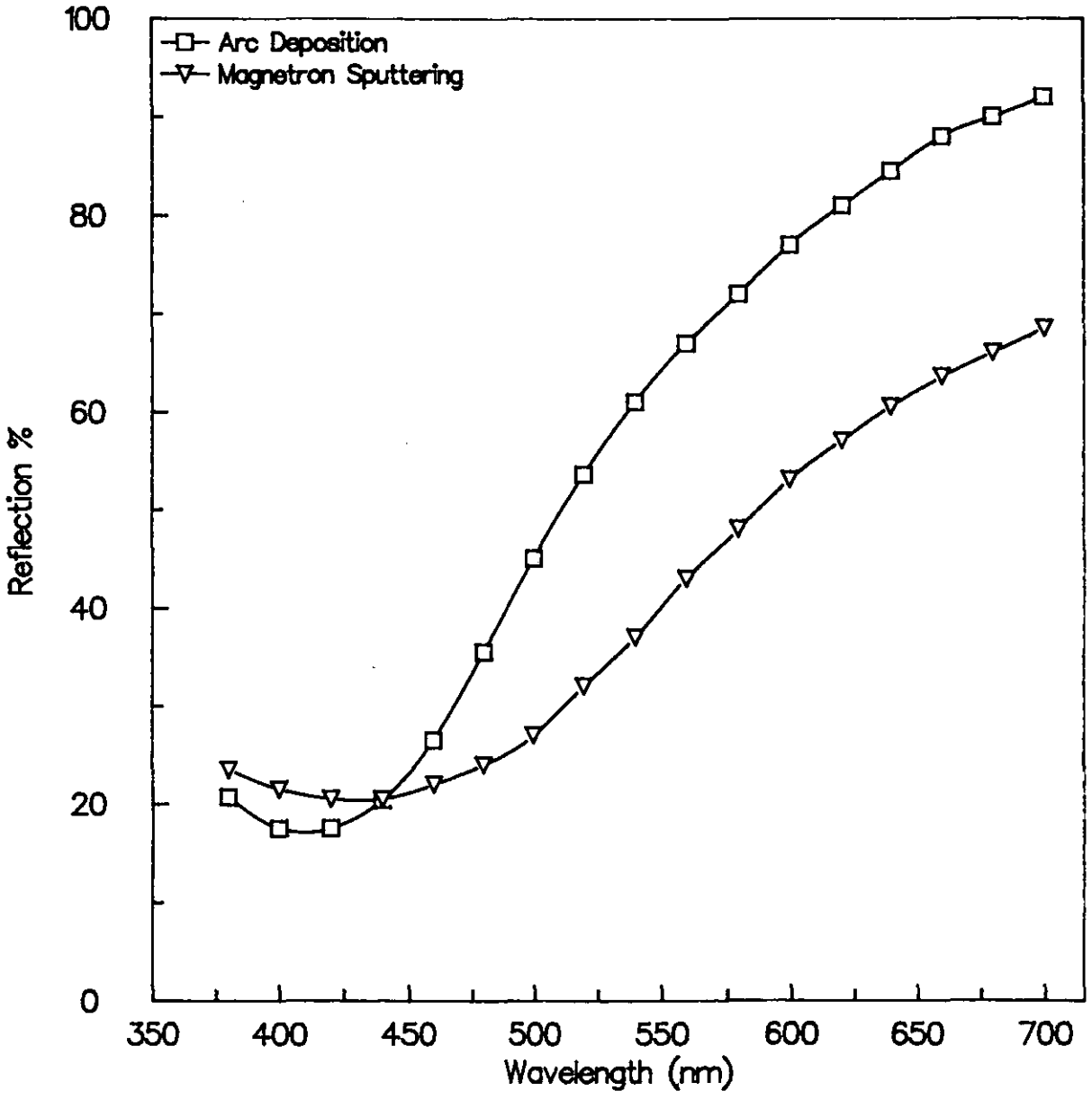

reaction and that made from arc used an atmosphere of 1.5 mTorr of nitrogen and 3.5 mTorr of argon.

The flux of the titanium particles striking the substrate surface in the case of reactive AE consists basically of positive titanium ions (Ti^+ and Ti^{++}). The reason for this is the low voltages present in an arc, for which there is a considerably greater cross section of ionization of atoms by electrons than at the higher voltages encountered in electron beam and magnetron systems (Ref. 2). The titanium ions have energies in the range of 20-30 eV (Ref. 3). When the deposition is carried out by reactive magnetron sputtering the titanium atoms predominate in the titanium flux (the concentration of the ions is about 0% in this case). The energy of the sputtered titanium atoms is about 10 eV. Hence, the energies of the metal particles bombarding the substrate are about 20 times larger in the case of arc than in the case of magnetron. The energetic titanium ions striking the film surface are neutralised and penetrate in the film, losing their energy. Thus, near and on the film surface, atoms with high mobility are formed.

The surface mobility of the nitrogen atoms is also larger during arc deposition than during magnetron sputtering (Ref. 3). This high mobility of the reacting components explains the higher reactivity of titanium and nitrogen during film growth by reactive arc evaporation. This is the reason behind the wide range of reactive gas pressure used by arc evaporation.

In a mixture of 3.5 mTorr argon and 1.5 mTorr oxygen the reactive evaporation of aluminium oxide was also processed. A clear film of refractive index of 1.66 was obtained. These films are notoriously difficult to sputter because of arcing on the cathode surface

6.4 Other Remarks

Magnetron sputtering enables a wide range of material to be used, even those with low melting points. The arc system is more popular with high melting point materials. In the case of arc system less contamination of the film has appeared during TiN deposition. That is because the bombardment of incident ions produces the equivalent of high temperatures in the film (Ref. 8). Rejection of TiO_2 may be the result of sublimation. The melting temperature of TiN is 2930 °C while the melting temperature of TiO_2 is 1825 °C. The reduction of oxygen concentration on TiN film give it a high degree of brightness (Ref. 9). Target-substrate distance, in the case of AE source can be longer than that in a MS system. Power loss in the cathode is about 30% in case of AE (Ref. 1) and about 80% in the case of unbalanced magnetron (Ref. 10).

Conclusions

The comparison between an arc evaporation source and the unbalanced magnetron has been described here. Demonstrating the general feature and the advantages and disadvantages of both systems. The magnetron enables a wide range of material to be used and less droplet contamination is observed. The magnetron can deposit onto a much larger substrate compared to the arc evaporation source.

The measurements of ion content of target material in plasma shows that the unbalanced magnetron has a considerably lower ion content than the arc evaporation system.

The presence of metal ions during deposition has a large influence on the optical and electrical properties of TiN and Al films.

6.5 References

1- J. Musil, S. Kadlec, J. Vyskocil and V. Poulek, Surf. Coat. Tech., 39/40 (1989) 301.

2- J. Vyskocil and J. Musil, Surf. Coat. Tech., 43/44 (1990) 299.

3- D. N. popov, Ts. D. Uzunov, E. I. Dimitrov, Bulg. J. Phys., 13 5, (1986) 470.

4- R. P. Howson, N. Mustapha, H. A. Ja'fer and M. Stenlake, IPAT, Bussels, 1991.

5- P. Robinson and A. Matthews, Surf. Coat. Tech., 43/44 (1990) 288.

6- P. C. Johnson, in "Thin film processes 2", (eds., J. L. Vossen and W. Kern), Academic press, New York (1991).

7- P. J. Martin, R. P. Netterfield and T. J. Kinder, Thin Soild Films 193/194 (1990) 77.

8- P. A. Lindfors, W. M. Mularie, and G. K. Wehner, Surf. Coat. Tech., 29 (1986) 275.

9- A. Mumtaz and W. H. Class, J. Vac. Sci. Technol., 20 (3), (1982) 345.

10- R. P. Howson, H. A. Ja'fer, A. G. Spencer, Thin Solid Films, 193/194 (1990) 127.

CHAPTER-7

HIGH ION CURRENT PERFORMANCE FROM AN UNBALANCED MAGNETRON

It is well known that ion bombardment of the growing films can strongly influence their microstructure and consequently their physical properties (Ref. 1). Magnetron sputtering is now a widely used deposition technique. Its essential disadvantage is a lack of substrate ion bombardment during deposition.

In principle there are many possible ways to increase the ion current density on the substrates in magnetron sputtering, these are:

1- In the area of sputter-deposited hard coatings, ion-bombardment is typically performed by extraction of ions from the discharge using a 10-200 Volts of negative bias applied to the substrate. For insulating substrates a RF bias can be used (Ref. 2).

2- Additional ionisation, for instance by a hot cathode electron beam (Ref. 3) or a hollow cathode arc electron source (Ref. 4).

3- A magnetic confinement for the plasma, for instance by an unbalanced magnetron geometries as a means of increasing the ionisation density in the region near the substrate (Refs. 5-7).

In plasma assisted PVD (PAPVD) processes, the plasma plays a very important role in deposition. In general, it can be said that (1) electrons control the plasma chemistry by excitation, dissociation and ionisation of a working atmosphere, and (2) ions control the microstructure of films.

The kind and degree of film modifications due to the ion bombardment of the growing

films depend on (1) the kinetic energy of incident ions and (2) the ratio of fluxes of bombarding ions and condensing atoms Fi/Fm. Ion energies near the threshold of resputtering, desorption and impact induced displacement of surface atoms during film deposition will take place. At energies below 100 eV, the yield of ion impact events strongly decreases. To ensure sufficient effects in the film, then, the impact ratio of ions and condensing particles must be very high (>10) (Ref. 7).

To achieve such a value, the field of the conventional unbalanced magnetron is not enough. Extra magnets fastened around and behind the substrate are used to confine the plasma extracted from the unbalanced magnetron (Refs. 9-11). The disadvantage of such a design is that it localises the plasma beam in a certain area rather than distributing it across the substrate surface. Musil and Kadlec (Refs. 7,12,13) have combined the use of the unbalanced magnetron with biased substrates to achieve a double-site-sustained discharge (DSSD). The yield of this system showed that the impact ratio F_i/F_m can be increased from 2 with the use of the unbalanced magnetron to >10 with using the DSSD. Recently a dual magnetron has been used for hard coatings purposes (Refs. 14-16). With this technique two unbalanced magnetrons are used facing each other (Ref. 14). The maximum ion current achievable between was 5 mA/cm^2. Despite , all the techniques illustrated above, there is no single system that can provide the high impact ratio without using an enhanced magnetron process, such as , biasing the substrate , using two magnetrons or using an additional cathode for gas ionisation. The design of a single unbalanced magnetron in such a way to provide high ion current density and bias voltage on the insulating or isolated substrate has been achieved (Ref. 17). The feature of this system is discussed in this chapter.

7.1 Magnetron Design

A configuration of an unbalanced magnetron (UM) has been considered which directs a significant amount of the plasma onto the substrate surface. This immersion of the insulating substrate in a dense dc plasma provides a high ion bombardment of the depositing film.

The unbalanced dc magnetron with its new construction and magnetic configuration is shown in Fig. 1a. Extra rings are used, fixed on the outer pole of the magnetron and extended to a considerable distance from the target surface. Leakage of magnetic field with better confinement can be achieved. The magnetic field configuration is compared with the original unbalanced magnetron, Fig. 1b.

The key factor of this approach is the magnetic field configuration. The field lines in the new UM generally leak further to the front with less divergence. More magnetic flux will strike the substrate than with the original UM, see Figures 1a and 1b. Figure 2 shows a photograph taken of the new UM, using iron fillings to highlight the field. This Figure shows the field configuration, the null point (zero magnetic field point), and the magnetron with its target. The maximum field strength measured at the cathode surface at a radial distance of 20-30 mm was 200 gauss. At this distance is the most intense glow in the plasma, in addition the highest etching rate of the cathode (target) took place here. This magnetic strength is lower than that of the old magnetron by 70 gauss. That is due to the extension of the outer pole, weakening the field strength that is attracted by the inner pole, which leads to less magnetic field strength at the cathode surface. With this design the null point moved forward. The critical point concerning the maximum magnetic field that leaks towards the substrate is observed to have larger distance than that of the original UM. These two points, however, can be controlled only by adjusting the number of mild steel rings that are fixed on the outer pole of the magnetron. With this technique it

Fig.7.1 A cross section of an unbalanced magnetron a) the new design and b) the conventional unbalanced magnetron.

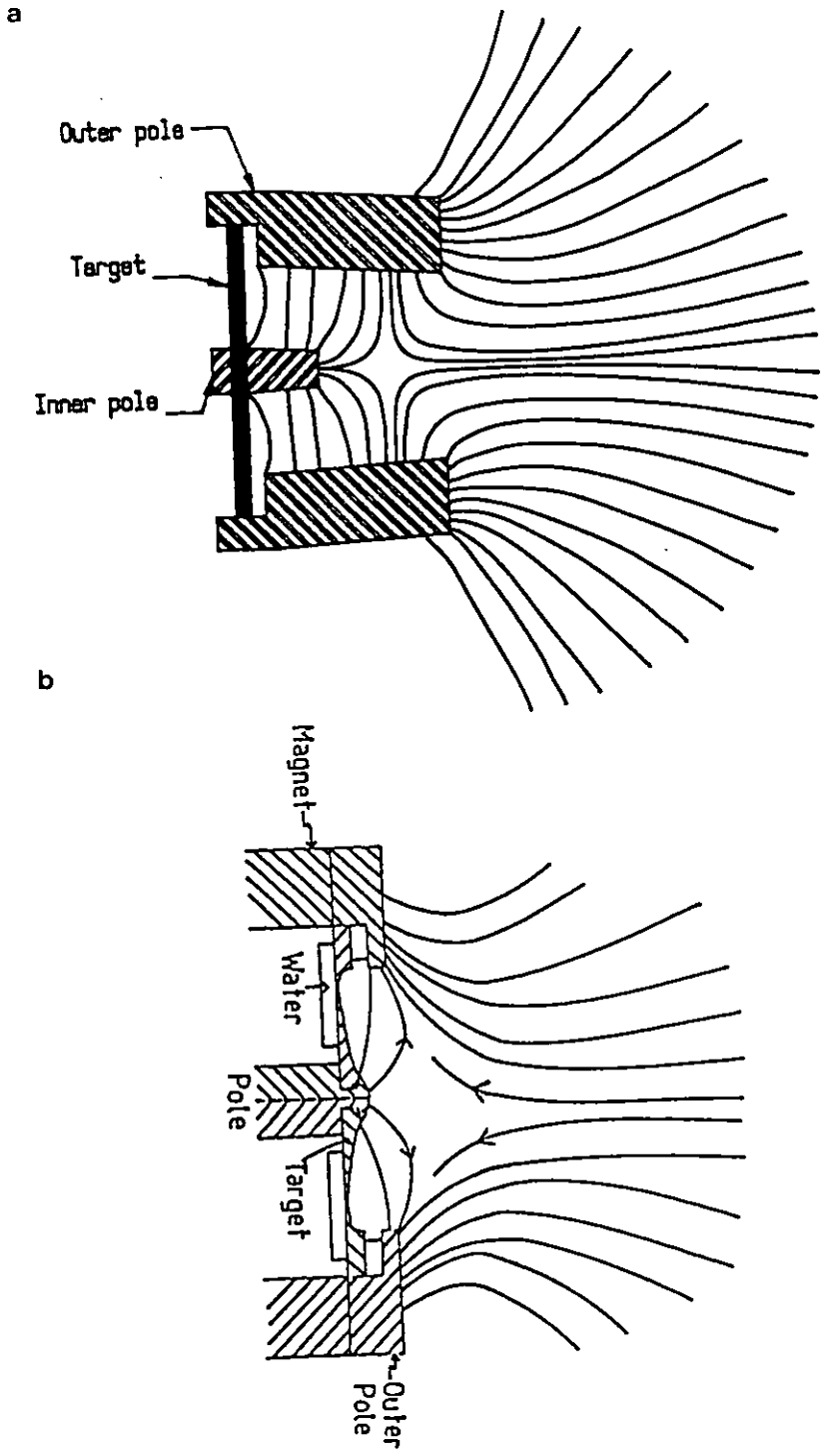

Fig.7.2 A photograph shows the magnetic field profile of the new unbalanced magnetron.

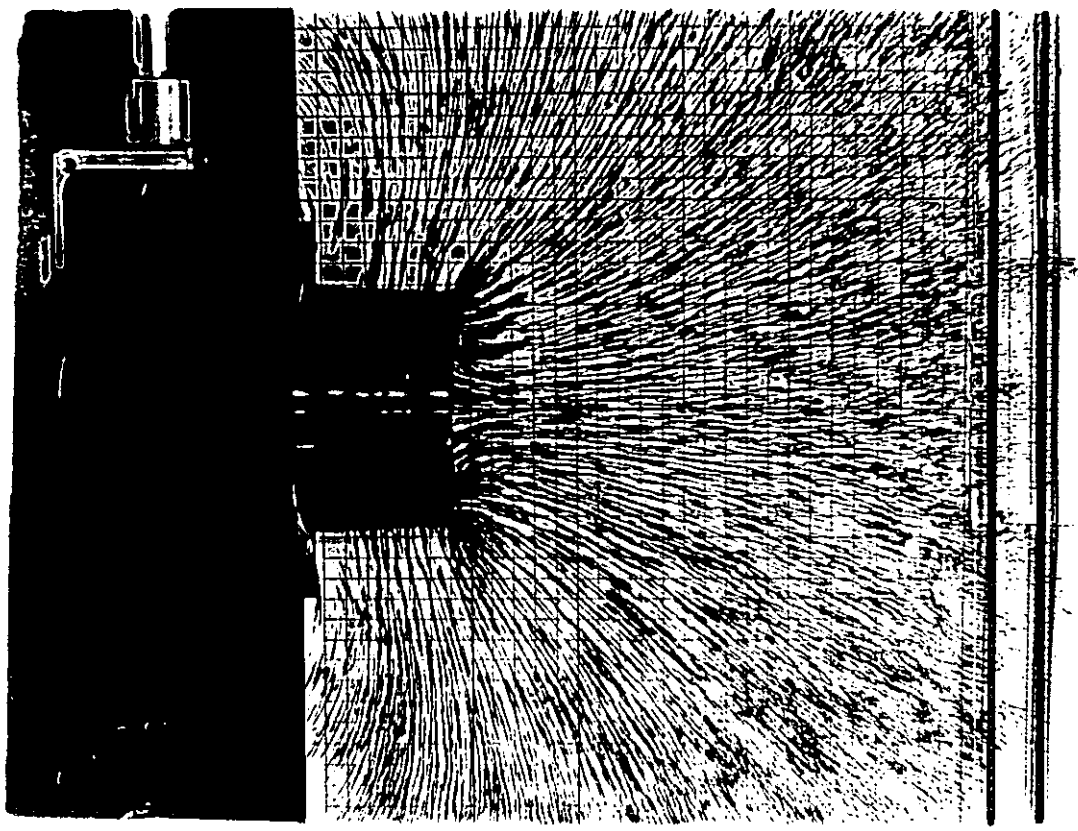

is not only desirable to control the critical point of the maximum field. It will optimise the leakage of the plasma and consequently by controlling the target-substrate distance and the number of the mild steel rings, the impact ratio of ions to condensing atoms can be adjusted.

7.1.1 I-V Characteristics of The New UM

Figure 3 shows the I-V characteristics of the magnetron discharge for both the original and the new unbalanced magnetrons. The measurements have been taken with argon pressure of 3 mTorr. The results that are shown in the figure confirm that better confinement has been achieved compared with the original one. The discharge characteristics of Fig. 3 are very similar to those observed for conventional magnetrons, and can be fitted to the same functional form:

$$I = K V^n$$

with values of n which depend on the magnetic field and gas pressure (Ref. 18) (see chapter 5 section 5.1.1).

7.2 Substrates Effects From UM

7.2.1 Floating Potential and Ion Current Measurement

A planar probe of area of 1 cm^2 has been used to investigate the plasma properties. Such a probe can be used effectively to measure substrate effects arising from the modification of the plasma used in sputtering. The observed dependence of the substrate parameters on the sputtering variables makes this technique useful for controlling the effects of ion bombardment during sputter deposition. The floating potential and the ion current bombarding the substrate are important parameters in thin film growth. For using an insulating or isolated substrate the floating potential represents almost the ion energy that

Fig.7.3 Unbalanced magnetron I-V characteristics.

Fig.7.4 Probe measurements of ion current density for oxygen and argon plasma.

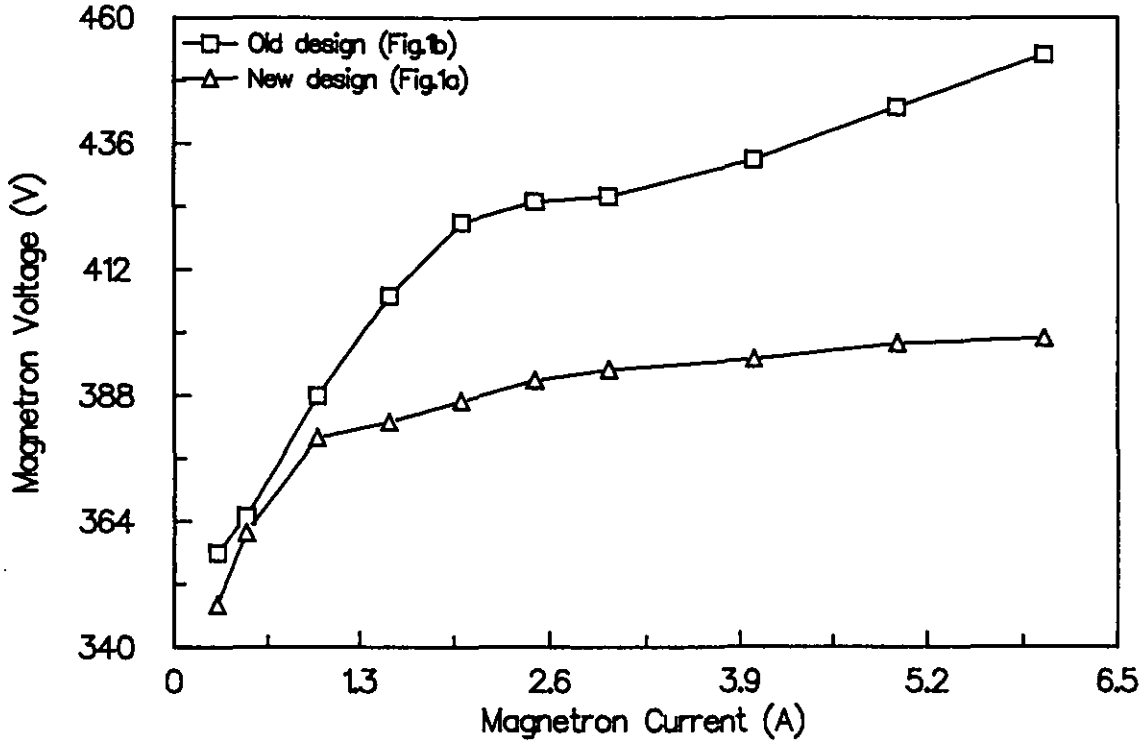

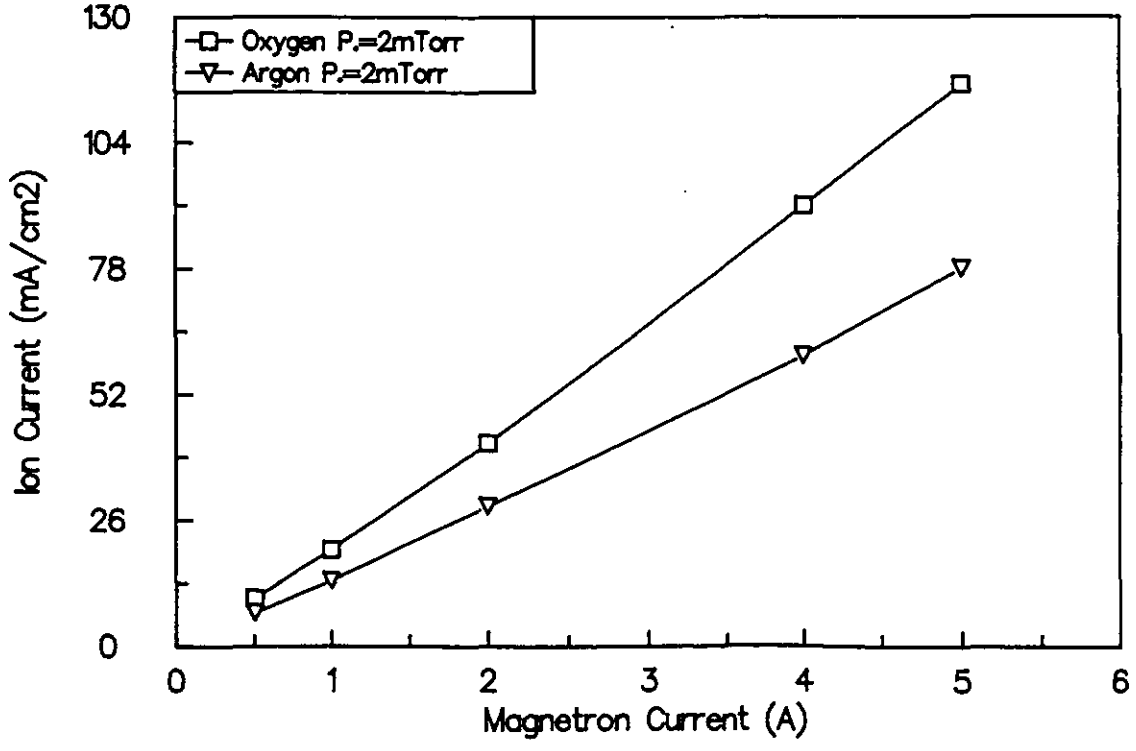

bombards the growing film.

Oxygen is used in many reactive sputtering applications, we have also used it in addition to argon in order to study the magnetron performance. In all the following Figures a comparison between the argon and oxygen uses is shown. Figs. 4 and 5 show the probe measurement of both ion current and the floating potential respectively. These measurements were taken as a function of the magnetron current. As the magnetron power increases additional ionisation to the working gas at constant pressure will occur. In turn, some of these ions will escape towards the substrate, following the electrons , and consequently the ion bombardment of the growing film will increase. For argon gas, a feature of magnetron discharge is that the floating potential is approximately constant. That is due to the energy accompanying the secondary electrons that enters the plasma is nearly constant at a fixed pressure.

Ionization in molecular gas discharges normally occurs predominantly by electron impact (Ref. 19). Reactions of this type include:

$$O_2 + e \text{ ---------- } O_2^+ + 2e$$

such a reaction predominates with high probability. In addition, other possible reactions involve $O2^{++}$ and O^+, the ion density in the oxygen plasma is higher than in argon plasma (see Fig. 4).

It is noted that plasma discharges often contain relatively large numbers of low energy electrons which have spent their energy in making inelastic collisions. These electrons can attach to electronegative molecules to form negative ions (Ref. 20), thus one has:

Fig.7.5 Probe measurements of floating potential for oxygen and argon plasma.

Fig.7.6 Plasma properties of unbalanced magnetron with oxygen partial pressure.

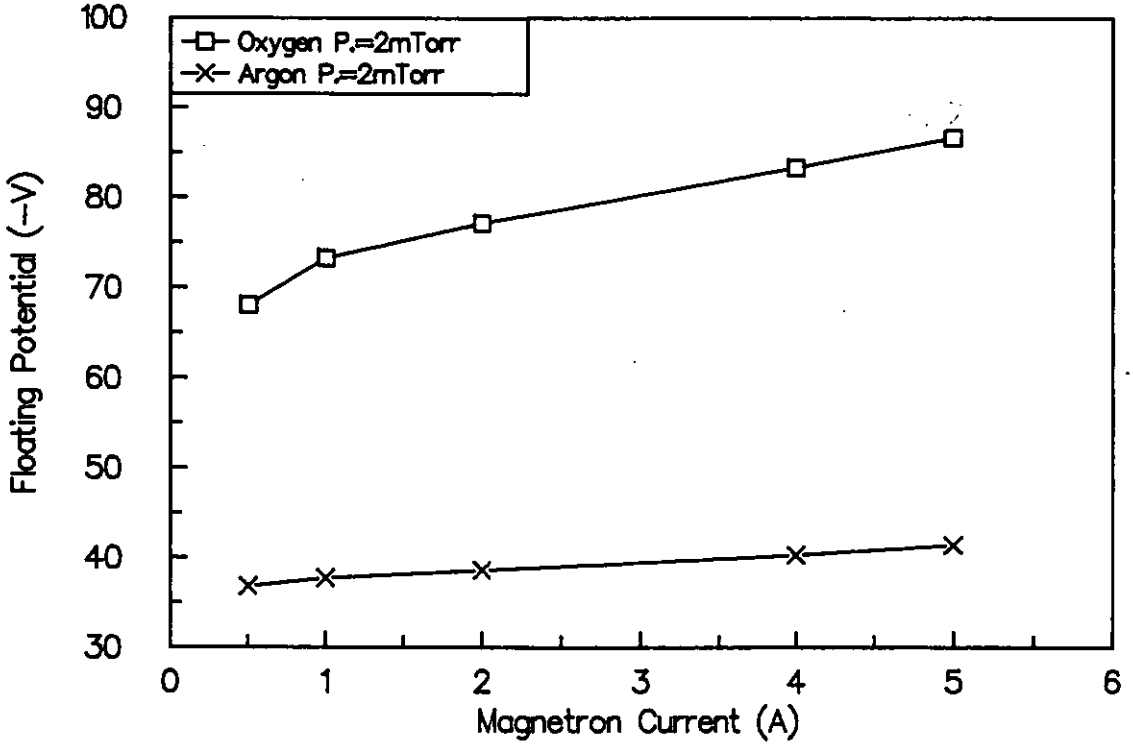

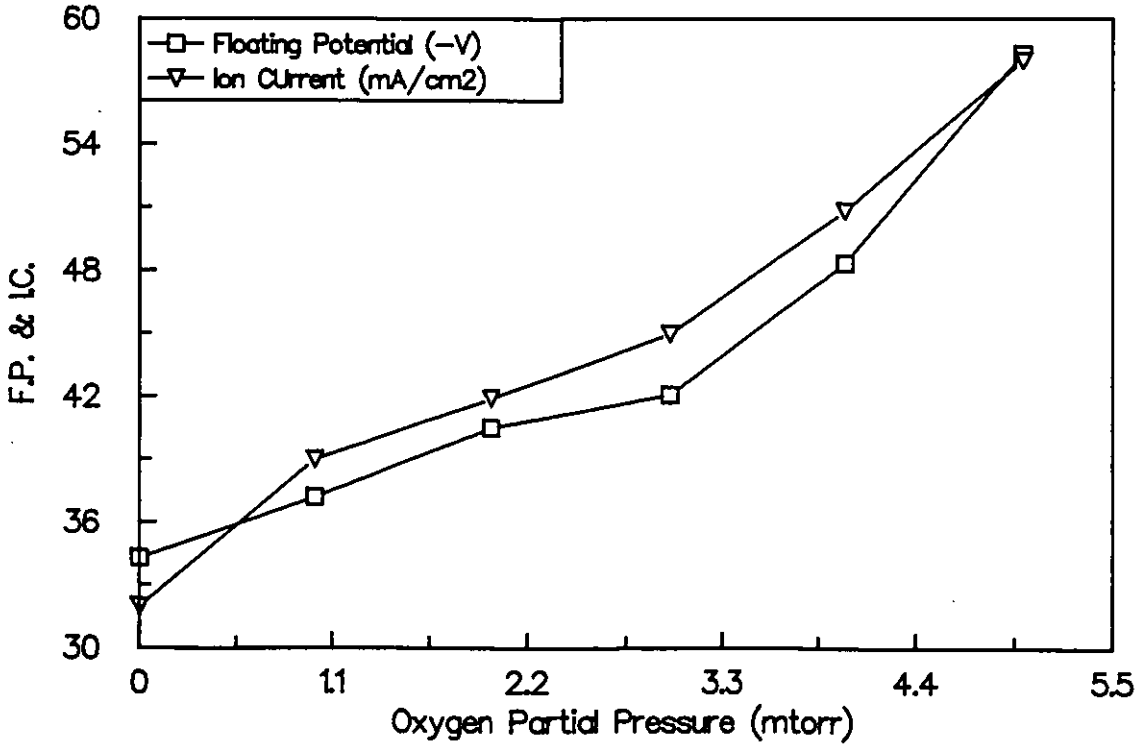

$$e^- + O_2 \text{ ---------- } O_2^-$$

The ion may then dissociate to give

$$O_2^- \text{ ---------- } O^- + O$$

Electron impact dissociation also occurs; reactions such as

$$e + O_2 \text{ ---------- } 2O + e$$

$$e + O_2 \text{ ---------- } O + O^-$$

There is a large supply of atoms, free radicals, and negative ions in the discharge. The high oxygen reactivity, the presence of the radical, excited atoms and molecules and negative ions, allow the substrate self-bias to assure a value double that when argon gas alone is used (see Fig. 5). As will be shown later, this energy is high enough for the etching of polymer. By using the oxygen and argon mixture the floating potential and ion current density can be adjusted merely by changing the oxygen partial pressure, Fig. 6. With such condition, and in addition to the reactions above, gas ionisation by oxygen-argon interaction can occur (Ref. 21). Reaction of this type includes:

$$O_2 + Ar \xrightarrow{h\upsilon} O_2^- + Ar^+$$

$$O_2^* + Ar \xrightarrow{h\upsilon} O_2 + Ar^+ + e$$

As shown in Figure 6 the ion current and the floating potential increase as the O_2 partial pressure increase.

7.2.2 Floating Potential and Ion Current Distribution with Axis Distance

The new unbalanced magnetron shown in Fig. 1a provides significant plasma confinement at the race-track. This provides a simple way of varying the ion bombardment to depositing species ratio at the substrate. This ratio can be estimated by dividing the ion current density by the deposition rate, at that distance from the target face. Fig. 7 illustrates the ion current density and the substrate self-bias with the plasma beam axis. This Figure shows the ion current extends to a larger distance compared with the original one.

7.2.3 Auxiliary Magnet Effects

Generally, magnetic bias has been used to increase or decrease the surface bombardment during deposition (Ref. 8). The configuration of such a design shows that the magnetic field is leaked forward a large distance from the front face of the ring before divergence far closure of the field lines. Hence a small magnetic field strength behind the substrate, opposing the magnetic polarity of the outer pole, can assist the magnetic field concentration and orient it perpendicular to the substrate surface. By using an electromagnetic coil positioned behind the substrate, the magnetic strength can be chosen by varying the biasing current of the coil. A 2 Amps current through the coil giving 150 gauss allows the self-bias voltage and probe ion current to be 15% higher. Figure 8 shows the experimental iron filling shape for N-S polarity.

The performance achieved from the new unbalanced magnetron ignores the use of magnetic bias. Alternatively, the use of magnetic bias in a such a way permits the plasma to be constricted to a 20 mm diameter. In turn, the substrate becomes red hot. The magnetic bias, then, is used to control the ion bombardment and floating potential, rather than enhance the plasma properties. Figure 9 shows a photograph of iron fillings, for N-N shape. Using N-N configuration, the substrate self-bias voltage and the ion

Fig.7.7 The distribution of the substrate self-bias and ion current with plasma beam axis.

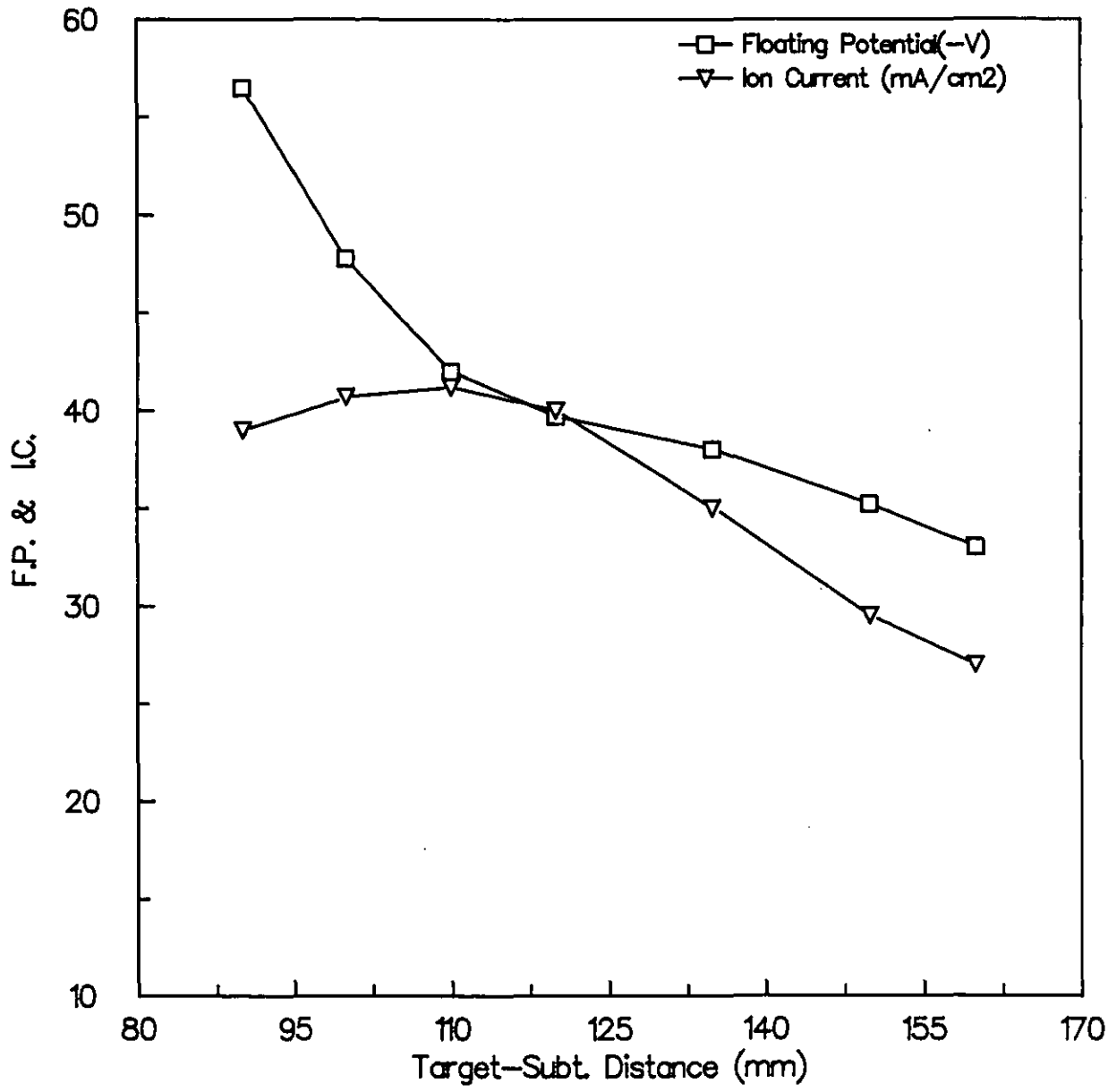

Fig.7.8 Magnetic field profile for N-S polarity.

Fig.7.9 Magnetic field profile for N_N polarity.

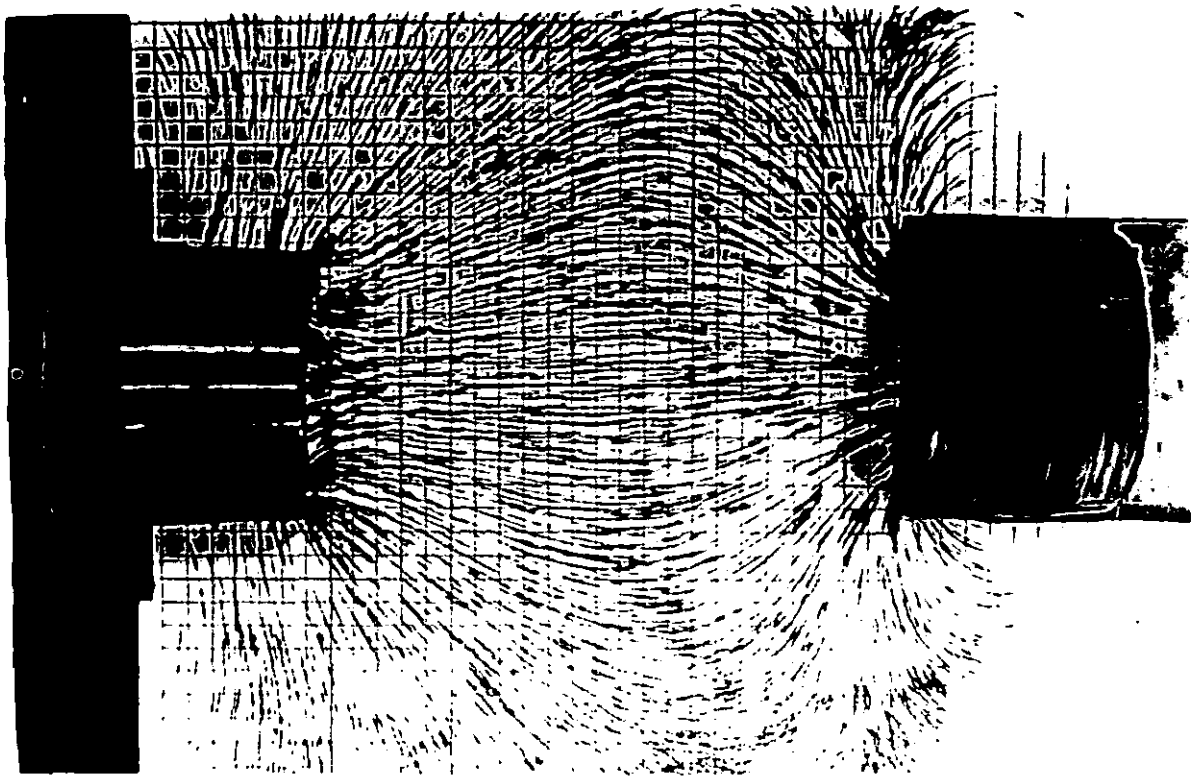

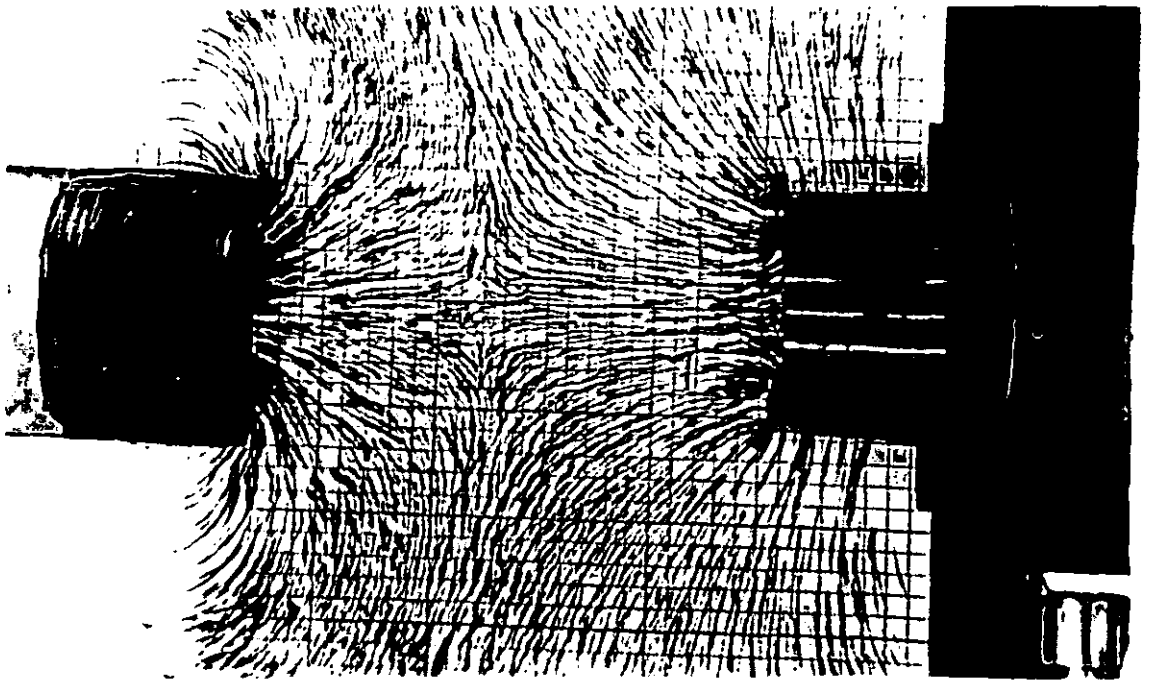

bombardment can be controlled with ease. By passing a dc current through the electromagnetic coil the magnetic strength at the substrate can be controlled and in turn, the plasma can be moved backward or forward.

7.3 Plasma Activation

Generally, by using the unbalanced magnetron, an increase in reactivity of the process on the substrate surface can be seen, giving a requirement for less reactive gas to be present, and hence a lower operating partial pressure (Refs. 22,23). Because of the highly confined plasma on the substrate and lower deposition rate with increasing distance, high plasma activation at the substrate surface, even with low base pressure occurs. In sputtering, film formation reactions at the substrate can be activated by the proximity of a plasma (Refs. 24,25) or by ion bombardment (Ref. 26). In order to estimate the extent of the concentrated plasma on the film purity, the reflection of a copper film in the visible range of the spectrum has been measured. These results are demonstrated in Figure 10 and compared with those of the original UM. As shown in this figure, the copper film that is deposited from using the new UM is more oxidised compared with the samples that were made with the original UM, but with less plasma intensity at the samples.

7.4 Applications

7.4.1 Plasma Enhanced Chemical Vapour Deposition (PECVD)

The earlier work on plasma-enhanced chemical vapour deposition (PECVD) is reviewed by Reif and Kern (Refs. 2,27). PECVD is an established commercial technique for the deposition of insulating films such as silicon nitride and silicon oxide. The major advantage of PECVD is its lower temperature capability compared with that of thermally driven CVD. Most of the glow discharges used for thin film plasma deposition are created by subjecting the gas to a radio-frequency (rf) electric field. Inelastic collisions between high-energy electrons and gas species generate highly reactive species, such as

Fig.7.10 The effects of the plasma activation on the film optical properties.

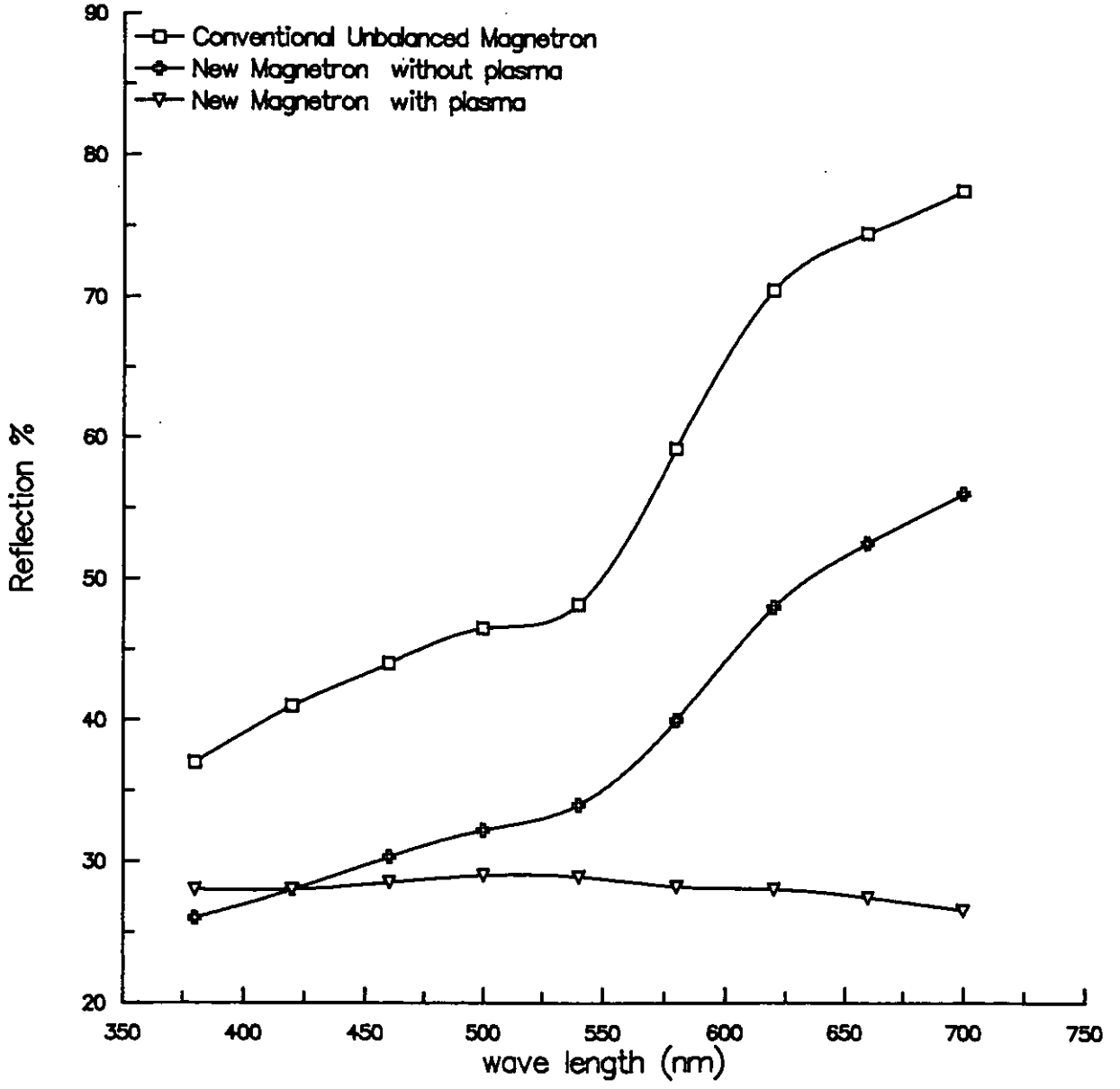

excited neutrals and free radicals, in addition to ions and electrons. By these mechanisms, the energy of the electrons creates reactive and charged species without substantially increasing the gas temperature. The reactive species that are generated in the plasma have a lower energy barrier to physical and chemical reactions than the parent species, and consequently can react at a lower temperature. In PECVD, these reactive species are utilised to form thin films at temperatures lower than those possible with thermally activated CVD. The charged species in the glow discharge may also affect the properties of the deposited film (Refs. 28,29).

7.4.1.1 Diamond-Like Carbon Deposition by PECVD

Hard diamond like amorphous carbon films offer extreme hardness, chemical inertness, and optical transparency over a wide spectral range. However, the realisation of these favourable properties depends sensitively on the microstructure, and thus on both the method and parameters of deposition. Much work has been done on the preparation of hard carbon films using rf (Refs. 30-33) and dc plasma deposition (Refs. 34,36), ion beam (Refs. 37,38), and sputtering technique (Refs. 39-43).

D.C. magnetron sputtering of carbon in an Ar-C_2H_2 gas mixture, using a metal cathode overcoated with a-C:H film, was reported by Carring and Harding (Ref. 43). Both post cathode and planar geometries were employed. Recently Savviides and Window (Ref. 41) reported 'DLC films' prepared by magnetron sputtering of graphite. Biederman et al (Ref. 40) used the same technique of Savvides. He compared the result of the unbalanced magnetron sputtering of a graphite target with that of using argon/propane mixture. Our experiment followed the same technique. The new unbalanced magnetron, graphite target, argon, oxygen, hydrogen and methane gases were used. In the first experiments the argon/methane mixture was used. The magnetron current range was between 0.5 and 5 A with corresponding voltages between 300 and 450 V. With these conditions, carbon

films were made at different argon and methane pressure, magnetron current and with addition of oxygen and hydrogen. In our investigation several measurements were made. For hardness estimation, a hard metal stylus was used. Other investigations were achieved by arbitrary examination of the appearance of the film, and by measuring the refractive index and the optical gap. The refractive index was measured by using an ellipsometry method. The optical gap was measured by following the procedure below (Refs. 17,40-43).

By using the spectrophotometer, the transmission T and reflection R can be measured. The optical absorption coefficient α was determined from this formula:

$$T = \frac{(1 - R)^2 \; e^{-\alpha d}}{1 - R^2 \; e^{-2\alpha d}}$$

The optical gap E_{opt} can be found by following this equation:

$$(\alpha E)^{1/2} = A \, (E - E_{opt})$$

where A is a constant.

The conclusions of this work can be illustrated by several points. In general, the film hardness was not satisfactory, but the film tended to be harder as methane pressure and magnetron current are decreased , and argon pressure is increased. The effects of oxygen partial pressure on the film properties show that general film features are improved. Biederman in his work demonstrates that the optical gap is increased as the propane partial pressure is increased. He witnessed the incorporation of hydrogen in the film structure and highlights that more polymeric inclusions are involved at the highest propane concentrations. This also happens when higher magnetron current is used.

In the second experiments, graphite sputtering when using pure argon and argon/oxygen-hydrogen mixtures was examined. Amorphous carbon was made by using pure argon. An optical gap of (1 ∓ 0.3 eV) was observed. This is in a good agreement with References 40 and 41. When oxygen is used, hard, transparent films of DLC were obtained. Oxygen partial pressures from 1 to 30 mTorr with magnetron currents of 3 to 5 A was used. These results demonstrate that the film becomes harder, more transparent and higher refractive indices between 1.98 and 2.4. There are no significant changes observed when additional hydrogen and nitrogen gas is used. For greater understanding of DLC properties the updated review of properties of diamond-like carbon in reference 44 is of great use.

7.4.1.2 Silicon Oxide (SiO_2)

Due to high magnetron performance and lower sputtere rate when Si is operated in oxygen partial pressures, this system is used as a plasma activation source rather than a sputter deposition system. PECVD of SiO is well explained by Reif and Kern (Ref. 2). Analysis of the silicon based compounds tetraethyoxysilane Si $(OC_2H_4)_4$ in the production of the silicon oxide was investigated using this system. This compound, liquid at room temperature, was contained in a glass chamber external to the evacuated reaction chamber. With reduced pressures in the reaction chamber of less than 10 mTorr, quite high flow rates of the compound vapour were achieved. No heating of the compound resulted whilst in the liquid stage was maintained.

Initially a small flow of silicon compound vapour was allowed into the system. Using this as the only gas present, a glow discharge was set up. Samples were produced with typical magnetron current of 1 Amp and exposure times of 6 minutes. These samples were found to have very high refractive indices, in the region of 2.3. This was far higher than the normal measured values for transparent silicon oxide film of 1.5 or less. We

have found, discharge deposited silicon compound does not oxidise the magnetron target and hence its sputtering is not reduced. These form a more dominant film formation process than that of the dissociation and reformation of the silicon molecules in an oxide form. In order to minimise this problem, oxygen gas was used and by controlling the argon and oxygen partial pressures the SiO refractive index of < 1.5 can be achieved, as shown in Figures 11 and 12. The argon optimises the activation process and oxygen enhances the film formation. In the use of this process, some problems had to be faced. Because direct PECVD was used rather than remote, SiO will be formed at the magnetron target and causes arcing and consequently the process has to be stopped. Other problems related to the pumping system occurred. The high flow rate of vapour into the reaction chamber caused contamination of the oil in the rotary pump and generally took a long time for the pump to recover and hence the efficiency of the pumps was reduced.

7.4.1.3 Titanium Oxide (TiO_2)

The oxides of interest are titanium dioxide TiO_2 and silicon dioxide SiO_2. These oxides have the physical properties of optical transparency, with TiO2 having very high refractive index of around 2.4 and SiO2 a lower refractive index of less than 1.5. This makes them ideal for use in multi layered thin film interference stacks which are used in the manufacture of frequency selective optical filters.

In plasma induced coating methods dissociation of the compound molecules takes place along with the normal ionization processes found in plasma discharges. Recombination of the ions to form the oxide on the substrate surface is then possible. This process has the advantage of much reduced thermal affects than the vapour deposition method. It has already been demonstrated that production of oxide films can take place using this method with the use of titanium chloride compounds (Ref. 45). It is hoped that a similar effect can be achieved using an organic titanium compound in the production of an oxide.

Fig.7.11 Variations in argon partial pressure on refractive index of SiO_2.

Fig.7.12 Variation in oxygen partial pressure on refractive index of SiO_2.

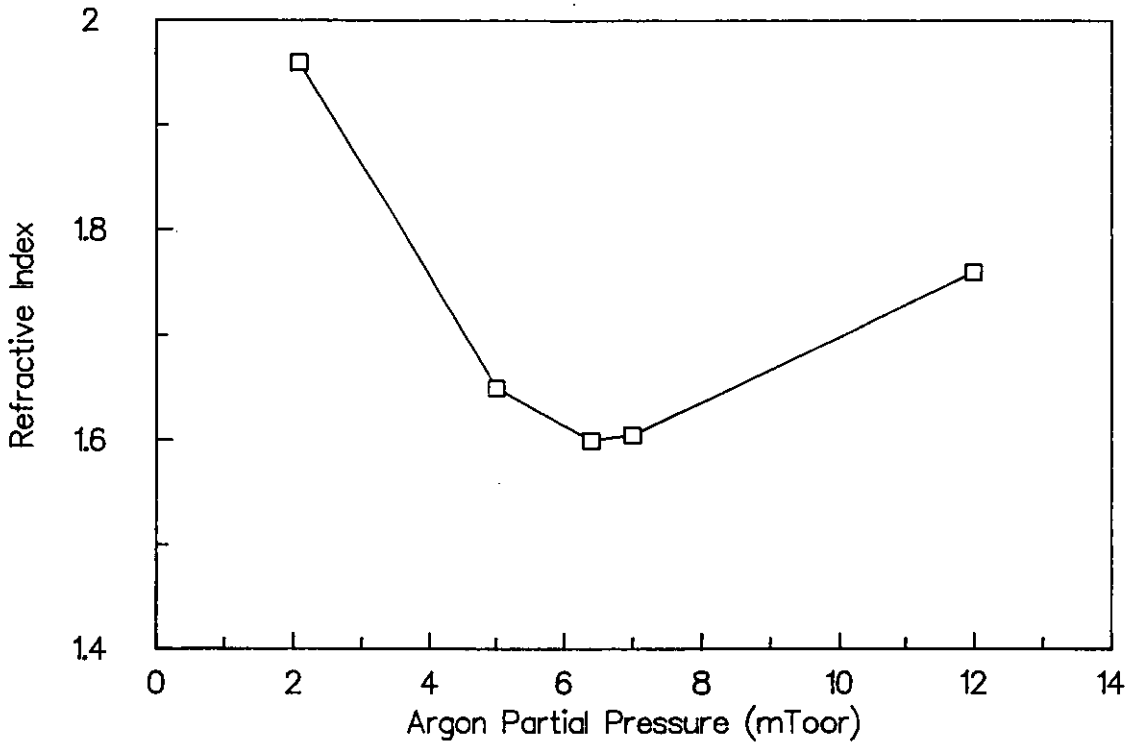

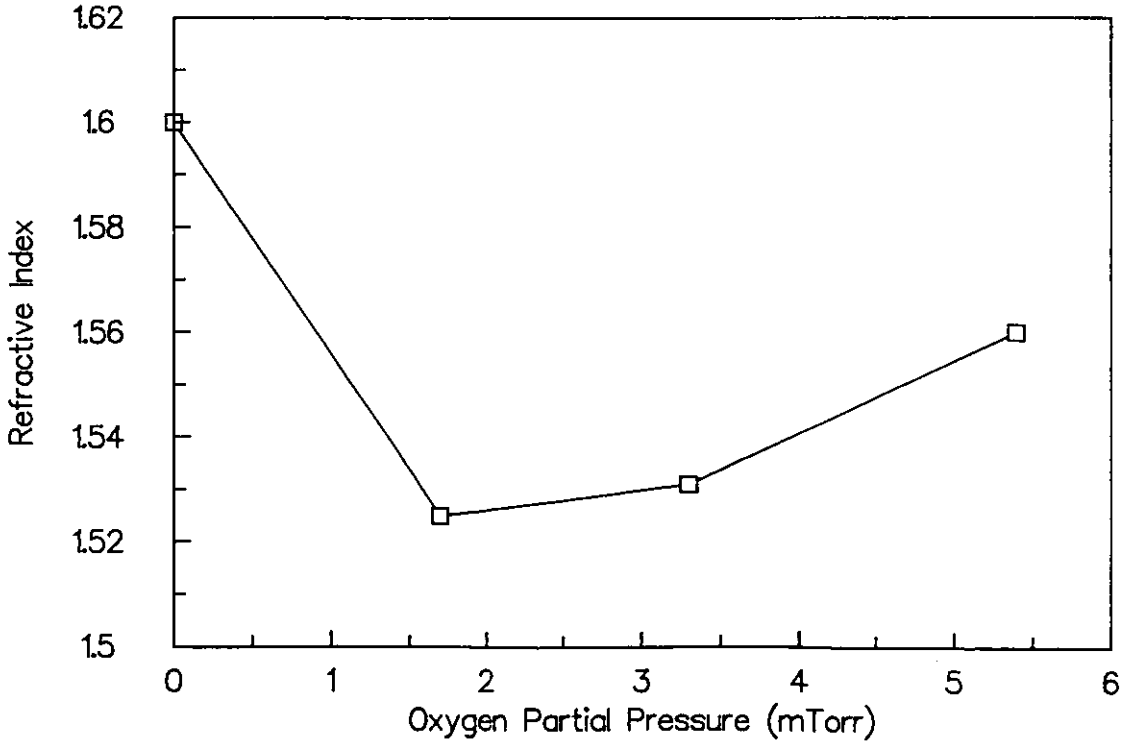

For this part of the investigations a tetraisopropylorth-otitante liquid $Ti\{OCH(CH_3)_2\}_4$ was used as in SiO deposition. The investigation of TiO2 is carried out by varying the titanium compound vapour partial pressure, argon pressure, oxygen partial pressure and plasma exposure time. The initial samples were made with the titanium compound vapour as the only gas present within the system. The magnetron used a carbon target. Typically short duration exposure times of around 3 minutes were used. These samples were found to have a dark powdery deposit laid down on substrate surface, later identified as contamination from the carbon target material. In order to reduce target sputtering, again argon and oxygen gas were used. With argon the refractive index of the deposited film shows very slight improvement. With oxygen, a series of samples were made using the optimised levels of the compound vapour and similar levels of argon vapour to those used in the experiments above. All the samples were made with magnetron currents of 1 amp and exposure times of 3 minutes. The resultant films are shown Figs. 13 and 14. As can be seen from these two Figures the best results were seen at lowest deposition rates. At levels below the optimum point, the ratio of oxygen ions to reactive titanium ions is insufficient to allow a high deposition rate of the required oxide film. As the ratio of oxygen to titanium ions varies, there will be a point where the ratio of the reactive ions will produce the purest possible form of the oxide coating. Beyond the stoichiometric point an excess of oxygen atoms exists, and production of another oxide form may begin altering the films properties. Figure 15 represents the deposited thickness for a range of exposure times. For this it can be seen that a linear relationship exists between the coating thickness and the exposure time.

Analysis of the refractive index of the film is shown in Fig. 16. With an increase in exposure time there is a marked increase in the refractive index, particularly for the exposure of 18 minutes, where a refractive index of almost 2.4 was measured. It is a

Fig 7.13 Effects on TiO_2 refractive index of variations in oxygen partial pressure.

Fig 7.14 Effects on TiO_2 deposition rate of variations in oxygen partial pressure.

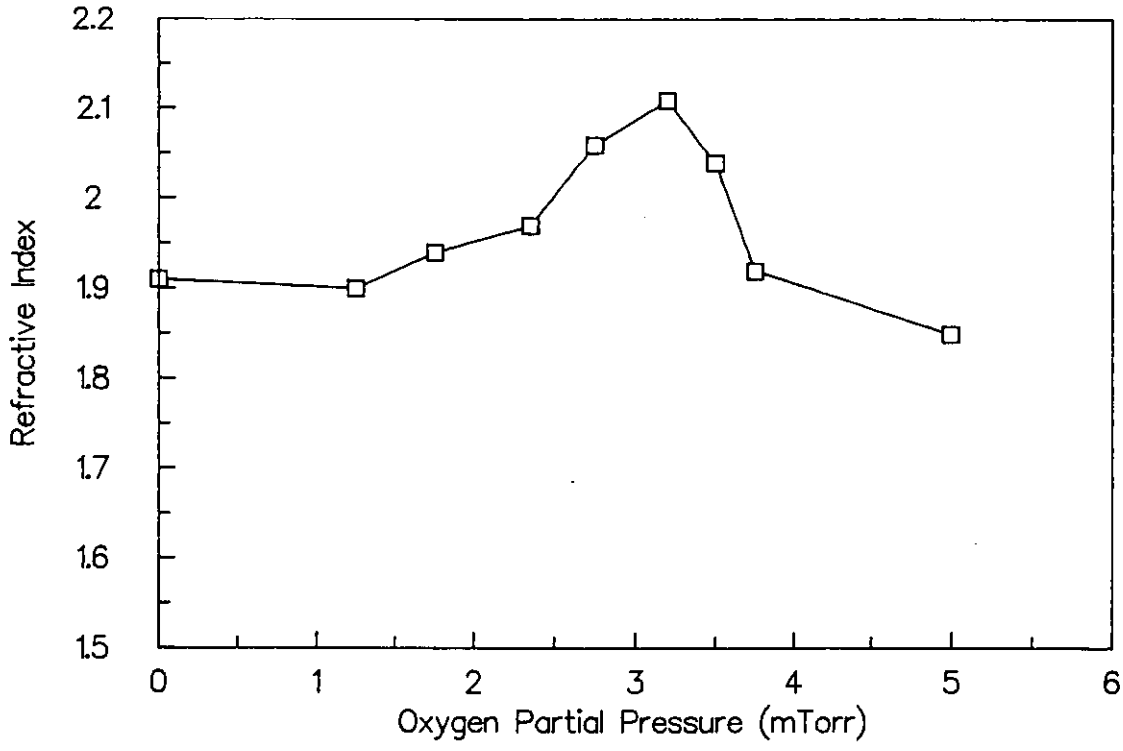

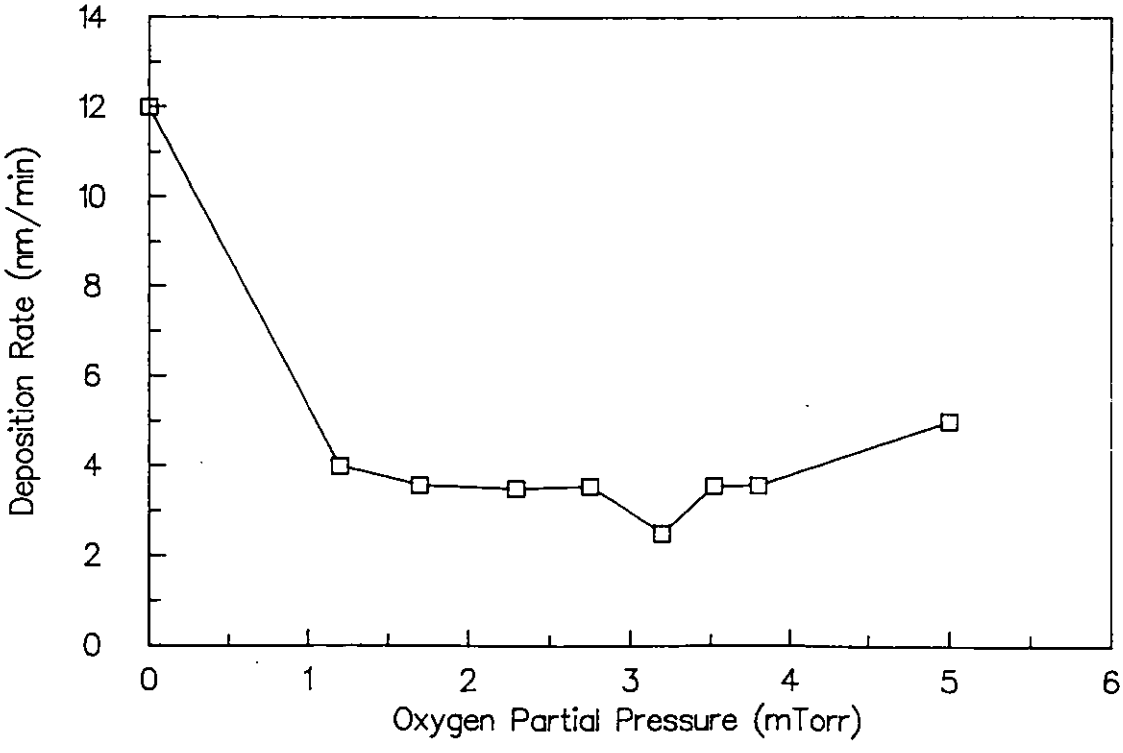

Fig.7.15 Variation in deposition thickness with increased exposure time.

Fig.7-16 Variation in refractive index with increased in exposure time

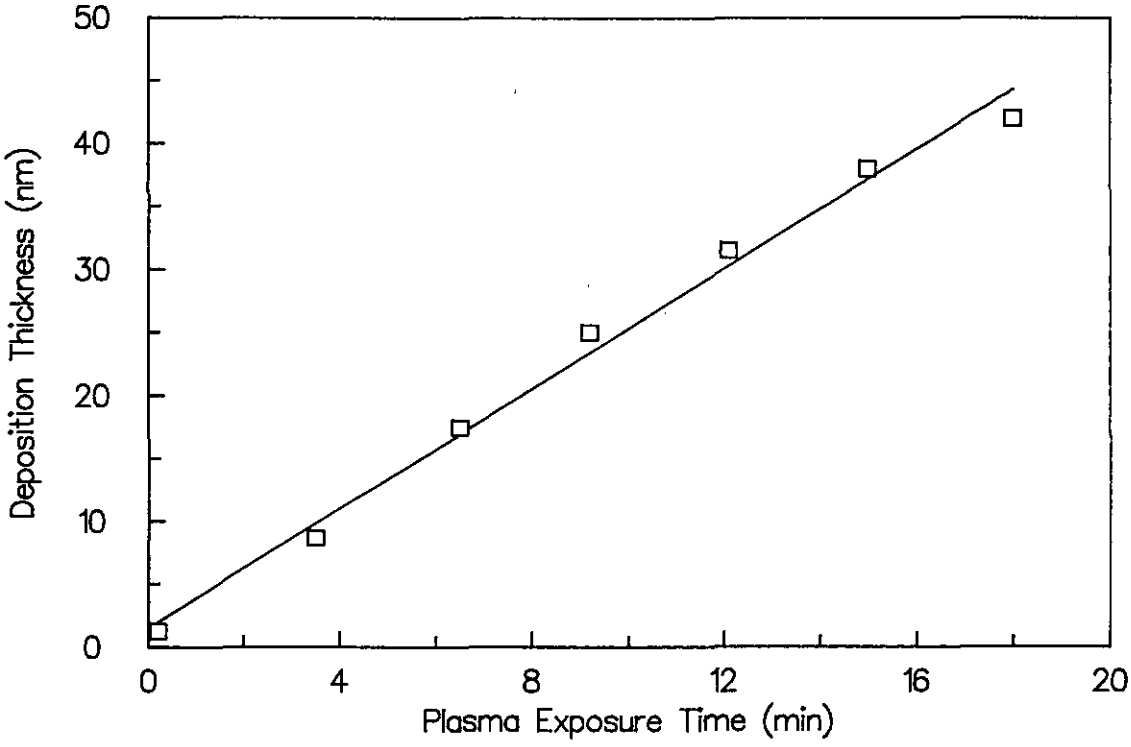

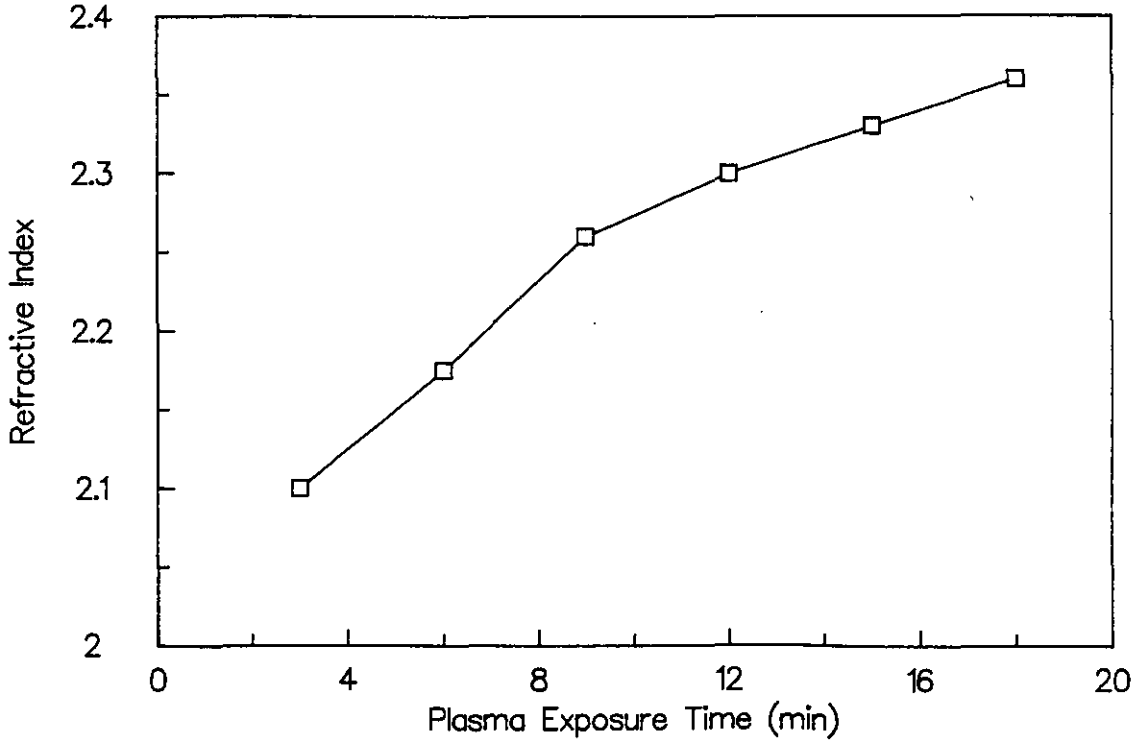

feature of thin films that the electrical and optical properties may be improved as the thickness of the deposited film increases.

The major problem with this process is to evaporate the titanium compound directly into a process chamber. It was too difficult to control the flow rate of the compound vapour. By heating the titanium compound container, the evaporation took place, but the flow rate control was still difficult. Once again these sorts of organic compounds contaminate the diffusion and rotary pump oil, in turn shortening their lives. The problems concerning the target contamination remained. The plasma source (see chapter 9) will be shown to adopt this technique for use as a remote PECVD rather than a direct process, which in turn, gives more control ability and less contamination.

7.4.2 Polymer and Positive Photoresist Etching

Dry plasma etching is a new approach for an environmentally safe cleaning and drying of metallic and polymer surfaces. In the case of plastics, plasma etching is accompanied by a modification of the polymer surface thus creating active sites for an improved adhesion of subsequent metallic or organic coatings. By using reactive ion etching, the textured surface consisting of submicrons columns for selective absorption and optical storage (Refs. 46-49). Some of optical properties in light scattering by diffuse reflectance and interface roughness have been investigated (Ref. 50). The influence of polymer temperature, ion current density, ion energy and ion dose on etch and deposition rate of PTFE and FEP has been investigated (Ref. 51). The results of an investigation of the effect of rf bias ion plating on CR 39 plastic and PET have been investigated (Ref. 52). It was shown that the plastic substrate is easily etched by ion bombardment and chemical /structural changes in the surface depend upon the bombardment condition. It was found that the etching rate increase directly with increasing the rf power (Refs. 19,53).

In this work, the plasma produced from the new unbalanced magnetron was employed for investigation the photoresist and PET polymer etching. This study has been carried out in a pure oxygen plasma.

7.4.2.1 Plasma Parameter Effects

It is really the evidence clarified in our early investigation that the intensity of ion bombardment and their energy can be increased by the addition of the oxygen. So that the reactivity of the process on the substrate surface and the radical species needed for this investigation will be enhanced. The dissociation of oxygen molecules by electron impact as well as the ionization will occur, so that reactions such as,

$$e + O_2 \text{ ---------- } 2O + e$$

$$e + O_2 \text{ ---------- } O_2^+ + 2e$$

are a major source of atoms, free radicals, and negative ions, in the discharge, and these reactions are quite important in photoresist etching or stripping (Ref. 2). Consequently these components are controlled by discharge condition like gas pressure and magnetron power which in turn, control the intensity and energy of ions and the generation rate of active species necessary to create a reaction for etching. As oxygen pressure is increased (at constant magnetron power) the collision rate will increase but the average electron energy will eventually decrease simply because the existing field will have less time accelerate an electron collision. So that the generation of active species or its precursor will be decreased. Hence, the etching rate must eventually decrease with increasing pressure as shown in Fig. 17.

With increasing the magnetron current (at constant pressure), the energy of species is relatively constant but the generation rate of radical atoms will increase. The latter leads to an increase of the etching rate as shown in Fig. 18. We have also found that the etching rate is inversely proportional to the argon partial pressure. We have also found that when

Fig.7.17 Variation of etching rate with oxygen pressure.

Fig.7.18 The effects of magnetron power on the etching rate.

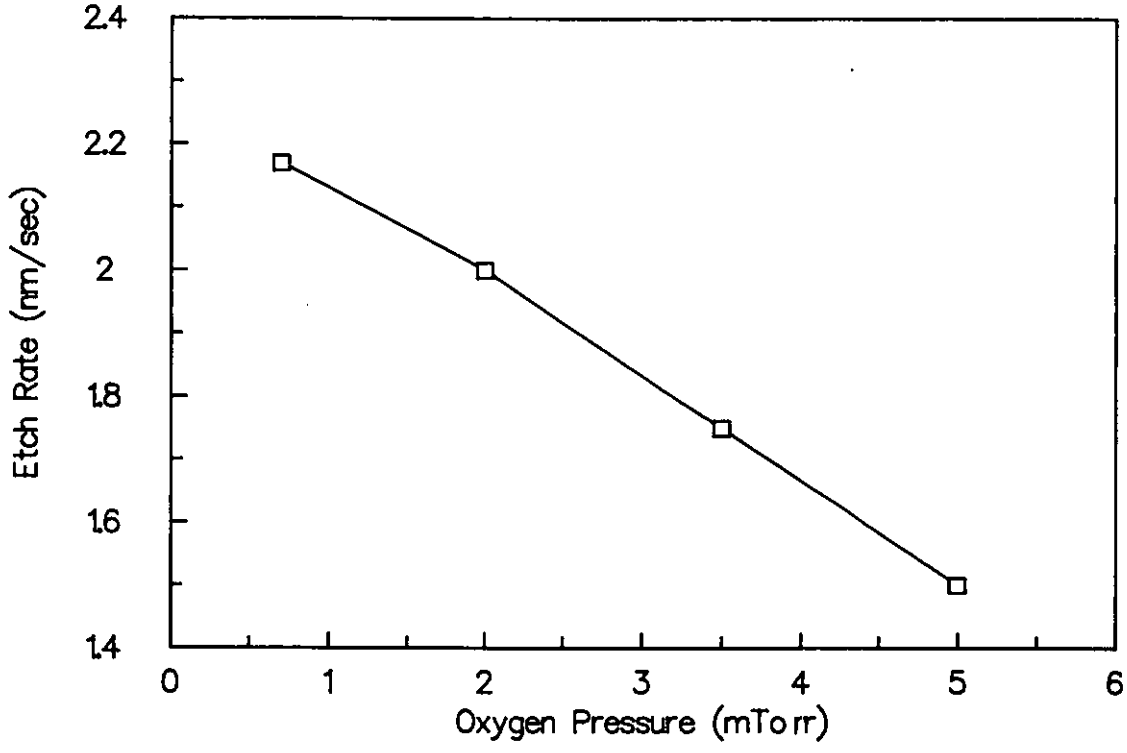

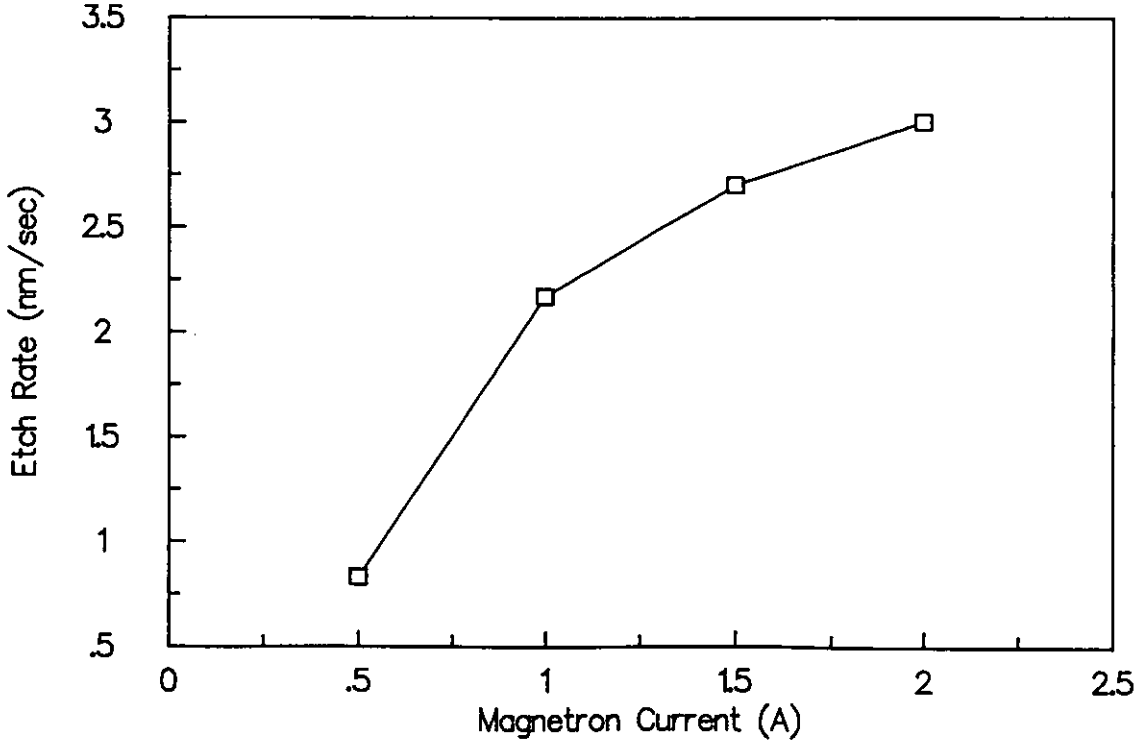

Fig.7.19 Variation of the etching rate with increasing exposure time.

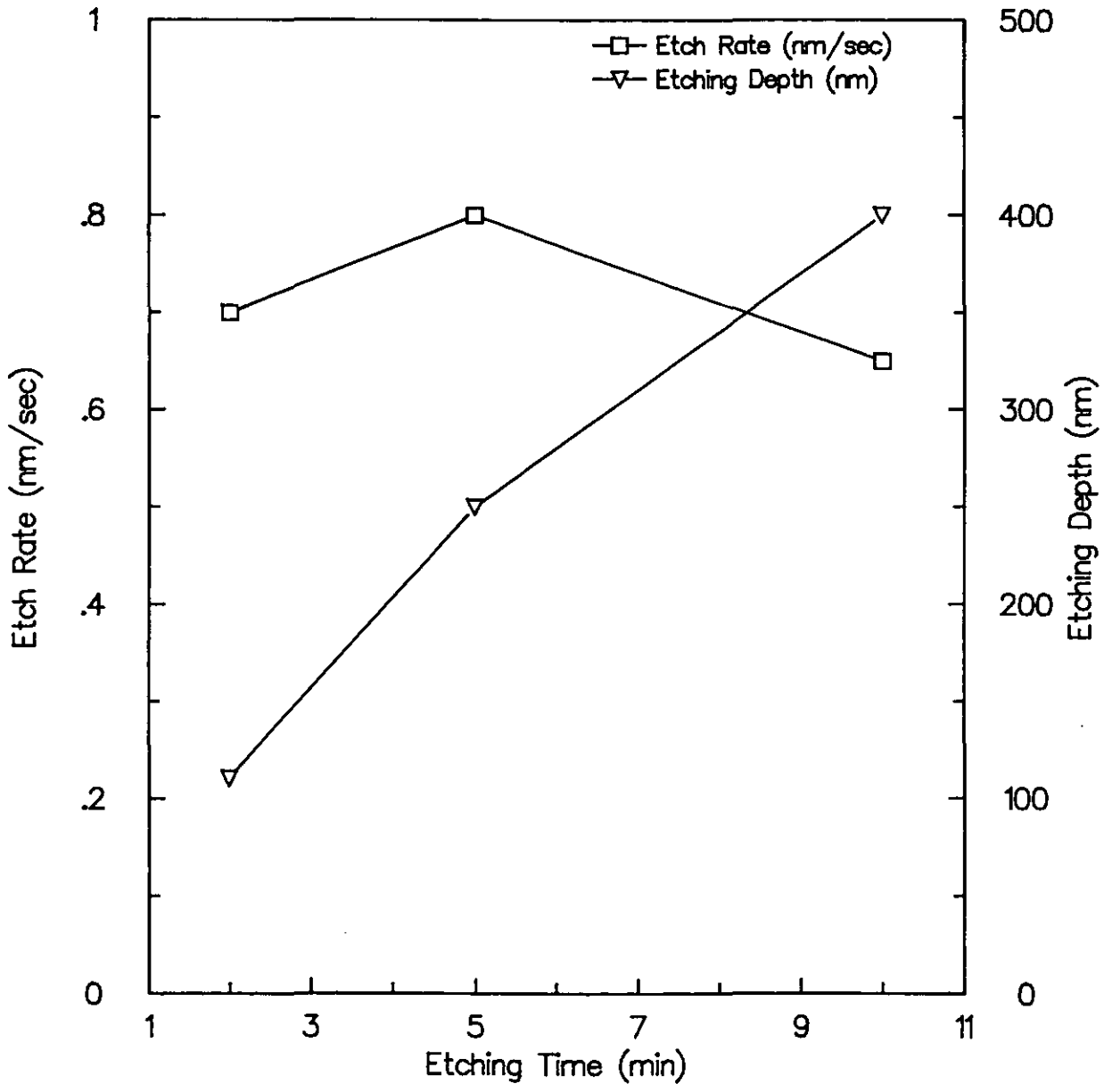

the partial pressure of argon exceeds 50% because there are less radical atoms, etching decreases and the deposition of a polymer film due to sputtering of the carbon target will be increased. In that sense, using the plasma beam free of oxygen reduces the etching rate so that it can not be measured by the talystep or estimated. Fig. 19 shows the etching depth and rate with increasing etching time. By using SEM, the surface morphology of the etched resist can be shown in Fig. 20. Figure 20a demonstrates the general aspect of the etched and unetched resist. The unetched surface was covered by a razor mask. Figs. 20b,c and d exhibits the surface morphology as a function of etching time. These three photographs are related to Figure 19, the time is increased from b to d.

7.4.2.2 Selective Surfaces

Selective surfaces are needed in many applications (Ref. 54). The most conceptually simple technique for fabricating a textural surface (Refs. 46,47) is to use a thin island film as a mask for an etching process. This film must resist the etching and able to form island of the correct size and density. Fig. 21 shows a schematic view of the mask pattern.

The Au and Al have been used in our investigations as a mask which is deposited on the resist film or the polymer by using magnetron sputtering. The nucleation and the structure of the growing stage have been investigated in the literature (Refs. 54-56). Fig. 22 shows the pertinent structure and thickness scales of thin Au film deposited onto glass for both ion-assisted and conventional evaporation technique. However, in our technique, there is a little information concerning the thickness of the thin island film of Au or Al mask. Hence, the resulting etching of different Au thickness has been carried out as a function of different Au deposition time as shown in Fig. 23. From This Figure , the etching rate decreases as the island of Au starts building up till film continuity is complete, the etching rate then becomes zero.

Fig.7.20 The morphology by SEM for etched resist. A) comparison between treated and untreated surface. B,C and D exhibit the surface morphology with different etching time.

A

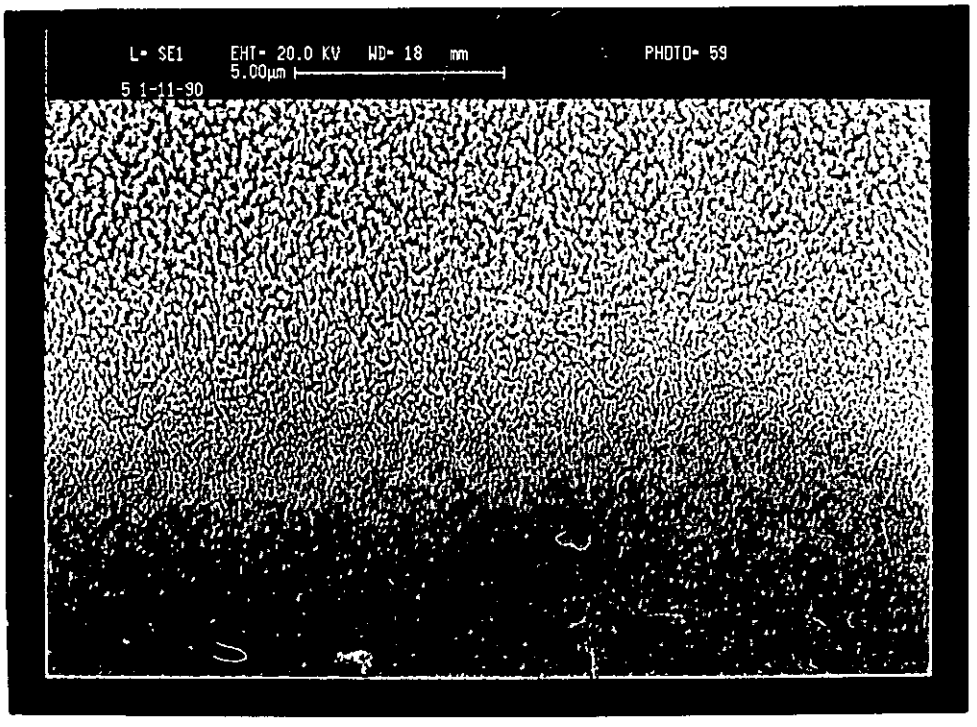

B

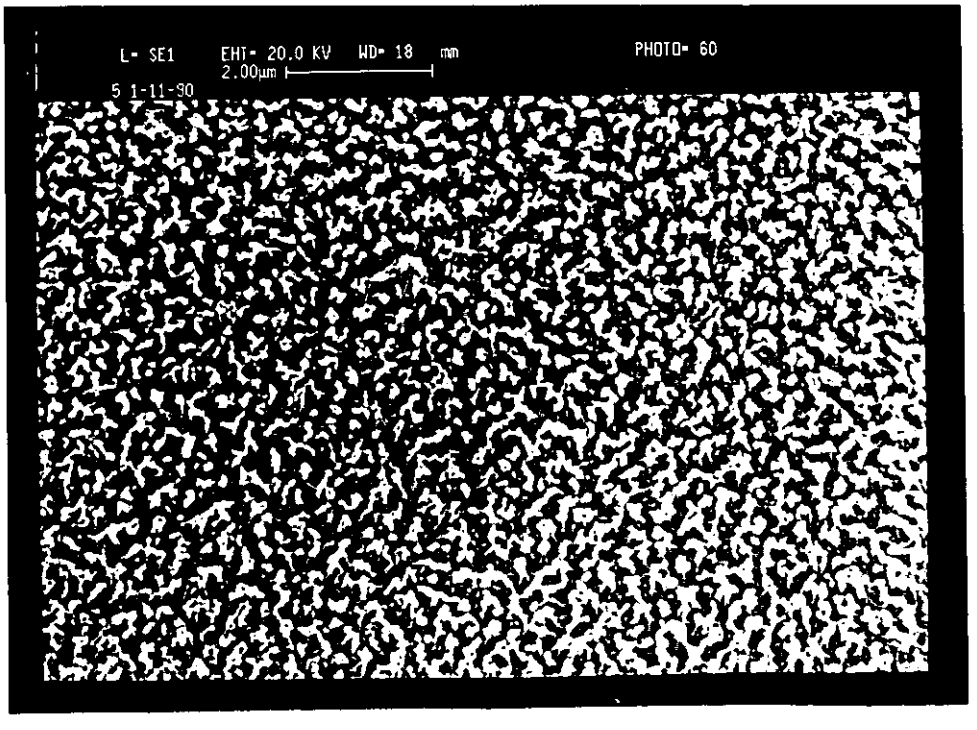

C

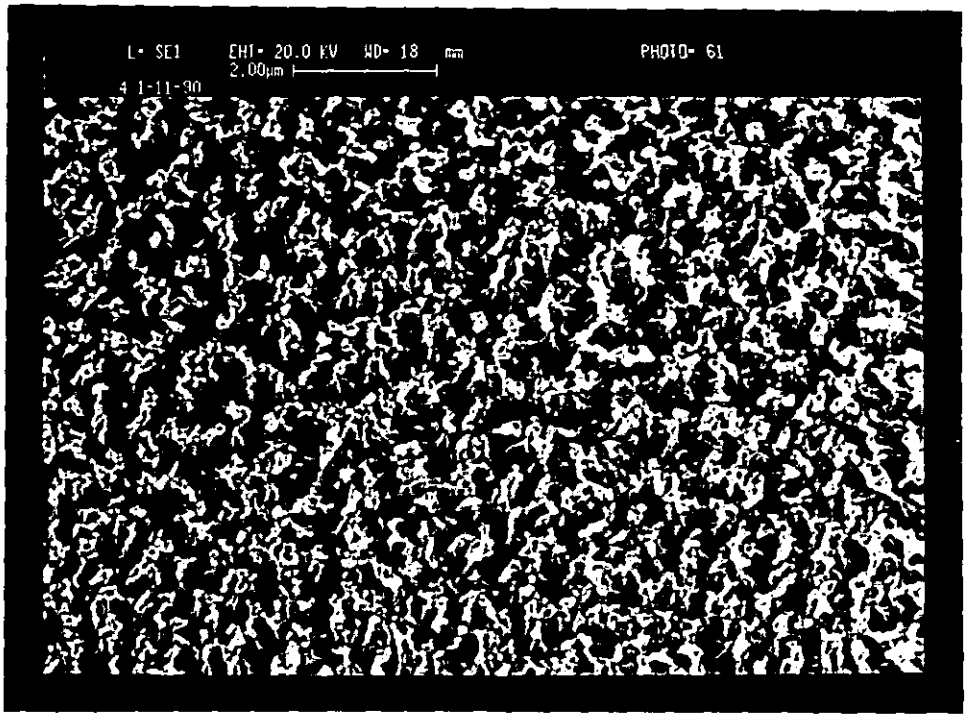
L- SE1 EHT- 20.0 KV WD- 18 mm
2.00µm
PHOTO- 61
4 1-11-90

D

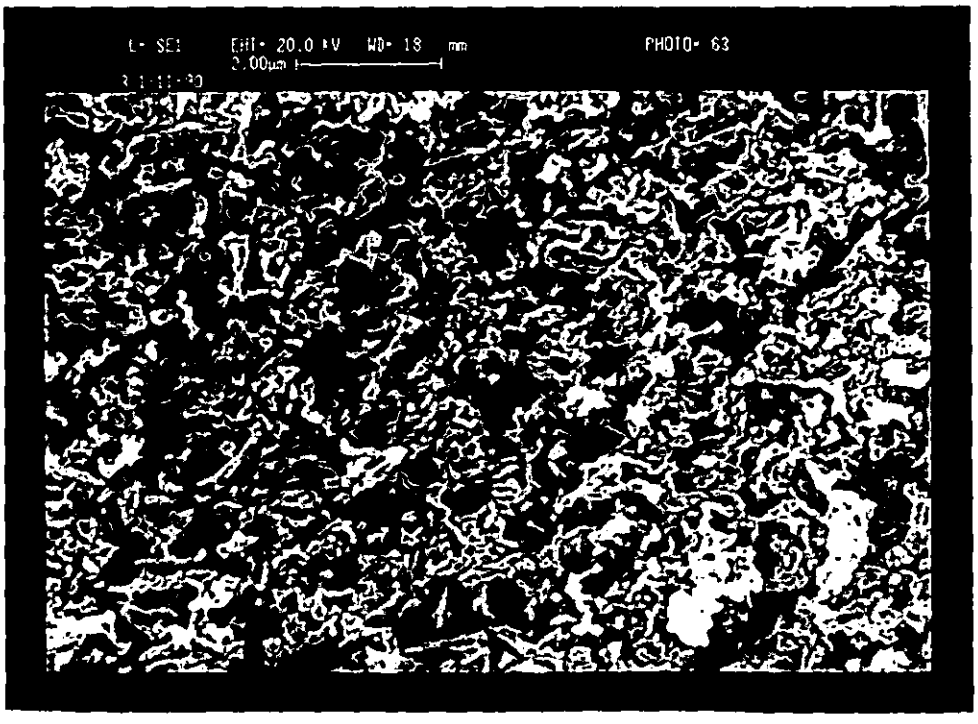
L- SE1 EHT- 20.0 KV WD- 18 mm
2.00µm
PHOTO- 63

FIg.7.21 A schematic view of the mask pattern. (ref.47).

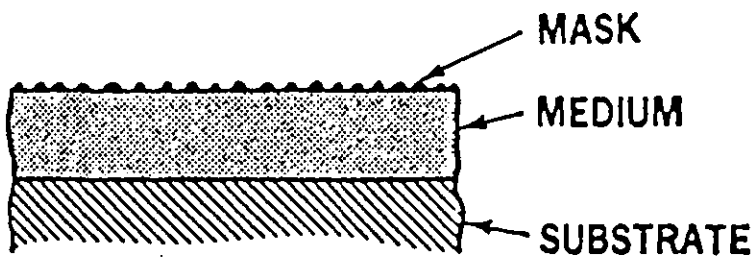

Fig.7.22 Survey over growth stages, structures, and thickness scales for thin Au films deposited onto glass by use of conventional evaporation and ion-assisted evaporation (ref.56).

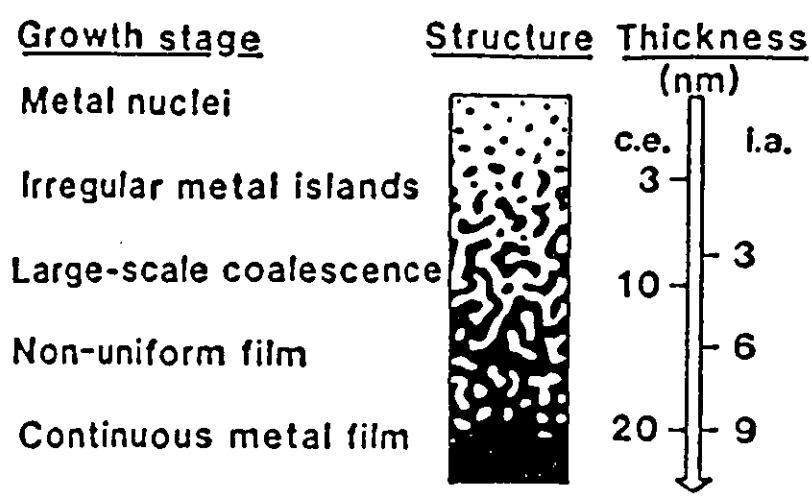

Fig.7.23 Variation of etching rate with different Au mask thickness

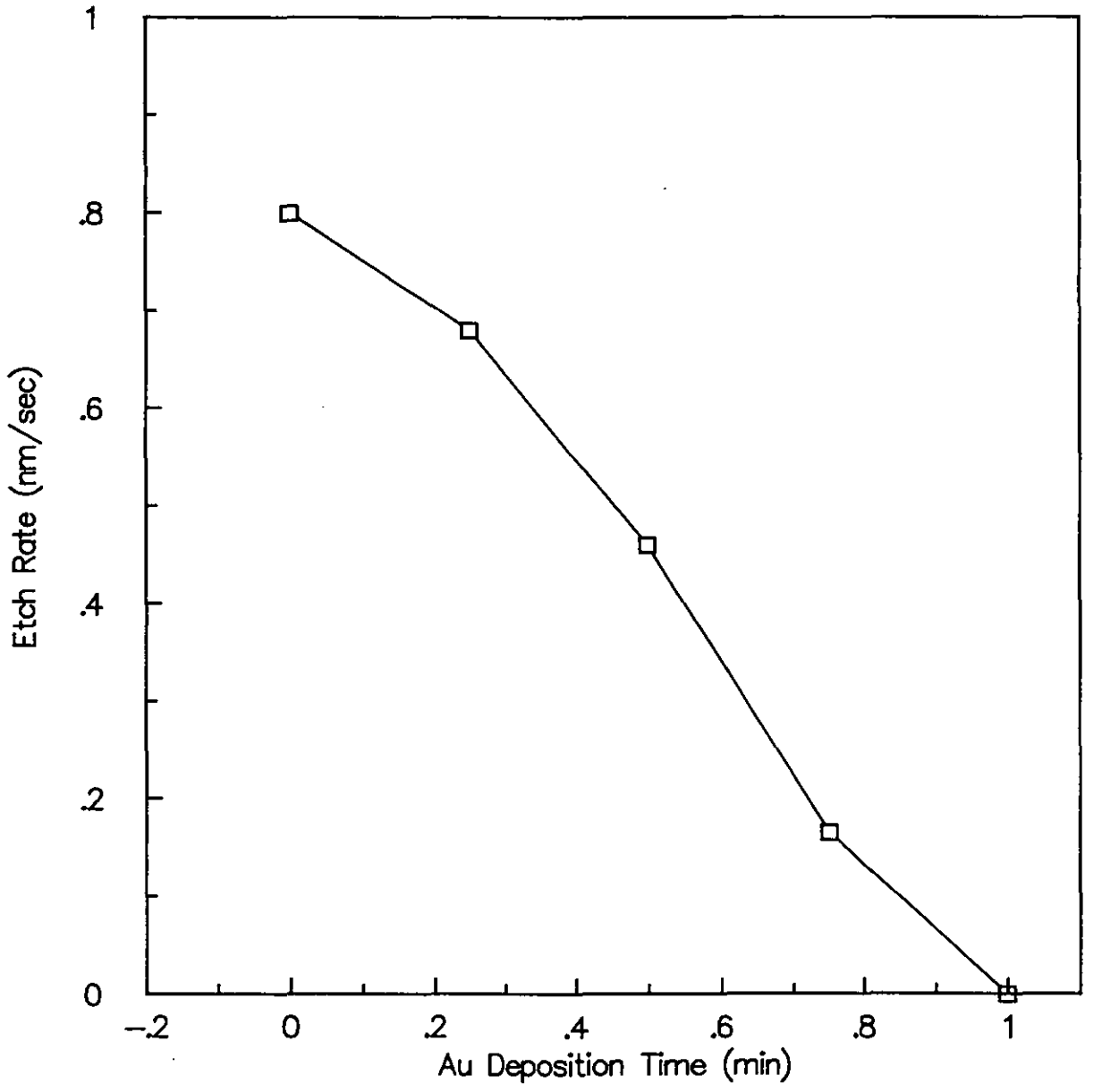

The morphology of the etched surface can be controlled by varying the etching parameters or the amount of mask thickness. The resulting microstructure of etched photoresist are shown in Fig. 24a,b for thin Au mask (a) and for thicker Au mask made at the same condition (b). Due to thermal effects, cracks on the etched resist surface have been observed. A deposition of discontinuous Au film on PET substrate was used for preparing a textured surface to study the optical properties like reflectance in the visible part of the spectrum. In this type of substrate special attention should be paid to avoid thermal effects. Fig. 25 shows a photograph of surface morphology of PET sample etched with a Au mask. Fig. 26 demonstrates the reflection spectra in the visible region of an etched PET sample compared with that of unetched sample. Microscopic surface roughness has been used as a mechanism for selective absorption (Ref. 57). For the columnar surface structure (Ref. 46), the graded refractive index reduces the reflection in a way that does not depend critically on the structure or film production conditions. Because the texture has dimensions of the order of the wavelength of visible light, these surfaces can be highly absorbing (Ref. 48). This is primarily due to multiple reflections of the incident photons between the relatively step sides of the surface structure and the consequent increase in absorption probability. However, polymer etching is quite important in thin film deposition. A film implanted to a polymer substrate, then, can be achieved with this technique more easier than using a graded metallization technique (Refs. 58,59).

Fig.7.24 Morphology by SEM for Photo resist, A) thinner Au mask and B) thicker Au mask.

A

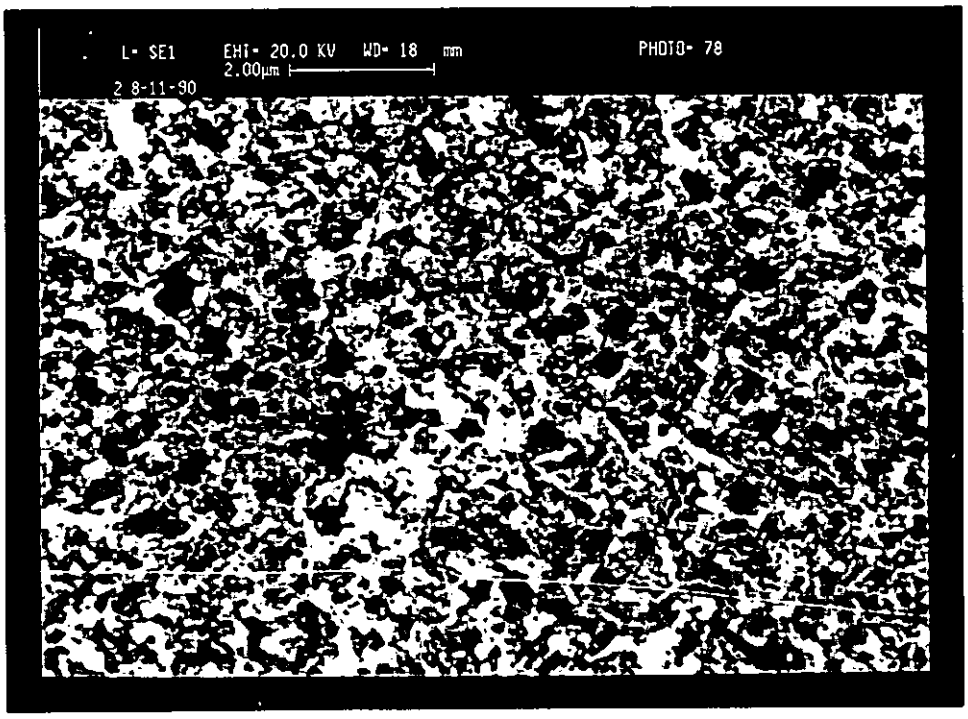

B

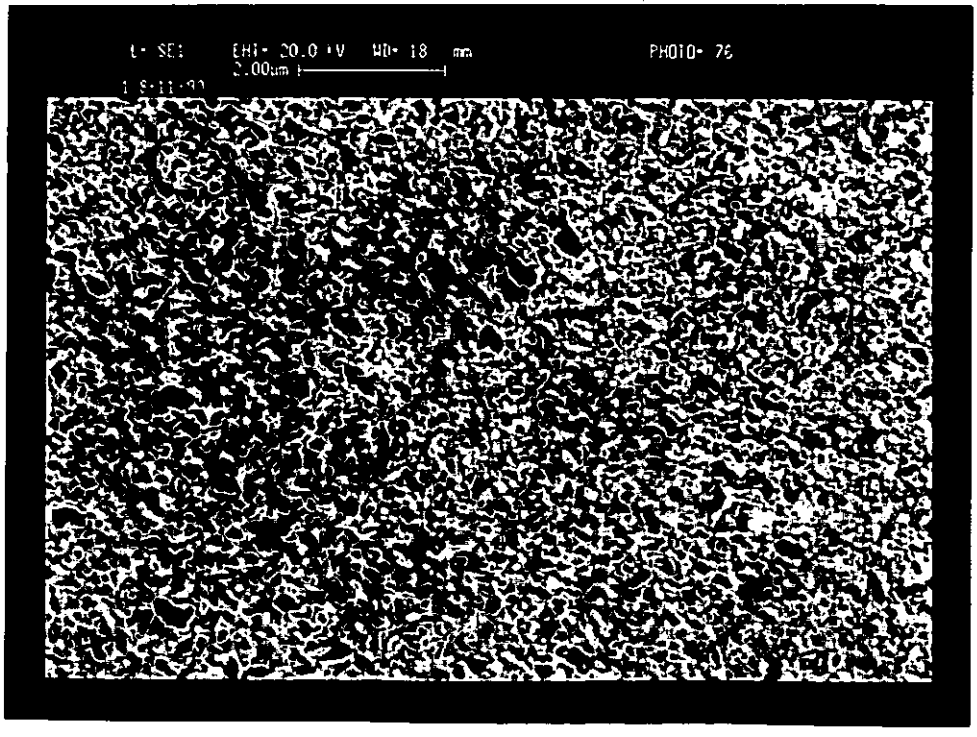

Fig.7.25 Surface morphology by SEM for PET etched with gold mask

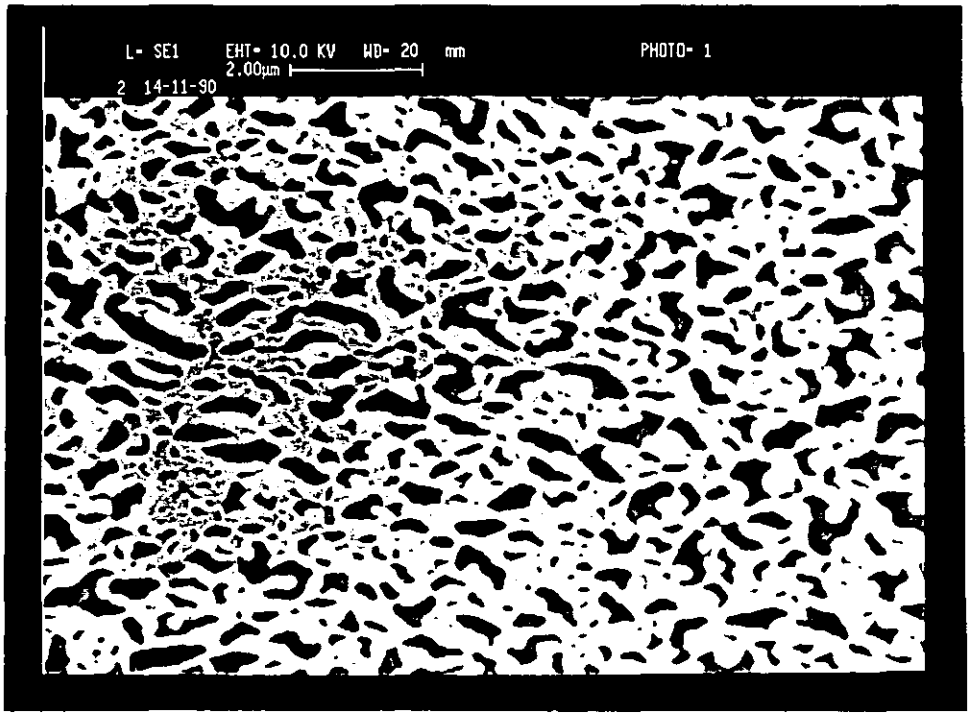

Fig.7.26 REflection spectra in the visible for etched PET samples compared with untreated one.

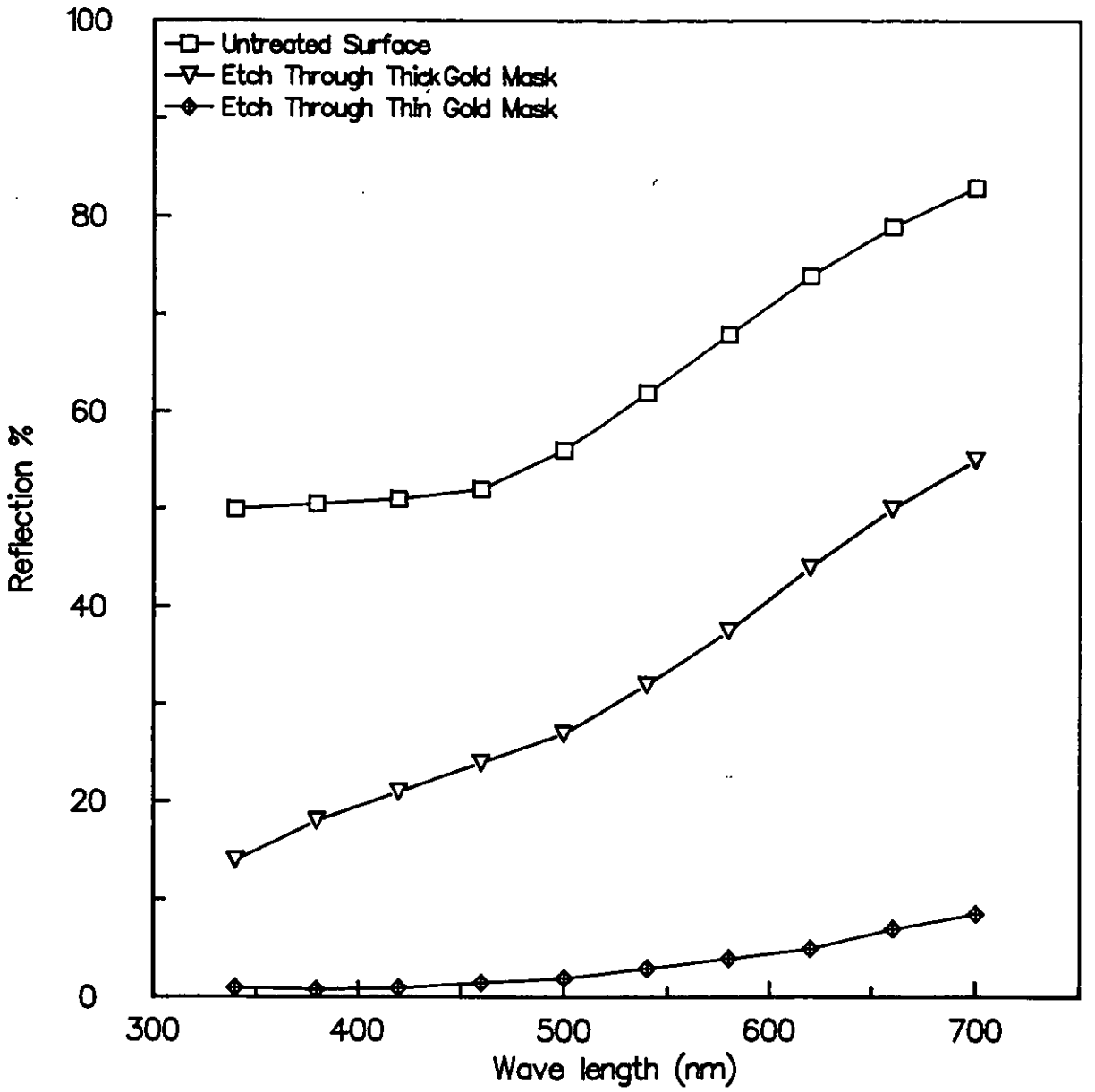

Conclusions

It has been shown here that the unbalanced magnetron can be modified to be used as a source of high ion current density and floating potential.

This system was used to deposit a diamond-like carbon film; as a source in Plasma Enhanced Chemical Vapour Deposition (PECVD) for silicon and titanium oxide; and to etche and modifying a polymer surface.

7.5 References

1- S. M. Rossnagel and J. J. Cuomo, Vacuum, 38 (1988) 73.

2- J. J. Vossen and W. Kern, "Thin film processes II", Academic press, New York, 1991.

3- R. Adachi and K. takeshita, J. Vac. Sci. Technol., 20 (1982) 98.

4- J. J. Cuomo and S. M. Rossnagel, J. Vac. Sci. Technol., A 4 (1986) 393.

5- B. Window and N. Savvides, J. Vac. Sci. Technol., A 4 (1986) 196.

6- A. G. Spencer, K. Oka, R. W. Iewin and R. P. Howson, Vacuum, 38 (1988) 857.

7- S. Kadlec, J. Musil, W. D. Munz, G. Hakanson and J. E. Sundgren, Surf. Coat. Tech., 39/40 (1989) 487.

8- T. Fukami, F. Shintani and M. Naoe, Thin Solid Films, 149 (1987) 373.

9- R. P. Howson, H. A. Ja'fer and A. G. Spencer, Thin Solid Films, 193/194 (1990) 127.

10- L. Kostandinov and D. Dobrev, Vacuum, 42 (1991) 35.

11- S. Kadlec and J. Musil, J. Vac. Sci. Technol., A 8 (1990) 1318.

12- J. Musil, S. Kadlec, J. Vyskocil and V. poulek, Surf. Coat. Tech., 39/40 (1989) 301.

13- S. Kadlec, J. Musil, V. Valvoda, W. D. Munz, H. Peterson and J. Schroeder, Vacuum, 41 (1990) 2233.

14- S. L. Rohde, L. Hultman, M. S. Wong and W. Sproul, Surf. Coat. tech., 50 (1992) 255.

15- K. Tominaga, Vacuum, 41 (1990) 1154.

16- D. G. Teer, Int. Conf. IPAT, Brussele, May, (1991).

17- H. A. Ja'fer, R. P. Howson, M. Stenelake, A. G. Spencer, Int. Conf. IPAT, Brussele, May, (1991).

18- J. A. Thornton and A. S. Penfold, in Thin Film Processes, edited by J. J. Vossen

and W. Kern, Academic press, New York, (1978).

19- J. L. Vossen and W. Kern, eds., "Thin Film Processes I", Academic press, New York, 1978.

20- R. F. Bunshah, ed., "Deposition Technologies for Films and Coatings, development and applications", Noyes Publication, New York, 1982.

21- A. G. Spencer, personal communications, Physics Dept., Loughborough Univ., 1992.

22- R. P. Howson, H. A. Ja'fer, J. Vac. Sci. Technol., A,Vol. 10, (1992) 1784-1790.

23- K. Oka and R. P. Howson, Proc. conf. on Ion Plating and Allied Techniques, Brighton, (1987), P. 158.

24- A. H. Eltoukhy, B. R. Natarajan, J. E. Greene, and T. L. Barr, Thin solid Films, 69 (1980) 229.

25- S. Maniv, C. Miner, and W. D. Westwood, J. Vac. Sci. Technol., A 1, 39 (1983) 1370.

26- s. M. Rossnagel and J. J. Cuomo, Vacuun, 38, 2 (1981) 73.

27- S. M. Rossnagel, ed.,"Handbook of Plasma processing Technology", Noyes Publication, New Jersey, U.S.A., (1990).

28- J. E. Greene and S. A. Barnett, J. Vac. Sci. Technol., 21 (1982) 285.

29- J. E. Greene, Solid State Technology, 30 (4), (1987) 115.

30- L. Holland and S. M. Ojha, Thin Solid Films, 38 (1976) L 17.

31- C. P. Chang. D. L. Flamm, D. E. Ibbotson, and J. A. Muchas, J. Appl. Phys., 63 (1988) 1744.

32- D. E. Meyer, N. I. Ianno, I. A. Woollam, A. B. Swartzlander, and A. J. Nelson, J. Mat. Res., 3 (1988) 1397.

33- H. Vora and T. J. Moravec, J. Appl. Phy., 52 (10), (1981) 6151.

34- D. S. Whitemal, R. Williamson, Thin Solid Films, 97 (1982) 345.

35- B. Meyerson and F. W. Smith, J. Non Cryst. Solids, 35-36, (1980) 435.

36- F. W. Smith, J. Appl. Phys., 55 (3), (1984) 764.

37- S. Aisenberg and R. Chabot, J. Appl. Phys., 42 (1971) 2953.

38- C. Weissmantel, Thin Solid Films, 92 (1982) 55.

39- B. A. Banks and S. K. Rutledge, J. Vac. Sci. Technol., 21 (1982) 807.

40- H. Biederman, R. P. Howson, I. McCabe, Int. Conf. IPAT, 1987.

41- N. Savvides and B. Window, J. Vac. Sci. Technol., A 3(6), (1985) 2386.

42- S. Craig, G. L. Harding, Thin Solid Films, 97 (1982) 345.

43- D. A. Anderson, Phill. Mag., 35 (1977) 17.

44- J. Robertson, Surf. Coat. Tech., 50 (1992) 185.

45- P. Turner, R. P. Howson, and C. A. Bishop, Thin Solid Films, (1981).

46- H. G. Grainghead, " Proceeding of the Society of Photo-Optical Inst. Eng., SPIE, 1983.

47- H. G. Grainghead, R. E. Howard, J. E. Sweeney, and D. M. Tennant, J. Vac. Sci. Technol., 20 (1982) 316.

48- S. M. Rossnagel and R. S. Robinson, J. Vac. Sci. Technol., 20 (1982) 336.

49- H. G. Grainghead, R. e. Howard and D. M. Tennant, Appl. Phys. Lett., 37 (1980) 653.

50- A. Ross, M. Bergkvist, and C. G. Ribbing, Appl. Opt., 27 (1988) 4314.

51- M. T. Mirtich and J. S. Vovey, J. Vac. Sci. Technol., 9, 6 (1979) 809.

52- K. Suzuki, A. B. Christie, and R. P. Howson, Vacuum, 00 (1983) 001.

53- D. M. Manos and D. I. Flamm, " Plasma Etching, an introduction", Academic Press, New York, (1989).

54- C. G. Granqvist, "Spectrally Selective Surfaces for Heating and Cooling Applications", V. TT1, A publication of SPIE, Washington, U.S.A., (1989).

55- C. A. Bishop, R. P. Howson and M. I. Ridge, Inst. Phys. Conf. Ser. No. 54: chapter 6, (1980).

56- G. B. Smith, G. A. Niklasson, J. S. E. M. Svensson and C. G. Granqvist, J. Appl.

Phys., 59 (1986) 571.

57- G. Pellegrinig, Solar Energy Materials, 3 (1980) 391.

58- K. L. Mittal and J. R. Susko, eds., "Mettalized Plastics 1, Fundamental and Applied Aspects", Plenum Press, London, (1989).

59- "Polymer Surfaces and Interfaces", eds., W. J. Feast and H. S. Munro, John Wiley and Sons Pub., Chichester, (1987).

CHAPTER-8

LOW VOLTAGE MAGNETRON

At the normal operating pressure of a diode magnetron, only 35-50% of the sputtered material from the target surface is deposited on the substrate (Ref. 1). The rest is lost through scattering with the background gas and is deposited either back on the target or on the wall of the chamber. Therefore, a lower working pressure is required. Because of this, a decrease in pressure is quite useful, as it converts the magnetron deposition process from partial scattering to direct line-of-sight deposition. The ability to operate in a line-of-sight mode without a reduction in deposition rate due to scattering allows the magnetron-substrate distance to be increased. The increased distance allows better film uniformity as well as removing the samples from any ion or electron bombardment caused by the proximity of the plasma. The increased distance also allows multiple processes to occur simultaneously, such as multiple magnetron deposition, combination with evaporation/deposition or ion beam bombardment during deposition. In addition by using diode magnetron sputtering in some processes, the effects on the growing film due to the radiation created damage by energetic atoms can be high (Ref. 1).

By using secondary ion mass spectra (SIMS) from an ITO target irradiated by 1 KeV Ar ions, S. Ishrbashi et al (Ref. 2) have found that in negative ions spectra, a stray peak of O^- was observed, and its relative intensity was about one tenth that of In^+. These negative ions, mainly O^-, are accelerated by the electric field of the cathode sheath and collide with the substrate. Radiation created-damage during ITO (Ref. 2) and Al-doped ZnO (Ref. 3) deposition has been observed.

In a conventional dc magnetron discharge, a negative potential of -350 to -450 V is

applied to the target. Energetic atoms and negative ions that are generated on the target surface are accelerated by the negative potential almost normal to the target and collide with the substrate to cause film-radiation damage, which in turn influences the microstructure and morphology, and hence the film properties and film stress.

A suitable way, then, to control this selective process and to reduce the deleterious effects in the growing film is by reducing the sputtering voltage i.e the magnetron voltage. To lower the sputtering voltage it has recently been demonstrated that the injection of electrons into the race track of a magnetron, independently of those supplied by the sputtering process at the cathode, can result in a much lower operating potential for the magnetron and allow it to operate at lower pressures (Refs. 4,5).

8.1 The Hollow Cathode Enhanced Magnetron Process

The use of a hollow cathode electron arc source in a triode configuration with a direct current (dc) magnetron sputtering source was first reported by Cuomo and Rossnagel (Ref. 4). Dawson-Elli et all (Ref. 6), found the use of the hollow cathode facilitates the magnetron sputtering of oxides from metallic target. The hollow cathode electron arc source (Refs. 7,8) consists of a short Ta tube, which is constricted at one end, through which Ar is passed. A low voltage cathode arc discharge is struck inside the tube, which couples, through the orifice, to a glow discharge outside the tube. The hollow cathode can be used to supply additional electrons to a magnetron discharge by placing the hollow cathode source in the fringe region of the magnetic field (Refs. 4,6). There are two principle reasons for this approach: the use of the hollow cathode source decouples the current-voltage relation of the diode plasma, and it allows operation of the plasma at any desired voltage or current as shown in Fig. 1. The second reason to use this technique is to lower the operating pressure of the chamber to less than 0.1 mTorr. This is much lower than the 3-30 mtorr range of the diode magnetron at equivalent operating power.

Fig.8.1 Magnetron I-V characteristics assisted by hollow cathode (ref.5).

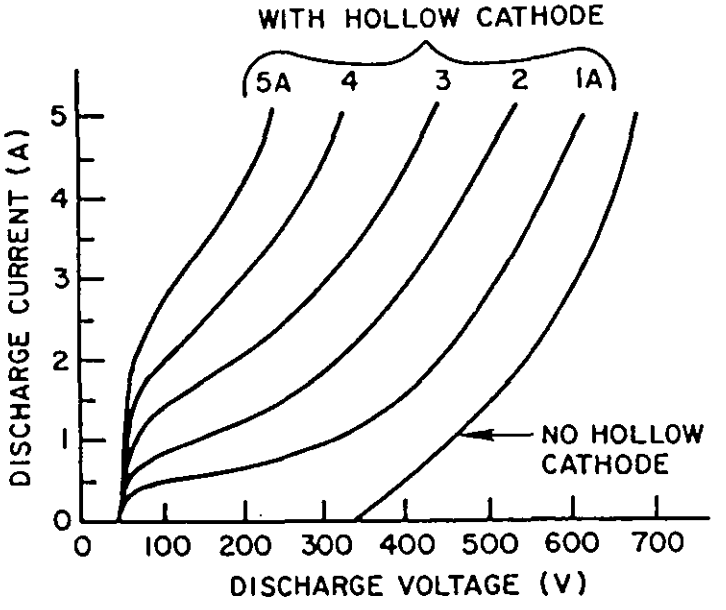

8.2 Thin Film Stress

Sputtered thin films, as with all vacuum deposited coatings, generally exist in a state of internal stress. The magnitude and sign (compressive stress is, by convention, negative) of this internal stress depends on many factors, including substrate temperature, sputter gas species, the material being sputtered, the gas pressure, and apparatus geometry (Refs. 9,10). These parameters affect the film microstructure and morphology through the interplay of the direction flux of the coating atoms and the mobility of those atoms upon reaching the substrate. The microstructure and morphology in turn influence film properties such as electrical resistivity and film stress (Ref. 11). The stress, specifically, is the result of the strain, "built in" to the film by the manner in which it is deposited.

In magnetron sputtering, the working gas pressure and ion bombardment during film deposition play a significant role for controlling film properties. For dense and less contaminated films, low working gas pressure is required. hence high energetic particles impinging the substrate result and higher internal film stress will occur. Occasionally, these stresses make the film crack and peel from the substrate. The change in film density with increasing deposition pressure is accompanied by an increase in the concentration of the entrapped argon in the films and by a decrease in the stress in the films (Ref. 12).

If the magnetron is driven at a lower voltage, essentially the resultant stresses due to high energetic particles impinging the substrate can readily be reduced. The strain (stress) in a film will cause a simply supported substrate to bend. Assuming the film to be on "top" of the substrate, tensile stress causes the substrate to bend concave upward, while compressive stress causes concave downward bending. Stress is therefore inferred from the deflection of a flexible substrate. The bending force S per unit width of the substrate, is given by (Ref. 12):

$$S = \int_0^d \sigma(z)\, dZ$$

where d is the film thickness and $\sigma(z)$ is the distribution of stress in the direction perpendicular to the substrate. An approximate solution to this equation for stresses in electro-deposited Ni was obtained by Stoney (Ref. 13) in 1909. Assuming $\sigma(z)$=constant, cylindrical curvature of the substrate, and Young's modulus for the film equals to the modulas of the substrate, he obtained:

$$\sigma = \frac{E_s\, d_s^2}{6\, R\, (1 - \upsilon_s)\, d_f}$$

where

υ_s= The poissons's ratio of the substrate

E_s = The substrate elastic modulas,

d_f = The film thickness,

ds = The substrate thickness,

R = The radius of the curvature of the substrate.

Brenner and Senderoff (Ref. 14) showed that Stoney's equation was accurate to within 5% if E_f=E_s and d_f/d_s <0.05. In situ stress measurements of NbN (Ref. 12) show that at low pressure, the films are highly compressive throughout their thickness. The intermediate pressure reveals that film growth starts highly compressive and then transforms to a mild tensile stress. As the pressure is increased further, the onset of tensile stress occurs at a reduced film thickness, i.e the films are predominantly tensile. The use of the hollow cathode assisted magnetron (Ref. 4,9) causes the transition from compressive to tensile stress to occur at a higher pressure. The hollow cathode injects 1-2

A of electron into the volume in front of the target face, only a fraction of which are coupled into the target. The remaining electrons, in search of ground, spiral down magnetic field lines towards the substrate, creating a situation near the substrate very similar to the highly unbalanced magnetrons. Hence, the above result shows the effect of ion and electron bombardment to the substrate as a result of extending the plasma towards the substrate, rather than the magnetron potential effect.

However, Windischmann (Ref. 15) relates the effect of pressure to the normalised momentum P_n of the particles bombarding the substrate, where:

$$P_n = \gamma\ E^{0.5}$$

where:

γ= Energetic particle/Sputtered atom arrival rate ratio and

E= Particle energy.

Where P_n is small, a porous film is indicated. The energetic species (sputtered atoms, reflected neutral gas atoms, etc) gain their energy at the target, and lose it through scattering in the surrounding gas. High P_n therefore occurs at low sputtering pressure, and therefore compressive stress occurs at low pressure. High gas pressure reduces P_n through scattering which allows the film to grow with an open microstructure and tensile stress. The projection of energetic species towards the substrate, similar to that obtained using the unbalanced magnetrons, would increase P_n and thereby add a degree of activation to the process and the stress will increase.

8.3 Thermionic Electron Assisted Magnetron Process

To supply additional electrons it is possible to use a hot cathode which emits electrons through thermionic rather than secondary emission. The potential supply of current by thermionic emission is given by the Richardson-Dushman equation:

$$J = A\,T^2 \exp\frac{e\varphi}{KT}$$

where:

φ = The work function of the metal

A = constant equal to 120 Amp/cm^2 deg^2

K = Boltezmann constant

e = Electron charge

Such a system will provide a finite current even in high vacuum. In the latter case, however, the available current is space-charge-limited (Refs. 7,16). In order to ignite the plasma a substantial voltages applied to the filament are required. In the presence of a gas at low pressure, however, ions will be produced by collisions, provided the applied voltage exceeds the ionisation potential of the gas. As with the case of the self-sustained glow discharge, the slow moving ions tend to accumulate in front of the cathode and a dark space is produced.

In most sputtering systems, the thermionic cathode is a heated tungsten filament which can tolerate ion bombardment for long periods. To increase the efficiency of the diode sputtering, the hot cathode technique is widely referred in the middle-to-late 1960's to as "triode sputtering". It was quickly overshadowed by the development of "magnetron sputtering" in the early 1970's, (Refs. 17,18). Magnetron sputtering technology led to many advances in thin-film devices and products. As always seems to be the case,

however, technological demands for increasing equipment performance, efficiency, and sophistication never stop. These demands, have led to the development of the Tri-Magnetron sputtering technique (Refs. 13,20). In such a device, filament cathode and an anode is used to provide a discharge. The discharge is mechanically, rather than magnetically, confined, as in the case of a magnetron, but uses the magnetic field to increase the plasma density and uniformity. Recently, the design of a triode device in which the cathode is a magnetron cathode and uses a hollow cathode electron source as a second cathode to increase the plasma density has been described by Cuomo and Rossnagel (Ref. 4). To the same end, and in order to avoid some disadvantages connected with the relatively large dimensions of such cathodes, the simple, directly heated tungsten filament has been used (Ref. 21).

8.4 Low Voltage Magnetron Design and Optimisation

In order to reduce the magnetron potential, a simple tungsten filament has been used. The filament is connected directly to the race track in front of the target. The same magnetron described in chapter 5 is used in our investigation. The layout of this design is shown in Fig. 2. The filament is connected to the same potential as the magnetron, because otherwise the process will not be achievable. However, that is because the available current is space-charge limited. In this case the electron cloud is present in the immediate vicinity of the cathode, and only the application of a substantial potential can allow full emission current to reach the anode. Thus, by the application of a relatively small voltage in the order of 30 V, the full emission current of the emitter can be drawn. If the total applied voltage is further increased, additional current may be drawn from the cathode because of enhanced heating of the cathode by the high energy ions. To create the required thermionic electrons emissions from the filament, this was heated by an isolated AC low voltage resistance heating supply (I^2R). The electron emission is increased by raising the temperature of the filament by passing more current. The unbalanced

Fig.8.2 Lay out of the low voltage magnetron with the filament connection.

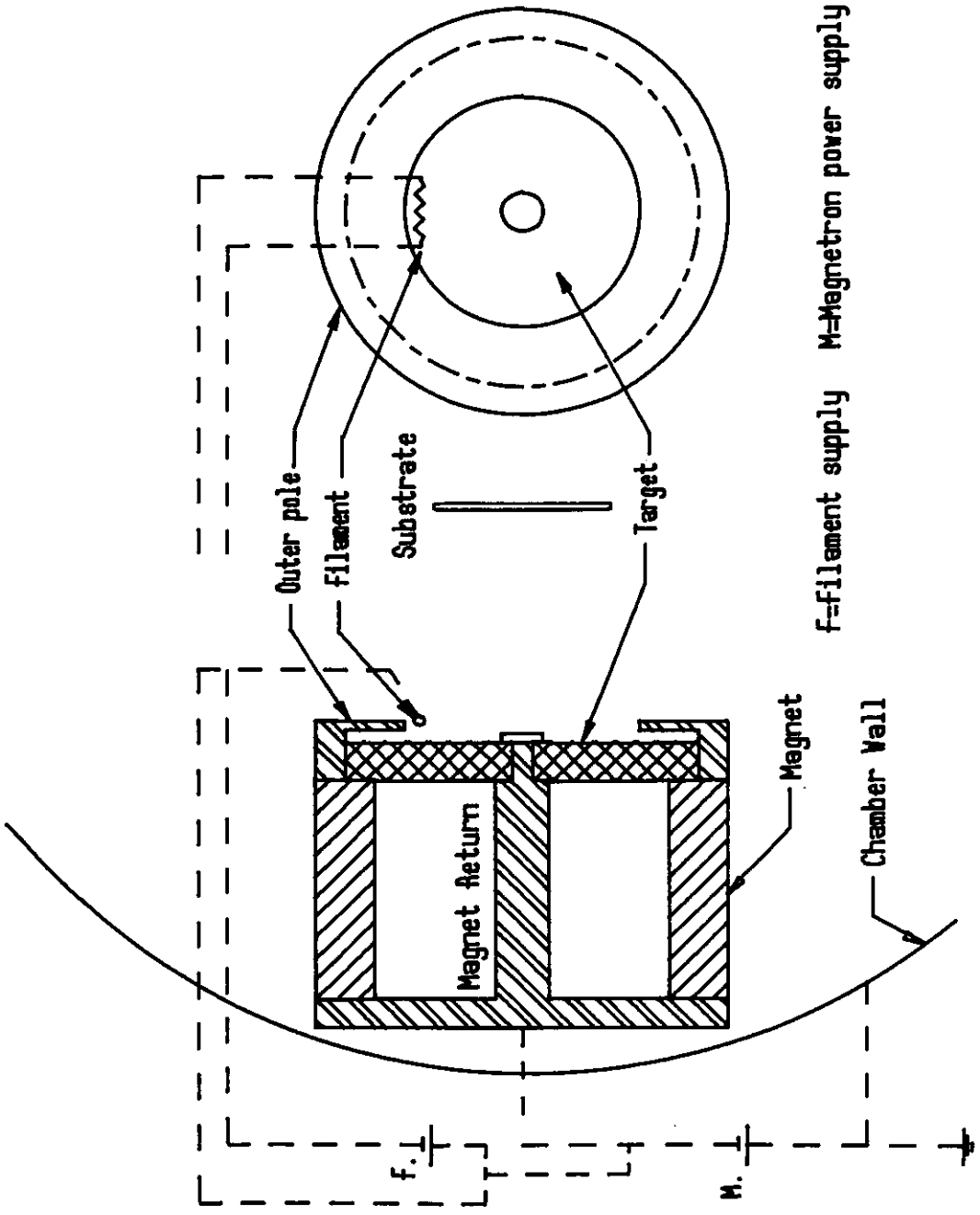

magnetron has been connected to an MDX magnetron driver. Key factors of the MDX supply are (i) constant power mode, where the current and voltage are automatically adjusted to maintain a power set-point, (ii) constant voltage mode where current is automatically adjusted and (iii) constant current mode where voltage is automatically adjusted.

The emitted electrons from the heated filament will be distributed around the magnetron drift loop by a modified ExB effect. The electrons are energetic enough to cause ionisation of the background gas. The increased ionisation forms a denser plasma than is produced by the magnetron alone. The plasma is characterised by a lower impedance, resulting in increased currents at constant voltage or constant magnetron power.

8.4.1 Filament Position Effects

In order to optimise the system efficiency, particular attention needs to be paid to the filament position with respect to the magnetic trap of the magnetron. The filament position plays a significant role in controlling the coupling of the filament emission current into the magnetron current. The small size of the filament helps to control its position anywhere on the race track of the magnetron with ease. Positioning the filament in the higher magnetic field area near the cathode surface leads to higher coupling. The degree of coupling can be determined from the effects on the magnetron features, especially the I-V characteristic. In our investigation, the filament has been fixed within 15 mm from the target face, and close to the outer pole, which is adjusted in such a manner that a better enhancement of the magnetron parameters can be achieved, and to be far enough away from the target erosion area in order to prolong its life.

8.4.2 I-V Magnetron Characteristic

The lowest potential operating voltage for the conventional diode magnetron cathode

Fig.8.3 Magnetron I-V characteristics assisted by thermionic electrons.

Fig.8.4 I-V characteristics of an unbalanced magnetron with different filament current (magnetron power 0.5 KW and argon pressure 3 mTorr).

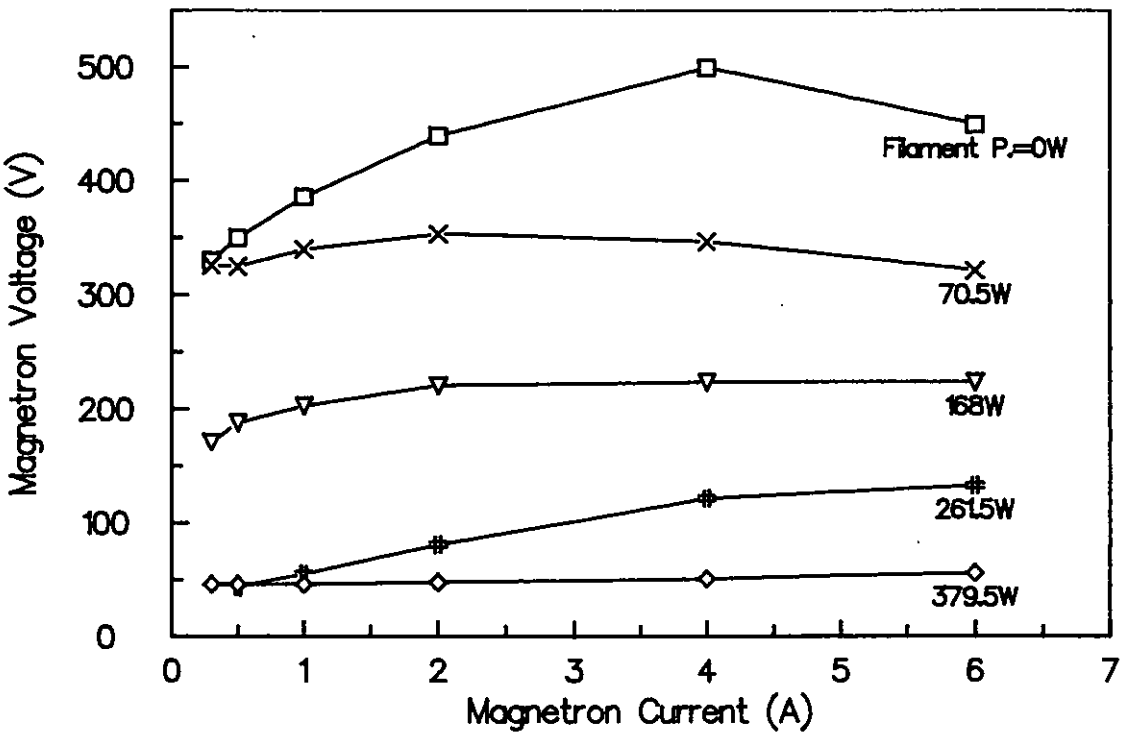

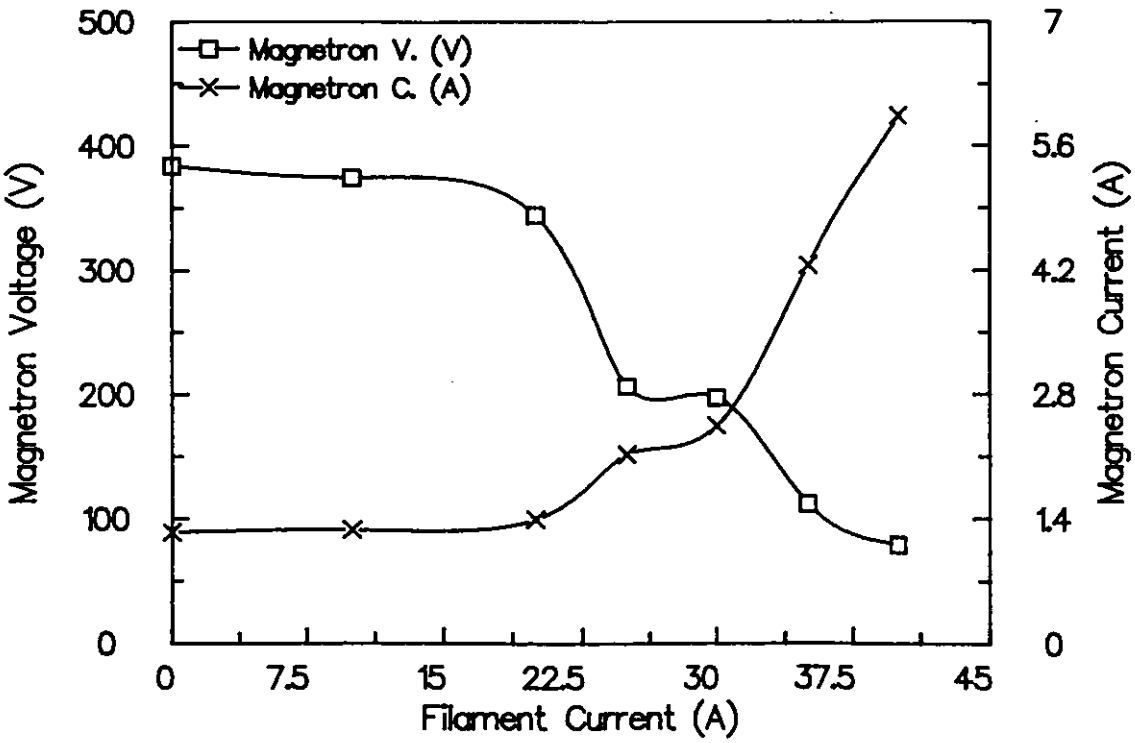

varies with pressure, target material, and gas species (Ref. 22), but is in the 300-500 V range. Below these voltages, no plasma is formed and no target bombardment takes place. This places a lower limit on the bombarding ion energy for magnetron sputtering. Operation at voltages just above the turn-on voltage is possible, but in general the ion current is very low. By using a filament enhanced magnetron mode, the magnetron target can be biased at any potential and still draw a significant bombardment current. This feature is shown in Fig. 3. The filament power is high, because of the larger scale process involved. Fig. 4 shows the I-V characteristic of the UM as a function of the filament current. These measurements were taken with an argon pressure of 3 mtorr and constant magnetron power of 0.5 KW.

8.4.3 Low Working Gas Pressure

In addition to effectively decoupling the voltage from the current in a magnetron device, two other significant feature are present which do not occur with a diode magnetron. The first is the ability to operate at low voltages, below the initiation voltage for the diode magnetron. The second feature is a significantly lowered operating pressure over conventional magnetron operation.

With the use of the filament supported magnetron discharge, the following expected effects were seen. The system would operate at a much lower voltage, and the threshold pressure for operation moved towards 0.2 mtorr as the electron emission from the filament was increased, Fig. 5. This is much lower than the 2-20 mtorr range of the diode magnetron operated at equivalent current. At lower pressures, there are simply too few gas atoms to be ionised efficiently by the secondary electrons from the magnetron. The additional supply of electrons from the filament remove this limitation and allows operation of the dc magnetron between 0 to 2 mtorr. These pressures are well into the long mean free path regime, and sputtered atoms or ions move in straight (line-of-sight)

Fig.8.5 Variations of filament current on magnetron potential and working gas pressure (magnetron p. = .5KW).

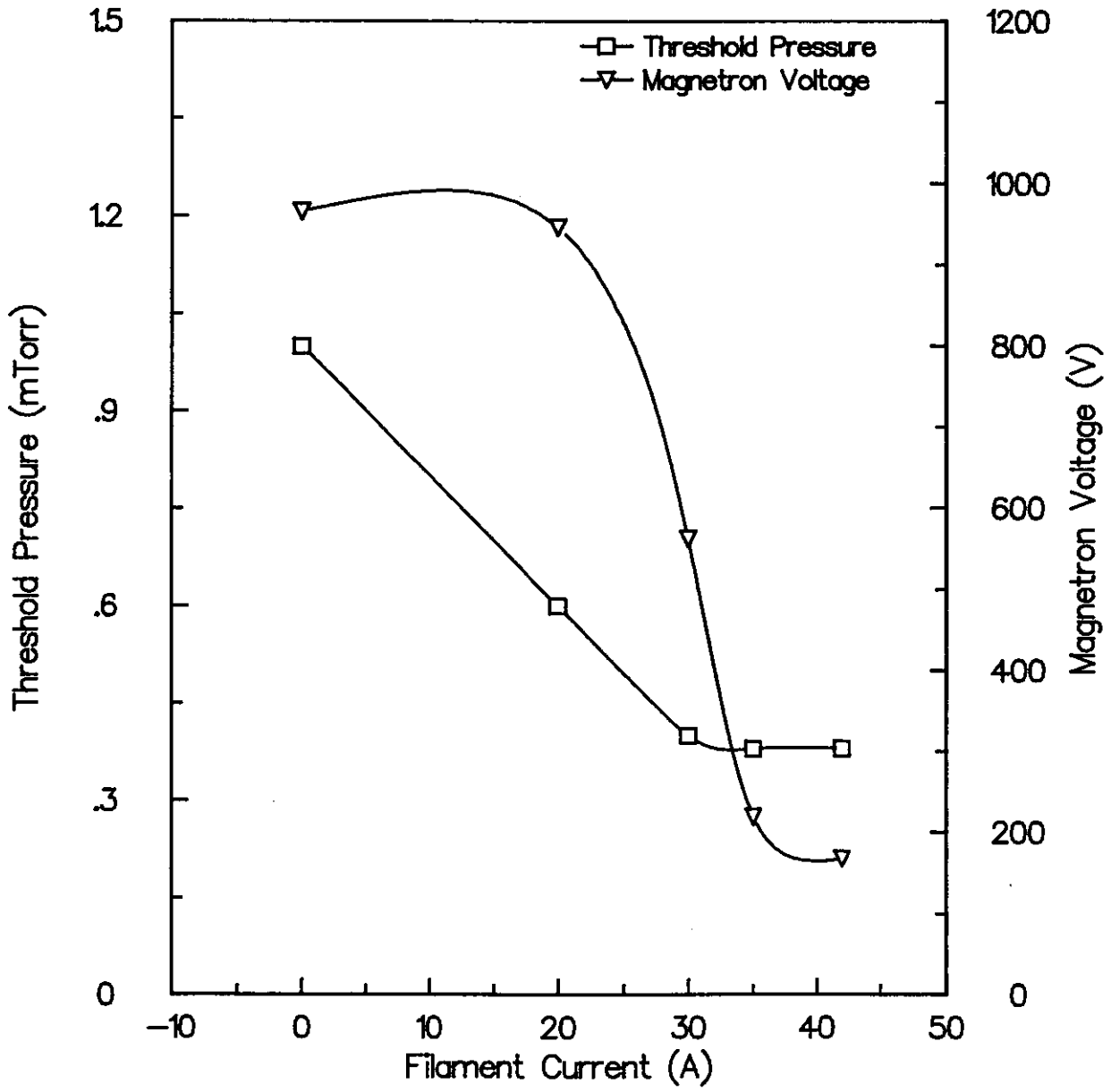

trajectories without gas scattering.

8.5 Plasma Properties

Measurement of plasma properties has been achieved by using an electrostatic probe of 1 cm^2 area. At 100 V bias on the probe, ion current density was measured. From the I-V probe characteristic the substrate self-bias (floating potential) can be obtained. The survey of these two parameters with magnetron potential is shown in Fig. 6. During this experiment the magnetron power and the argon pressure were fixed at 0.5 KW and 3 mtorr respectively. As seen in Fig. 6 the plasma properties of an unbalanced magnetron were improved, and the magnetron voltage was reduced. The ionisation that is created by the thermionic electrons not only couples with the magnetron and reduces its voltage, but some of them will leak to the front following the magnetic field, which leads to enhancement of the magnetron performance by increasing the ion bombardment of the substrate. By lowering the argon pressure, so that it approaches the operating threshold pressure, the potential drop at the substrate (floating potential) can be higher than that on the magnetron. This is illustrated in Fig. 7.

8.6 Sputtering Rate of Low Voltage Magnetron

The theory of Sigmund, modified for low-energy sputtering by Steinbruchel (Ref. 23) identifies four parameters affecting the sputtering yield. These parameters are the surface binding energy, target and projectile atomic numbers and the projectile energies (see section 2.3 of chapter 2). In our experiment, a copper magnetron target has been used. Target sputtering rate was measured in order to measure the effect of magnetron potential on the sputtering yield. As mentioned in section 8.4, with the use of an MDX power supply in power mode, the voltage and the current will be adjusted to maintain a power set-point. By fixing the magnetron at 0.75 KW and the argon pressure at 3 mtorr, the copper deposition rate was measured. The ensuing results are shown in Fig. 8. Because

Fig.8.6 Plasma characteristic with different filament current.

Fig.8.7 The improvement in the plasma properties and lower magnetron potential for lower argon pressure.

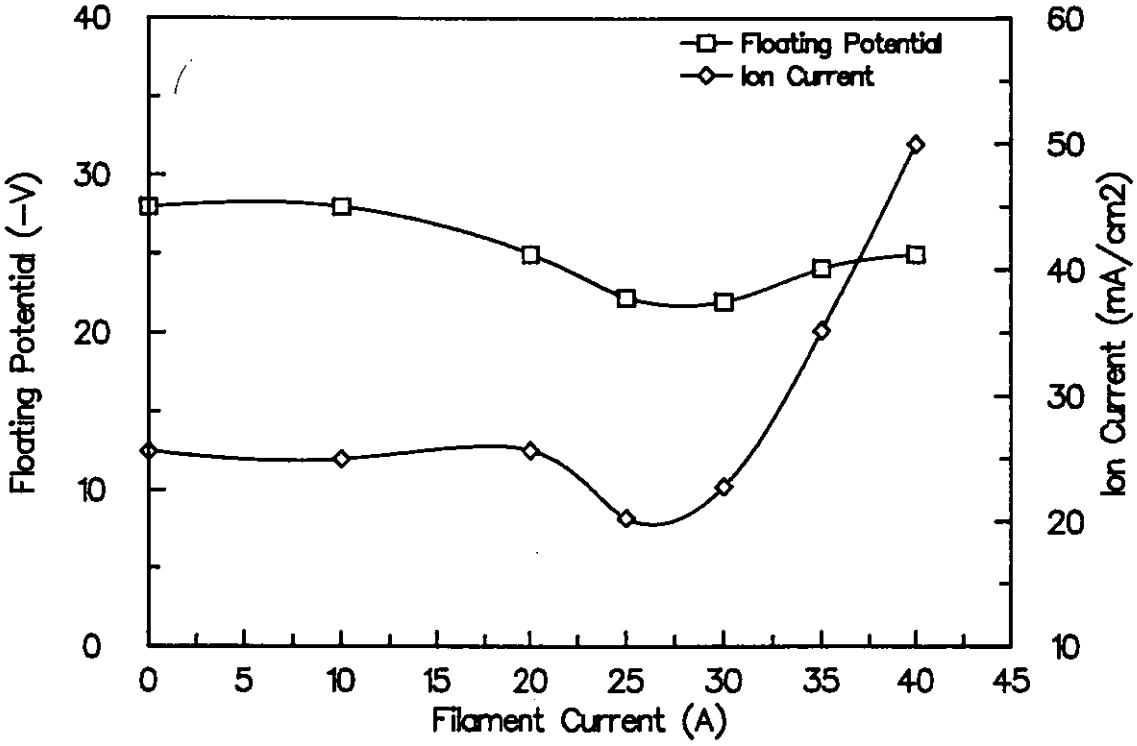

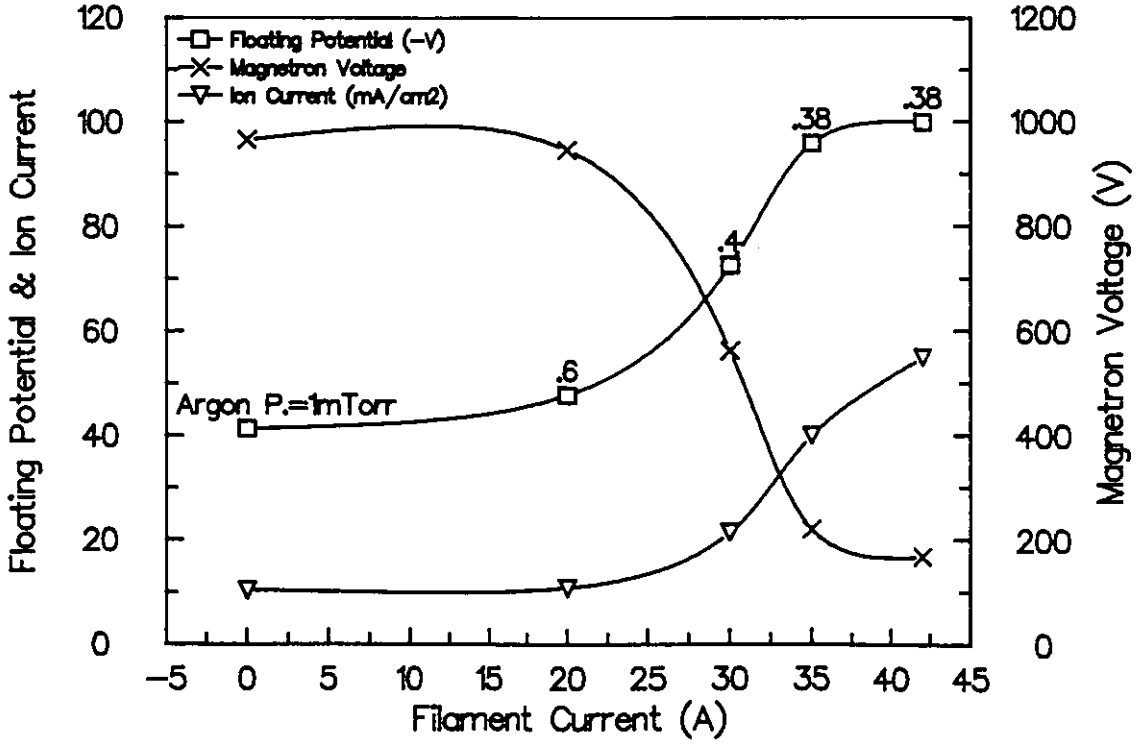

Fig.8.8 Effects on deposition rate of variation in magnetron voltage (magnetron power fixed to 0.75 KW).

Fig.8.9 Effects on deposition rate of variation in magnetron voltage (magnetron current fixed to 4 A).

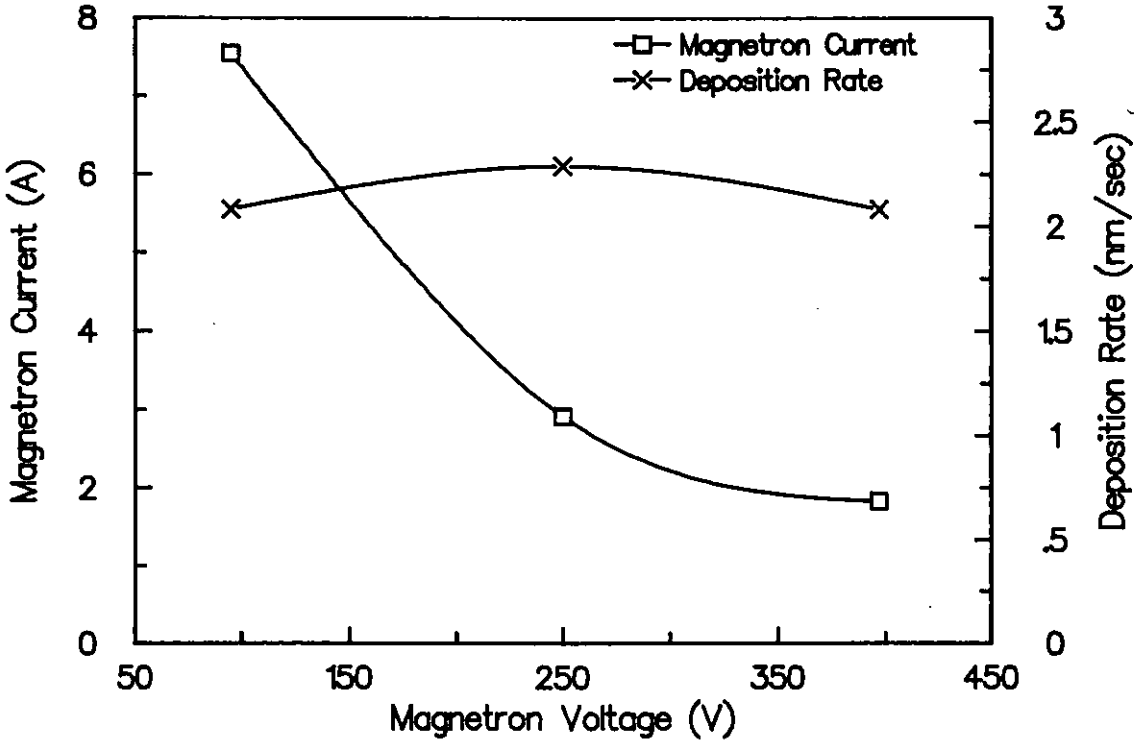

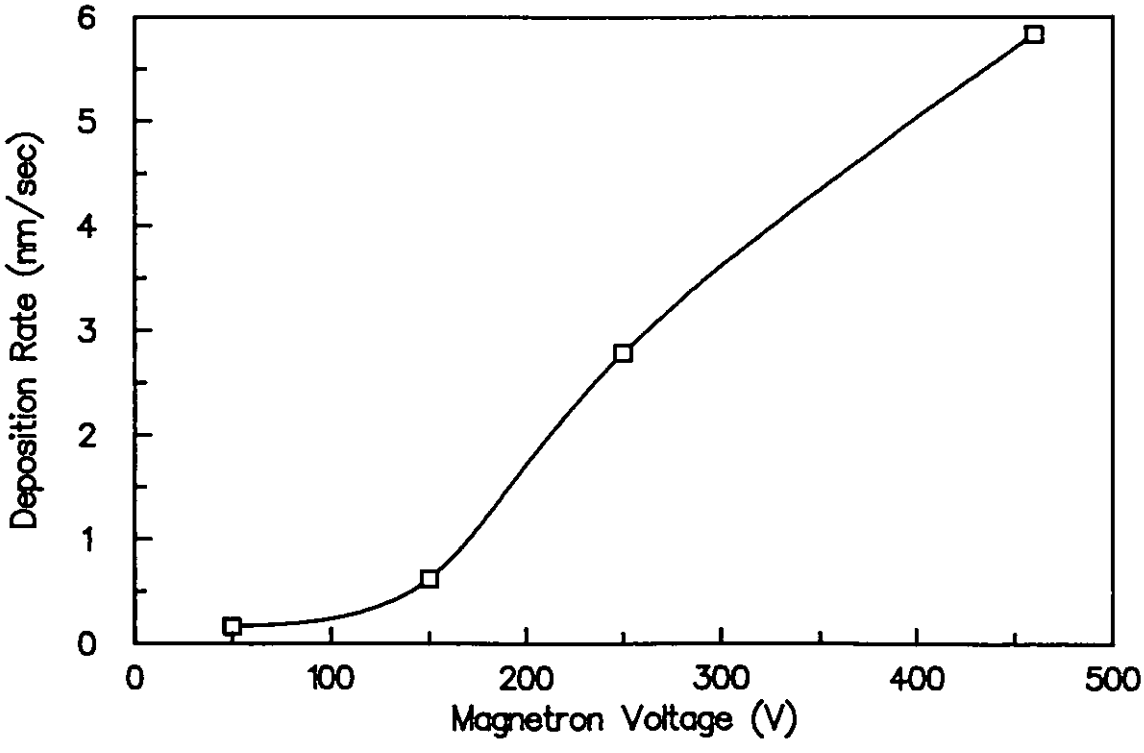

the magnetron power is kept constant, reducing the magnetron voltage will lead to increased magnetron current, in order to maintain the input power. Consequently, the deposition rate is kept constant just above the threshold voltage, and the sputtering rate will reduce dramatically below 100 V. If the sputtering yield of a material is considered in terms of the amount of material sputtered related to input power, rather than the more usual number of sputtering ions. Then it can be seen to peak at the voltage of operation of the discharge of around 120 volts. The ionisation cross-section of the noble gases peaks at around the same value, allowing operation of the process with a smaller amount of gas; i.e. lower partial pressure.

The relationship between magnetron voltage and the sputtering yield can be better understood if the magnetron current is fixed rather than the input power. Fig. 9 shows the copper deposition rate as a function of the magnetron voltage. With a fixed magnetron current of 4 Amps. It can be seen from this Figure that deposition rate decreases linearly with magnetron potential, until it reaches 100 V. Below 100 V the deposition rate decreases to a minimum until it reaches its zero value at about 30-40 V.

8.7 Applications

8.7.1 Low Voltage Reactive Sputtering of TiN

In recent years particular attention has been dedicated to characterising and improvement of the electrical and optical properties of TiN. As illustrated in Chapter 5, reactive magnetron sputtering of TiN can be improved by using a vacuum system provided with a load-lock. Because of the high vacuum achieved, the film resistivity of TiN can be reduced to 0.77 Ω μm. To achieve this value, magnetron powers as high as 2 KW are required, or argon pressure is lowered to a minimum. These results were compared with those achieved by the use of the getter box. Depositing TiN onto glass substrates at room temperature with high magnetron power, or low argon pressure, in general results in

stresses in the film. These stresses ordinarily cause film cracking and adhesion failure. With the use of the low voltage magnetron, this problem may be solved. By reducing the magnetron voltage, radiation-type damage induced by high energy neutral atoms will reduce. The film properties will thus improve as well.

The use of low voltage unbalanced magnetron sputtering to deposit TiN was achieved. The results show the film resistivity reduces from 2.1 Ω μm at 355 V magnetron voltage to 1.01 Ω μm at 200 V. This result has been collected using magnetron power of 0.5 KW and argon pressure of 3 mtorr. By increasing the magnetron power to 1.5 KW, the resistivity of TiN film in the optimum region can be reduced from 0.77 Ω μm to 0.6 Ω μm at 280 V. Current limitation of MDX power supply limits the reduction in magnetron voltage. Using such a design, however, means there are two problem to be faced relating to film damage. The first is the filament heat radiation directed to the substrate, which causes unmatched heating during film deposition, which in turn leads to stress in the film. This problem has been solved by covering the filament with high melting point material such as stainless steel. The second problem is ion bombardment from the unbalanced magnetron. Recently, it has been found that in order to modify TiN film structure, it is necessary for the ion current to the substrate to be between 1 and 3 mA/cm^2 (Ref. 24).

The filament assisted magnetron improves the unbalanced magnetron performance, in that the ion current and floating potential at the substrate will increase as the magnetron is driven at lower voltage. In order to control these two parameters, a water cooled copper electrode has been used. This electrode was fixed close to the centre pole of the magnetron at a distance of 5 to 10 mm, and is connected through a resistance to earth. The use of such a technique in order to control ion bombardment of the substrate will reduce it, but not to the required level. This is because the magnetic field configuration of

an unbalanced magnetron causes electrons, followed by ions, to escape from the outer pole side and to intercept the substrate. With these conditions the results mentioned above were determined.

It was later found that the use of two unbalanced magnetrons, configured in such a way that the magnetron target is positioned 15 degree from other helps to minimise the electron ion radiation damage to zero level. This process is clearly demonstrated in the Figures presented in chapter 9. Full investigation of low voltage TiN sputtering magnetrons, using the batch getter box system rather than open-load-lock system is explained in the following section.

8.7.2 Low Voltage Magnetron Sputtering of TiN Using a Getter Box System

TiN deposition onto glass substrates by using a load lock system (air to air) and the small volume of a getter box was discussed in chapter 5. It was again decided to produce films of TiN in a tightly enclosed volume, using the self-gettering effect to give greater purity, plasma emission-monitoring (PEM) to provide stability for the reactive sputtering process, and unbalanced magnetron (UM), with electron injection to allow operation at low cathode potential, using the same design of Fig. 2. It is reported that operation of the process at low magnetron potentials and under conditions that provide considerable ion bombardment of the growing film leads to TiN of better quality, where this is assessed by improved specular selectivity in their reflectivity and lower resistivity (Ref. 25). Figs. 10,11 and 12 show nitrogen consumption, film thickness, and film resistivity as a function of percentage of Ti line respectively at three different magnetron potentials. As can be seen from these figures, the nitrogen consumption reduces as the magnetron potential reduces. That may be attributed to lower deposition rate at lower magnetron voltages (see Figure 10). We have seen that the PEM (input) signal does increase as the

Fig.8.10 Nitrogen consumption versus the Ti line set point at three magnetron voltages.

Fig.8.11 Variation of film thickness with the Ti line at three magnetron voltages.

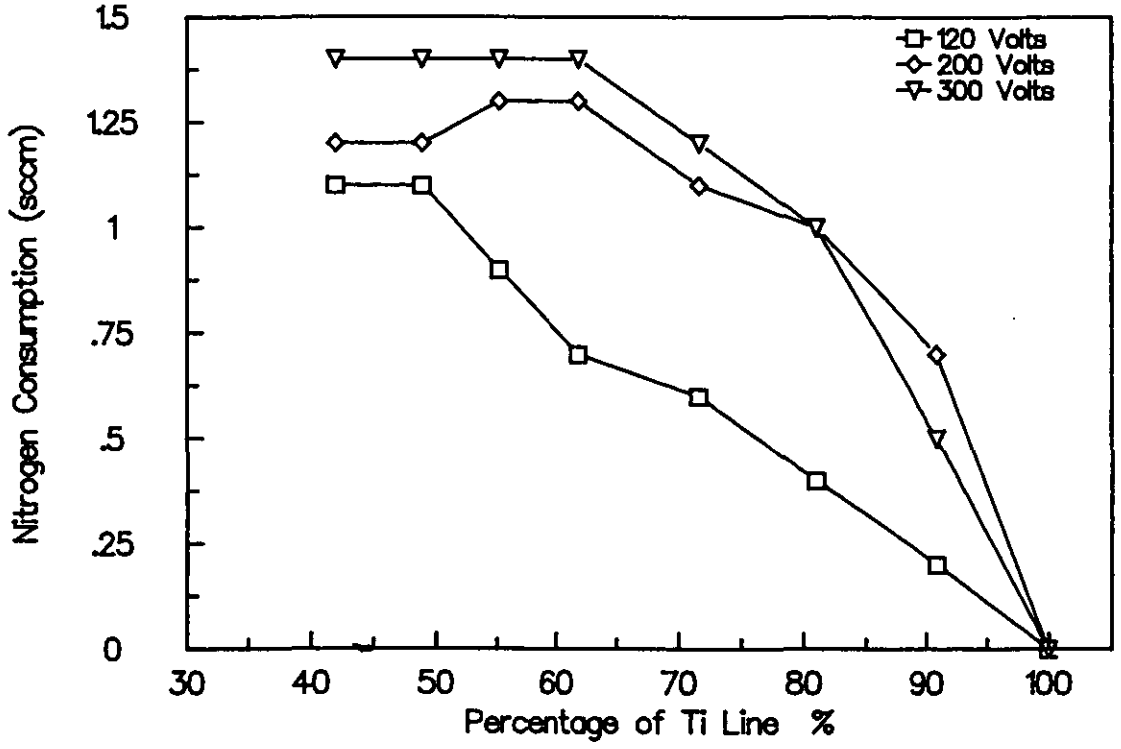

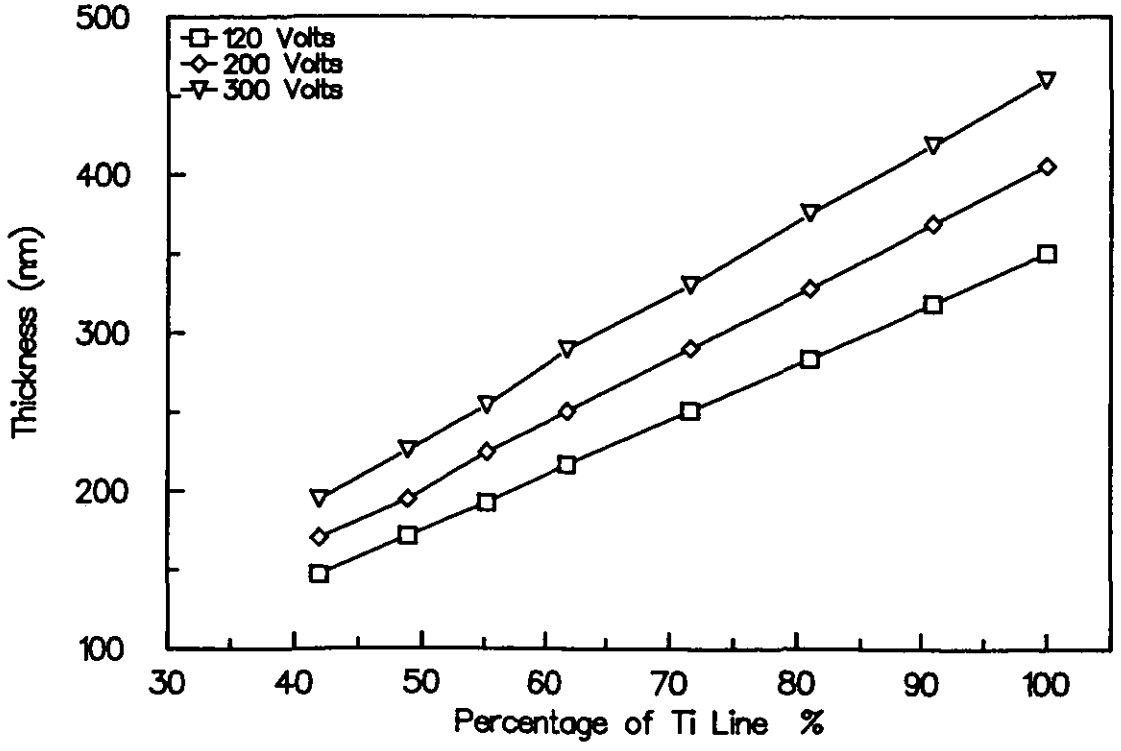

Fig.8.12 Film resistivity for different magnetron potential.

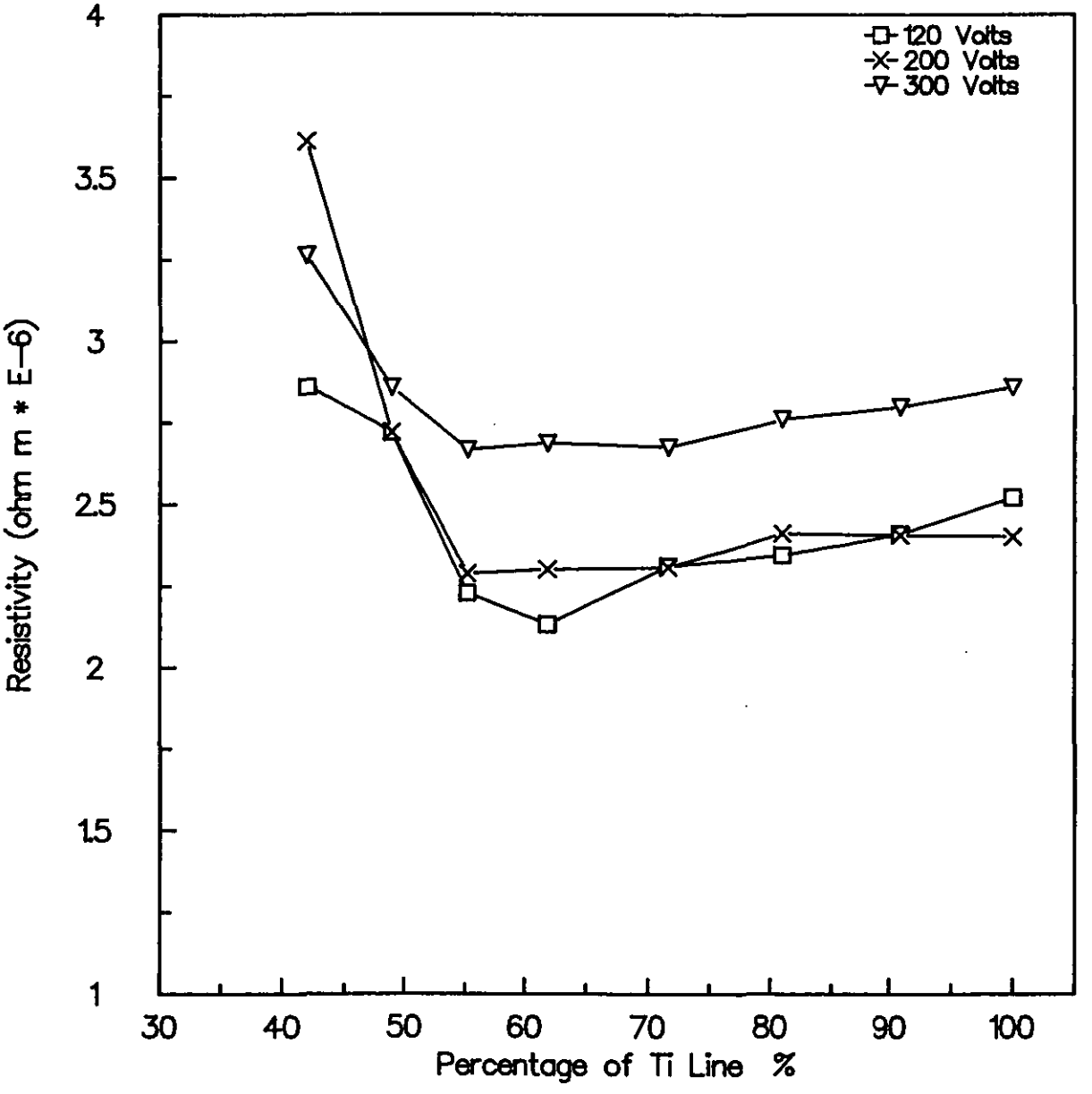

magnetron is operated at lower voltages. That reveals not an increase in the metal emission line but due to the increase in electron emission at constant energy from the filament as the magnetron operated at low voltage. It was seen (Ref. 26) that the emission signal is related to the electron intensity and its energy in the dense plasma region (almost in front of the magnetron target). When the filament assisted magnetron is used the existing electrons are emitted, almost, at constant energy.

However, the influence of operating the magnetron at lower potentials in making titanium nitride is shown in Figure 12, where it can be seen that films made at lower potential had a lower resistivity. This reduction of film resistivity can be attributed to two reasons:

1- As the magnetron operates at lower voltage, better unbalanced magnetron performance concerning high ion bombardment and floating potential will be achieved (see Figure 6). As a result increased ion assisted film improvement may be seen. That is because the ion to atom arrival rate is altered, which causes better film properties. this factor has a significant role in controlling the film microstructure and consequent properties as demonstrated in chapter 5 and 7.

2- Lowering the magnetron potential will reduce the high neutrals energy that bombard the growing film, causing radiation-type damage. During ITO deposition (Ref. 2) it was seen that at lower magnetron potentials the films resistivity drop dromaticaly, that because the higher carrier constration and mobility were found.

Conclusions

The design and characterization of an unbalanced magnetron that operates at a low voltages has been given here.

This system shows a better plasma performance compared to that of a conventional unbalanced magnetron.

The use of this source in TiN deposition leads to better electrical and optical properties.

8.8 References

1- J. A. Thornton, Thin Solid Films, 80 (1981) 1.

2- S. Ishibashi, Y. Higuchi, H. Nakamura, T. Komatsu, Y. Ota and K. Nakamura, Proc. 1st. Int'l. Symp. on ISSP, 91, Tokyo, (1991).

3- K. Tominaga, K. Kuroda and O. Tada, Japanese Journal of Applied Physics, 27 (1988) 1176.

4- J. J. Cuomo and S. M. Rossnagel, J. Vac. Sci. Technol., A 4 (3), (1986) 393.

5- K. Steenbeck, E. Steinbeiss, G. Schmidt and G. Bruchlos, Vacuum, 42 (1991) 39.

6- D. F. Dawson-Elli, A. R. Lefkow, and J. E. Nordman, J. Vac. Sci. Technol., A 8 (1990) 1294.

7- J. L. Vossen and W. Kern, "Thin film process II", academic press, Ney York, 1991.

8- L. Delcroix and A. R. Trindade, Advances in Electronics and electro physics, Academic, New York, Vol. 36, 1974, P. 265.

9- J. A. Thornton, J. Vac. Sci. Technol., A 4 (1986) 305.

10- J. A. Thornton and D. W. Hoffman, J. Vac. Sci. Technol., 18 (1981) 203.

11- R. Messier, J. Vac, Sci. Technol., A 4 (1986) 490.

12- D. F. Dawson-Elli, D. Plantz, D. S. Stone and J. E. Nordman, J. Vac. Sci. Technol., A 9 (1991) 2442.

13- G. G. Stoney, Proc. R. Soc. London, A 82, (1909) 172.

14- A. Brenner and S. Senderoff, J. Res. N.B.S., 42 (1949) 105.

15- H. Windischmann, J. Vac. Sci. Technol., A 9 ( ) 666.

16- B. Chapmann, "Glow discharge process", Wiley Publication, New york, 1980.

17- J. A. Thornton, J. Vac. Sci. Technol., 15 (1978) 171.

18- R. K. waits, J. Vac. Sci. Technol., 15 (1978) 179.

19- Tri-Mag sputtering source, manufactured by L. M. Simard, Santa Barbara, California 93111.

20- E. J. McClanahan, batelle Northwest, presented at American Vacuum Society Symposium, San Diego, CA, 1984.

21- R. P. Howson, H. A. Ja'fer, presented at American Vacuum Society Symposium, san Diego, CA, 1991.

22- R. P. Howson, H. A. Ja'fer, A. G. Spencer,Thin Solid Films, 193/194 (1990) 127.

23- Ch. Steinberuchel, Appl. Phys., A 36, (1985) 37.

24- W. D. Munz, presented at the combined 17th Int. Conf. on Metallurgical Coatings and the 8th Int. Confer. on Thin Films, san Diego, CA, April, 1990.

25- R. A. Swady, H. A. Ja'fer and R. P. Howson, to be published in Vacuum, 1993.

26- A. G. Spencer, "High rate reactive magnetron sputtering", LUT, 1988.

CHAPTER-9

PLASMA SOURCE BASED AN UNBALANCED MAGNETRON

9.1 Hall Effect Ion Source

Hall-effect ion sources are closely related to work done in Soviet Union, much of which was reported in their All-Union conferences (Ref. 1). This work is acknowledged by the use of the names "closed drift" and "End Hall" as types of Hall-effect ion sources. Hall-effect ion source can be defined as a plasma device operating in approximately the glow-discharge regime. The ions are electrostatically accelerated into a beam with the accelerating electric field established by an electron current of comparable magnitude to the beam current, interacting with a magnetic field. One component of the electron motion is counter to the ion flow. Another component is normal to the direction. The current associated with this normal component is called the Hall current. In Hall-effect ion sources there is a complete, or closed, path for the Hall current. In addition, for the ions to be accelerated into a beam, rather than much more diffusely, the ion cyclotron radius must be much larger than the total acceleration length. The high-current, low-energy capabilities of these sources make them particularly suited to process improvement during thin-film deposition or thin-film property enhancement.

9.1.1 Operation

There are several types of Hall-effect ion sources. The well known ones are the end-hall type (Refs. 1,2) so named because the exits the acceleration region at the end (axis) of the magnetic field, and the closed-drift type (Refs. 1,3) in which the ion-acceleration channel is annular,rather than circular as it is in the end-hall. The operation mechanism of end-Hall ion source is described here to be compared with our result.

The source is shown in cross-section in Fig. 1 (Ref. 2). The cathode is a heated filament in the front of the source that is employed to emit electrons both for primary discharge, and to charge-neutralize the ion beam. The anode is configured conically, with a magnetic field that traverses the anode surface and diverges along the central axis of the source. The gas is fed through a plate below the anode. Electrons from the cathode are accelerated towards the anode and can cause ionisation, both through direct collisions and through heating of the background electron population. In the anode region, there exists an ExB drift, which helps confine the electrons and causes additional ionisation. The current to the anode is almost entirely composed of electrons, both the electrons from the cathode and the secondary electrons that result from the ionisation of neutrals.

In normal operation, the gas flow is adjusted at constant anode current until the anode voltage is also at the desired value. A weak potential difference is set up along the axis of the source, of the form

$$dV = \left(\frac{KT_e}{e}\right) \ln \left(\frac{B}{B_o}\right)$$

where:

B and B_o = The magnetic field at two locations on the axis of the source

K = Boltzmann constant

T_e = Electron temperature in K and

e = Electron charge

Ions are accelerated by this weak potential gradient, and the net ion energy has been found experimentally to follow this relation (Ref. 1) The typical ion energies from these sources are related to the anode-cathode potential as well as the field gradient. They can be controllably varied from 20 to 100 ev. The beams, however, tend to be rather divergent compared with the Kaufman source.

Fig.9.1 A cross section of a Hall-effect ion source {ref2}

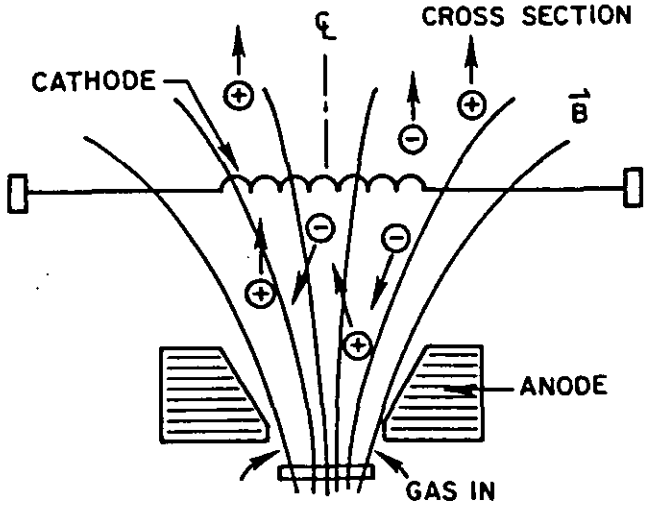

9.2 Plasma-Source Based an Unbalanced Magnetron

9.2.1 Design and Optimisation

The most recent techniques for building ungridded ion-sources are based on plasma (Ref. 4) or hot filaments (Ref. 5). These designs result from a combination of the plasma discharge into an ion source. All of these sources show that there are too many variables to control the output satisfactorily. To do so, system complexity is necessary. In turn, their cost will be high. Using our approach, the unbalanced magnetron principle, combined with a hot filament discharge aided by a magnetic field, result in high ion current density. The controllability of such devices is achieved from the control of the process parameters, these being argon pressure and the thermionic electron emission from the filament (in general).

From previous chapters, we have seen that the high performance of an unbalanced magnetron plasma can be achieved by optimising the magnetic field configuration that leaks from the outer pole to the front, striking either the subjected target or the substrate. The created electrons (both from ionisations and the secondary electron emission), will react with the magnetic field lines and follow them taking the ions with them by electrostatic means. To create a high ion-beam source, then, there are two points to consider. Firstly, design a magnetic configuration for better plasma confinement, then, optimised high electron generation source. By using additional mild steel rings fixed to the outer pole of the magnetron, thus extending it a considerable distance from the target surface, a larger, better defined leakage of magnetic field, can be achieved (chapter 7). The majority of electron generation will be accounted for by secondary electrons emitted from the target surface by ion bombardment. The electrons are trapped by the magnetic field lines creating an ExB drift which in turn will cause more ionisation. This system provides a high ion current density of between 5 and 100 mA/cm^2 and with self-bias of between 20 and 100 V at the substrate . Recently it has been found that such performance

can improve the film property of AR ophthalmic coating and film adhesion (Ref. 6). The operating voltage range of this source is 350-600 V. in this range of voltage the plasma beam will be accompanied by sputtered target material. Even when operated in an oxygen environment, the contamination is not eliminated.

From the low voltage magnetron sputtering process we have seen that the plasma properties are improved. That was interpreted as being due to the lower plasma impedance as the discharge transfer from the cold-cathode discharge regime to the hot-cathode discharge (Refs. 7,8). The electrons emitted from the filament are energetic enough to cause ionisation of the background gas. The increased ionisation forms a denser plasma than that produced by the magnetron alone. The plasma is characterised by a lower impedance, resulting in increased current at constant voltage or decreased voltage at constant current. Of all the electron current injected into the volume in front of the target face, only a fraction are coupled into the target. The rest of electrons, spiral down magnetic field lines toward the substrate. In turn,the plasma properties the ion current density and substrate self-bias are improved.

By accompanying the magnetic configuration of unbalanced magnetron (Figure 1 chapter-7) with that of the low voltage magnetron performance, both pure and high flux ion beam sources can be achieved. The plasma source with its magnetic field shape, connected with its circuit is shown in Fig. 2. The filament position is different from that in the low magnetron voltage configuration. The filament is connected in the centre of the source axis in front of the reflector (so called because it can no longer be a sputtered target). It is used as a biased surface to reflect the electrons to be diffused to the front, following the magnetic line.

To use the magnetron as a low voltage sputtering system, the filament is positioned in the

Fig.9.2 A cross section of a plasma source and the magnetic Configuration

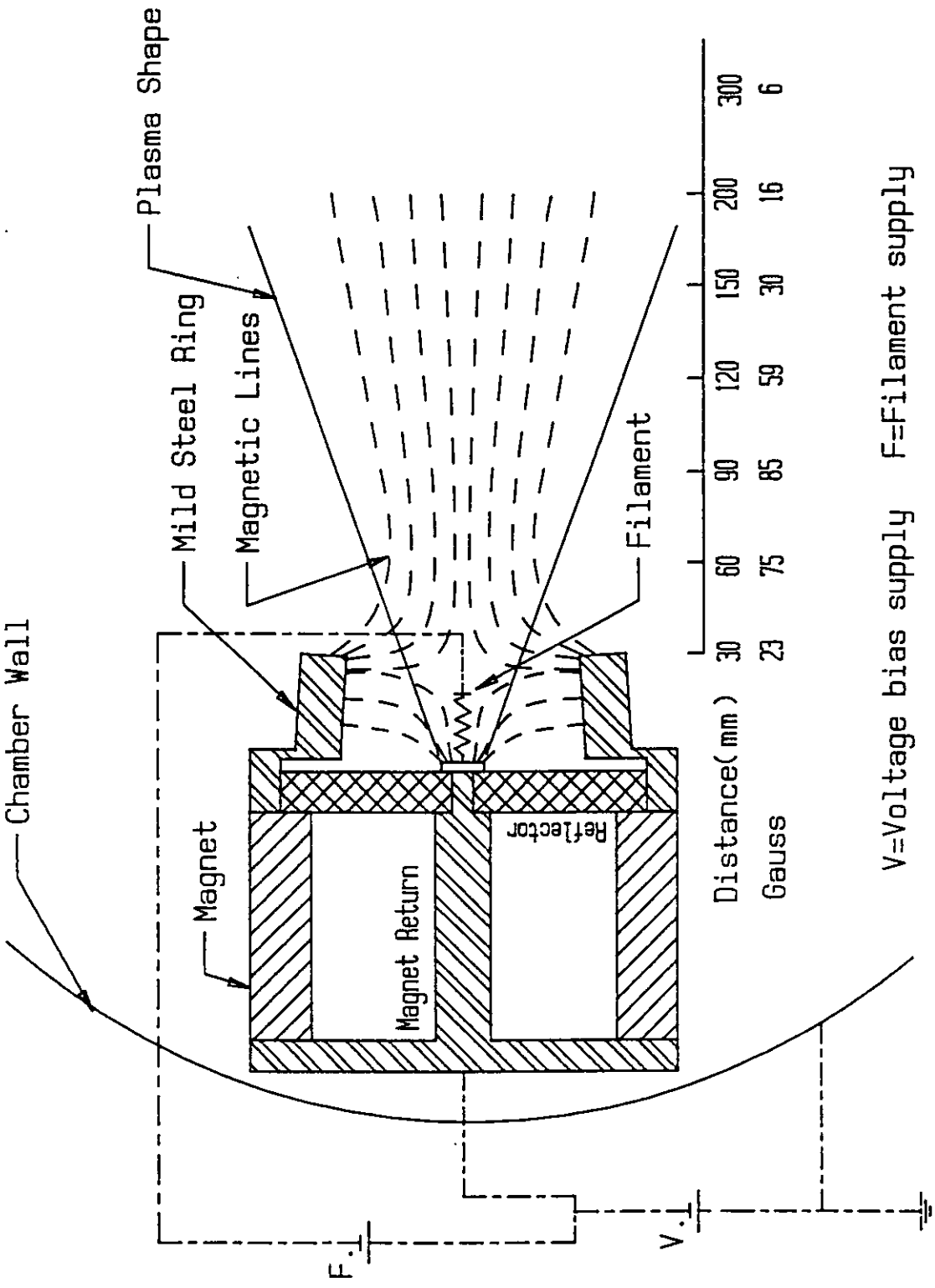

race track close to the outer pole and parallel to the target surface. Despite the magnetron operated at a lower voltage, the ExB drift in front of the target will still occur. The existence of a dense plasma in front of the target causes the target material to be sputtered and contaminate the plasma beam. The existence of the ExB will confine a large proportion of the plasma produced; that remaining being constricted to the front following the magnetic field lines leaked from the outer pole of the magnetron. In other words, this design is more applicable as a controllable voltage sputtering technique than as a plasma source. With the connection of the filament at the centre of the plasma source, accompanied by a magnetic field taking the shape shown in Figure 2, a Penning-like discharge will take place. The resultant plasma is confined within a diameter close to the filament, diffusing to the front in a cone-like shape. This is shown as a dotted line in the same figure. Fig. 3 Shows a photograph of plasma beam produced by this plasma source. The filament-reflector distance and the filament position within the magnetic field both play major roles for optimising the source performance.

The filament, which is normally tungsten,is connected to a resistance heating supply, either AC or DC. To ignite the plasma the filament and the reflector are biased to a particular voltage by using a DC supply. An MDX magnetron driver supply having voltage and current ranges of 0 to 600 Volts and 0 to 8 Amperes respectively, has been used in our experiment. Consequently, the reflector current will be limited by the supply current. When the reflector current reaches 8 A, arcing initiates and the MDX supply will start flashing, so the plasma will be extinguished. A more convenient supply for such a plasma source is one providing higher current in the voltage range 0 to 200 Volts. To prevent the filament sputtering and hence prolong its life, it is necessary to bias it below 100 V. There is a threshold voltage which is related more to the filament-magnetic field configuration than the filament-reflector distance.

Fig.9.3 A photogragh of plasma source in use showing the plasma beam shape.

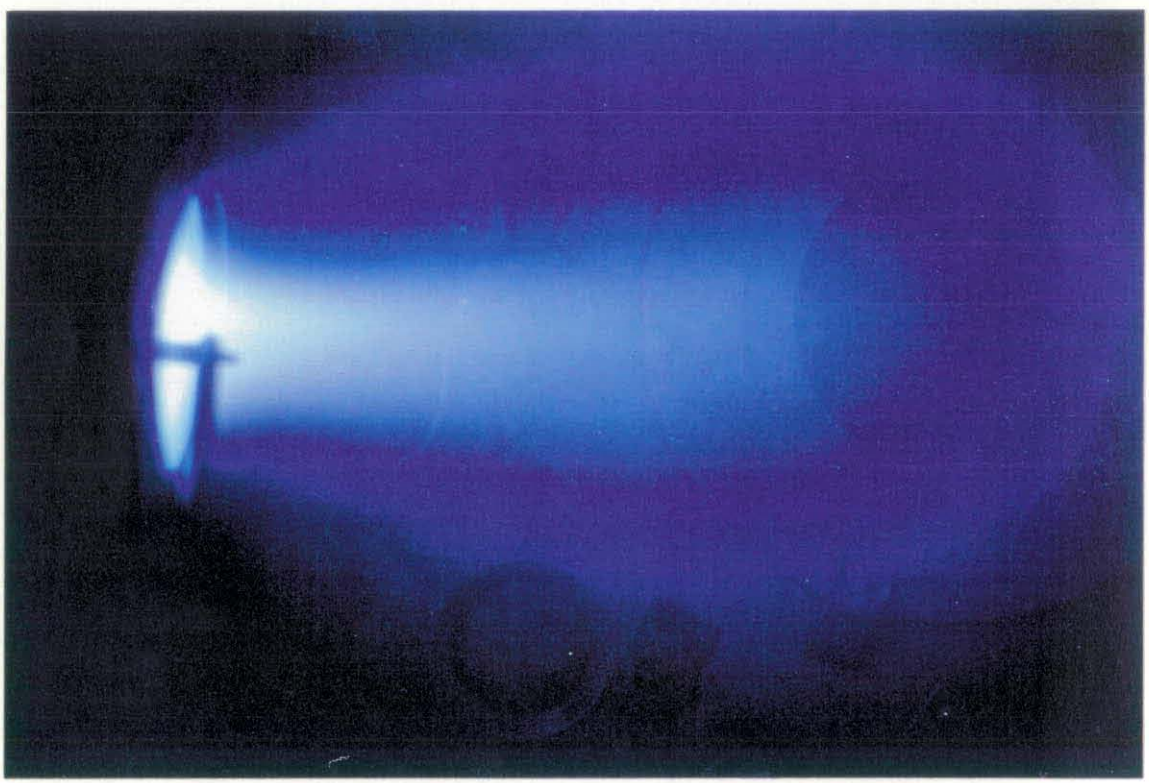

Within the bias voltage applied to the reflector and the filament, the plasma will be ignited immediately when the filament reaches incandescence. At such an elevated temperature, the filament will become a copious source of thermionically emitted electrons. These electron have enough energy to ionise the background gas and initiate the plasma. Because of the negative bias reflector, a fraction of the produced ions will be directed towards it and reflect the electrons to the front. The resultant reflector current can be read from the supply meter. Reflector current will increase as the filament temperature increases. Electron emission is increased by raising the temperature of the filament by passing more current through it. The relationship between the reflector current and the filament current is shown in Fig. 4. As shown in the figure, the utilised temperature is achieved between 40 and 60 Amperes. This range of current is related to the filament size. A narrower gauge filament requires less current, but with broader filaments longer life times can be reached. Hereafter, plasma properties will be related to the reflector current rather than the filament current.

9.2.2 The Source Performance

Ion current, and the energy associated with it, is the most interesting parameter for ion beam investigation. The use of electrostatic probe the source performance has been studied (Ref. 9). Fig. 5 shows the floating potential and ion current density as a function of the reflector current, as measured by the probe at a distance of 120 mm from the reflector surface with 3 mtorr argon pressure. By increasing or decreasing the filament emission, the required ion current and floating potential can be achieved. As the filament temperature rises, therefore it will heat the background electron population, adding not only a degree of ionisation and increased ion current, but also accelerating the ions to higher energies.

Fig.9.4 Reflector current as a function of the filament current.

fig.9.5 Probe measurement of floating potential and ion current density versus the reflector current.

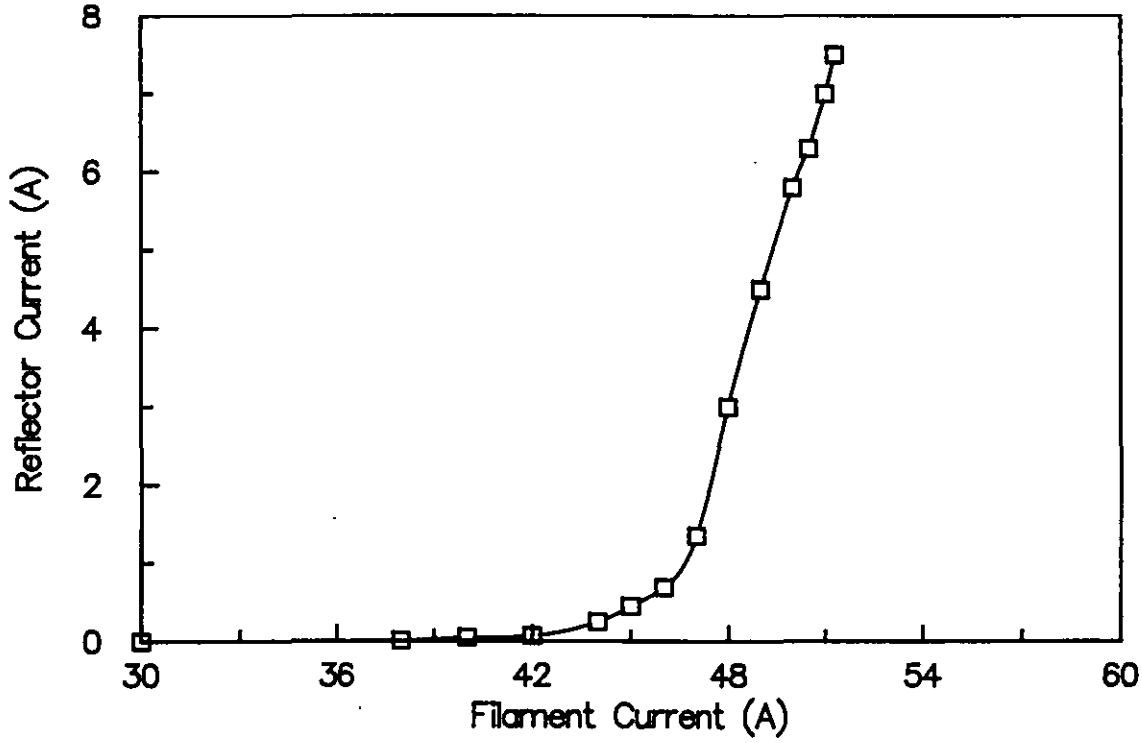

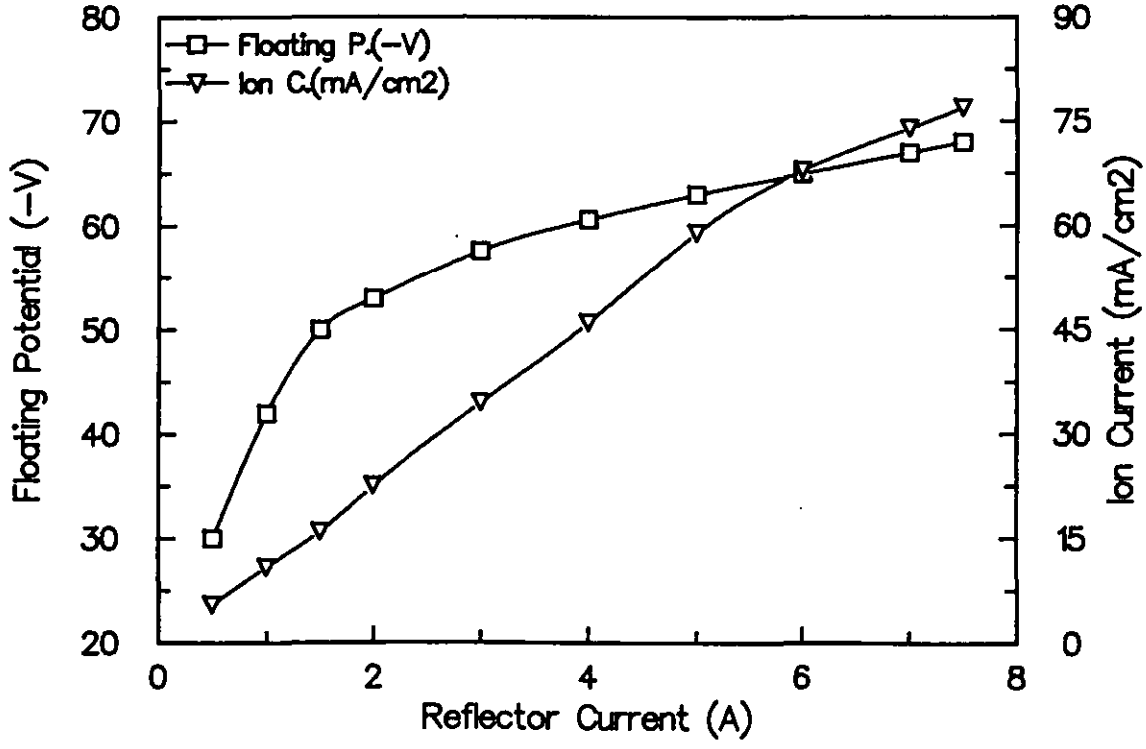

9.2.3 Axis and Radial Beam Profile

The probe described above was used to investigate the beam distribution along the beam axis and with a radial distance from the centre line of the plasma beam. By fixing the reflector current at 7 A and argon pressure at 3 mTorr, the ion current density and floating potential profiles have been measured, shown in Fig. 6. If we combine the result of Fig. 6 with the magnetic strength along the beam axis Fig. 2, the ion current and the floating potential profile can be understood. From the unbalanced magnetron principle, the magnetic field distribution demonstrates that the magnetic strength approaches a maximum at a distance of 90 mm from the reflector surface. That occurs where maximum divergence of the magnetic field takes place. At this point, as we can see from Fig. 6, the ion current density will reach the maximum. Either side of this critical point the ion current will decrease. The plasma beam reduces as we follow the beam axis. At the first three points, the floating potential profile is slightly different from that of the ion current profile. When the maximum is achieved the floating potential is a minimum and starts to rise again until it reaches a maximum and ultimately follows the magnetic field strength. This may be due to maximum confinement of the plasma beam taking place at maximum magnetic field strength. Consequently, that will result in plasma disturbance ,recombination and collision of the plasma and gas species.

Fig. 7 shows the ion current density and the floating potential profile as a function of the radial distance. These measurements have been taken at a distance of 120 mm from the reflector face and 3 mtorr argon pressure. As shown in the figure, ion current density is greater at the centre of the beam than at larger radius. With further distance from the reflector surface better beam uniformity can be achieved as shown in Fig. 7b.

fig.9.6 Ion current and floating potential profile with beam axis.

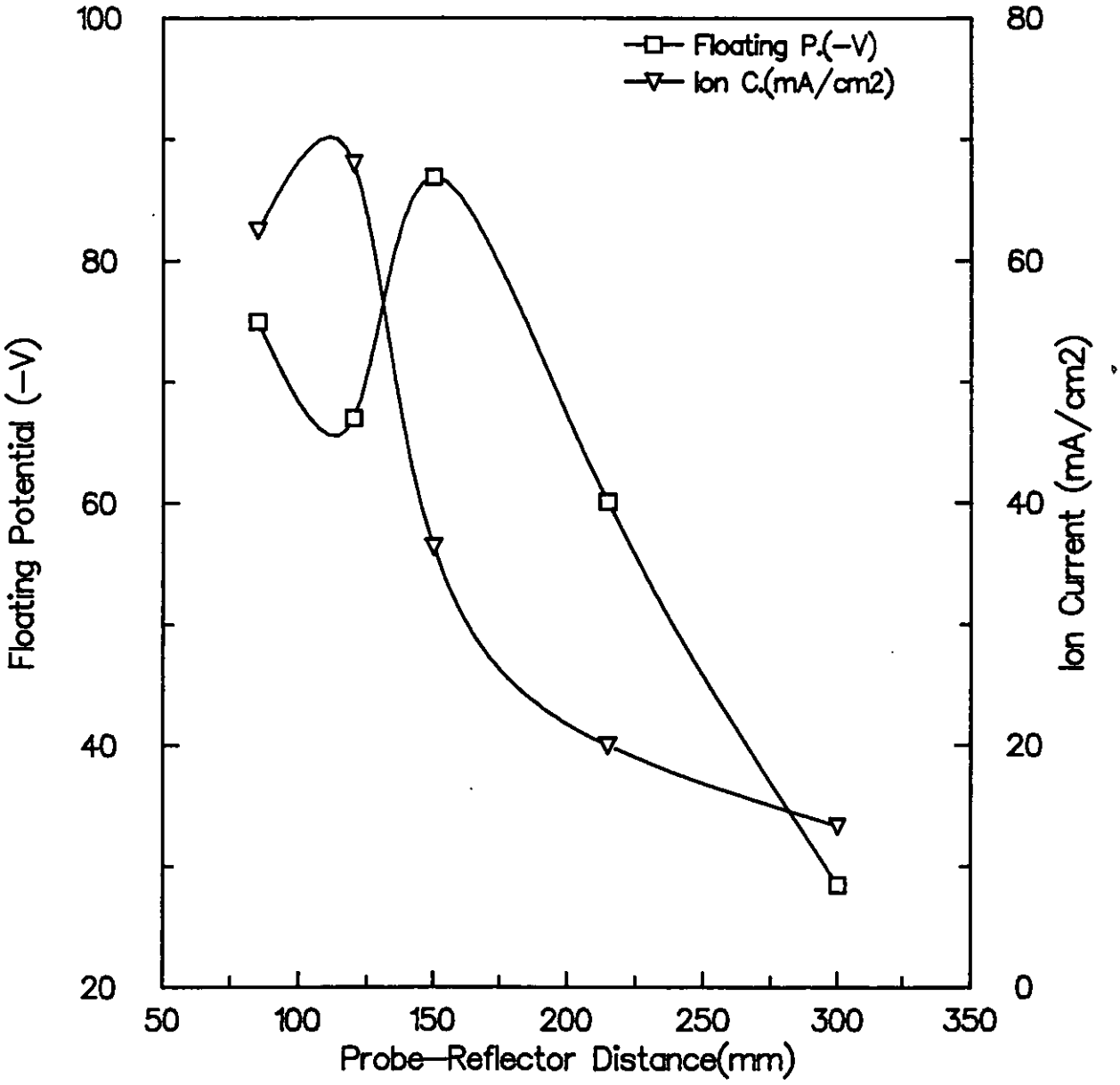

fig.9.7 Floating potential and the ion current profile with the radial distribution a) at 120mm distance and b) at 160 mm

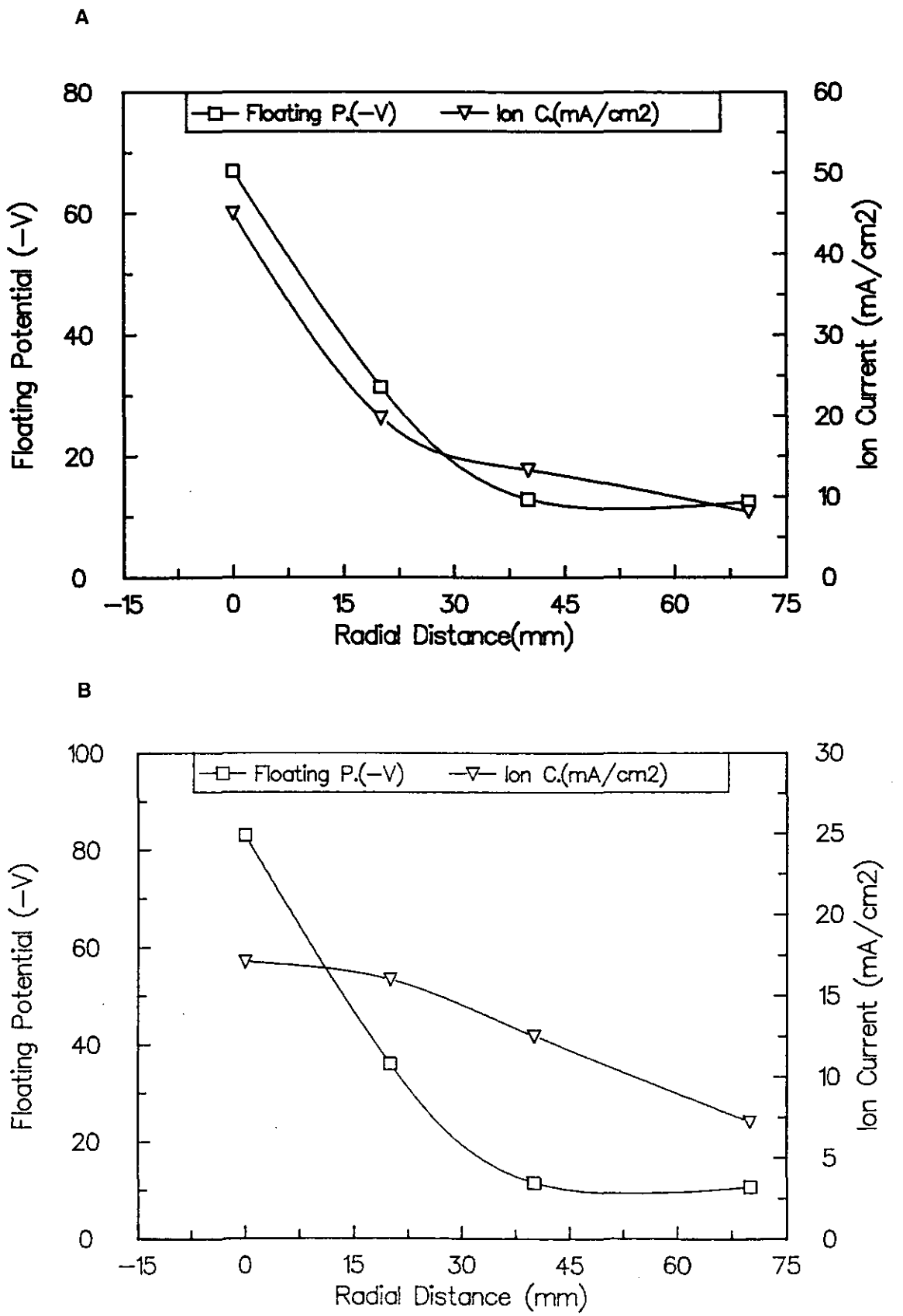

9.2.4 Argon and Oxygen Pressure Effects

Features of the unbalanced magnetron are increasing ion current and the substrate self-bias with decreasing the argon pressure (Ref. 10). The energy of the secondary electrons entering the plasma in magnetron sputtering is approximately constant. Thus as the pressure decreases, the probability of ionisation in the plasma decreases, as does the recombination and charge exchange. Therefore, the ion current and floating potential will increase.

Fig. 8 shows the probe measurements as a function of argon pressure for plasma processes. Reflector current was 7 A, and probe-reflector distance 120 mm. The emission current from the filament will be severely limited by the electron space charge surrounding it, but with an anode located in the vacuum to withdraw the electrons, and a suitable gas introduced to a pressure of a few millitorr, a glow discharge can easily be generated. In our system the anode is the chamber wall and as such does not attract electrons. Other factors influencing emission current are the filament potential and the argon pressure. If the bias voltage to the filament is maintained in our experiment, then the only remaining parameter which can initiate the discharge and release electrons is an increased argon partial pressure. Because we are dealing with a copious source of thermionic electrons, the probability of ionisation will increase as the argon pressure increases until reaching the maximum value. After that, gaseous recombination and charge exchange will take place, and the ion current will decrease. As shown in Fig. 8, the ion energy will decrease as the argon pressure increases. That is due to higher scattering with the background gas as the pressure increases, and hence, reduction of the ion and electron energies.

The use of oxygen partial in magnetron processes has a large influence on the plasma parameters. The influence of the oxygen partial pressure combined with argon shows

fig.9.8 Probe measurement of ion current and floating potential versus the argon pressure.

fig.9.9 ion current and floating potential with oxygen partial pressure.

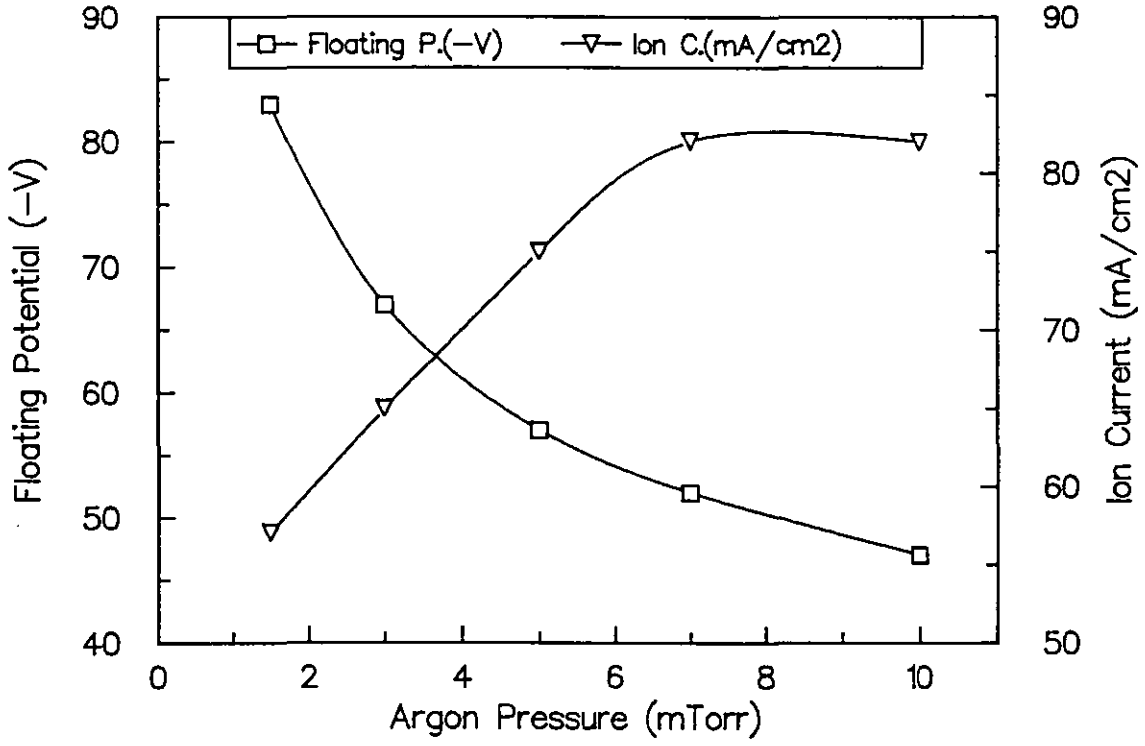

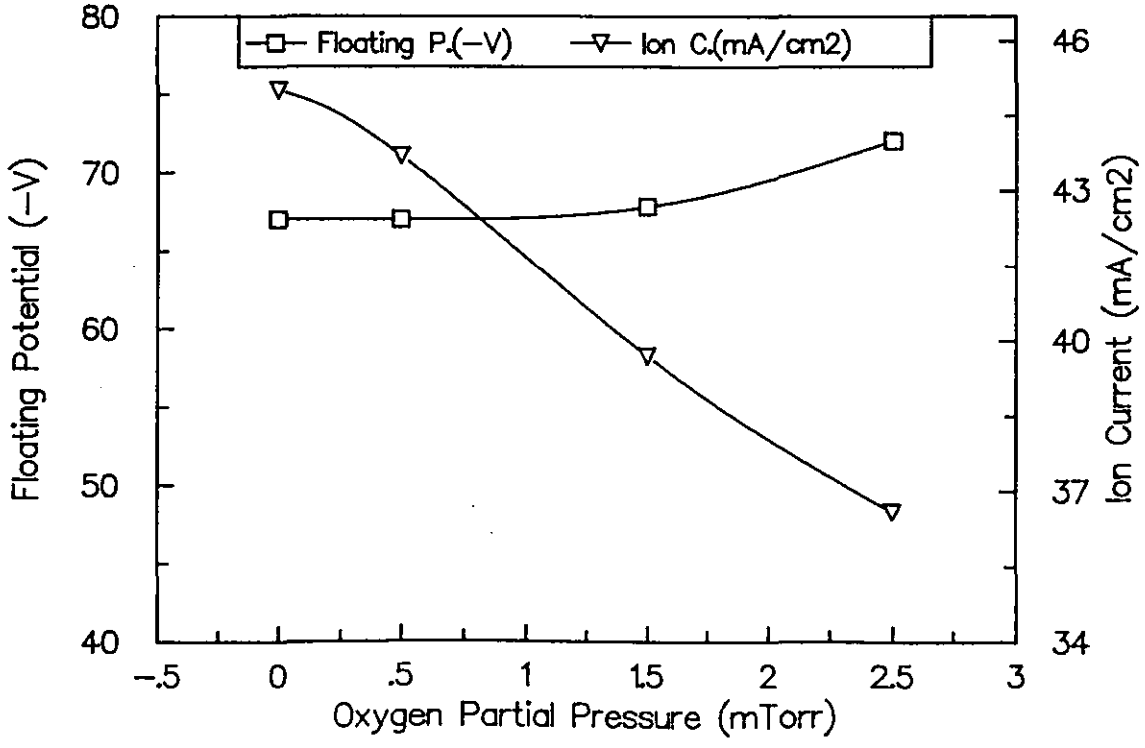

that the ion current and the floating potential are improved as the oxygen partial pressure increases. The presence of oxygen in magnetron sputtering, will result in the dissociation of the oxygen molecular by electron impact. Some of the dissociative events will be accompanied by ionisation, so that the discharge can be sustained. Such reaction will be accompanied by a free radical and positive and negative ions in the discharge. In the presence of the negative ions and the electrons, the potential drop at the substrate will increase in order to equalise the charge flow to it.

Fig. 9 shows the probe characteristic of oxygen used in plasma sources. The total pressure and the reflector current were 3 mTorr and 7 A respectively. As we can see from this figure, the electron impact dissociation of oxygen molecular is not accompanied by ionisation. As the oxygen partial pressure is increased the ion current is decreases, and there is a slight increase in the floating potential as a result of the presence of negative oxygen ions. In magnetron sputtering, the existence of highly energetic sputtered atoms, the E×B drift current, and the high voltage process, all may lead to impact dissociation oxygen molecular accompanied by ionisation, in turn enhancing the plasma properties (see chapter 7).

9.2.5 Auxiliary Magnet Effects

From the previous discussion, the parameters that influence the plasma characteristics are argon pressure, electron-emission current and the distance from the source body. The use of additional magnets behind the substrate, enable the plasma beam to be better characterised. For this purpose, an electromagnetic coil has been fastened at 40 mm from the probe area. By passing 1.5 A through the coil the magnetic strength at the the probe will be equal to 115 gauss.

Fig. 10 shows the relation between the ion current and the floating potential with the

fig.9.10 auxilary magnet affects on the probe reading of ion current andthe floating potential.

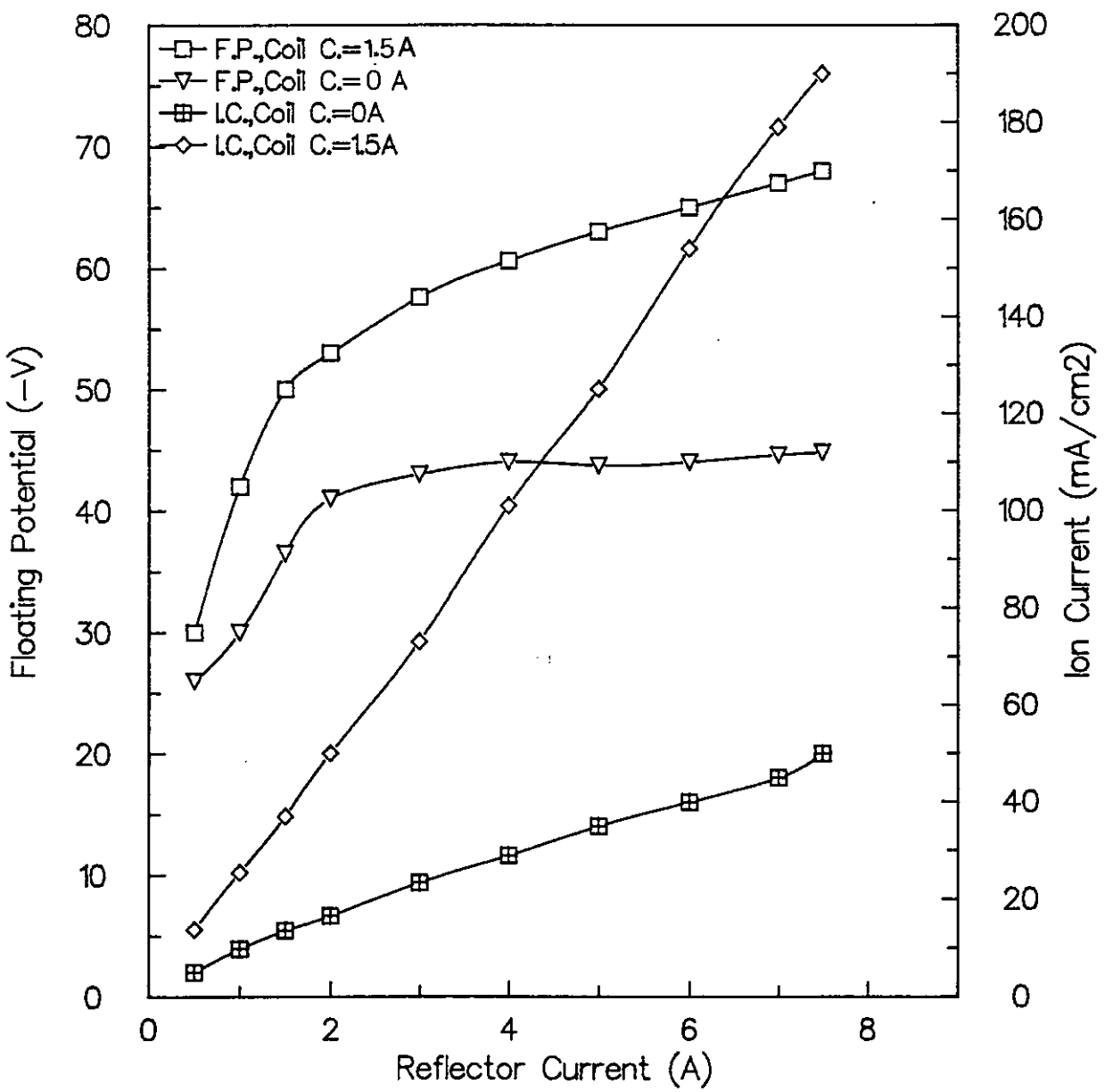

reflector current, both with and without the additional magnet. The ion current and the floating potential are improved as the magnetic bias is added. As will be shown later, such performance can be used as a device to form a dense plasma source for low-magnetron sputtering technique. using the same coil the plasma beam can be directed to anywhere in the process chamber. Fig. 11 shows a photograph of the plasma beam when it is bent by 90 degree from the beam axis.

9.3 Applications

9.3.1 Metal Low Voltage Sputtering

The theory of filament assisted magnetron sputtering, used as a low voltage magnetron was introduced in the previous chapter. For TiN depositions, the ensuing results indicate that the film properties are improved when the magnetron operates at lower voltage (Ref. 11). Material such as Indium-Tin alloy cannot be deposited using this technique, because of target melting initiated by the close proximity of the high temperature filament.

The use of a plasma source to provide a high ion bombardment directed to an independently biased target enables low voltage sputtering to be achieved, even with low melting point material. The investigations of metal sputterings of copper plate, the use of targets based on unbalanced magnetron and reactive sputtering of ITO are selected.

9.3.1.1 Copper Plate Sputtering

A Cooled copper plate with a 120 mm diameter was chosen to be the sputtered target. This plate is fixed at a distance of 120 mm from the reflector face with an angle of 45 degree from the centre. It is biased independently by using a dc power supply. An electromagnet coil is used to confine the plasma beam to be more concentrated at the plate target. The substrate is fixed in front of the copper plate at a distance of 100 mm. The layout of this design is shown in Fig. 12. For such process, however, high ion current

fig.9.11 A photogragh of plasma source with bend plasma by 90:

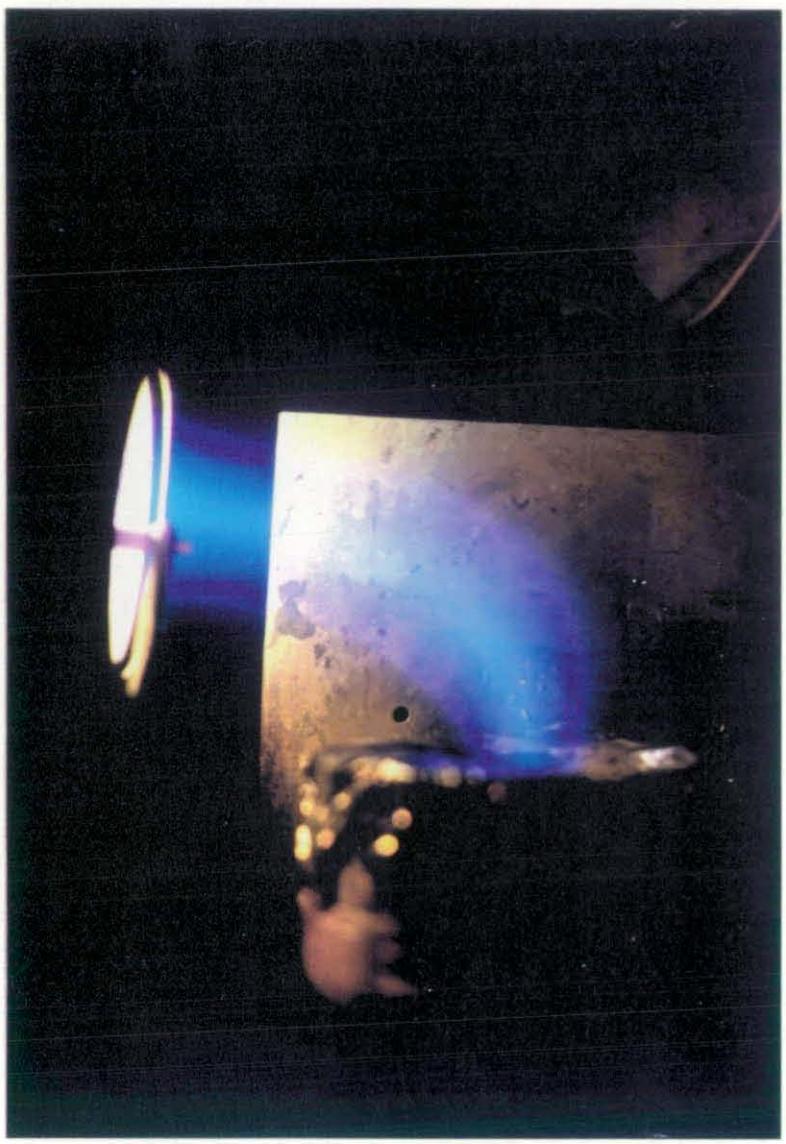

fig.9.12 Layout of the plasma source and the use of copper plate target.

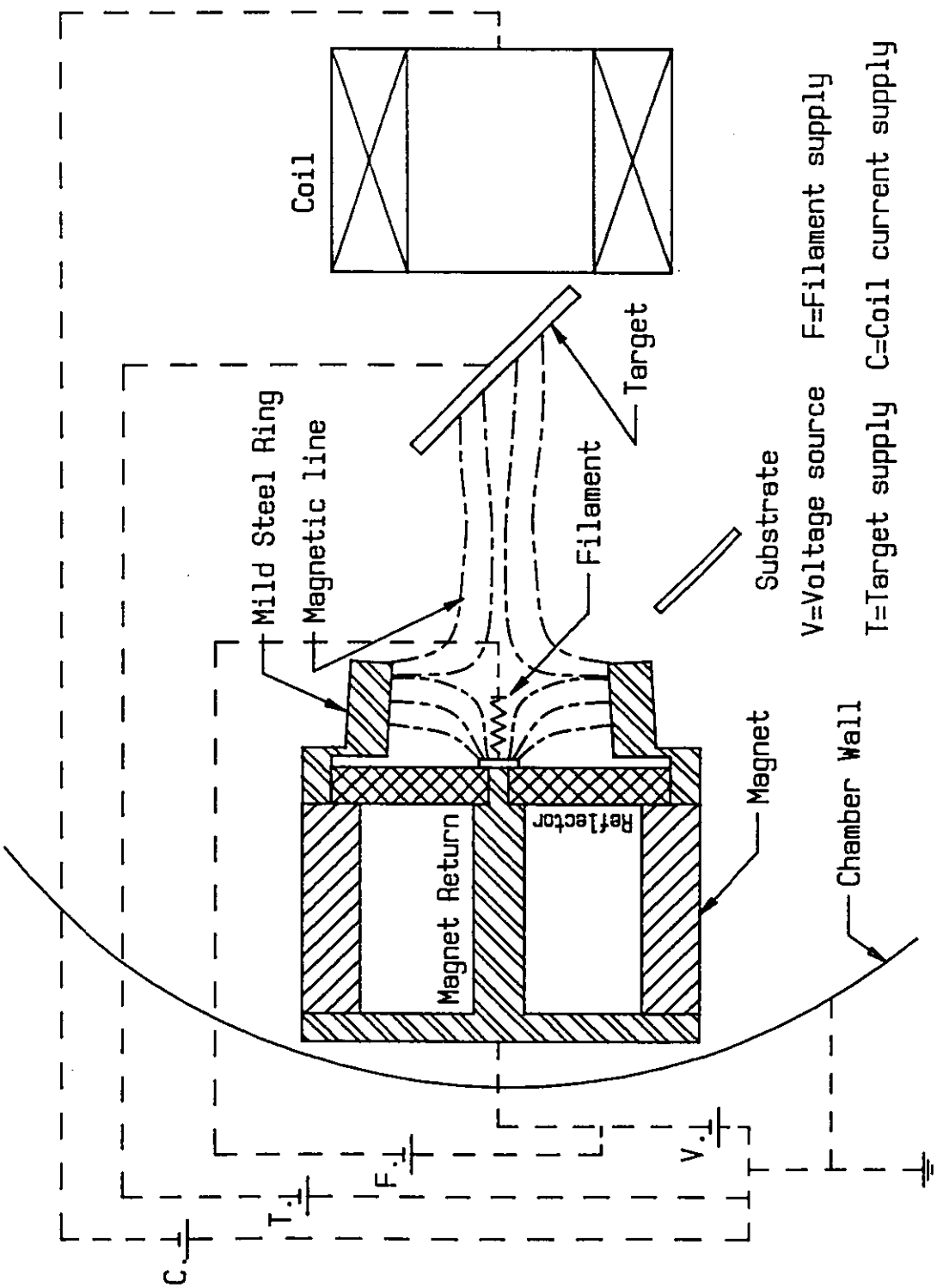

density is required rather than high energy. As shown in section 9.2, this can be achieved by controlling plasma operating parameters. such as electron emission, argon pressure and the magnetic strength at the target. Using a fairly large target diameter, most of the plasma ions will strike the target with energies equal to the target potential. Hence, the use of the coil in this situation acts to localise the beam at the target centre rather than increasing plasma beam efficiency.

Fig. 13 shows the I-V characteristic of the copper plate target. Copper deposition rate has been measured as a function of the target potential, illustrated in Fig. 14. As shown in Fig. 13, at a bias voltage between 50 and 100 Volts the target current is related to the target potential. This is because the applied potential at the target is not high enough to repel all the plasma electrons, especially those at high energy. Above 100 V all ions will be attracted and the current will keep constant. Then, the deposition rate of the plate target will be related more to the target potential than the ion density. As will be shown in the following section, such behaviour does not occur if the magnetron target has been used instead. For the same purpose, bending the plasma beam to be directed onto a plate target backed by electromagnetic coil will enable the target to be sputtered. Such a design is shown in Fig. 15. When the plasma beam is bent by a magnetic means, some of these ions that have a high energy will not follow the electrons. Thereby, the beam efficiency will reduce. When the plasma is bent, the low magnetic strength will be sufficient to influence the electrons into taking the ions with them by electrostatic means. Some ions and electrons that gain a high energy during the ionisation have enough momentum to accelerate to the front. To insure that all ions are bent, a high magnetic strength is required. The escaped ions reduce the ion current density by 35% from the original, of (Fig. 11). Essentially this technique is advantageous if the plasma beam is to be used in a remote, shielded environment, similar to some applications of PECVD or for cold plasma applications. With reference to Fig. 12, during deposition, and because there is no

fig.9.13 I-V characteristic of copper plate target.

fig.9.14 Copper deposition rate as a function of the target potential.

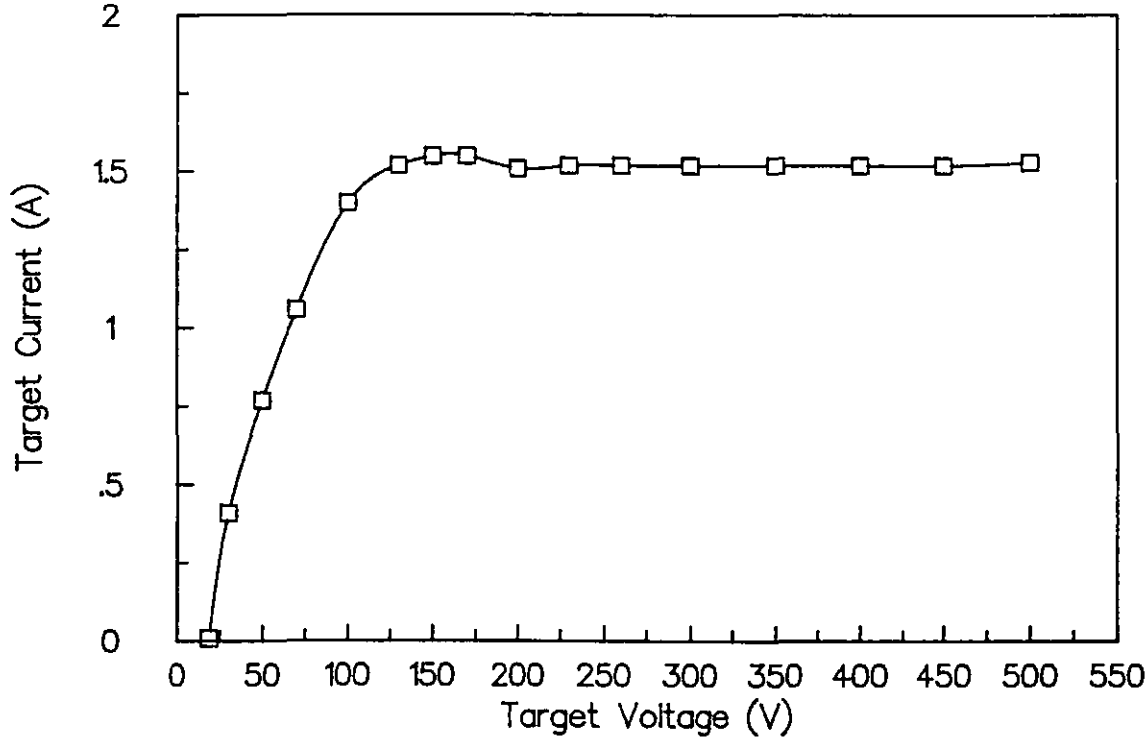

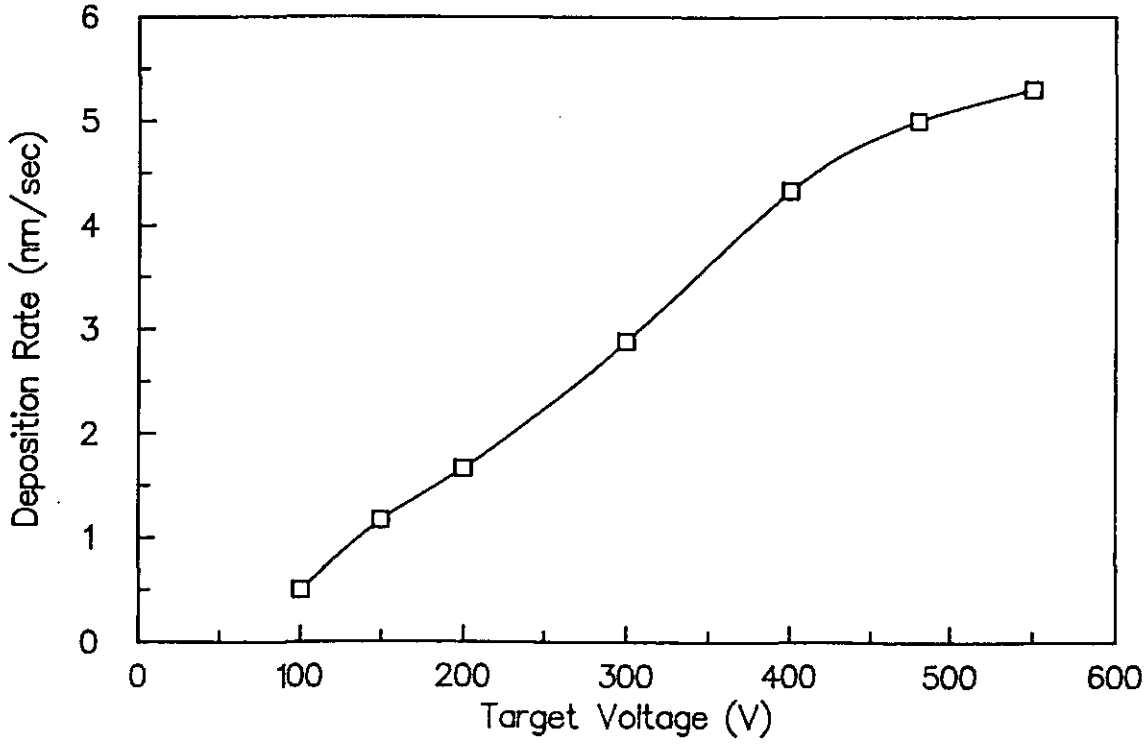

fig.9.15 Layout of copper plate target subjected to a plasma beam at 90° to the plasma source.

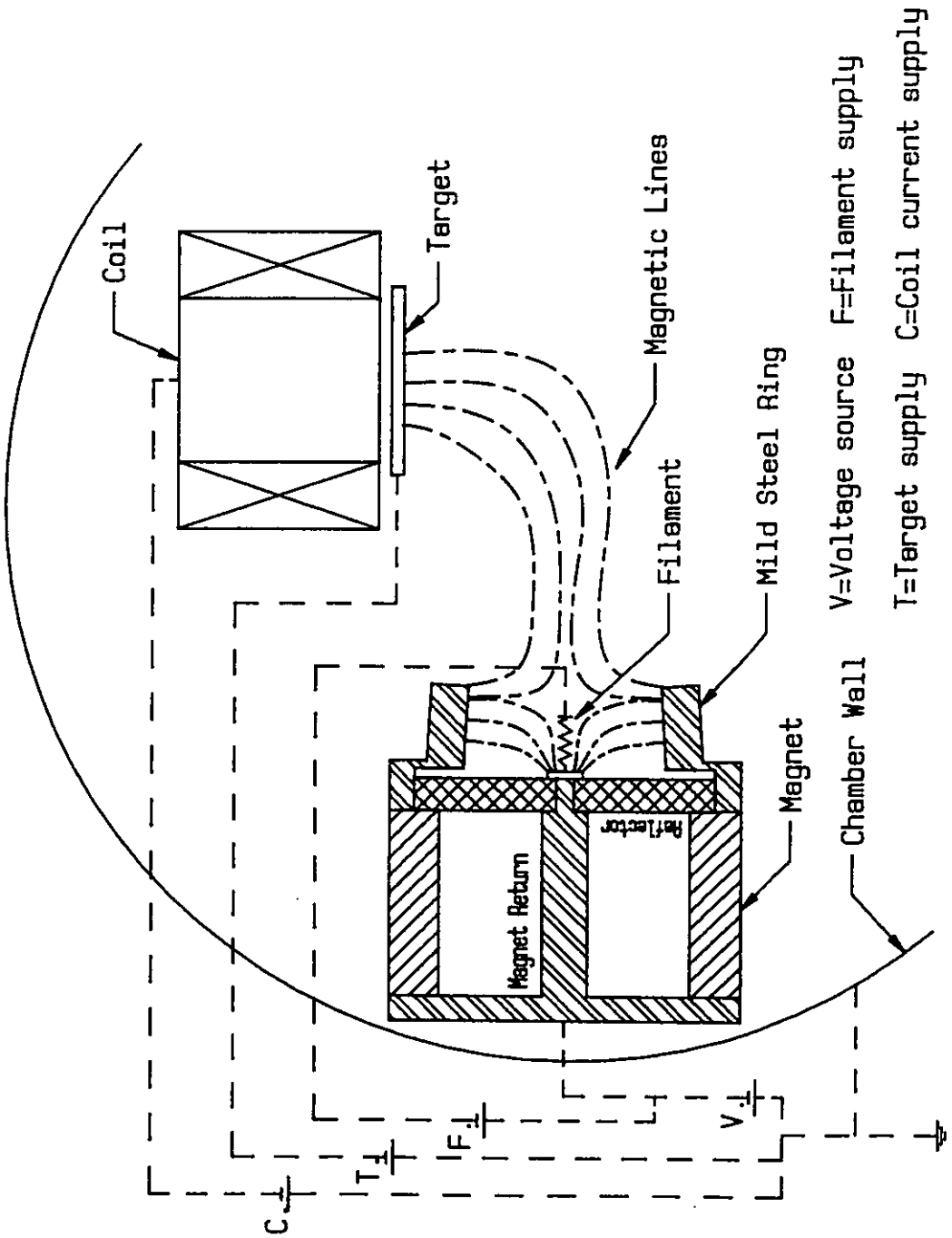

racetrack in front of the target, the secondary electrons emitted from the target at a bias voltage more than 170 V will escape to the front resulting in heating of the substrate and stress in the film.

9.3.1.2 Copper Target Based an Unbalanced Magnetron Sputtering

By replacing the copper plate with a target-based magnetron, the process, in general, can be improved. The set up of such geometry with the magnetic field configuration is shown in Fig. 16. Fig. 17 shows a photograph for the plasma beam directed to a target based unbalanced magnetron. The use of gas pressure as a factor for optimising plasma beam utilisation is shown very clearly by this process, and Fig. 18 demonstrates this fact.

From the basic theory of the magnetron, the secondary electrons emanating from the target as a result of ion bombardment will react with those magnetic field lines those parallel to the target, creating an ExB drift current. In turn, The trapped electrons, will create ionisation and enhance the input power to the biased target. Fig. 19 shows the I-V characteristic of this design compared with that of the copper plate target, and with the unbalanced magnetron not subjected to a plasma beam. From the ion current and target potential, the input power for each process can be obtained. As shown in this figure, the target based magnetron is more efficient than that of the plate target in this respect. The investigation of copper sputtering rate with the former has been carried out. Ensuing results are compared with those of copper plate target and the unbalanced magnetron. The sputtering rate as a function of the target voltage is shown in Fig. 20. Because the ExB drift current exists in front of the biased magnetron, the deposition rate is higher than that of both the plate target and the conventional unbalanced magnetron without plasma source. This process, then, enhances the efficiency of magnetron sputtering, such that the magnetron deposition rate increases by a factor 10 for a given voltage. In addition, using this system for low voltage sputtering, result in deposited films showing no stress.

fig.9.16 Layout of target based unbalanced magnetron subjected to the plasma source.

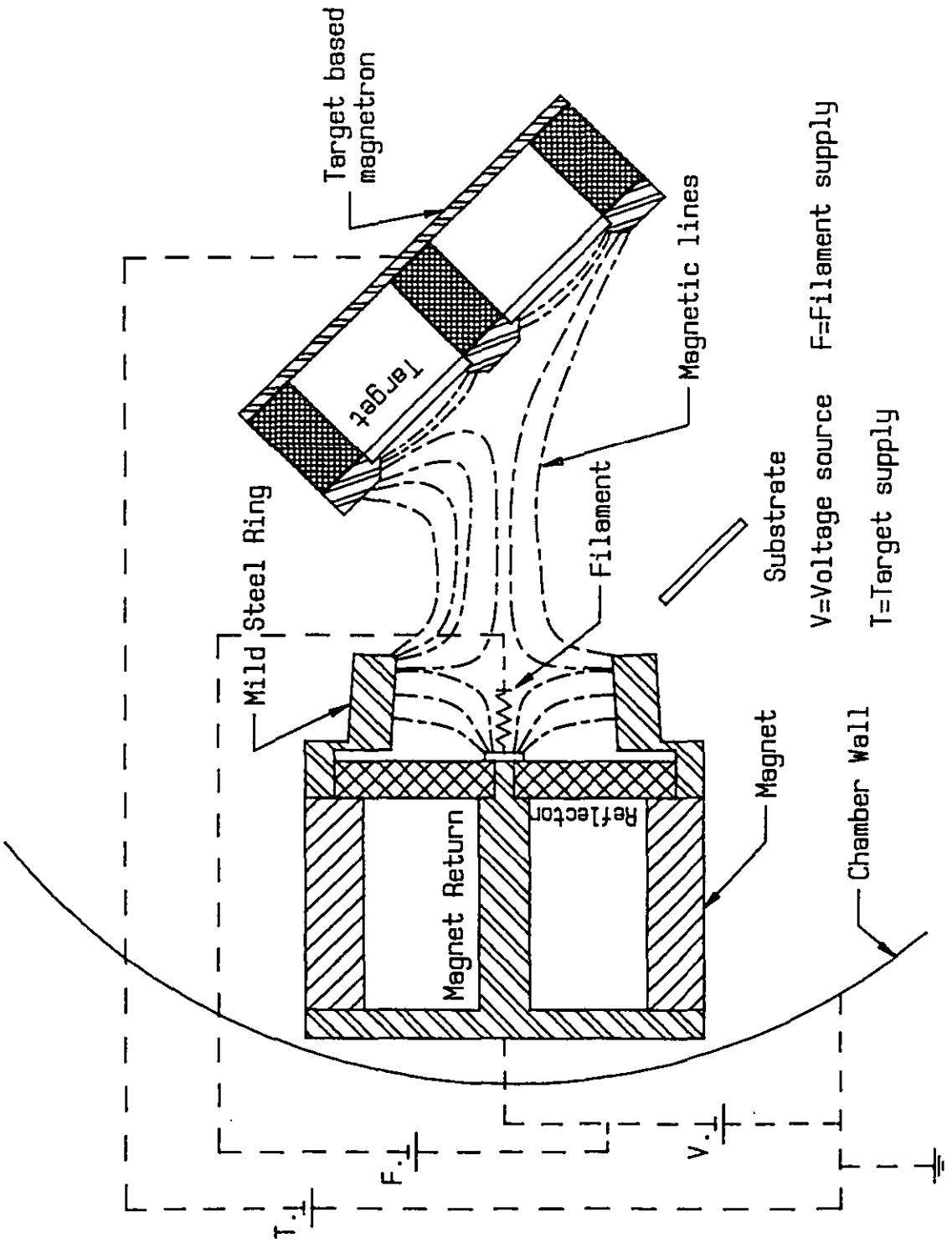

fig.9.17 A photograph showing the plasma beam trapped by the magnetron target

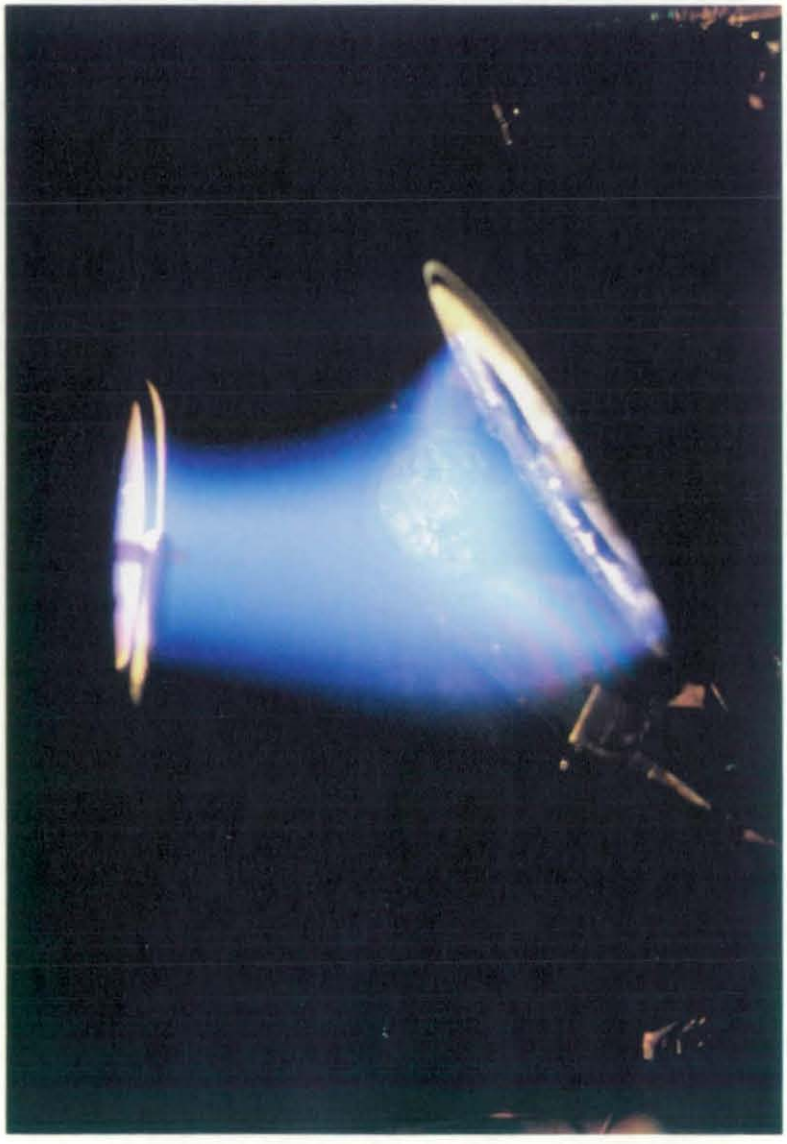

fig.9.18 I-V characteristic of target based unbalanced magnetron versus the argon pressure.

fig.9.19 I-V characteristic of target based unbalanced magnetron compared with that of plate target and conventional magnetron.

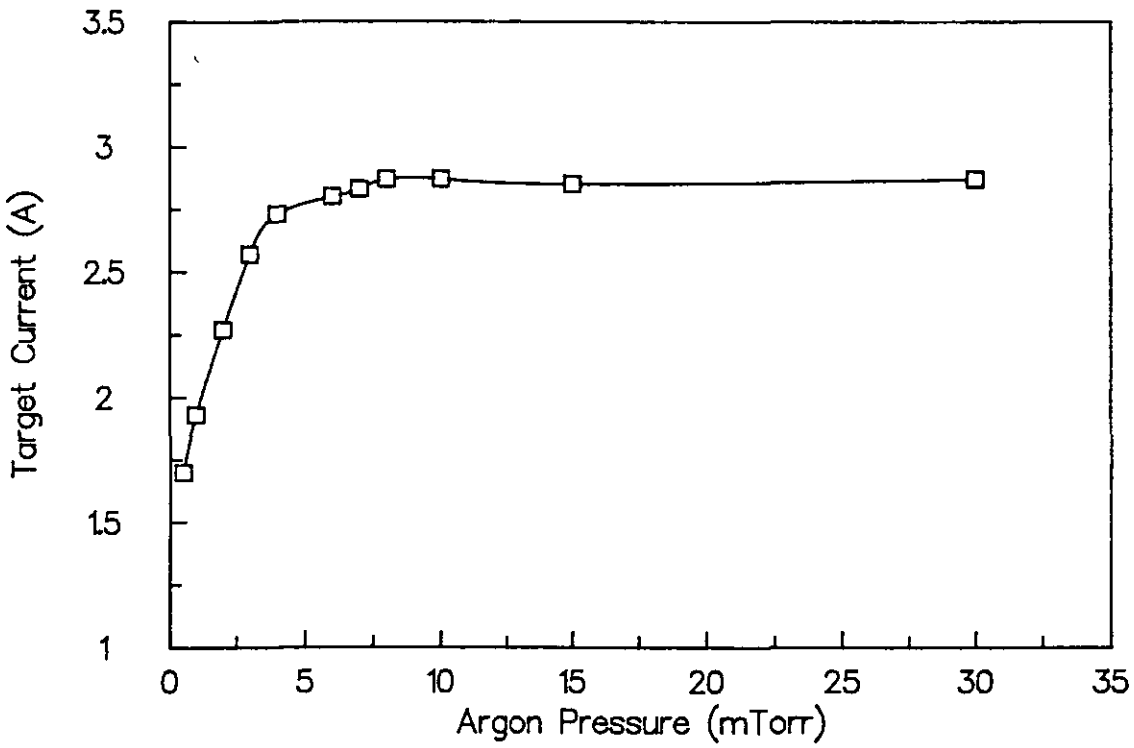

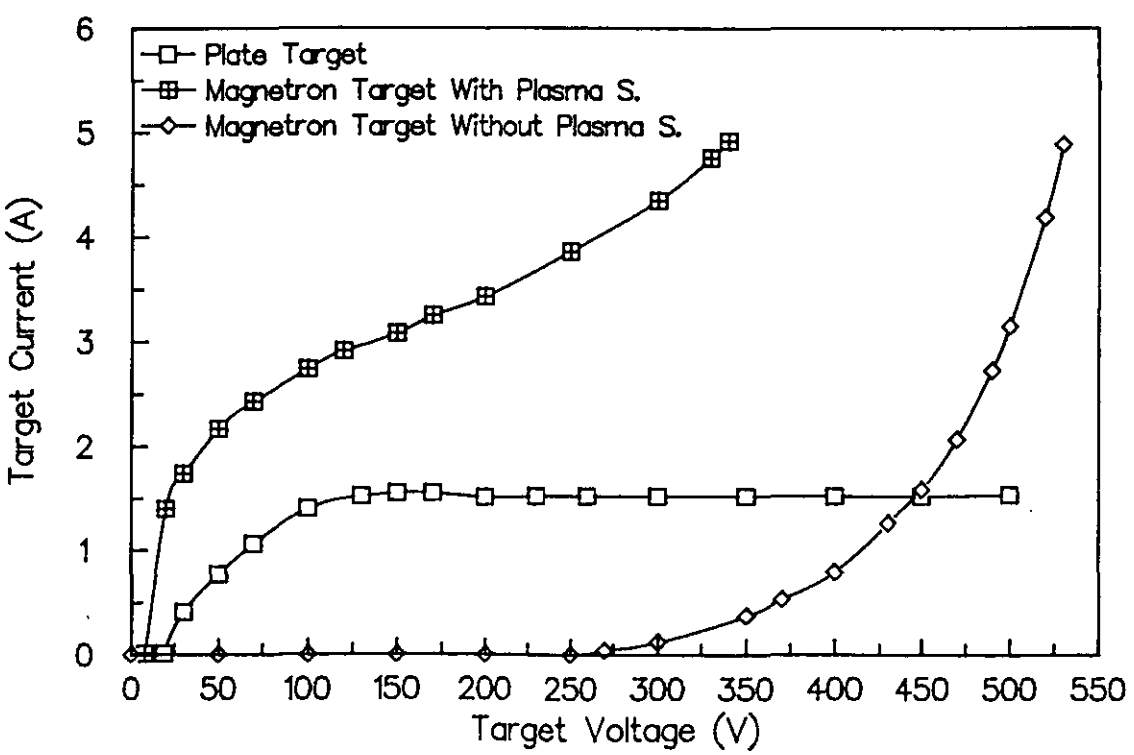

Further, the magnetic configuration of this system enables it to be used for low potential sputtering at room temperature for any target material.

In order to optimise the target utilisation, the target angle with respect to the centre line of the plasma beam should be considered. The input power to the biased target is very sensitive to this angle. Fig. 21 shows the target I-V characteristic for different target angles. At 0°, the plasma beam will be normal to the target surface.

9.3.2 Low Voltage ITO Sputtering.

Recently, Ishibashi et al, (Ref. 12) found that the discharge voltage during sputtering did affect the resistivity of ITO films. By using a lower sputtering voltage, it was possible to obtain low ITO film resistivity. In their investigation, an oxide indium tin target was used. At normal voltage magnetron operation highly energetic oxygen ions created at the target surface are accelerated by the electric field of the cathode sheath and collide with the substrate, causing ITO film damage. The resultant films deposited at room temperature show that film resistivity is reduced from 10×10^{-4} Ω cm at 400 V (normal magnetron operation voltage) to 4×10^{-4} Ω cm at 100 V magnetron voltage. The latter can be reduced to 1×10^{-4} Ω cm when the substrate is heated to 350° C.

ITO films produced by reactive magnetron sputtering in normal operation of target potential (300-400 V), and at room temperature demonstrate that low film resistivities of approximately 4×10^{-4} Ω cm can be achieved (Refs. 13,14). In such circumstances the ITO films deposited in normal reactive magnetron operation at room temperature are better than these deposited from an indium-tin oxide target. Interesting results of low ITO resistivity at room temperature can be achieved when reducing the discharge potential (magnetron voltage).

fig.9.20 Copper deposition rate of target based unbalanced magnetron copaired with that of plate target and conventional magnetron.

fig.9.21 Target current as a function of the target angle.

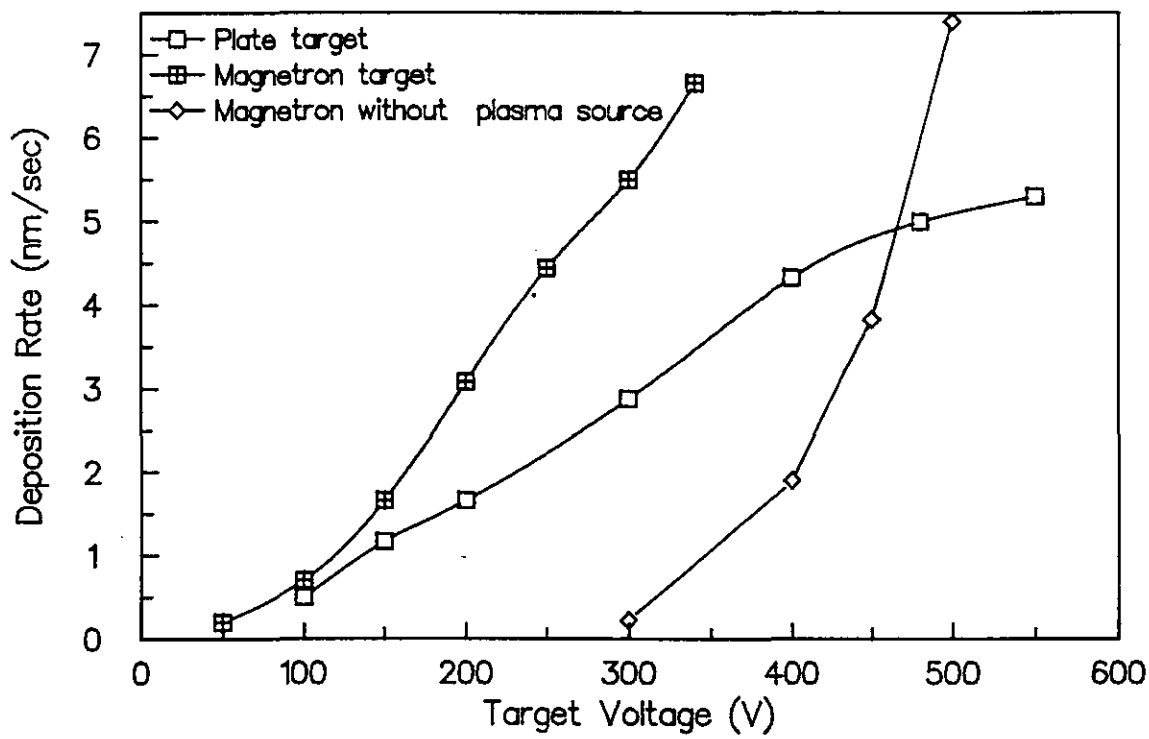

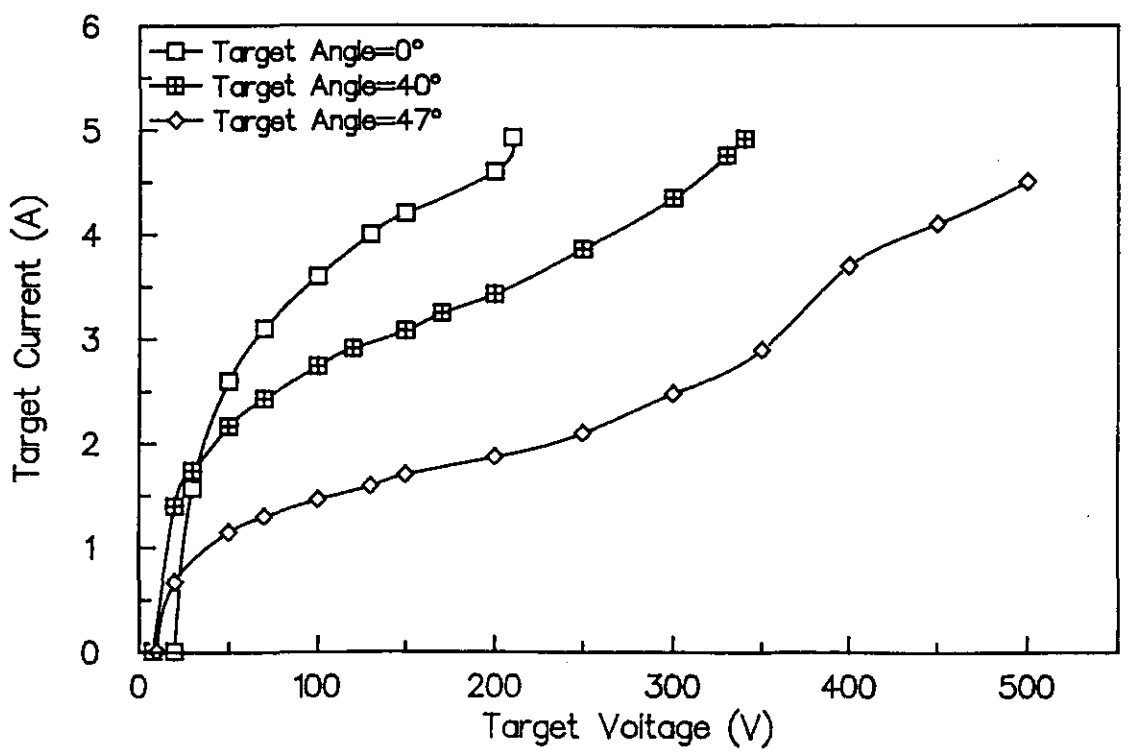

Much attention has been paid to the filament assisted magnetron (so called low voltage magnetron), described in the previous chapter. Material such as indium-tin alloy cannot be deposited using this technique, because of target melting initiated by the close proximity of the high temperature filament. Our attempts were therefore concentrated on using the plasma source as in metal target sputtering of the previous section. The system of Fig. 16, with an indium-tin target has been used. In order to control the oxygen gas pressure at the correct level, especially in the pressure instability region, the Plasma Emission Monitor, PEM, is required. However, when using this technique some problems had to be faced, which led the experiment to end with uncertainty. The main problem was oxygen pressure instability, because the incoming signal from the emission fibre was noisy, in turn making the control unstable. Another approach was to use the pressure signal as an input signal to the control system. unfortunately the output of the pirani pressure gauge was affected by the plasma generation, in turn disrupting the input signal and making the process uncontrollable. Ultimately manual control was used. Using this method, the oxygen flow is controlled rather than the oxygen partial pressure. Hence, in the stoichiometric region where the film is conducting, pressure instability exists. Results achieved near to this point are not optimum. To achieved better stoichiometry, then, a high pumping speed is required so that the diffusion pump port was fully opened. At 3 mTorr argon pressure, 7 A reflector current and 150 V magnetron bias voltage, ITO films were deposited. The resultant resistivity shows the same order as the conventional magnetron. This is about 4×10^{-4} Ω cm. A deposition rate as high as 3.3 nm/sec has been achieved with an input power of 300 W. Observations on a variety of ITO films produced from the bias target magnetron, even when using PEM or pressure signal control, show that the ITO film resistivity reaches saturation.

Using an ITO target, sputtered by Ar ions, generates black, high resistivity suboxide on

the surface, which can be explained by the following Ion Collision reaction

$$In_2O_3 \text{ ---------- } 2InO + O$$

In the ITO film itself, a high sputtering voltage can generate the above reaction by the negative ion collision of oxygen to form black and high resistivity suboxide (InO). The film resistivity will be increased by this material. When the operation voltage reduced below 100 V the oxygen ion energy was reduced, in turn, forming less suboxide at the film, and the resistivity will be lower.

By using reactive magnetron sputtering less oxygen ion damage results. That is because the resulting films is not only from the ITO sputtered from the target surface but mostly from the reaction which exists at the substrate between the sputtered target atoms and the oxygen gas. Reducing the target voltage will only reduce the energy of that fraction of oxygen ions that are formed at the target surface.

Conclusions

The design of a plasma source based on the unbalanced magnetron principle has been described here. This source can be used as a tool in thin film modifications and as an activation source in thin film production. The source can be used as a plasma beam assisted magnetron system for low voltage sputtering of a sensitive materials (the deposition of ITO thin film).

9.4 References

1- J.J.Couomo and S.M.Rossnagel, "Handbook of Ion Beam Processing Technology" Noyes publication, (1989)

2- H.R.Kaufman, R.S.Robinson, and R.I.Seddon, J. Vac. Sci. Technol, A5, 2081 (1987).

3- H.R.Kaufman. AIAA, 78, (1985).

4- E.Yade, A.Tonegawa, D.Satoh and K.Takayama, Vacuum, 36, 43, (1986).

5- J.H.Freeman, Nucl. Inst. Meth. 22, 306 (1960).

6- M.Wool, Private comminication, Physics Dep. Loughbourough Uni. Leics. UK (1992).

7- B.Chapman, "Glow Discharge Processing" Jhon Wiley and Son, New York, (1980).

8- J.J.Coumo and S.M.Rossangel, J. Vac. Sci. Technol. a4, 393, (1986).

9- H.A.Ja'fer And R.P.Howson, to be published in Vacuum J. (1993).

10- R.P.Howson, H.A.Ja'fer and A.G.Spencer, Thin Solid Films, 193/194. 127 (1990).

11- R.A.Swady, H.A.Ja'fer and R.P.Howson, to be published in Vacuum J. (1993).

12- I.Ishibashi, Y.Higachi, H.Nakamura, T.Komatsu, Y.Ota and K.nakamura, Proc. 1st Int'l Symp. on ISSP'91 Tokyo (1991).

13- A.G.Spencer, Ph.D. Theses, Physics Dept.,Loughbourough Uni. (1988).

14- C.A.Bishop, Ph.D. Thesis, Physics Dept.,Loughborough Uni. (1986).

CHAPTER-10

CONCLUSIONS

The principle of the magnetron which is used to create low voltage sources operating in low pressure is that crossed electric and magnetic fields can contain electrons within a volume close to the cathode, making them available to ionise the residual atmosphere. Implicit in this is that there is a continuous path for the circulation of these electrons. Sputtering magnetrons can be planar or cylindrical. A recent modification to the planar design has been the "unbalanced" magnetron, where some of the electrons can leak from the region near to the cathode through magnetic field lines leaving one pole, hence the magnetic field is not completely balanced. If this pole is the one in the centre of a circular, planar magnetron the leakage field can form a field along the axis of the circle which can also contain an extension of the cathode forming a cylindrical magnetron with leakage of electrons from the open end. When the device is used to create a plasma, the leaking electrons take ions with them for charge neutralisation. This plasma will impinge on the substrate which, if it is isolated, will acquire a negative charge to equalise the flow of the charge to it. The use of an unbalanced magnetron shows that the reactivity and the film properties can be improved. As the reactivity increases at the substrate, the partial pressure of oxygen is seen to be considerably lower for high floating potential and ion bombardment on the deposited film. The use of the unbalanced magnetron for reactively sputtered titanium nitride and oxide on glass substrate at room temperature exhibits an improvement in its optical and electrical properties.

The combination of both the planar and post magnetron in one system result in a high performance unbalanced magnetron. This design has been achieved by adding extra pole pieces to the magnetron outer pole this extend the magnetic field and the trapped plasma far from the sputtering target. As a result ion current densities as high as 100 mA/cm^2

and floating potentials of up to 70 V have been achieved. using this system shows a possibilities of depositing diamond like carbon. Because of the high plasma densities and low amounts of sputtered material when operated in oxygen gas, the system was used as plasma source rather than a sputter deposition system. Using it in PEVCD demonstrated the deposition of SiO_2 and TiO_2. Also the use of this system as a tool for dry etching of photoresist and PET have been demonstrated.

For selective processes there are some disadvantages when the above technique is used; either problems consistent with low pressure operation or deleterious effects in the growing film. It has been witnessed that the high energy reflected neutrals at magnetron voltages around 500 V may cause a radiation type damage, which in turn influences the microstructure and morphology and hence the film properties and film stress. Reducing the magnetron voltage, then, can be beneficial. The injection of electrons into the magnetic trap of the magnetron can result in a much lower operating potential for the magnetron and allow it to operate at lower pressure. Coupling in thermionic electrons emitted from a filament connected at the magnetron race track can reduce the magnetron voltages from 500 to 100 V. This technique shows a better plasma performance and gives a good quality film. Operation of the process at low magnetron potential and under conditions that provide considerable ion bombardment of the growing film was shown to give TiN of better quality. Where this assessed by improved specular selectivity in their reflectivity and lower resistivity.

The magnetic field configuration provided by an unbalanced magnetron combined with the hot filament discharge achieves a high ion current density at the substrate (plasma source). This gives the substrate a self-bias of between 10 and 100 V, with an ion current of between 5 and 100 mA/cm^2. These parameters can be controlled easily by adjusting

the electron emission and the process conditions. The use of magnetic field enables the plasma beam direction to be controlled and bent into remote or shielded environments. The dense plasma emanating from this device enables it to be used for low voltage sputtering. The use of this device fore low voltage reactive sputtering is also possible. My results showing that a high deposition rate of ITO at the low resistivity region can be achieved. In order to optimise the use of the plasma beam in future work the target angle with respect to the centre line of the plasma beam should be considered.

Conferences and Publications List

1- "Substrate effects from an unbalanced magnetron" R.P.Howson, H.A.Ja'fer and A.G.Spencer, "Thin Solid Film" 193/194 (1990) 127.

2- "Design, construction and performance of an unbalanced magnetron for use with insulating substrate" H.A.Ja'fer, R.P.Howson, E.M.Stenlake, and A.G.Spencer, 8th international Conference IPAT, Brussels, May-1991.

3- "Ion-assisted processing with an unbalanced magnetron" R.P.Howson, H.A.Ja'fer, G.W.Hall, E.M.Stenlake, R.A.Swady, A.G.Spencer, H.Barankova, S.Kadlec, Proc. 1st Int'l Sympo. on ISSP, Tokyo, 1991.

4- "Reactive sputtering with an unbalanced magnetron" R.P.Howson and H.A.Ja'fer, J. Vac. Sci. Technol. , A, Vol. 10, (1992) 1784-1790.

5- "Reactive ion plating at low ion energies with an unbalanced magnetron" R.P.Howson and H.A.Ja'fer, to be published in Vacuum 1993.

6- "The reactive sputtering of thin films of TiN at low target voltages" R.A.Swady, H.A.Ja'fer, and R.P.Howson, to be published in Vacuum (1993).

7- "A comparison between the performance of an arc evaporation source and an unbalanced magnetron sputtering source", R.P.Howson, N.Mustapha, H.A.Ja'fer, and E.M.Stenlake, 8th international cof. IPAT, Brussels, May-1991.

8- "A low-voltage, high-current, ion-bombardment source using magnetron principles" H.A.Ja'fer and R.P.Howson, to be published in Vacuum (1993).